Mechanisms of Human Immunodeficiency Virus (HIV) Persistence and Strategies to Elicit Cytotoxic T Lymphocyte-Mediated Clearance of HIV-Infected Cells

by

Mark M. Painter

A dissertation submitted in partial fulfillment
of the requirements for the degree of
Doctor of Philosophy
(Immunology)
in the University of Michigan
2020

Doctoral Committee:

       Professor Kathleen L. Collins, Chair
       Professor Malini Raghavan
       Professor David H. Sherman
       Professor Weiping Zou

Mark M. Painter

markmp@umich.edu

ORCID iD: 0000-0002-0180-2748

DEDICATION

To Matt and Michael

ACKNOWLEDGMENTS

Compiling this dissertation has afforded me the priceless opportunity to reflect on all of the people who made necessary contributions, large and small, in science and in life, that have carried me to this point. I need to begin by thanking Dr. Kathleen Collins for her mentorship during my time in graduate school. I arrived in Ann Arbor rich in spirit but poor in experience. To the extent that I am a capable scientist today, it is because of the foundation Kathy provided through her guidance and support. She created the culture for me to grow and become a scientist of my own, always willing to risk my independence and never subduing my ideas and interpretations, even when we passionately disagreed about the data. A lot of life happens during 6 years, and she has been unendingly patient and persistent despite my extended periods of distraction and stubbornness. For all of this, I owe a sincere debt of gratitude.

I also need to thank Dr. Thomas Zaikos and Dr. Megan McLeod. They taught my hands most of what they know how to do in the lab and were exceedingly generous with their time and attention when I was learning how to do almost everything from scratch. As I have tried to pay it forward in training newer members of the lab, I often see myself lacking the tenderness and generosity that they never failed to show me. It is impossible to claim this work as my own, as the ideas presented in this dissertation are the fruit of the efforts of generations of Collins lab members, many of whom I have never met. I owe particular thanks to the people with whom I shared time in the lab, who contributed their

of inspiration to me, and I will forever be grateful to have been given each of you to share

life with, from the beginning to the end.

TABLE OF CONTENTS

LIST OF FIGURES

ABSTRACT

Human immunodeficiency virus (HIV), the cause of a decades-long pandemic responsible for over 30 million deaths and 38 million ongoing infections, establishes a chronic infection for which there is no cure. While the development of combination antiretroviral therapy (ART) has radically transformed the course of the pandemic, individuals living with HIV must maintain therapy for the remainder of their lives. This is the result of cells harboring latent HIV proviruses, which are stably integrated in the host cell DNA but remain transcriptionally silent. These latent proviruses are not targeted by ART and evade clearance by the host immune response, but can begin to express viral genes and re-establish an ongoing infection in the event of ART interruption. The leading theoretical framework to achieve an HIV cure is the "shock and kill" approach, in which latent proviruses are therapeutically reactivated to express viral genes and subsequently killed by the cytopathic effects of the virus or the host immune response.

The latent reservoir of replication-competent HIV is found in a multitude of quiescent cell types residing in diverse tissues, including resting memory $CD4^+$ T cells and hematopoietic stem and progenitor cells (HSPCs). Understanding the mechanisms regulating HIV latency and reactivation in quiescent cells will enable the development of targeted latency reversing agents (LRAs). Chapter 2 describes two modifications to *in vitro* cultures that independently maintain primary HSPCs in a quiescent state. These quiescent HSPCs are susceptible to HIV infection, but preferentially harbor latent

proviruses that have a significantly reduced likelihood of spontaneous reactivation. Latent proviruses in quiescent cells are resistant to therapeutic reactivation by histone deacetylase inhibition or P-TEFb activation, but are responsive to NFκB activation. Collectively, this work provides a path forward to identify mechanisms contributing to latency and latency reversal in quiescent primary cells.

In the event that a potent shock or sequential shocks successfully induce HIV gene expression in every cell harboring a replication-competent provirus, these cells need to be killed before the latent reservoir can be reseeded. Cytotoxic T lymphocytes (CTLs) are the main effectors of the adaptive immune system responsible for eliminating HIV-infected cells by recognizing HIV peptides presented by MHC-I on the cell surface. HIV evades these responses through the activity of the accessory protein Nef, which downregulates MHC-I by redirecting it to the lysosome instead of the plasma membrane. The work described in Chapter 3 led to the identification of concanamycin A (CMA) as a potent inhibitor of HIV Nef. CMA counteracted Nef at sub-nanomolar concentrations that did not interfere with lysosomal acidification or degradation and were non-toxic in primary cell cultures. CMA specifically reversed Nef-mediated downregulation of MHC-I, but not CD4, and cells treated with CMA showed reduced formation of the AP-1:Nef:MHC-I complex required for MHC-I downregulation. CMA restored expression of diverse allotypes of MHC-I in Nef-expressing cells and inhibited Nef alleles from divergent clades of HIV and SIV, including from primary patient isolates. Importantly, restoration of MHC-I in HIV-infected cells was accompanied by enhanced CTL-mediated clearance of infected cells comparable to genetic deletion of Nef. Thus, CMA is a promising lead compound for therapeutic inhibition of Nef to enhance immune-mediated clearance of HIV-infected cells.

CHAPTER 1

Introduction[1]

Human immunodeficiency virus (HIV) is the etiologic agent of acquired immunodeficiency syndrome (AIDS) and the cause of a global pandemic responsible for approximately 700,000 deaths and 1.7 million new infections in 2019, over 32 million AIDS-associated deaths since the start of the pandemic, and approximately 38 million ongoing infections for which there is no cure[1]. HIV belongs to the family of viruses called retroviruses (Retroviridae), a unique and fascinating family of RNA viruses found throughout vertebrate life, characterized by the two defining features of their life cycle: reverse transcription and integration. The process of reverse transcription, where the viral genomic RNA is reverse-transcribed to genomic DNA by the enzyme reverse transcriptase, was believed to be impossible prior to the discovery of retroviruses[2,3]. While reverse transcription has since been described in other viruses, such as hepadnaviruses[4] and caulimoviruses[5], the discovery of reverse transcriptase in retroviruses fundamentally transformed the field of microbiology[6]. Integration of the viral genome into the host cell DNA is unique to retroviruses and endows them with the capacity to establish persistent infections that can remain undetectable by the host immune response when the virus is

---

[1] Portions of this chapter were published previously:

Painter Mark M., and Collins Kathleen L. (2019) HIV and Retroviruses. In: Schmidt, Thomas M. (ed.) Encyclopedia of Microbiology, 4th Edition. vol. 2, pp. 613-628. UK: Elsevier.

transcriptionally silent. Integration also implies the possibility of altering host cell gene expression, as is the case with oncogenic activation and tumor formation observed in some retroviruses. The beginning of this chapter aims to place the work described in Chapters 2-4 in the context of the existing knowledge of the biology of retroviruses, providing a broad overview focusing on the retroviral life cycle. Particular emphasis will be placed on human immunodeficiency virus type 1 (HIV), the retrovirus responsible for the greatest disease burden in humans and the focus of the research presented here. This chapter will conclude by introducing the specific topics to be explored in Chapters 2-4, discussing the host immune response to HIV and the obstacles that stand in the way of curing HIV infection.

Taxonomy and Classification

All retroviruses share three genes that are essential to the viral life cycle: *gag*, *pol*, and *env*. *Gag* encodes the structural proteins required for virion formation, *pol* encodes the viral enzymes, and *env* encodes the transmembrane envelope protein, which mediates receptor binding and entry into the target cell. Retroviruses share a common genomic organization, in which Gag and a Gag-Pol polyprotein are generated via various mechanisms from the full-length genomic RNA (gRNA), and Env is produced from a singly spliced subgenomic RNA. The viral protease (Pro), an enzyme required for viral particle maturation and infectivity, is often referred to as part of the *pol* gene, although it can be produced from a separate open reading frame (ORF) from *pol*, or as part of *gag*. Retroviruses encoding only *gag*, *pol*, and *env* are considered simple retroviruses, while

those that encode additional genes, such as HIV, are known as complex retroviruses. The retrovirus family is divided into two subfamilies: orthoretrovirinae, which is further divided into six genera, including the lentiviruses, and spumaretrovirinae, which includes only the spumavirus genus[7].

Lentiviruses

Lentiviruses are complex retroviruses encoding *gag* in one ORF and *pro-pol* in another. Production of the Gag-Pro-Pol polyprotein requires a ribosomal frameshift at the end of *gag*. Lentivirus particles assemble at the cell membrane and have distinctive conical cores, and the viral genome is approximately 9.3 kb in length. Lentiviruses include HIV-1 and HIV-2, SIV, caprine arthritis encephalitis virus, and Maedi-visna virus[7]. They encode several additional proteins, which vary among members of the genus. Lentiviruses are capable of infecting non-dividing cells and are named for the characteristically slow onset of the associated disease. HIV-1 and HIV-2 are the etiologic agents of acquired immunodeficiency syndrome (AIDS) and are the retroviruses responsible for the greatest disease burden in humans.
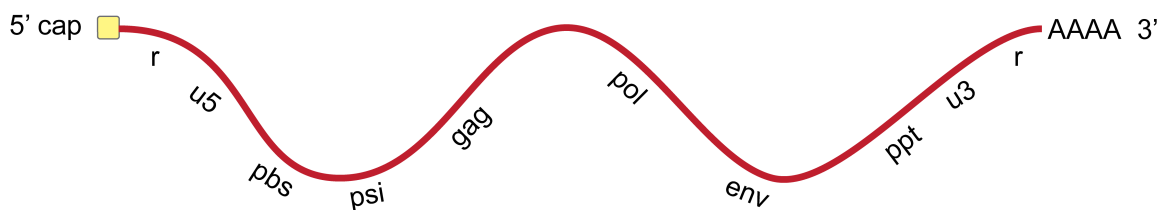
Fig. 1.1: Diagram of the retroviral genomic RNA (gRNA) highlighting important features.[2] The components of the gRNA are shown from 5' to 3'. A 5' methyl cap is present, as with all host mRNA

---

[2] All figures and data from figures throughout were generated by Mark M. Painter unless otherwise indicated in footnotes.

molecules. R is the repeated sequence found at both ends of the gRNA. U5 is the unique 5' sequence containing an "att" site for integration. PBS is the primer binding site, an 18 nucleotide tRNA hybridization sequence which is complementary to the tRNA primer that initiates reverse transcription. The Psi element (Ψ) is the encapsidation signal for packaging of the gRNA. *Gag, pol*, and *env* are the coding regions of the retroviral proteins, and complex retroviruses have additional coding regions in this section of the genome. Ppt is the polypurine tract, the initiation site for plus-strand DNA synthesis. U3 is the unique 3' sequence containing an "att" site for integration. A 3' poly-A tail is present, as with all host mRNA molecules.

Structure and Composition

Genomic RNA and protein nomenclature

The retroviral genome is packaged into viral particles as a dimer of single-stranded, positive-sense, linear RNA molecules. The genomic RNA (gRNA) is produced by the host RNA polymerase II (Pol II) machinery and processed as a host mRNA, with addition of a 5' methyl cap and a 3' poly-A tail. The gRNA includes many important regulatory sequences, shown in Fig. 1.1. The coding region encodes the Gag, Pol, and Env polyproteins, which are further processed to produce the functional products listed in Table 1.1[8].

Precursor	Protein	Abbreviation	HIV-1
Gag	Matrix	MA	p17
	Capsid	CA	p24
	Nucleocapsid	NC	p9
Pol	Protease	PR	p10
	Reverse Transcriptase	RT	p65/p51
	Integrase	IN	p31
Env	Surface	SU	gp120
	Transmembrane	TM	gp41

Table 1.1: Protein products common to all retroviruses. All retroviruses generate Gag, Pol, and Env precursor proteins, which are then cleaved to generate the functional protein products. These products are named in common for all retroviruses with the shown two-letter abbreviations, and the specific names for HIV-1 are also shown.
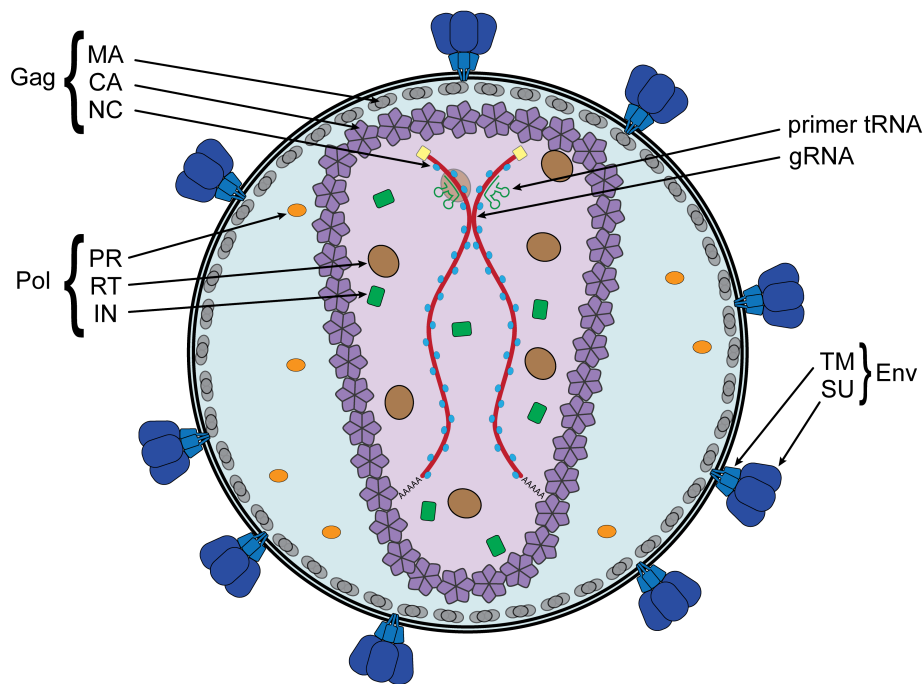
Fig. 1.2: Diagram of the mature retroviral virion. The essential components of mature retroviral virions are depicted, with the protein products labeled in groups according to their unprocessed precursor proteins, Gag, Pol, and Env.

Structure of virions

Retroviral virions are initially assembled when unprocessed Gag and Gag-Pol precursors multimerize within the cytoplasm or at the plasma membrane, which is likely mediated by initial interactions between Gag and dimerized gRNA[9-12]. The immature virion is spherical and appears translucent by electron microscopy. The virion matures when the viral protease (Pro) cleaves Gag and Gag-Pol to the functional products listed in Table 1.1. The mature virion is roughly spherical, but the cleaved CA forms a more ordered viral core around the highly condensed gRNA, which is coated with NC[13,14]. The viral particle typically contains 1500-2000 Gag precursors, with 5-10% as much Gag-Pol in HIV virions[15,16]. The capsid core is made up of primarily hexamers of CA, while some

pentamers stabilize the structure[17]. The capsid core is surrounded by a sphere of MA proteins, which is surrounded by a lipid bilayer envelope acquired during budding from the host cell membrane. The lipid envelope includes host transmembrane proteins as well as the heavily glycosylated viral SU and TM proteins, which exist as trimers[18]. SU is entirely extracellular, but remains associated with the envelope through interactions with the single-pass transmembrane TM protein[19]. The number of Env trimers varies among retroviruses, with lentiviruses having as few as 2-10[18,20].

Retroviral Life Cycle
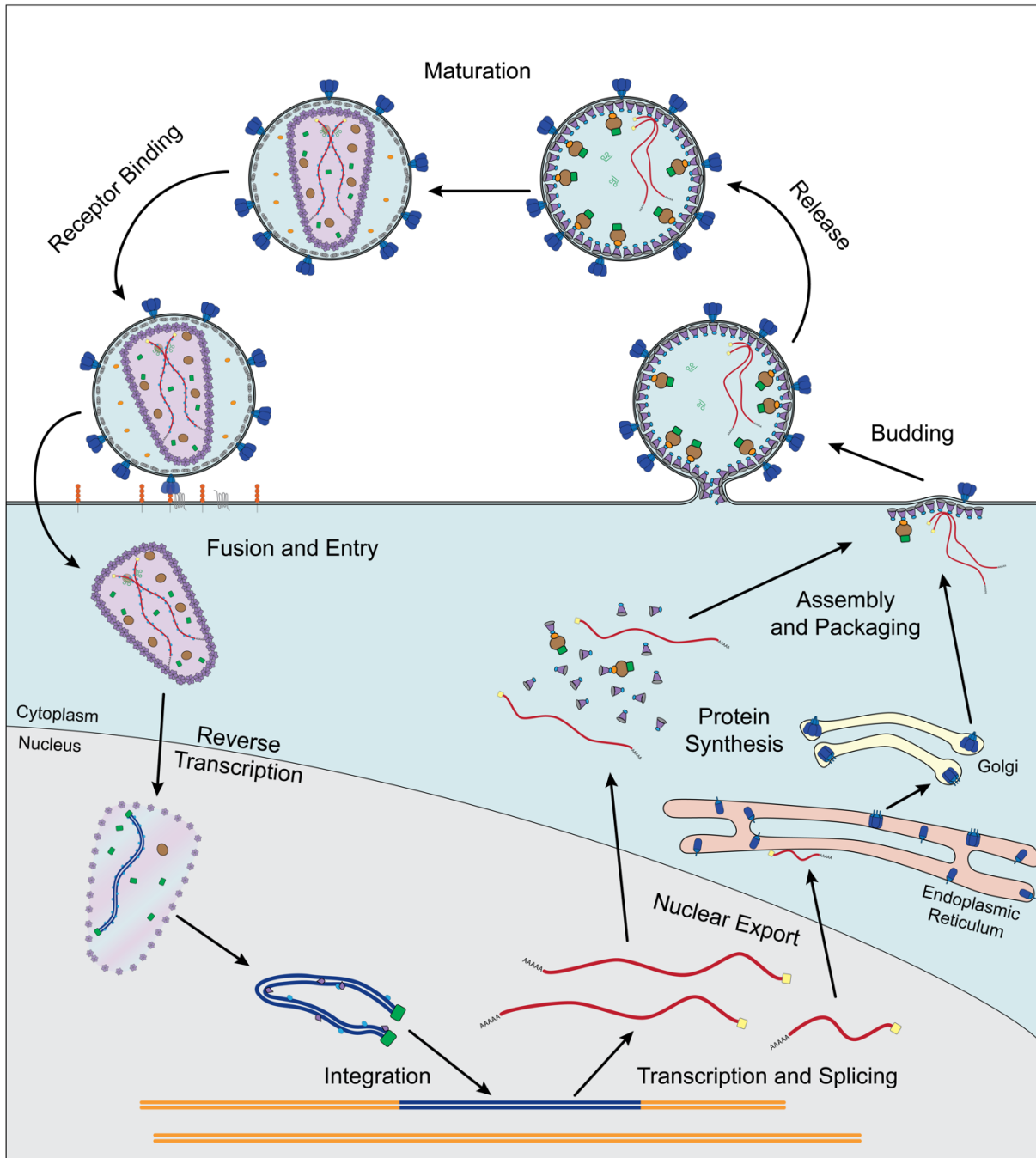
Fig. 1.3: Diagram of the retroviral life cycle. The critical stages of the retroviral life cycle within a single host cell are depicted, from the infection of a target cell with a mature virus particle to the production of mature virus particles from the infected cell.

Receptor binding and membrane fusion

The retroviral life cycle begins when SU trimers on the outside of the virion envelope bind with high specificity to a protein or proteins on the surface of the target cell, which act as the viral receptor. Receptor usage is determined by the structure of the SU protein, and thus SU is responsible for defining the range of host cells that are susceptible to infection. The SU protein of HIV (gp120) binds to the viral receptor CD4[21,22], as well as one of two co-receptors, either CXCR4[23] or CCR5[24,25]. As CD4 is predominantly expressed on a subset of T cells, as well as to a lesser extent on macrophages[26,27] and hematopoietic stem and progenitor cells (HSPCs)[28-32], these cells represent the primary targets of HIV infection. Upon receptor binding, the SU-TM trimers undergo a structural change that exposes the N-terminal fusion peptide of TM[19]. TM mediates fusion of the viral envelope with the target cell plasma membrane, and the viral core is released into the target cell cytoplasm.

Internalization and capsid core disassembly

The initial stages following membrane fusion and internalization of the capsid core are poorly understood. After internalization, it remains unclear precisely what must take place with the capsid core, made up of CA hexamers and pentamers, for productive infection[33]. Maturation of Gag precursors is essential for reverse transcription to proceed, and mutations that destabilize or hyperstabilize the capsid core severely hinder reverse transcription[34,35]. The capsid core may also play a role in shielding the cytoplasmic viral DNA from recognition by innate immune sensors[36,37]. Recent studies indicate that CA can be detected in the nucleus, suggesting that some amount of CA remains associated with

the viral genome throughout the reverse transcription process[38-41]. Furthermore, CA is the major determinant that allows HIV-1 and other lentiviruses to infect non-dividing cells[42,43], and many interactions between nuclear import machinery and domains of CA that are only present when it is assembled in the capsid core are essential for this to occur[44,45]. More recent evidence suggests that the fully assembled capsid core may be translocated into the nucleus, casting doubt on the importance of cytoplasmic disassembly altogether. A recent study indicates clearly that uncoating and reverse transcription occur in the nucleus after nuclear import[46], shifting the widely-accepted paradigm that reverse transcription occurs in the cytoplasm and casting further doubt on the temporal relationships between post-entry events, including nuclear translocation, capsid core disassembly, and reverse transcription.

Nuclear entry

Many host proteins are involved in the nuclear import of lentiviruses. NUP358 (also known as RANBP2) is located on the cytoplasmic side of the NPC[47] and interacts with HIV-1 CA to facilitate docking of the PIC at the NPC[48]. NUP153 is located on the nuclear side of the NPC[47] and interacts with residues on CA that are only present when CA is assembled in multimers as in the capsid core[40,44], and this interaction is important for HIV-1 integration[48,49]. TNPO3 also binds CA[50] and facilitates nuclear import of the PIC[51], and may be involved in removing CA from the PIC once it enters the nucleus[41,52]. CPSF6 binds CA[53] and is essential for proper trafficking of the PIC to the nucleus and nuclear import[54], as well as maintaining the characteristic integration site preferences of HIV[48,55,56].

Reverse transcription

Upon entry into the target cell, the virus must complete the reverse transcription of its RNA genome into a double-stranded DNA genome, allowing the virus to integrate into the host cell DNA and generate new viral progeny. Reverse transcription is a complex but remarkable process, proceeding through a series of essential steps, facilitated by the reverse transcriptase (RT) enzyme, that ultimately produce the reverse transcribed complementary DNA (cDNA) (see reviews for the details presented below[57,58]). Reverse transcription was previously believed to begin shortly after the viral core enters the cytoplasm, although recent findings indicate that reverse transcription occur in the nucleus[46]. The precise signals regulating the initiation of reverse transcription are unknown, but the reaction proceeds within the reverse transcription complex (RTC). The RTC is likely enclosed in a partially-assembled capsid core containing the gRNA dimer and 50-100 RT enzymes[59,60].
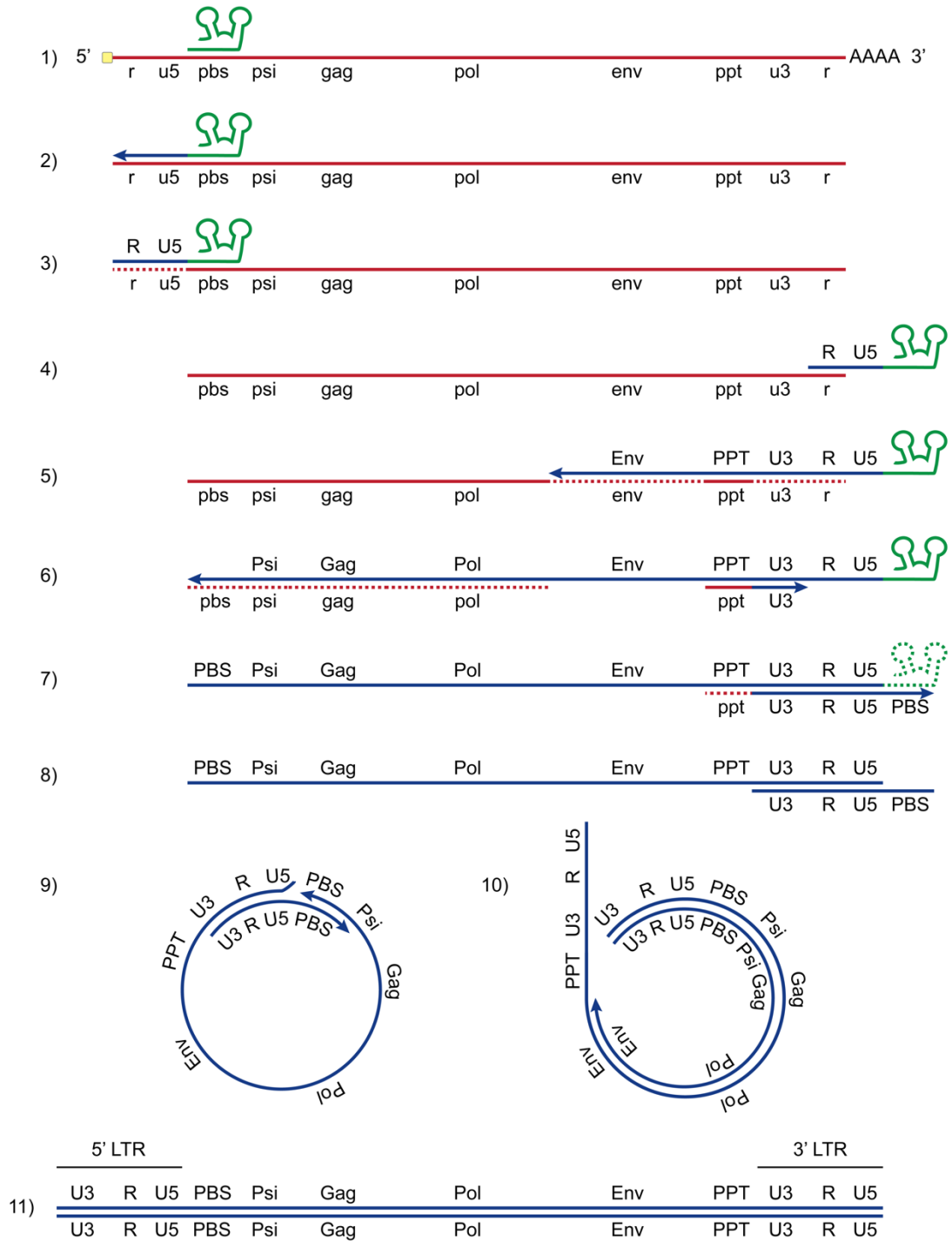
Fig. 1.4: Schematic of the process of reverse transcription. 1) gRNA with primer tRNA bound. 2) initiation of minus-strand synthesis. 3) formation of the 3' strong-stop DNA and degradation by RNase H. 4) first translocation. 5) minus-strand elongation and generation of the ppt primer. 6) completion of minus-strand synthesis and initiation of plus-strand synthesis. 7) completion of 5' strong-stop DNA and degradation of ppt and tRNA primer. 8) linear product prior to second translocation. 9) second translocation and formation of circular intermediate with simultaneous minus- and plus-strand synthesis. 10) completion of minus- and plus-strand synthesis. 11) finished cDNA product differing from gRNA with the presence of LTRs at both ends.

11

Initiation of minus-strand DNA synthesis

Reverse transcription begins when the 3'-terminal 18 nucleotides of the primer tRNA hybridize with complementarity to the 18-nucletoide pbs near the 5' end of the gRNA. Each virus uses a preferred tRNA molecule as the primer, which varies among the different retroviruses and for HIV is tRNA[Lys3]. The 3'-OH of the tRNA serves as the primer for the initial DNA synthesis, which proceeds toward the 5' end of the gRNA. This generates the U5 and R sequences of the minus-strand DNA, known as the minus-strand strong-stop DNA.

First translocation

The RNase H activity of RT degrades the region of the gRNA complementary to the newly synthesized DNA, which exposes the DNA as a single strand. The R sequence of the minus-strand DNA is translocated and anneals to the 3' r sequence of the gRNA, leaving a 5' overhang of U5 and the tRNA primer. This translocation is facilitated by NC[61], and can result in annealing to either of the two gRNAs packaged in the virion.

Long minus-strand DNA synthesis

Synthesis of the minus-strand DNA proceeds along the length of the gRNA, beginning with the strong-stop 3'-OH as the primer. Thus, the entire minus-strand DNA copy of the gRNA is generated. As the DNA polymerase activity of RT synthesizes the minus-strand DNA, the RNase H activity of RT degrades the gRNA from the RNA-DNA hybrid that is generated. This can be performed by the same RT enzyme that is

synthesizing the DNA, with degradation occurring 17-18 base pairs behind the elongating 3' end, or by a separate RT enzyme[62,63].

Initiation of plus-strand DNA synthesis

In order for synthesis of the DNA plus-strand to begin, a 3'-OH primer is required. The ppt, a purine-rich region of the genome located near the 3' end of the gRNA, is resistant to RNase H degradation and remains intact and bound to the fully-synthesized minus-strand DNA as an RNA-DNA hybrid. The ppt RNA oligonucleotide serves as the primer for initial plus-strand DNA synthesis, which proceeds through U3, R, and U5, continuing up to base 19 of the primer tRNA. The first 18 base pairs of the tRNA are copied, generating the PBS and the plus-strand strong-stop DNA product. The RNase H activity of RT degrades the ppt, which is susceptible to degradation after deoxynucleotides are added. In addition to the ppt near the 3' end of the gRNA, spumaviruses and lentiviruses encode a central polypurine tract that acts as a second primer for plus-strand DNA synthesis, allowing for more efficient production of the plus-strand DNA[64,65].

Removal of tRNA and second translocation

The RNase H activity of RT removes the tRNA, exposing the 3' end of the plus-strand DNA, which contains the PBS. The exposed PBS at the 3' end of each DNA strand anneals, generating a circular intermediate with both 3' ends ready for elongation. Each strand serves as the template for the other strand.

Completion of both strands

Elongation of the minus strand continues from the PBS through U5-R-U3, displacing the plus strand as it proceeds, creating a ssDNA template for synthesis of the plus-strand 3' LTR. Simultaneously, elongation of the plus strand proceeds along the minus strand from the PBS, through the viral genome, and through the PPT-U3-R-U5 region at the 5' end of the minus strand. Lentiviruses, which have also initiated plus-strand elongation from a central ppt, generate breaks in the plus-strand DNA with flaps of overlapping sequence[66]. These are eventually corrected by the host cell DNA repair machinery prior to integration.

Upon completion of reverse transcription, it is important to note that the cDNA genome is modified relative to the template gRNA. The overhangs from the two translocations result in the duplication of U5 and U3. The viral DNA now has 2 long terminal repeats (LTRs), one at each end of the genome, composed of U3-R-U5.

Biochemistry and structure of RT

The amino-terminal domain of RT has DNA polymerase activity[67], which is unique among DNA polymerases in its ability to use either RNA or DNA as the primer or the template (see review[68]). The DNA polymerase activity of RT is slow relative to host DNA polymerases, ranging from 1-100 nucleotide additions per second, with estimates for minus-strand synthesis around 70 nucleotides per minute[69]. It also possesses poor processivity, releasing frequently from the template, and is relatively low-fidelity, generating 10^{-4}-10^{-5} mutations per base[70,71]. This low fidelity is exacerbated by the fact that RT lacks any proofreading activity. RT also has a helicase activity that is capable of

displacing a DNA strand that is annealed to the template being used, which is essential during synthesis of the minus-strand 5' LTR[72]. The carboxy-terminal domain of RT possesses RNase H activity, which generates oligonucleotides with a 3'-OH, creating a suitable primer from the ppt to initiate plus-strand synthesis[67]. RNase H only degrades RNA in duplex form, either with DNA or RNA, and can act in concert with the DNA polymerase activity of RT[62,63]. Lentiviruses produce RT as a heterodimer, which for HIV-1 is composed of a p66 subunit with both DNA polymerase and RNase H, and a p51 subunit, which lacks the RNase H domain but is essential for proper positioning of the p66 subunit for RNase activity[73-75].

Recombination between the two co-packaged virion gRNAs happens frequently during reverse transcription and contributes to the generation of genetic diversity within the viral population[76-78]. In order for recombination between the two gRNAs to produce significant changes in the viral sequence, the producer cell must be co-infected with multiple viral genomes[77]. Usually the two gRNAs that are packaged are identical, limiting the effects of recombination events. Recombination is most common during template switching, and is thus a frequent event during minus-strand synthesis, when the template routinely switches back and forth between the two RNA strands[79,80]. This switching can occur when RNase H degrades the template and allows annealing to the other RNA strand, which may occur more frequently at sites with RNA secondary structures that slow RT DNA polymerase activity[81-83], or when nicks in the template strand force a switch to the other strand[84]. Template switching requires that the two gRNAs be similar enough for the 3' end of the growing DNA strand to anneal, and similar enough for the two gRNAs to successfully dimerize and be co-packaged into a single virion[85-87]. Recombination

between two gRNAs only occurs between the pairs of a packaged dimer, suggesting that each virion performs its own RT reaction, and the gRNAs packaged in other virions are not accessible for the duration of RT.

Integration

After reverse transcription has been completed, the RTC transitions to become the pre-integration complex (PIC), as the next important step of the viral life cycle is the integration of the double stranded genomic DNA into the host cell genome (reviewed in detail here[88,89]). Integration is the truly unique and defining feature of retroviruses, as it is not an essential step in the life cycle of any other family of viruses. Despite being present in the nucleus, unintegrated retroviral cDNA is a relatively poor substrate for transcription, and an integrated provirus is essential for persistent and efficient expression of retroviral genes[90,91]. Integration allows retroviruses to occasionally enter the germline and become transmitted vertically[92,93], and is also responsible for retroviral-mediated mutational and insertional oncogenesis[94,95]. Integration is mediated by the IN enzyme, which forms a dimer of dimers structure called the intasome via interactions in the N-terminal oligomerization domain[96,97]. The catalytic core domain contains three acidic residues that interact with two Mg^{2+} ions[98] and is highly conserved[99]. The integration reaction proceeds via two steps:

3'-end processing

To initiate the integration reaction, IN recognizes an 'A-T-T' sequence at each end of the viral cDNA and removes 2-3 nucleotides (2 for HIV-1) on the 3' strand at each blunt

end of the cDNA in a concerted manner, with both ends being trimmed simultaneously[100-102]. The cleavage occurs at a highly conserved 'C-A' sequence in the cDNA, releasing the dinucleotide and leaving C-A-OH 3'-hydroxyl ends. This generates short 5' overhangs at each end of the cDNA.

Strand Transfer

After 3' end processing, the target capture complex is formed. The free 3'-OH from the trimmed ends attack the target DNA in a concerted manner, with the two cDNA strands attacking the two strands of the host DNA simultaneously and only a few base pairs apart. This generates two nicks in the host DNA on opposite strands. The two nicks leave an equal number of unpaired complementary bases on either side of the integrated viral DNA, which were annealed to each other prior to the integration reaction. Host DNA polymerase fills in the empty bases on either side of the viral genome, generating a short duplication of the host integration site sequence. The length of the duplication is characteristic for each retrovirus and is 5 bp for HIV. 5' flap endonuclease removes the short 5' overhang generated on the viral DNA during 3' end processing, and DNA ligase seals the gaps to complete the integration of the retroviral provirus. Thus the integrated HIV-1 provirus contains a 2 bp deletion from the end of each LTR, as well as a 5 bp duplication of the host integration site sequence found immediately adjacent to each LTR[103].

Integration Sites

The integration site has the potential to dramatically affect host cell function by altering gene expression or disrupting functional genomic elements. Integration near oncogenes can cause increases in oncogene expression and drive tumor development[94,95]. Retroviral integration sites are not sequence-specific, and for the alpharetroviruses and betaretroviruses, the integration site is essentially random through the entire host genome[104-106]. However, despite the absence of a specific integration site sequence, other retroviruses demonstrate preferential integration into certain locations in the host cell genome. Lentiviruses, including HIV, preferentially integrate within expressed genes, intron-rich regions, and in chromatin located near the nuclear envelope, while avoiding chromatin in lamina associated domains[49,107-110].

Transcription

The integration of the virus into the host cell DNA, establishing a permanent provirus within the genome of the infected cell, marks the end of the early phase of retrovirus infection, shifting the focus to the production of new virus particles. The first step in virion production is the initiation of transcription from the promoter found within the 5' LTR, which is responsible for producing both the mRNAs needed to encode the viral structural proteins and the viral gRNA. Initiation of transcription at the 5' LTR is stochastic, although the U3 region contains a promoter, with both a TATA box and CCAAT box, as well as a range of enhancers[111]. U3 enhancer regions recruit several transcription factors, including NFκB[112], AP-1[113,114], NFAT[115,116], and SP-1[117,118], among others. Transcription of the provirus is performed by the host Pol II enzyme and initiates at the U3-R border.

Many complex retroviruses encode additional trans-activating proteins to enhance expression of the viral genes. HIV encodes Tat, which binds to the TAR element, a secondary structure near the 5' end of the nascent viral RNA[119]. Tat then recruits P-TEFb, increasing the processivity of Pol II, which tends to stall early in the transcription of the HIV genome, by phosphorylating the Pol II C-terminal domain[120,121].

Transcription proceeds through the 5' LTR and the coding region of the viral genes and concludes in the 3' LTR, where transcription stops at the R-U5 border. A 5' methyl cap is added, and the 3' end is polyadenylated. This generates the full-length viral RNA, which serves as both the packaged gRNA and as the mRNA template for translation of Gag and Gag-Pol polyproteins.

Splicing and nuclear export

Upon generation of the full-length viral RNA, simple retroviruses require the successful nuclear export of two RNA forms: a singly-spliced variant that is used to produce Env proteins, and the full-length RNA for production of Gag-Pol and packaging into nascent virions. Complex retroviruses like HIV include other alternatively-spliced or multiply-spliced subgenomic RNAs. The splicing of the singly-spliced variants uses host cell machinery and behaves similarly to any cellular mRNA (reviewed here[122]). Export of unspliced or incompletely spliced RNA, however, is inefficient, as host nuclear export factors are often recruited during splicing, and splicing factors that bind introns provide signals to prevent nuclear export[123]. Thus, most host RNAs are properly and completely spliced prior to nuclear export. Splicing of HIV is very complex, with at least four 5' splice donor sites and eight 3' splice acceptor sites[124]. The major splice donor site is used in

generating each of the spliced RNA products. Thus, there are many incompletely spliced subgenomic RNAs, as well as the unspliced gRNA, that must be exported. HIV encodes Rev to facilitate this process[125]. Rev exports incompletely-spliced HIV RNA products by binding to a specific element on the viral RNA, the Rev-response element (RRE), and then binding to the host CRM1 protein, which is responsible for the export of proteins containing a nuclear export signal (NES)[126,127].

Translation and protein processing

The Gag, Pol, and Env proteins are essential to the production of infectious virions for all retroviruses. Each of these proteins is translated as a precursor that is eventually cleaved and processed into the functional subunits that form a mature virus particle[128]. Producing precursors likely benefits retroviruses in many ways, including the ability to produce many functional proteins from a single ORF, guaranteeing that proteins are produced and packaged in the appropriate ratio, and targeting many proteins to the site of virion assembly simultaneously.

Gag

The Gag precursor is produced from the full-length RNA. Some retroviruses may employ an internal ribosomal entry site (IRES) near the *gag* start codon to prevent the need for translational initiation at the 5' cap, which requires an elongated scanning through the R-U5 region of the genome[129-134]. The major form of Gag is myristylated by myristyl CoA transferase, increasing the hydrophobicity of Gag and facilitating membrane association and packaging into the virion[135].

Pro-Pol

The viral protease is also produced from the full-length RNA and exists between the *gag* and *pol* genes. It can be fused to the 3' end of *gag*, the 5' end of *pol*, or neither, and is often produced along with Pol, which includes RT and IN, by translational readthrough[136] or frameshifting[133,137-139]. Lentiviruses require a single -1 frameshift to occur during the junction between *gag* and *pol*, as they exist in separate ORFs. This is facilitated by a slippery region near the *gag* stop codon, which includes homopolymeric bases such as poly-A or poly-U and a large hairpin, stem-loop, or pseudoknot structure[140,141]. The -1 frameshift results in an out of frame *gag* stop codon, and translation continues through the Pol ORF[139]. This occurs in 5-10% of translation events, resulting in Gag-Pol being 10-20-fold less abundant than Gag[142]. In lentiviruses, *pro* is in the *pol* ORF and is produced equimolar to Pol.

Env

All retroviruses produce the Env precursor from a singly-spliced subgenomic RNA, with a 5' leader sequence joined directly to the *env* coding region after *gag-pol* is removed as an intron. Env is synthesized as a single-pass transmembrane protein in the ER, where it is folded, glycosylated, and oligomerizes to form Env trimers[143]. Unlike the other retroviral precursor proteins, the Env precursor is not processed by the viral protease, but rather by host furin proteases in the Golgi, which separate the SU and TM subunits[144,145]. SU is wholly extracellular and remains associated with the virion via interactions with TM. It is heavily glycosylated[146-149], protecting the virion from neutralizing antibodies by

shielding antibody epitopes[150-153], and contains hypervariable regions that determine receptor binding[154,155]. TM has extracellular, transmembrane, and cytoplasmic domains, with the extracellular N-terminus containing the fusion peptide, which is essential for membrane fusion during entry into the target cell[156]. TM also contains the major contacts for oligomerization[157], and trimers of SU-TM heterodimers are transported to the cell surface for assembly.

Assembly and packaging

Assembly of retroviral virions is predominantly mediated by Gag precursors, as these are sufficient for production of virus-like particles in the absence of any other viral factors (see reviews[9,158]). The C-type viruses assemble at the plasma membrane, with Gag targeted there by hydrophobic residues, basic residues, and myristic acid[159-161]. For HIV, the MA domain of Gag, which has a myristic acid added to the N-terminal glycine, embeds in the plasma membrane and forms stable anchors only upon binding to $PI(4,5)P_2$, which is specifically localized to the plasma membrane[162,163]. This prevents improper virion assembly at internal membranes. The MA domain of Gag also localizes HIV to budding lipid rafts[164] and incorporates the glycosphingolipid GM3 into the envelope[165], which is later recognized by CD169/Siglec-1 on dendritic cells (DCs) to enhance trans-infection of $CD4^+$ T cells[166-169]. The Gag proteins aggregate, causing curvature in the plasma membrane and initiation of budding[161,170].

The SU and TM trimers of heterodimers are incorporated via contacts between the cytoplasmic tail of TM and the N-terminus of Gag[171-175], although there are likely additional mechanisms involved[176]. HIV incorporates Vpr into virions at a high level, roughly

equimolar with Gag. The recruitment of Vpr into virions requires the Gag p6 domain, although the function of Vpr remains unclear[177-179]. Host proteins are also incorporated into virions[180], including Cyclophilin A[181], which has many different effects on Gag stabilization and disassembly and can promote or reduce retroviral infectivity depending on the experimental context, but is generally considered an essential host cofactor of HIV[182-184].

The proper packaging of the gRNA represents a challenge for retroviral assembly, as the gRNA comprises only a small fraction of the total cytoplasmic RNA in the host cell, and many viral subgenomic RNAs are also present and must be excluded from the assembling virion[185]. The gRNA is packaged as a dimer, which is usually a homodimer of two identical gRNAs, except in rare cases where co-infection or expression of an endogenous retrovirus causes packaging of an RNA heterodimer[186]. Packaging is mediated by the Psi (Ψ) sequence in the 5' UTR[187], which interacts specifically with the NC subunit of the Gag precursor[188,189]. In the absence of a Psi signal, virions package a random sampling of host mRNAs, and non-gRNAs can be packaged if they are engineered to contain a Psi sequence[10]. HIV-1 splices the Psi sequence out of the subgenomic RNAs to prevent packaging interference with the gRNA. Psi functions via cis-acting structural elements of the RNA, including stem loop structures containing purine-rich loops. For HIV-1, stem-loops 1 and 3 (SL1 and SL3) are especially important for packaging[190,191].

Dimerization of the genome

Dimerization of the two packaged gRNAs is mediated by interactions in a complementary sequence near the 5' end of the genome called the dimerization initiation site (DIS)[192,193]. For HIV, the DIS is in SL1[194]. The DIS and *gag* start codon are both near the 5' end of the viral RNA and determine whether the RNA dimerizes for packaging as a gRNA or is translated to produce Gag or Gag-Pol proteins[195-198]. When the DIS of two gRNAs bind, they form the dimer linkage structure (DLS). The NC subunit of the Gag precursor protein binds the DLS with high specificity, initiating Gag multimerization and assembly[11]. These interactions are more specific than the generic affinity of NC for RNA[199], ensuring that dimerized gRNAs are packaged[200]. Other domains of the Gag precursor may be involved in this interaction as well[201,202]. The dimerized gRNAs are non-covalently associated and do not form significant base-pairing interactions[203], and dimerization is stabilized during virion maturation after release from the producer cell[204,205]. HIV-1 dimerization initiates in the cytoplasm.

Dimerization has several purported benefits for retroviral replication. Nicks in the gRNA are common, and proper completion of reverse transcription would be impossible from a single nicked genome. Co-packaging a second copy can greatly increase the fidelity of reverse transcription by increasing the likelihood that an intact template exists for each region of the genome. Dimerization also distinguishes the gRNA from spliced mRNA, as only dimerized gRNA has the DLS as a signal for Gag recruitment and assembly. Furthermore, recombination can drive evolution, as there are approximately 3-15 strand transfers per replication cycle[206-208]. Retroviruses have higher rates of recombination than other RNA viruses, which may contribute to the adaptability of the virus[77,209].

Budding and maturation

Gag precursors assemble at the plasma membrane, inducing membrane curvature and initiating the budding process[210]. The p6 domain of the HIV-1 Gag precursor recruits the endosomal sorting complexes required for transport (ESCRT) machinery by binding to TSG101 and ALIX[211,212], and the NC domain of Gag may be involved in ESCRT recruitment as well[213]. ESCRT machinery is responsible for release of the immature virion[214-216].

Upon virion release, the viral PR enzyme cleaves itself out of its precursor form[217]. PR acts as a homodimer[218] and subsequently cleaves the remaining Gag and Gag-Pol precursors in hydrophobic regions[219,220], triggering a number of events that generate the mature, infectious virion[221,222]. Prior to PR processing of the precursors, retroviral virions are immature and non-infectious[221,223-225]. Thus, mutations to or inhibition of PR can prevent retroviral infection.

Processing of Gag precursor

The MA protein remains bound to the inner face of the membrane via the N-terminal myristyl group[160,161]. It interacts with TM for proper incorporation of Env trimers into the virion[171-175], and is referred to as p17 in HIV-1. The CA protein contains the major homology region and is conserved among all retroviruses[226]. Upon cleavage, CA undergoes a dramatic rearrangement that is visible by electron microscopy, forming the condensed inner capsid core[227]. The shape of the capsid core depends on the individual virus, but it is made up of CA-CA interactions that form primarily hexamers and some

pentamers[17]. For HIV-1, the CA protein is called p24. The NC protein is small, highly basic, and contains two highly conserved zinc-finger domains that coordinate a zinc ion, with a few exceptions in the retrovirus family[228,229]. After release from the Gag precursor, the basic NC coats the entire gRNA[230], with each NC protein bound to 5-8 nucleotides[231-236]. NC acts as an RNA chaperone, and this binding is essential for reverse transcription[237]. NC enables RT to proceed through regions with significant secondary structures, and also facilitates the various strand transfers that take place. NC processing results in pbs remodeling, exposing the 18 nucleotides with perfect complementarity to the 3' end of the primer tRNA and allowing binding of the primer tRNAs to the pbs of each gRNA[233,238-240]. This sets the stage for reverse transcription upon infection of a new target cell. For HIV-1, NC is referred to as p7.

The Gag-Pol precursor is processed by PR into RT, IN, and the same mature subunits of Gag.

Innate Immune Response to Retroviral Infection

As retroviruses have been circulating in vertebrates throughout evolutionary history, the host species have evolved a number of innate mechanisms to defend against retroviral infections. Likewise, retroviruses have evolved to counteract these defense mechanisms, which is the role of many of the accessory proteins encoded by the complex retroviruses. This evolutionary race determines the tropism of the retroviruses, as each species is able to prevent infection by all but a few specific viruses that have evolved to overcome these restrictions in a species-specific manner (see reviews[241-243]).

The APOBEC3 family of host proteins are packaged into retroviral virions in a NC- and RNA-dependent manner[244,245] and restrict multiple retroviruses, including HIV, by inducing hypermutation[246-249]. Although APOBEC3G is the most widely studied, other APOBEC3 family members, including 3B, 3D, 3F, and 3H are also active against HIV. APOBEC3G is a cytidine deaminase that deaminates cytidine nucleotides, generating uracil in the minus-strand ssDNA after RNA degradation but before plus-strand synthesis, resulting in a G-A mutation in the plus-strand DNA[250-252]. It is expressed at high levels in human CD4^{+} T cells and macrophages, the primary targets of HIV infection[253]. This may explain the presence of the central ppt of HIV-1, which hastens positive-strand synthesis and reduces the exposure of the minus-strand DNA to APOBEC3[254]. Vif, an accessory protein encoded by almost all lentiviruses[247], counteracts APOBEC3 proteins by inducing their polyubiquitination and proteasomal degradation[255,256], preventing their packaging in budding virions[246,257].

During cytoplasmic reverse transcription, retroviruses can generate RNA-DNA, ssDNA, and dsDNA in the cytoplasm of the host cell, none of which are present in the cytoplasm during normal host cell processes. As with other viruses, many sensors of retroviral nucleic acids have been described, including cGAS and IFI16. Cytosolic DNA is detected by cGAS, which interacts with STING to signal the production of interferon-β (IFN-β) via IRF3[258]. HIV evades cGAS, however, by recruiting the host TREX1 protein to degrade viral DNA products that are susceptible to sensing by cGAS[259,260]. IFI16 also senses cytoplasmic DNA, acting via STING to induce IFN-β [261]. For HIV-1, this pathway may contribute to loss of CD4 cells and progression to AIDS, as pyroptotic CD4^{+} cell death following abortive HIV-1 infection requires IFI16[262,263].

SAMHD1 is a host protein that restricts HIV-1 in some cell types, such as DCs, macrophages, and resting CD4^{+} T cells, by depleting the cellular pool of dNTPs needed for cDNA synthesis[264-267]. HIV-2 and SIV overcome this restriction by encoding the accessory protein Vpx, which recruits the E3 ubiquitin ligase DCAF1-DDB1 to induce degradation of SAMHD1[266,267]. Vpx is absent in HIV-1, allowing SAMHD1 to reduce HIV-1 infection of SAMHD1-expressing cells, including DCs[268], resting CD4^{+} T cells[269] and, to a lesser extent, macrophages[265].

SERINC3 and SERINC5 were recently discovered as membrane-bound restriction factors of HIV-1, which are incorporated into the virion to reduce particle infectivity[270,271]. HIV-1 counteracts this restriction with the accessory protein Nef, which redirects SERINC3 and SERINC5 away from the cell surface via the endolysosomal system to prevent their incorporation into virions[270-272]. Nef also facilitates HIV-1 infection in a number of other ways, including redirecting MHC-I to the lysosome for degradation to prevent antigen presentation to CD8^{+} T cells[273-277] and internalizing CD4 from the cell surface to prevent superinfection and Env interactions with CD4 during virion budding, which are described in more detail below[278].

The TRIM5α protein, which was previously called Ref1 and Lv1, binds to the retroviral capsid core and accelerates uncoating in a proteasome-dependent manner, inhibiting reverse transcription and formation of a functional PIC[279-283]. Trim5α proteins vary from species to species, and the species-specificity of primate lentiviruses is largely determined by their ability to evade restriction by TRIM5α in their native host species, but not in other primates[279-282,284].

Tetherin, also known as BST2, tethers budding retroviral virions to the cell surface, preventing virion release and leading to internalization and degradation[285,286]. HIV-1 overcomes the tetherin restriction with the accessory protein Vpu, which prevents tetherin from reaching the cell surface and leads to its degradation[285-288]. HIV-2 and SIV do not encode Vpu, but SIV Nef facilitates the AP-2-dependent internalization of tetherin at the cell surface[289,290], while the HIV-2 Env protein is sufficient for HIV-2 to overcome tetherin restriction[291,292].

Other restriction factors that have recently been described for HIV-1 include MxB/Mx2, which is IFN-inducible and binds CA to inhibit nuclear import or uncoating[293-296], and IFITM1, which is a plasma membrane protein preventing fusion and entry[297]. The precise mechanisms of action for these recently discovered restriction factors are still being elucidated. ZAP was recently discovered as restriction factor that detects CG dinucleotides in cytoplasmic RNA. Given that vertebrate genomes demonstrate marked CG suppression, this enables antiviral defense by distinguishing CG-rich viral genomes from CG-poor host mRNA. HIV evades ZAP by mimicking the CG suppression of the human genome[298].

Acquired Immunodeficiency Syndrome (AIDS)

By far the most significant retroviral disease burden in humans is the acquired immunodeficiency syndrome (AIDS), which is caused by untreated infection with either HIV-1 or HIV-2. AIDS was first recognized in the United States in 1981[299], a series of investigators from 1983-1984 identified that retroviruses may be the cause of AIDS[300-303],

and by 1986 these retroviruses were identified as HIV[304], which was subsequently named HIV-1 upon the discovery of HIV-2. HIV-2 has only 45% sequence homology to HIV-1. HIV-2 differs from HIV-1 in that it encodes Vpx, which counteracts SAMHD1[266,267,305]. In addition, HIV-2 lacks Vpu, which downregulates tetherin and CD4, although HIV-2 has evolved to use other viral proteins to mediate these effects, and is less pathogenic than HIV-1[306]. HIV-1 is separated into 4 groups: M, N, O, and P, of which M is responsible for the majority of infections worldwide[307]. Group M is separated into 9 subtypes, of which subtype B is most common in Europe and North and South America, while subtype C is by far the most prevalent subtype worldwide. HIV-2 is divided into 8 groups, named A-H[308]. Most clinical HIV research is done on HIV-1, group M, subtype B viruses.

HIV is transmitted primarily through sexual contact or exposure to blood, such as during blood transfusions or intravenous drug use[309,310]. It can also be transmitted perinatally between mother and child during pregnancy, labor, or breastfeeding[311]. During acute infection, some individuals can experience flu-like symptoms[312,313]. After an initial peak in plasma viremia is established within a few weeks of exposure, immune responses primarily dependent on HIV-specific CD8$^+$ T cells begin to control the virus, suppressing the plasma viral load to the viral set point, but failing to completely prevent viral replication or clear the infection[314-317]. The viral load averages roughly 10^4-10^5 particles per mL of plasma, with approximately 10^{10} new virions produced each day and infected cells having a half-life of about 2 days[318-320].

The virus requires its receptor, CD4[22,321,322], plus a co-receptor, either CCR5[323-327] or CXCR4[23], to enter cells. Thus, the virus replicates primarily in CD4$^+$ T cells, which express high levels of CD4. HIV-1 can also infect cells with lower levels of CD4, including

macrophages, as infected macrophages have been found in the brain[328], lymph nodes[26], and urethra[329], and hematopoietic stem and progenitor cells in the bone marrow[28-32,330]. Infection of CD4^{+} T cells leads to cell death[263], and persistent viremia leads to a steadily decreasing CD4^{+} cell count during the course of infection[326,327]. This depletion occurs gradually during a prolonged asymptomatic phase of infection, which can last for several years[331]. AIDS is associated with a suite of rare opportunistic infections and tumors that are typically suppressed by normal immune responses, and these opportunistic infections and tumors are responsible for most AIDS-related deaths.

In addition to infecting and depleting CD4-expressing cells, HIV infection can affect other cell types as well. CD8^{+} T cells and B cells can both be killed by bystander activation[332]. While dendritic cells (DCs) aren't productively infected by HIV-1, as they express high levels of SAMHD1 to restrict the infection, they are susceptible to infection by HIV-2 and SIV, which encode Vpx to counteract SAMHD1[266,267]. In the context of HIV-1, DCs can still contribute to infection through trans-infection of T cells, in which DCs capture viral particles, maintain their infectivity, and transfer them to T cells at the virological synapse. Initial studies implicated DC-SIGN and similar receptors as essential for trans-infection via DCs[333], although recent studies have shown that GM3 incorporated in the HIV-1 envelope is recognized by CD169/Siglec-1 to facilitate trans-infection[166-169,334]. DCs can also produce interferon during acute infection, and are especially sensitive to HIV-2, where DC infection proceeds sufficiently for cGAS recognition of viral DNA[36,335].

Throughout the world, and even within a single individual, HIV demonstrates tremendous genetic diversity[336]. This genetic diversity allows the virus to rapidly evolve

to evade host adaptive immune responses, as well as antiretroviral monotherapies. The RT enzyme has a particularly low fidelity among DNA polymerases, which is likely the major contributor to HIV mutagenesis[71]. HIV is especially variable in the exposed regions of the envelope protein[337,338]. This variability likely benefits the virus in evading the host humoral response, which is directed predominantly against exposed residues of gp120 (SU) and gp41 (TM)[151].

Adaptive Immunity to HIV

Humoral immunity

Humoral immunity to HIV-1 and SIV is observed, with both neutralizing and non-neutralizing antibodies generated against the virus within the first 2 weeks of infection, although these fail to suppress viral replication[339,340]. Neutralizing antibodies predominantly target the HIV-1 Env receptor binding domains: the V1, V2, and V3 loops and the CD4-binding domain of the HIV-1 gp120 (SU) and interfere with the ability of the virus to interact with the receptor and prevent entry into the target cell[341]. As V1, V2, and V3 are hypervariable regions of gp120, the virus rapidly evolves to avoid these neutralizing antibody responses, which fail to control spread and suppress viral loads. HIV may also evade the humoral response through the activity of Nef, which can be secreted by infected CD4$^+$ T cells and taken up by B cells, where it can inhibit class-switching to more functional IgA and IgG isotypes[342]. Neutralizing antibodies isolated from an infected individual often successfully neutralize previous isolates of virus from that individual, but fail to neutralize the virus that is currently circulating[151,340,343,344]. Non-

neutralizing antibodies can mediate antibody-dependent cell cytotoxicity (ADCC) and facilitate killing of infected cells by NK cells and macrophages, although the significance of this mechanism in controlling viral replication is poorly understood[345].

Some neutralizing antibodies that have undergone extensive somatic hypermutation following years of exposure to high viral loads have developed the capacity to neutralize a broad range of HIV isolates and are known as broadly neutralizing antibodies (bNAbs)[346-349]. Passive transfer of broadly neutralizing antibodies can offer protection from infection in a SHIV model[350] and can suppress viral load[351,352] or delay rebound upon therapy interruption[353] in humans. However, after initial suppression of viremia, resistance mutations that evade neutralization are rapidly detected in many individuals, indicating that bNAbs do not entirely suppress viral replication[351-353]. While the existence of broadly neutralizing antibodies offers some promise for HIV-1 vaccine development, as broad neutralization may be effective to prevent transmission prior to robust infection and selection for escape variants, various vaccination strategies have failed to elicit these responses due to their rarity and high degree of somatic hypermutation[354]. This is an area of intense ongoing research, and one bNAb with minimal somatic hypermutation was isolated from an infant, offering some promise that similar responses could be elicited by vaccination[355].

Cytotoxic T lymphocytes (CTLs; CD8+ T cells)

CD8+ T cells, commonly referred to as cytotoxic T lymphocytes (CTLs) for their cytolytic activity, represent the primary antiviral effectors of cellular adaptive immunity, and massive HIV-specific CTL responses are observed shortly after the initial detection

33

of HIV RNA in the plasma[317,356,357]. While these responses shape the viral landscape[358], correlate with the viral set point[317], and motivate viral evolution[359,360], they are unable to successfully control the infection in most individuals, and fail to clear the virus entirely[317,357]. These CTLs eventually become exhausted, losing their ability to control the evolution and spread of the virus[361,362]. Exhaustion is likely in part mediated by the upregulation of inhibitory receptor ligands PD-L1 and PD-L2 on the surface of HIV-infected cells and the secretion of IL-10[363,364]. Upregulation of PD-L1 can also directly protect HIV-infected cells from CTL killing[365]. HIV-1 and HIV-2 also encode the accessory protein Nef, which redirects newly-synthesized MHC-I away from the surface of infected cells to prevent presentation of viral peptides and recognition by HIV-specific CTLs[366].

CTLs recognize virally-infected cells by responding to peptide antigens presented in the context of major histocompatibility complex class-I (MHC-I) on the surface of infected cells[367]. Each CTL expresses a unique T cell receptor (TCR), positively- and negatively-selected in the thymus for moderate affinity for self MHC-I but low affinity for MHC-I presenting self-peptides, respectively[368]. High-affinity interactions between the TCR and cognate peptide antigens presented by MHC-I on the surface of a target cell lead to the formation of the immune synapse and the subsequent killing of the target cell[369]. Killing is mediated by the release of lytic granules containing perforin and granzyme, which induce apoptosis in the target cell[370-374].

MHC-I is both polygenic, with genes encoding HLA-A, -B, -C, -E, -F, and -G, and polymorphic, with remarkable allelic variation particularly in HLA-A, -B, and -C[375]. Polygeny allows for functional separation of MHC-I genes. HLA-A and -B, and to a lesser extent -C, are responsible for presenting peptides to CTLs. HLA-A and HLA-B are

expressed at 5-20-fold higher levels than HLA-C on B cells and peripheral blood leukocytes[376], and this likely contributes to the fact that most CTLs are restricted to HLA-A or HLA-B[377]. HLA-C also presents a narrower range of peptide antigens[378], although when HLA-C-restricted CTL responses do arise, they have similar functionality to those restricted to HLA-A or -B[379-381]. Allelic variation in the MHC-I loci responsible for antigen presentation contributes to population-level protection from diverse pathogens through the presence of alleles that are optimized for presentation of a wide spectrum of peptides[382]. Beyond presenting peptide antigens to CTLs, the MHC-I proteins HLA-C[383], -E[384], and -G[385] interact with inhibitory receptors on natural killer (NK) cells, which recognize cells with a combination of low MHC-I, a signal of viruses or tumors evading CTL responses[386], and elevated natural killer cell activating ligands[387].

A small subset of individuals, known as elite controllers (ECs) or long-term non-progressors (LTNPs), naturally suppress HIV-1 viral load and prevent progression to AIDS, and this control is due to their unusually effective CTL responses[388-391]. Many studies have attempted to describe the factors that promote elite control of HIV. In genome-wide association studies, the most common correlates with HIV control or unusually rapid progression to AIDS are alleles of HLA-B. While these alleles are enriched in EC cohorts, many individuals possessing these protective alleles do not successfully suppress viral replication, and many ECs do not possess a protective allele[392-394]. A recent study demonstrated that ECs possess CTL responses, particularly immunodominant responses, directed against peptide epitopes in the HIV genome that are highly networked. Highly networked amino acid residues are predicted to be critical to maintaining the structure of the folded protein and are thus mutationally constrained.

Protective alleles preferentially present highly networked peptides, and risk alleles tend to present less networked peptides. Regardless of HLA allele, the presence of CTL responses within an individual that were directed against highly networked peptides was predictive of elite control of HIV[391]. CTLs from LTNPs also do not upregulate PD-1 or display exhaustion phenotypes, as CTLs from progressors do[361,395]. Yet, despite spontaneous control of the virus, elite controllers are not cured and the virus persists throughout life, except in one recently-described possible exception[396].

Most of the disease burden of HIV resides in lymphoid tissues, but most studies of HIV-specific CD8$^+$ T cells responses survey circulating lymphocytes in the blood. Tissue resident memory T cells (T_{RM}) express the surface markers CD69 and CD103, reside in the tissues, rarely enter circulation, and are the primary effectors of memory responses in tissues[397,398]. Human lymphoid tissue T_{RM} cells were recently described, and elite controllers had increased HIV-specific T_{RM}s in the lymph node[399]. Elite controller CD8$^+$ T_{RM} cells in the lymph node also have a distinct transcriptional profile, with reduced expression of inhibitory markers and cytolytic molecules, and increased expression of cytokines compared to chronic progressors, suggesting that control may not be associated with cytolytic activities of CD8$^+$ T cells. However, it is not clear if this is a result of the reduced viral load in controllers as compared to progressors, which could reduce apparent cytolytic activities as a result of having fewer infected targets to respond to *in vivo*[400]. Regulatory T cells (T_{reg}) can suppress antigen-specific effector T cell functions and have increased prevalence in some HIV-infected patients[401]. Increased T_{reg} frequencies in lymphoid tissues correlates with disease progression[402], and elite controllers may have fewer T_{reg} or express HLA alleles that are less susceptible to T_{reg}-

mediated suppression[401,403]. Thus, inducing the suppressive effects of T_{regs} may be an important mechanism of immune evasion for HIV.

Pursuit of an HIV Cure

Antiretroviral therapy (ART)

The HIV/AIDS pandemic has been radically transformed by the development of effective combination antiretroviral therapy (ART, see reviews[404,405]). While HIV rapidly evolves to evade antiretroviral monotherapy[406], combination therapy is effective in suppressing viral load and dramatically prolonging survival, allowing infected individuals to live relatively healthy lives with an infection that until recently meant almost certain death[407-409]. As of 2019, 67% of people living with HIV are accessing ART, which is estimated to have prevented 12 million AIDS-related deaths in the last decade[1]. Different classes of antiretroviral drugs target various stages of the viral life cycle, from entry to proteolytic maturation.

Entry inhibitors interfere with the interactions between HIV Env (gp120) and the coreceptor CCR5 by binding directly to CCR5, preventing associations with either natural ligands or gp120[410,411]. Fusion inhibitors are alpha-helical peptides that block the fusion step of viral entry by mimicking a critical domain of gp41, which must form a homodimer to mediate entry[412]. Nucleoside analogs (NRTIs) function as reverse transcriptase inhibitors through their capacity to be incorporated by RT during DNA synthesis. Since these nucleoside analogs lack the 3'-OH, DNA synthesis cannot proceed upon NRTI incorporation[413,414]. Resistance to NRTIs occurs when mutations are accumulated that

either confer the ability to excise the NRTI from the nascent strand[415-417] or increase the efficiency of incorporation of the natural substrates relative to the nucleoside analog[418,419]. While the NRTIs inhibit reverse transcription by mimicking the natural substrates of RT, non-nucleoside reverse transcriptase inhibitors (NNRTIs) function as small, hydrophobic molecules that inhibit RT by an allosteric mechanism[75,420,421]. NNRTIs are only effective against RT from subtypes B and C of HIV-1, as most retroviral RT enzymes, including those of HIV-1 group O, HIV-2, and SIV, lack the NNRTI binding pocket and are naturally resistant[422-424]. Even in HIV-1 subtypes B and C, resistance mutations to NNRTIs develop easily[425,426]. Integrase strand transfer inhibitors (INSTIs) target HIV integrase, preventing successful integration of the viral DNA genome and promoting the formation of non-productive intermediates, such as 2-LTR circles[427]. INSTIs are broadly active against HIV-1 subtypes and HIV-2[428,429]. Protease inhibitors mimic the transition state for normal HIV protease substrates and block the enzyme active site[430]. These inhibitors, however, carry particularly burdensome side effects, and thus are not utilized in first-line ART in most cases. New classes of antiretroviral drugs are in development, including inhibitors of CA such as GS-CA1[431] and the derivative GS-6207, which act by hyperstabilizing the capsid core to prevent disassembly[432].

HIV Latency

Despite the success of ART, it does not represent a cure, and infected individuals must remain on ART for the remainder of their lives. Although viral loads are suppressed below clinically detectable levels, viral rebound occurs within a few weeks of cessation of ART. Thus, despite the capacity of ART to virtually eliminate the pool of replicating virus

in an individual, latent reservoirs of the virus exist in which an integrated provirus remains transcriptionally silent, evading detection by host immune responses[433,434]. These latent reservoirs are established early during the course of infection and are continuously re-seeded with circulating virus until the time of therapy initiation[435]. Studies characterizing the half-life of the latent reservoir indicate that the virus will persist for the duration of life[436], representing a major barrier to curing HIV-infected individuals[437,438]. SIV RNA and DNA is detected in a broad range of tissues distal from the initial site of infection within a few days of first exposure[439]. Latent HIV DNA capable of generating rebound viremia is present even following early initiation of ART during acute infection[437]. Initiation of treatment during hyperacute infection may be beneficial in individuals where infection is detected early, as it could contribute to a reduced latent reservoir[440,441], delayed rebound upon treatment interruption[442,443], and enhanced functionality of anti-HIV T cell responses[444], although humoral responses may be blunted if viral replication is blocked before they are generated[445].

The majority of HIV DNA in optimally-treated individuals is defective and unlikely to replicate as a result of major deletions or hypermutation, and these defective proviruses accumulate during ART[446,447]. Nevertheless, replication-competent proviruses do persist, and the presence of full-length HIV genomes that are resistant to induction represent major barriers to the goal of eliminating replication-competent HIV from the body[448].
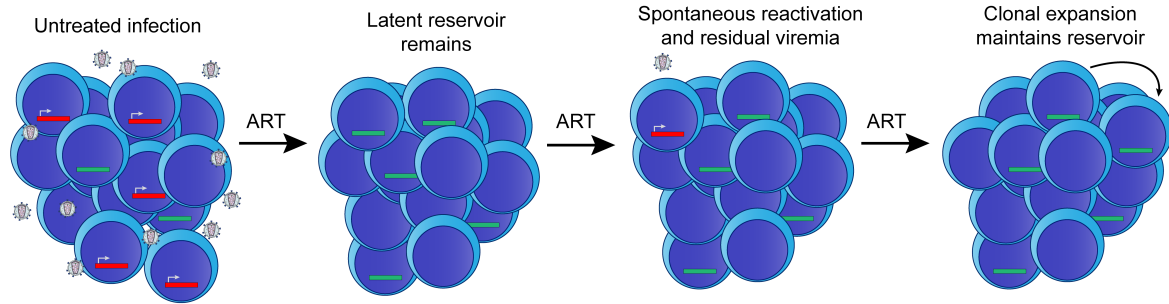
Fig. 1.5: Dynamics of the latent reservoir of HIV during antiretroviral therapy (ART). ART blocks HIV replication and prevents the infection of new cells, but latent proviruses can reactivate spontaneously to contribute to residual viremia. Cells harboring latent provirus can maintain the reservoir through proliferation and clonal expansion of the virus. *Red* represents a transcriptionally active provirus; *green* represents a transcriptionally silent latent provirus.

Cellular reservoirs of latent HIV

CD4^{+} T cells are the primary cellular target of HIV, and they likewise represent the most abundant cellular reservoir of latent HIV proviruses[433,449]. Latency is not equally prevalent in all subsets of CD4^{+} T cells and is particularly enriched in quiescent resting memory T cells, especially central memory T cells (T_{CM})[450]. T_{CM} can also proliferate to clonally expand the HIV reservoir without reactivating latent HIV[451]. In general, quiescence has been shown to correlate with HIV latency, although quiescence is a term that is loosely defined[452-454], and less-quiescent T effector memory cells (T_{EM}) may be enriched for replication-competent HIV[455].

Notably, an assessment of whole-body HIV burden in an SIV model suggests that the T cells harboring HIV may primarily be located in lymphoid and other tissues rather than circulating in the blood[456]. CD4^{+} T_{RM} cells in the cervical mucosa represent the major reservoir of latent HIV in cervical tissue[457], and latent reservoirs are detectable in tissues throughout the body, including gut-associated lymphoid tissue (GALT)[458,459], central nervous system (CNS)[460], genital tract[461], and especially lymph nodes[462]. The lymph

nodes are a particularly critical reservoir of latent HIV, as many CD4^{+} T cells reside in lymph nodes, and the B cell follicle is a privileged immune site where T follicular helper cells (T_{FH}) infected with HIV may be protected from CD8^{+} T cells[463-465]. T_{FH} may also contribute disproportionately to residual viremia during ART and are enriched for replication-competent provirus, which may result from their anatomical segregation from anti-HIV CTLs that gradually eliminate accessible cells harboring full-length provirus[466,467].

Although CD4^{+} T cells are the primary target of HIV-1 infection and the main cellular reservoir of latent HIV during ART, HIV can infect other cell types that express CD4 and CXCR4 or CCR5. Latent proviruses can be found in circulating and tissue-resident macrophages[26,27,468,469] as well as hematopoietic stem and progenitor cells (HSPCs)[29-32]. Importantly, several studies have failed to attribute residual viremia in treated patients exclusively to T cell reservoirs, suggesting these alternative cellular reservoirs may be critical to HIV persistence and rebound viremia upon ART interruption[470,471]. One study indicated that the GALT is not the major source of rebound viremia upon ART interruption[472], and a recent work demonstrated that proviruses isolated from HSPCs are a key source of residual viremia during ART[330].

HSPCs reside in the bone marrow and are responsible for generating the hematopoietic cell compartment throughout the life of an individual. The most stem-like HSPCs, hematopoietic stem cells (HSCs), exist in a quiescent state and are long-lived and capable of self-renewal[473,474]. HSCs undergo asymmetric cell division, yielding daughter cells that are more lineage-committed progenitors, which in turn continue to differentiate and give rise to the entire repertoire of mature hematopoietic cells[475]. While

several publications had described HIV-1 infection of HSPCs, both *in vitro* and from patient bone marrow[29-32], other studies had failed to detect HIV-1 provirus in HSPCs from ART-treated individuals[476,477]. Two recent publications seem to have definitively established that HSPCs can be productively infected with HIV *in vivo*. Sebastian et al. shed light on the discrepancy, demonstrating that prior negative studies lacked the necessary statistical power to reliably detect HIV DNA from HSPCs, which have significantly lower abundance of HIV DNA than T cells. Through rigorous statistical analyses accounting for $CD3^+$ T cell contamination, Sebastian et al. observed the *in vivo* expansion of HSPC-derived defective HIV proviruses in differentiated hematopoietic progeny cells. Due to the defective nature of the clonal genomes, this observation could not have been attributed to coincident infection with identical virus, pointing to the existence of an infected parental progenitor cell as the source of these cells[28]. Further evidence supporting this conclusion was provided by Zaikos et al., who demonstrated that proviruses found in HSPCs are clonally expanded, harbor replication-competent provirus, and contribute to residual plasma viremia in optimally treated individuals. Thus, there is substantial evidence supporting the conclusion that HSPCs form a critical reservoir of HIV *in vivo* and must be accounted for in cure efforts focused on eliminating the replication-competent HIV responsible for rebound viremia after ART interruption.

Shock and Kill

The major barrier to an HIV cure is the persistence of transcriptionally silent , replication-competent HIV DNA that can reactivate to cause rebound viremia upon ART

interruption, even after decades of ART. Thus, the current approaches to developing a cure for HIV involve reactivating the latent reservoirs of replication-competent HIV in a so-called "shock and kill" approach[478]. First, the previously latent proviruses are "shocked" with a therapeutic agent that induces HIV gene expression from proviruses that were previously transcriptionally silent. With the induction of HIV gene expression, the cells harboring reactivated provirus begin to produce HIV proteins and epitopes, rendering them susceptible to being "killed" by viral cytopathic effect or by the host immune system while ART prevents infection of new cells from reseeding of the latent reservoir. In order to successfully achieve a cure, every replication-competent provirus that could ever be induced to express HIV gene products must be reactivated and killed before proliferating and returning to latency.
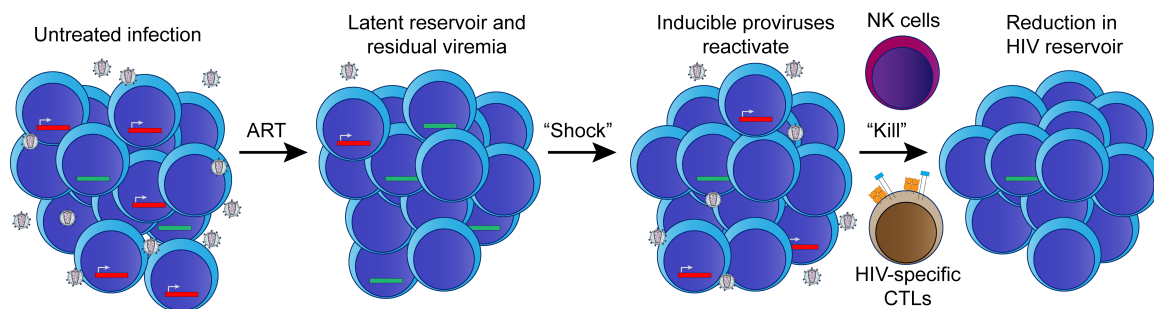
Fig. 1.6: Shock and kill strategy to reduce the HIV reservoir. Maintenance of ART throughout blocks HIV replication and prevents the infection of new cells. A therapeutic "shock" induces HIV gene expression from latent proviruses. Expression of viral genes generates HIV epitopes enabling the clearance of reactivated cells by natural killer cells (NK cells) or cytotoxic T lymphocytes (CTLs). *Red* represents a transcriptionally active provirus; *green* represents a transcriptionally silent latent provirus.

Latency Reversal Agents

Given the aforementioned heterogeneity of the cellular and anatomical reservoirs of latent HIV, latency reversal agents (LRAs) will have to be broadly effective, and their

43

ability to reactivate proviruses in every relevant reservoir must be assessed[479]. A large body of literature has attempted to characterize and define the mechanisms regulating the establishment and maintenance of HIV latency in various cell culture models, though these almost exclusively focus on studying the CD4^{+} T cell reservoir using immortalized cell lines or various manipulations to encourage latency in primary cells[480]. Many mechanisms that can contribute to latency have been identified, and these are accompanied by therapeutic approaches to reactivate latent proviruses (see review[481]).

As with cellular genes, the promoter in the 5' LTR of HIV is heavily regulated by epigenetic influences on gene expression. Many LRAs target epigenetic factors with the aim of enhancing transcription. Multiple studies have indicated that the silencing effects of methyl-cytosine in CpG islands is associated with HIV latency in cell culture models and *in vivo*, and heavily methylated HIV promoters can be induced with the DNA methylation inhibitor 5-aza-2'deoxycytidine (aza-CdR)[482,483]. DNA methylation does not entirely explain latency *in vivo* nor does it account for every aspect of latency reversal, as aza-CdR synergized with activators of NFκB[482], and alternative LRAs can overcome hypermethylation[483]. Histone acetylation, counteracted by histone deacetylases (HDACs), specifically class-1 HDACs, can also enhance HIV gene expression, and the lack of histone acetylation is associated with latency[484-486]. HDAC inhibitors, such as vorinostat[487,488] and romidepsin[489-491], are among the most widely-used and promising LRAs, which are believed to achieve reactivation through chromatin remodeling, increasing histone acetylation and improving accessibility for RNA polymerase II (Pol II). Extensive clinical trials of histone deacetylase inhibitors have shown some evidence of increased HIV RNA expression, but no reduction in the proviral reservoir[492-494].

Several key transcription factors can regulate HIV gene expression by binding directly to the LTR promoter. NFκB is essential for efficient transcription from the promoter in the HIV 5' LTR[112]. Canonical NFκB consists of the p50/p65 heterodimer, which is sequestered by IκB, enabling activation of the pathway via IκB phosphorylation. The non-canonical NFκB pathway culminates with the activation of the RelB/p52 heterodimer by inducing alternative processing of the precursor p100[495]. Canonical NFκB signaling can be induced by TNFα stimulation[30] or protein kinase C (PKC) activation with agonists such as bryostatin-1[496] or ingenols[497]. While PKC agonists are among the most promising LRAs *in vitro*[480,498], they are generally considered too toxic for clinical use, and bryostatin-1 showed little effect on HIV gene expression at tolerable levels *in vivo*[499]. Smac mimetics like ciapivir can activate the non-canonical NFκB pathway to reactivate latently infected cells *in vitro*[500] and *in vivo* in a humanized mouse model[501] with no effect on T cell activation, indicating that these compounds may have fewer associated toxicities in patients than activators of the canonical NFκB pathway.

After recruitment of Pol II to the HIV promoter, efficient elongation requires the interaction of HIV Tat with P-TEFb.[120,502]. Tat binds to the TAR element, a secondary structure near the 5' end of the nascent viral RNA[119]. When bound to the TAR element, Tat recruits activated P-TEFb, composed of cyclin T1 and phosphorylated CDK9, which increasing the processivity of Pol II by phosphorylating the Pol II C-terminal domain[120,121]. The low level of phosphorylated CDK9 in resting CD4$^+$ T cells contributes to HIV latency[503]. P-TEFb can also be held in an inactive state by the 7SK snRNP complex[504,505], but can be released from this complex and activated following treatment with the LRA HMBA, inducing HIV gene expression[506].

Combinations of LRAs targeting diverse mechanisms that can contribute to HIV latency have demonstrated increased efficacy *in vitro*[484,500,507-509]. Despite the robust body of literature and reproducible evidence that these agents can induce HIV gene expression, to date none of these approaches have proved successful in significantly reducing the size of the latent reservoir and substantially delaying rebound upon cessation of ART[492,493,510-516]. This suggests possible failures in reactivating all or even a large proportion of the replication-competent reservoir, failures in killing the cells harboring induced proviruses before the virus returns to latency, or both.

To address the inability to reactivate the entirety of the replication-competent reservoir, it will be essential to identify reactivation strategies that are likely to be broadly effective in reversing latency, given the heterogenous nature of the reservoir *in vivo*. Thus, it is of critical importance to develop *in vitro* models of HIV-1 latent infection that reflect the true nature of the cells harboring provirus *in vivo*, including their quiescent state. While latent HIV-1 infection has been observed in several *in vitro* systems[480], these are all focused exclusively on latency in T cells, and there is notable absence of primary cell models in which HIV-1 preferentially establishes a latent infection in quiescent cells. Furthermore, the treatments that were most effective in many of these models are the same approaches that have failed to reduce the viral reservoir *in vivo*, reaffirming the need to develop better cell culture models to predict LRA efficacy[492,493,498,510-512].

Chapter 2 of this dissertation details the development of a primary cell model of HIV latency in quiescent HSPCs, which can provide key insights into the mechanisms regulating the establishment and maintenance of HIV latency and the efficacy of LRAs in quiescent primary cells.

Nef-Mediated Immune Evasion Impairs CTL Killing

In addition to improving shock therapies to achieve maximal reactivation of latent HIV from heterogenous cellular reservoirs, the cells harboring reactivated provirus will need to be eliminated before proliferating or returning to latency. CTLs are the primary effectors responsible for killing cells expressing HIV proteins, presented as HIV-derived peptides by MHC-I. While evidence suggests a single molecule of peptide:MHC-I can be sufficient to induce CTL-mediated killing[517,518], many studies have shown a proportional relationship between the abundance of peptide:MHC-I on the target cell surface and the potency of CTL-mediated activation or clearance[519-523]. MHC-I is loaded in the endoplasmic reticulum (ER) with peptides that were first generated by cytoplasmic proteasomal processing and subsequently actively imported into the ER. Peptide-loaded MHC-I transits from the ER and is processed through the cis-, medial- and trans-Golgi, exits via the trans-Golgi network (TGN), and ultimately proceeds through the secretory pathway via secretory vesicles until it reaches the plasma membrane. Upon reaching the plasma membrane, peptide:MHC-I complexes can interact with CD8^{+} T cells expressing a TCR with high affinity for both the allele of MHC-I and the peptide being presented[524].

The HIV accessory protein Nef interferes with the proper trafficking of MHC-I by first binding to the cytoplasmic tail of MHC-I early in the secretory pathway[525]. Binding of Nef to the MHC-I cytoplasmic tail stabilizes an interaction between a tyrosine residue (Y320) in the MHC-I tail and the tyrosine-binding pocket in the μ subunit of clathrin adaptor protein 1 (AP-1), exposing a cryptic AP-1 sorting signal that is not present in the absence

of Nef[273,274]. AP-1 is a heterotetrameric complex consisting of $\mu 1$, $\beta 1$, $\sigma 1$, and γ subunits, which recognizes Yxxφ or [D/E] xxxLL sorting signals and induces clathrin coat formation[526]. Formation of the AP-1:Nef:MHC-I complex mediates the redirection of MHC-I into the endolysosomal trafficking pathway via clathrin-coated vesicles in an ADP-ribosylation factor-1 (ARF-1)-dependent manner, and trafficking proceeds until MHC-I is delivered to the lysosome, where it is degraded. An alternative model proposed that Nef promoted the internalization of MHC-I from the cell surface[527], which was purported to occur via a pathway involving PACS-1, PI3K, and ARF6[528]. The contributions of this model to MHC-I downregulation, however, have not been reproducible[275,529]. The direct contacts between Nef, MHC-I, AP-1, and ARF-1, on the other hand, have been confirmed by X-ray crystallography[530] and cryo-electron microscopy analyses[531], elucidating the structural basis for these interactions and confirming this as the essential mechanism by which Nef induces degradation of MHC-I in the lysosome[532].

The lysosome is the organelle responsible for the degradation of proteins within the cell. Lysosomal proteases are the effectors of lysosomal degradation, and their proteolytic activity is only activated in an acidic environment, preventing premature degradation of host proteins prior to successful delivery of the proteases to the lysosome[533]. Lysosomal acidification is maintained by the vacuolar H^+-ATPase (V-ATPase), a rotary proton-pumping motor[534] consisting of two domains, an integral domain (V_0) and a cytoplasmic domain (V_1). V-ATPase maintains acidic intracellular compartments by using the energy from the hydrolysis of ATP, catalyzed by V_1, to pump H^+ ions against a pH gradient, which is catalyzed by V_0.

Nef does not exclusively downregulate MHC-I, and in fact hijacks host trafficking adaptor proteins to promote the degradation of many host proteins in the lysosome (see review[532]). Nef is expressed early in the viral life cycle and is conserved among primate lentiviruses, although some functional differences exist, as SIV Nef can downregulate CD3 and tetherin[535]. Nef is anchored to membranes via myristoylation of the N-terminal glycine[536] and additional key residues at the N-terminus of Nef[537], although the majority of Nef protein remains cytoplasmic rather than associated with membranes[538]. While dimers and trimers of Nef can be detected in cells, and oligomerization of Nef was believed to be critical for all Nef functions due to the deleterious effects of mutations to the D123 domain involved in oligomerization[539], the myristoylated form of Nef that associates with membranes predominantly exists as a monomer[538], and myristoylation is also essential for all Nef functions[540-543]. Nef downregulates CD4[544] via internalization from the cell surface via the clathrin adaptor protein 2 (AP-2) complex[278,545,546]. Downregulation of CD4 likely prevents superinfection, which is assisted by concomitant downregulation of CCR5[547], and protects infected cells from antibody-mediated cell cytotoxicity[548-550]. One of the original and elusive activities of Nef is its critical role to enhance virion infectivity[551,552]. This activity was recently mapped to the restriction factors SERINC3 and SERINC5, which are internalized from the cell surface and degraded in the lysosome in the presence of Nef[270-272]. HIV-1 Nef also downregulates the T cell costimulatory molecule CD28[553], interacts with Src family kinases[554], modulates T cell activation[555-557] and promotes survival through activation of PAK, which activates PI3-kinase to inactivate the pro-apoptotic Bad protein[558]. Though Nef interacts with many host proteins, the mechanism of recruiting AP-1 at the TGN is, to date, unique to MHC-I.
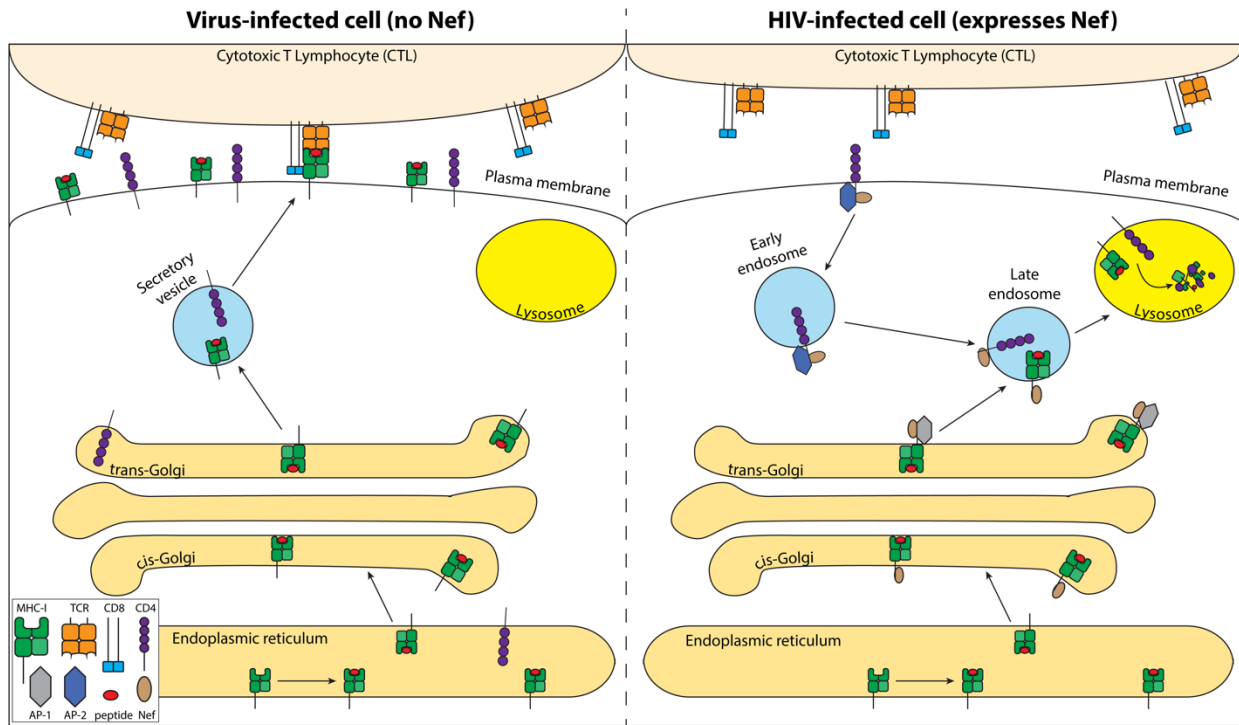
Fig. 1.7: Nef alters the trafficking of MHC-I and CD4 and prevents the recognition of HIV-infected cells by cytotoxic T lymphocytes. Left panel: a cell infected with a virus successfully presents a virus-derived peptide to a virus-specific CTL. Right: HIV-infected cells express Nef, reducing cell-surface MHC-I and evading CTL recognition. Nef also downregulates CD4 by a different mechanism, as indicated.

With recruitment of AP-1 to the cytoplasmic tail of MHC-I mediated by Nef, newly synthesized MHC-I that could be loaded with virus-derived peptides is redirected away from the cell surface in HIV-infected cells. The resulting loss of MHC-I presenting HIV-derived peptides reduces the efficiency of HIV-specific CTLs, protecting a portion of Nef-expressing cells from CTL clearance[277]. Nef binds specifically to the cytoplasmic domains of HLA-A and -B, but not HLA-C and -E. This selective targeting is the result of alterations in the key binding residues Y320, A324, and D324 in the cytoplasmic tails of HLA-C and -E[274]. The preservation of HLA-C and -E on the cell surface is thought to provide a selective advantage, given the NK inhibitory properties of HLA-C and -E. This differentiation from HLA-A and-B, which play a larger role in presenting peptides to CTLs

50

and are strongly targeted by Nef, may optimize evasion of both CTL and NK cell responses and is conserved across primate lentiviruses[559-561]. The existence of HLA-C-restricted CTL responses to HIV would seem to challenge this framework[379-381]. The recent discovery that HLA-C is downregulated by the Vpu proteins from some primary isolates of HIV-1, and by the Vif protein of HIV-2, suggests that HIV can evolve to evade HLA-C-restricted CTL responses in settings where these exert stronger selective pressures than NK cells[562-564]. Predictably, downregulation of HLA-C involves evolutionary tradeoffs, since downregulation of HLA-C by Vpu does indeed sensitize HIV-infected cells to NK cell-mediated clearance[565].

The urgent need for a therapeutic Nef inhibitor is evident given that 1) shock alone is insufficient to induce killing of reactivated cells harboring HIV proviruses, 2) CTLs are the primary effectors of immune control of HIV, and 3) Nef protects some HIV-infected cells from even potent HIV-specific CTLs. In fact, the identification of a potent inhibitor of Nef that restores MHC-I to the surface of HIV-infected cells may be an essential step toward the goal of efficiently clearing HIV reservoirs following therapeutic latency reversal. While previous studies have identified compounds that inhibit some activities of Nef *in vitro,* they have not been shown to dramatically and reproducibly restore MHC-I to the surface of Nef-expressing cells[566-568]. Thus, their effects on CTL killing of HIV-infected cells are predictably small, necessitating the discovery of compounds that can potently restore MHC-I to the surface of Nef-expressing cells[567,569].

Natural products continue to represent the most prosperous source of lead-drug candidates[570]. Continued interest in natural products discovery originates from the plethora of clinically relevant biological activities exhibited by these compounds. The

Actinobacteria genera *Streptomyces* represents one of the most well studied families of bacteria as a source of bioactive metabolites, as natural products isolated from this family are estimated to account for approximately 30% of all identified bioactive metabolites[571-573]. The enormous potential for chemical diversity has inspired the assembly of diverse microbial natural products extract (NPE) libraries for screening against a variety of disease targets. This methodology has been historically successful, with approximately 60% of all approved drugs between 1981 and 2014 identified as natural products, natural product-derived, or inspired by natural products[574]. Despite this extensive history of success, only a select few examples of natural products used in the treatment of HIV have been described to date[575-577].

Chapter 3 of this dissertation details the discovery that the plecomacrolide family of natural products are potent inhibitors of HIV Nef that restore MHC-I to the surface of HIV-infected cells and can enhance the elimination of HIV-infected cells by HIV-specific CTLs.

References

1. Joint-United-Nations-Program-on-HIV/AIDS. UNAIDS data 2020. *Geneva: UNAIDS.* 2020:1-436.
2. Baltimore D. Viral RNA-dependent DNA polymerase: RNA-dependent DNA polymerase in virions of RNA tumour viruses. *Nature.* 1970;226(5252):1209-1211.
3. Temin HM, Mizutami S. RNA-dependent DNA polymerase in virions of Rous sarcoma virus. *nature.* 1970;226:1211-1213.
4. Summers J, Mason WS. Replication of the genome of a hepatitis B-like virus by reverse transcription of an RNA intermediate. *Cell.* 1982;29(2):403-415.
5. Hohn T, Hohn B, Pfeiffer P. Reverse transcription in CaMV. *Trends in biochemical Sciences.* 1985;10(5):205-209.
6. Coffin JM, Fan H. The discovery of reverse transcriptase. *Annual review of virology.* 2016;3:29-51.
7. Stoye J, Blomberg J, Coffin J, et al. Retroviridae. In: Elsevier Inc.: London, UK; 2012:477-495.
8. Leis J, Baltimore D, Bishop J, et al. Standardized and simplified nomenclature for proteins common to all retroviruses. *Journal of virology.* 1988;62(5):1808-1809.
9. Ganser-Pornillos BK, Yeager M, Sundquist WI. The structural biology of HIV assembly. *Current opinion in structural biology.* 2008;18(2):203-217.
10. Muriaux D, Mirro J, Harvin D, Rein A. RNA is a structural element in retrovirus particles. *Proceedings of the National Academy of Sciences.* 2001;98(9):5246-5251.
11. Darlix J-L, Gabus C, Nugeyre M-T, Clavel F, Barré-Sinoussi F. Cis elements and trans-acting factors involved in the RNA dimerization of the human immunodeficiency virus HIV-1. *Journal of molecular biology.* 1990;216(3):689-699.
12. Burniston MT, Cimarelli A, Colgan J, Curtis SP, Luban J. Human immunodeficiency virus type 1 Gag polyprotein multimerization requires the nucleocapsid domain and RNA and is promoted by the capsid-dimer interface and the basic region of matrix protein. *Journal of virology.* 1999;73(10):8527-8540.
13. Yeager M, Wilson-Kubalek EM, Weiner SG, Brown PO, Rein A. Supramolecular organization of immature and mature murine leukemia virus revealed by electron cryo-microscopy: implications for retroviral assembly mechanisms. *Proceedings of the National Academy of Sciences.* 1998;95(13):7299-7304.
14. Muriaux D, De Rocquigny H, Roques B-P, Paoletti J. NCp7 activates HIV-1Lai RNA dimerization by converting a transient loop-loop complex into a stable dimer. *Journal of Biological Chemistry.* 1996;271(52):33686-33692.
15. Briggs JA, Simon MN, Gross I, et al. The stoichiometry of Gag protein in HIV-1. *Nature structural & molecular biology.* 2004;11(7):672-675.
16. Briggs JA, Wilk T, Welker R, Kräusslich HG, Fuller SD. Structural organization of authentic, mature HIV-1 virions and cores. *The EMBO journal.* 2003;22(7):1707-1715.

17. Mattei S, Glass B, Hagen WJ, Kräusslich H-G, Briggs JA. The structure and flexibility of conical HIV-1 capsids determined within intact virions. *Science.* 2016;354(6318):1434-1437.

18. Zhu P, Chertova E, Bess J, et al. Electron tomography analysis of envelope glycoprotein trimers on HIV and simian immunodeficiency virus virions. *Proceedings of the National Academy of Sciences.* 2003;100(26):15812-15817.

19. Liu J, Bartesaghi A, Borgnia MJ, Sapiro G, Subramaniam S. Molecular architecture of native HIV-1 gp120 trimers. *Nature.* 2008;455(7209):109-113.

20. Chertova E, Bess Jr JW, Crise BJ, et al. Envelope glycoprotein incorporation, not shedding of surface envelope glycoprotein (gp120/SU), is the primary determinant of SU content of purified human immunodeficiency virus type 1 and simian immunodeficiency virus. *Journal of virology.* 2002;76(11):5315-5325.

21. Lasky LA, Nakamura G, Smith DH, et al. Delineation of a region of the human immunodeficiency virus type 1 gp120 glycoprotein critical for interaction with the CD4 receptor. *Cell.* 1987;50(6):975-985.

22. Maddon PJ, Dalgleish AG, McDougal JS, Clapham PR, Weiss RA, Axel R. The T4 gene encodes the AIDS virus receptor and is expressed in the immune system and the brain. *Cell.* 1986;47(3):333-348.

23. Feng Y, Broder CC, Kennedy PE, Berger EA. HIV-1 entry cofactor: functional cDNA cloning of a seven-transmembrane, G protein-coupled receptor. *Science.* 1996;272(5263):872-877.

24. Trkola A, Dragic T, Arthos J, et al. CD4-dependent, antibody-sensitive interactions between HIV-1 and its co-receptor CCR-5. *Nature.* 1996;384(6605):184-187.

25. Wu L, Gerard NP, Wyatt R, et al. CD4-induced interaction of primary HIV-1 gp120 glycoproteins with the chemokine receptor CCR-5. *Nature.* 1996;384(6605):179-183.

26. Embretson J, Zupancic M, Ribas JL, et al. Massive covert infection of helper T lymphocytes and macrophages by HIV during the incubation period of AIDS. *Nature.* 1993;362(6418):359-362.

27. Koenig S, Fauci AS. Detection of AIDS virus in macrophages in brain tissue from AIDS patients with encephalopathy. *Science.* 1986;233:1089-1094.

28. Sebastian NT, Zaikos TD, Terry V, et al. CD4 is expressed on a heterogeneous subset of hematopoietic progenitors, which persistently harbor CXCR4 and CCR5-tropic HIV proviral genomes in vivo. *PLoS Pathogens.* 2017;13(7):e1006509.

29. McNamara LA, Onafuwa-Nuga A, Sebastian NT, Riddell J, Bixby D, Collins KL. CD133+ hematopoietic progenitor cells harbor HIV genomes in a subset of optimally treated people with long-term viral suppression. *Journal of Infectious Diseases.* 2013:jit118.

30. McNamara LA, Ganesh JA, Collins KL. Latent HIV-1 infection occurs in multiple subsets of hematopoietic progenitor cells and is reversed by NF-kappaB activation. *J Virol.* 2012;86(17):9337-9350.

31. Carter CC, Onafuwa-Nuga A, McNamara LA, et al. HIV-1 infects multipotent progenitor cells causing cell death and establishing latent cellular reservoirs. *Nature medicine.* 2010;16(4):446-451.

32. Redd AD, Avalos A, Essex M. Infection of hematopoietic progenitor cells by HIV-1 subtype C, and its association with anemia in southern Africa. *Blood.* 2007;110(9):3143-3149.
33. Campbell EM, Hope TJ. HIV-1 capsid: the multifaceted key player in HIV-1 infection. *Nature Reviews Microbiology.* 2015;13(8):471-483.
34. Yang R, Shi J, Byeon I-JL, et al. Second-site suppressors of HIV-1 capsid mutations: restoration of intracellular activities without correction of intrinsic capsid stability defects. *Retrovirology.* 2012;9(1):1-14.
35. Forshey BM, von Schwedler U, Sundquist WI, Aiken C. Formation of a human immunodeficiency virus type 1 core of optimal stability is crucial for viral replication. *Journal of virology.* 2002;76(11):5667-5677.
36. Lahaye X, Satoh T, Gentili M, et al. The capsids of HIV-1 and HIV-2 determine immune detection of the viral cDNA by the innate sensor cGAS in dendritic cells. *Immunity.* 2013;39(6):1132-1142.
37. Le Sage V, Mouland AJ, Valiente-Echeverría F. Roles of HIV-1 capsid in viral replication and immune evasion. *Virus research.* 2014;193:116-129.
38. Peng K, Muranyi W, Glass B, et al. Quantitative microscopy of functional HIV post-entry complexes reveals association of replication with the viral capsid. *Elife.* 2014;3:e04114.
39. Matreyek KA, Yücel SS, Li X, Engelman A. Nucleoporin NUP153 phenylalanine-glycine motifs engage a common binding pocket within the HIV-1 capsid protein to mediate lentiviral infectivity. *PLoS Pathog.* 2013;9(10):e1003693.
40. Matreyek KA, Engelman A. The requirement for nucleoporin NUP153 during human immunodeficiency virus type 1 infection is determined by the viral capsid. *Journal of virology.* 2011;85(15):7818-7827.
41. Zhou L, Sokolskaja E, Jolly C, James W, Cowley SA, Fassati A. Transportin 3 promotes a nuclear maturation step required for efficient HIV-1 integration. *PLoS pathogens.* 2011;7(8):e1002194.
42. Yamashita M, Perez O, Hope TJ, Emerman M. Evidence for direct involvement of the capsid protein in HIV infection of nondividing cells. *PLoS Pathog.* 2007;3(10):e156.
43. Yamashita M, Emerman M. Capsid is a dominant determinant of retrovirus infectivity in nondividing cells. *Journal of virology.* 2004;78(11):5670-5678.
44. Price AJ, Jacques DA, McEwan WA, et al. Host cofactors and pharmacologic ligands share an essential interface in HIV-1 capsid that is lost upon disassembly. *PLoS Pathog.* 2014;10(10):e1004459.
45. Bhattacharya A, Alam SL, Fricke T, et al. Structural basis of HIV-1 capsid recognition by PF74 and CPSF6. *Proceedings of the National Academy of Sciences.* 2014;111(52):18625-18630.
46. Selyutina A, Persaud M, Lee K, KewalRamani V, Diaz-Griffero F. Nuclear Import of the HIV-1 Core Precedes Reverse Transcription and Uncoating. *Cell Reports.* 2020;32(13).
47. Strambio-De-Castillia C, Niepel M, Rout MP. The nuclear pore complex: bridging nuclear transport and gene regulation. *Nature reviews Molecular cell biology.* 2010;11(7):490-501.

48. Schaller T, Ocwieja KE, Rasaiyaah J, et al. HIV-1 capsid-cyclophilin interactions determine nuclear import pathway, integration targeting and replication efficiency. *PLoS Pathog.* 2011;7(12):e1002439.

49. Marini B, Kertesz-Farkas A, Ali H, et al. Nuclear architecture dictates HIV-1 integration site selection. *Nature.* 2015;521(7551):227-231.

50. Krishnan L, Matreyek KA, Oztop I, et al. The requirement for cellular transportin 3 (TNPO3 or TRN-SR2) during infection maps to human immunodeficiency virus type 1 capsid and not integrase. *Journal of virology.* 2010;84(1):397-406.

51. Valle-Casuso JC, Di Nunzio F, Yang Y, et al. TNPO3 is required for HIV-1 replication after nuclear import but prior to integration and binds the HIV-1 core. *Journal of virology.* 2012;86(10):5931-5936.

52. Christ F, Thys W, De Rijck J, et al. Transportin-SR2 imports HIV into the nucleus. *Current Biology.* 2008;18(16):1192-1202.

53. Lee K, Mulky A, Yuen W, et al. HIV-1 capsid-targeting domain of cleavage and polyadenylation specificity factor 6. *Journal of virology.* 2012;86(7):3851-3860.

54. Lee K, Ambrose Z, Martin TD, et al. Flexible use of nuclear import pathways by HIV-1. *Cell host & microbe.* 2010;7(3):221-233.

55. Koh Y, Wu X, Ferris AL, et al. Differential effects of human immunodeficiency virus type 1 capsid and cellular factors nucleoporin 153 and LEDGF/p75 on the efficiency and specificity of viral DNA integration. *Journal of virology.* 2013;87(1):648-658.

56. Sowd GA, Serrao E, Wang H, et al. A critical role for alternative polyadenylation factor CPSF6 in targeting HIV-1 integration to transcriptionally active chromatin. *Proceedings of the National Academy of Sciences.* 2016;113(8):E1054-E1063.

57. Telesnitsky A, Goff S. Reverse transcriptase and the generation of retroviral DNA. 1997.

58. Skalka AM, Goff S. *Reverse transcriptase.* Vol 23: Cold Spring Harbor Laboratory Press; 1993.

59. Iordanskiy SN, Bukrinsky MI. Reverse transcription complex: the key player of the early phase of HIV replication. 2007.

60. Warrilow D, Tachedjian G, Harrich D. Maturation of the HIV reverse transcription complex: putting the jigsaw together. *Reviews in medical virology.* 2009;19(6):324-337.

61. Johnson PE, Turner RB, Wu ZR, et al. A mechanism for plus-strand transfer enhancement by the HIV-1 nucleocapsid protein during reverse transcription. *Biochemistry.* 2000;39(31):9084-9091.

62. Gopalakrishnan V, Peliska JA, Benkovic SJ. Human immunodeficiency virus type 1 reverse transcriptase: spatial and temporal relationship between the polymerase and RNase H activities. *Proceedings of the National Academy of Sciences.* 1992;89(22):10763-10767.

63. Götte M, Fackler S, Hermann T, et al. HIV-1 reverse transcriptase-associated RNase H cleaves RNA/RNA in arrested complexes: implications for the mechanism by which RNase H discriminates between RNA/RNA and RNA/DNA. *The EMBO journal.* 1995;14(4):833-841.

64. Hungnesi O, Tjøtta E, Grinde B. Mutations in the central polypurine tract of HIV-1 result in delayed replication. *Virology.* 1992;190(1):440-442.

65. Charneau P, Alizon M, Clavel F. A second origin of DNA plus-strand synthesis is required for optimal human immunodeficiency virus replication. *Journal of virology.* 1992;66(5):2814-2820.

66. Zennou V, Petit C, Guetard D, Nerhbass U, Montagnier L, Charneau P. HIV-1 genome nuclear import is mediated by a central DNA flap. *Cell.* 2000;101(2):173-185.

67. Tanese N, Goff SP. Domain structure of the Moloney murine leukemia virus reverse transcriptase: mutational analysis and separate expression of the DNA polymerase and RNase H activities. *Proceedings of the national academy of sciences.* 1988;85(6):1777-1781.

68. Sarafianos SG, Marchand B, Das K, et al. Structure and function of HIV-1 reverse transcriptase: molecular mechanisms of polymerization and inhibition. *Journal of molecular biology.* 2009;385(3):693-713.

69. Reardon JE. Human immunodeficiency virus reverse transcriptase: steady-state and pre-steady-state kinetics of nucleotide incorporation. *Biochemistry.* 1992;31(18):4473-4479.

70. Roberts J, Preston B, Johnston L, Soni A, Loeb L, Kunkel T. Fidelity of two retroviral reverse transcriptases during DNA-dependent DNA synthesis in vitro. *Molecular and cellular biology.* 1989;9(2):469-476.

71. Preston BD, Poiesz BJ, Loeb LA. Fidelity of HIV-1 reverse transcriptase. *Science.* 1988;242(4882):1168-1171.

72. Hottiger M, Podust VN, Thimmig RL, McHenry C, Hübscher U. Strand displacement activity of the human immunodeficiency virus type 1 reverse transcriptase heterodimer and its individual subunits. *Journal of Biological Chemistry.* 1994;269(2):986-991.

73. di Marzo Veronese F, Copeland TD, DeVico AL, et al. Characterization of highly immunogenic p66/p51 as the reverse transcriptase of HTLV-III/LAV. *Science.* 1986;231(4743):1289-1291.

74. Lowe DM, Aitken A, Bradley C, et al. HIV-1 reverse transcriptase: crystallization and analysis of domain structure by limited proteolysis. *Biochemistry.* 1988;27(25):8884-8889.

75. Kohlstaedt L, Wang J, Friedman J, Rice P, Steitz T. Crystal structure at 3.5 A resolution of HIV-1 reverse transcriptase complexed with an inhibitor. *Science.* 1992;256(5065):1783-1790.

76. Onafuwa A, An W, Robson ND, Telesnitsky A. Human immunodeficiency virus type 1 genetic recombination is more frequent than that of Moloney murine leukemia virus despite similar template switching rates. *Journal of virology.* 2003;77(8):4577-4587.

77. Hu W-S, Temin HM. Genetic consequences of packaging two RNA genomes in one retroviral particle: pseudodiploidy and high rate of genetic recombination. *Proceedings of the National Academy of Sciences.* 1990;87(4):1556-1560.

78. Robertson DL, Sharp PM, McCutchan FE, Hahn BH. Recombination in HIV-1. *Nature.* 1995;374(6518):124-126.

79. Hwang CK, Svarovskaia ES, Pathak VK. Dynamic copy choice: steady state between murine leukemia virus polymerase and polymerase-dependent RNase H

activity determines frequency of in vivo template switching. *Proceedings of the National Academy of Sciences.* 2001;98(21):12209-12214.

80. Luo G, Taylor J. Template switching by reverse transcriptase during DNA synthesis. *Journal of virology.* 1990;64(9):4321-4328.

81. Lanciault C, Champoux JJ. Pausing during reverse transcription increases the rate of retroviral recombination. *Journal of virology.* 2006;80(5):2483-2494.

82. Galetto R, Moumen A, Giacomoni V, Véron M, Charneau P, Negroni M. The structure of HIV-1 genomic RNA in the gp120 gene determines a recombination hot spot in vivo. *Journal of Biological Chemistry.* 2004;279(35):36625-36632.

83. Harrison GP, Mayo MS, Hunter E, Lever AM. Pausing of reverse transcriptase on retroviral RNA templates is influenced by secondary structures both 5′ and 3′ of the catalytic site. *Nucleic acids research.* 1998;26(14):3433-3442.

84. Coffin JM. Structure, replication, and recombination of retrovirus genomes: some unifying hypotheses. *Journal of General Virology.* 1979;42(1):1-26.

85. Chin MP, Chen J, Nikolaitchik OA, Hu W-S. Molecular determinants of HIV-1 intersubtype recombination potential. *Virology.* 2007;363(2):437-446.

86. Louis DCS, Gotte D, Sanders-Buell E, et al. Infectious molecular clones with the nonhomologous dimer initiation sequences found in different subtypes of human immunodeficiency virus type 1 can recombine and initiate a spreading infection in vitro. *Journal of virology.* 1998;72(5):3991-3998.

87. Moore MD, Fu W, Nikolaitchik O, Chen J, Ptak RG, Hu W-S. Dimer initiation signal of human immunodeficiency virus type 1: its role in partner selection during RNA copackaging and its effects on recombination. *Journal of virology.* 2007;81(8):4002-4011.

88. Hansen MS, Carteau S, Hoffmann C, Li L, Bushman F. Retroviral cDNA integration: mechanism, applications and inhibition. In: *Genetic engineering.* Springer; 1998:41-61.

89. Krishnan L, Engelman A. Retroviral integrase proteins and HIV-1 DNA integration. *Journal of Biological Chemistry.* 2012;287(49):40858-40866.

90. Engelman A, Englund G, Orenstein JM, Martin MA, Craigie R. Multiple effects of mutations in human immunodeficiency virus type 1 integrase on viral replication. *Journal of virology.* 1995;69(5):2729-2736.

91. Sakai H, Kawamura M, Sakuragi J-I, et al. Integration is essential for efficient gene expression of human immunodeficiency virus type 1. *Journal of virology.* 1993;67(3):1169-1174.

92. Tarlinton RE, Meers J, Young PR. Retroviral invasion of the koala genome. *Nature.* 2006;442(7098):79-81.

93. O'NEIL LL, BURKHARD MJ, DIEHL LJ, HOOVER EA. Vertical transmission of feline immunodeficiency virus. *AIDS research and human retroviruses.* 1995;11(1):171-182.

94. Du Y, Spence SE, Jenkins NA, Copeland NG. Cooperating cancer-gene identification through oncogenic-retrovirus–induced insertional mutagenesis. *Blood.* 2005;106(7):2498-2505.

95. Hacein-Bey-Abina S, Garrigue A, Wang GP, et al. Insertional oncogenesis in 4 patients after retrovirus-mediated gene therapy of SCID-X1. *The Journal of clinical investigation.* 2008;118(9):3132-3142.

96.   Li X, Krishnan L, Cherepanov P, Engelman A. Structural biology of retroviral DNA integration. *Virology.* 2011;411(2):194-205.
97.   Hare S, Gupta SS, Valkov E, Engelman A, Cherepanov P. Retroviral intasome assembly and inhibition of DNA strand transfer. *Nature.* 2010;464(7286):232-236.
98.   Yang W, Lee JY, Nowotny M. Making and breaking nucleic acids: two-Mg2+-ion catalysis and substrate specificity. *Molecular cell.* 2006;22(1):5-13.
99.   Kulkosky J, Jones KS, Katz RA, Mack J, Skalka A. Residues critical for retroviral integrative recombination in a region that is highly conserved among retroviral/retrotransposon integrases and bacterial insertion sequence transposases. *Molecular and cellular biology.* 1992;12(5):2331-2338.
100.   Sherman PA, Fyfe JA. Human immunodeficiency virus integration protein expressed in Escherichia coli possesses selective DNA cleaving activity. *Proceedings of the National Academy of Sciences.* 1990;87(13):5119-5123.
101.   Bushman FD, Craigie R. Activities of human immunodeficiency virus (HIV) integration protein in vitro: specific cleavage and integration of HIV DNA. *Proceedings of the National Academy of Sciences.* 1991;88(4):1339-1343.
102.   Engelman A, Mizuuchi K, Craigie R. HIV-1 DNA integration: mechanism of viral DNA cleavage and DNA strand transfer. *Cell.* 1991;67(6):1211-1221.
103.   Bushman FD, Fujiwara T, Craigie R. Retroviral DNA integration directed by HIV integration protein in vitro. *Science.* 1990;249(4976):1555-1558.
104.   Faschinger A, Rouault F, Sollner J, et al. Mouse mammary tumor virus integration site selection in human and mouse genomes. *Journal of virology.* 2008;82(3):1360-1367.
105.   Mitchell RS, Beitzel BF, Schroder AR, et al. Retroviral DNA integration: ASLV, HIV, and MLV show distinct target site preferences. *PLoS Biol.* 2004;2(8):e234.
106.   Moiani A, Suerth JD, Gandolfi F, et al. Genome-wide analysis of alpharetroviral integration in human hematopoietic stem/progenitor cells. *Genes.* 2014;5(2):415-429.
107.   Achuthan V, Perreira JM, Sowd GA, et al. Capsid-CPSF6 interaction licenses nuclear HIV-1 trafficking to sites of viral DNA integration. *Cell host & microbe.* 2018;24(3):392-404. e398.
108.   Han Y, Lassen K, Monie D, et al. Resting CD4+ T cells from human immunodeficiency virus type 1 (HIV-1)-infected individuals carry integrated HIV-1 genomes within actively transcribed host genes. *Journal of virology.* 2004;78(12):6122-6133.
109.   Wang GP, Ciuffi A, Leipzig J, Berry CC, Bushman FD. HIV integration site selection: analysis by massively parallel pyrosequencing reveals association with epigenetic modifications. *Genome research.* 2007;17(8):1186-1194.
110.   Schröder AR, Shinn P, Chen H, Berry C, Ecker JR, Bushman F. HIV-1 integration in the human genome favors active genes and local hotspots. *Cell.* 2002;110(4):521-529.
111.   Garcia JA, Harrich D, Soultanakis E, Wu F, Mitsuyasu R, Gaynor RB. Human immunodeficiency virus type 1 LTR TATA and TAR region sequences required for transcriptional regulation. *The EMBO journal.* 1989;8(3):765-778.
112.   Nabel G, Baltimore D. An inducible transcription factor activates expression of human immunodeficiency virus in T cells. *Nature.* 1987;326(6114):711-713.

113. el Kharroubi A, Verdin E. Protein-DNA interactions within DNase I-hypersensitive sites located downstream of the HIV-1 promoter. *Journal of Biological Chemistry.* 1994;269(31):19916-19924.

114. Van Lint C, Amella CA, Emiliani S, John M, Jie T, Verdin E. Transcription factor binding sites downstream of the human immunodeficiency virus type 1 transcription start site are important for virus infectivity. *Journal of virology.* 1997;71(8):6113-6127.

115. Kinoshita S, Chen BK, Kaneshima H, Nolan GP. Host control of HIV-1 parasitism in T cells by the nuclear factor of activated T cells. *Cell.* 1998;95(5):595-604.

116. Cron RQ, Bartz SR, Clausell A, Bort SJ, Klebanoff SJ, Lewis DB. NFAT1 enhances HIV-1 gene expression in primary human CD4 T cells. *Clinical immunology.* 2000;94(3):179-191.

117. Jones KA, Kadonaga JT, Luciw PA, Tjian R. Activation of the AIDS retrovirus promoter by the cellular transcription factor, Sp1. *Science.* 1986;232(4751):755-759.

118. Harrich D, Garcia J, Wu F, Mitsuyasu R, Gonazalez J, Gaynor R. Role of SP1-binding domains in in vivo transcriptional regulation of the human immunodeficiency virus type 1 long terminal repeat. *Journal of virology.* 1989;63(6):2585-2591.

119. Weeks KM, Ampe C, Schultz SC, Steitz TA, Crothers DM. Fragments of the HIV-1 Tat protein specifically bind TAR RNA. *Science.* 1990;249(4974):1281-1285.

120. Wei P, Garber ME, Fang S-M, Fischer WH, Jones KA. A novel CDK9-associated C-type cyclin interacts directly with HIV-1 Tat and mediates its high-affinity, loop-specific binding to TAR RNA. *Cell.* 1998;92(4):451-462.

121. Isel C, Karn J. Direct evidence that HIV-1 Tat stimulates RNA polymerase II carboxyl-terminal domain hyperphosphorylation during transcriptional elongation. *Journal of molecular biology.* 1999;290(5):929-941.

122. Wang Z, Burge CB. Splicing regulation: from a parts list of regulatory elements to an integrated splicing code. *Rna.* 2008;14(5):802-813.

123. Nakielny S, Fischer U, Michael WM, Dreyfuss G. RNA transport. *Annual review of neuroscience.* 1997;20(1):269-301.

124. Purcell D, Martin MA. Alternative splicing of human immunodeficiency virus type 1 mRNA modulates viral protein expression, replication, and infectivity. *Journal of virology.* 1993;67(11):6365-6378.

125. Fischer U, Huber J, Boelens WC, Mattajt LW, Lührmann R. The HIV-1 Rev activation domain is a nuclear export signal that accesses an export pathway used by specific cellular RNAs. *Cell.* 1995;82(3):475-483.

126. Malim MH, Hauber J, Le S-Y, Maizel JV, Cullen BR. The HIV-1 rev trans-activator acts through a structured target sequence to activate nuclear export of unspliced viral mRNA. *Nature.* 1989;338(6212):254-257.

127. Fornerod M, Ohno M, Yoshida M, Mattaj IW. CRM1 is an export receptor for leucine-rich nuclear export signals. *Cell.* 1997;90(6):1051-1060.

128. Balvay L, Lastra ML, Sargueil B, Darlix J-L, Ohlmann T. Translational control of retroviruses. *Nature Reviews Microbiology.* 2007;5(2):128-140.

129. Ohlmann T, Lopez-Lastra M, Darlix J-L. An internal ribosome entry segment promotes translation of the simian immunodeficiency virus genomic RNA. *Journal of Biological Chemistry.* 2000;275(16):11899-11906.

130. Deffaud C, Darlix J-L. Rous sarcoma virus translation revisited: characterization of an internal ribosome entry segment in the 5′ leader of the genomic RNA. *Journal of Virology.* 2000;74(24):11581-11588.

131. Berlioz C, Darlix J-L. An internal ribosomal entry mechanism promotes translation of murine leukemia virus gag polyprotein precursors. *Journal of Virology.* 1995;69(4):2214-2222.

132. Buck CB, Shen X, Egan MA, Pierson TC, Walker CM, Siliciano RF. The human immunodeficiency virus type 1gag gene encodes an internal ribosome entry site. *Journal of virology.* 2001;75(1):181-191.

133. Bolinger C, Boris-Lawrie K. Mechanisms employed by retroviruses to exploit host factors for translational control of a complicated proteome. *Retrovirology.* 2009;6(1):8.

134. Miele G, Mouland A, Harrison GP, Cohen E, Lever A. The human immunodeficiency virus type 1 5'packaging signal structure affects translation but does not function as an internal ribosome entry site structure. *Journal of Virology.* 1996;70(2):944-951.

135. PAL R, REITZ JR MS, TSCHACHLER E, Gallo R, Sarngadharan M, DI MARZO VERONESE F. Myristoylation of gag proteins of HIV-1 plays an important role in virus assembly. *AIDS research and human retroviruses.* 1990;6(6):721-730.

136. Yoshinaka Y, Katoh I, Copeland TD, Oroszlan S. Murine leukemia virus protease is encoded by the gag-pol gene and is synthesized through suppression of an amber termination codon. *Proceedings of the National Academy of Sciences.* 1985;82(6):1618-1622.

137. Falk H, Mador N, Udi R, Panet A, Honigman A. Two cis-acting signals control ribosomal frameshift between human T-cell leukemia virus type II gag and pro genes. *Journal of virology.* 1993;67(10):6273-6277.

138. Jacks T, Varmus HE. Expression of the Rous sarcoma virus pol gene by ribosomal frameshifting. *Science.* 1985;230(4731):1237-1242.

139. Jacks T, Power MD, Masiarz FR, Luciw PA, Barr PJ, Varmus HE. Characterization of ribosomal frameshifting in HIV-1 gag-pol expression. *Nature.* 1988;331(6153):280-283.

140. Jacks T, Madhani HD, Masiarz FR, Varmus HE. Signals for ribosomal frameshifting in the Rous sarcoma virus gag-pol region. *Cell.* 1988;55(3):447-458.

141. Staple DW, Butcher SE. Solution structure and thermodynamic investigation of the HIV-1 frameshift inducing element. *Journal of molecular biology.* 2005;349(5):1011-1023.

142. Shehu-Xhilaga M, Crowe SM, Mak J. Maintenance of the Gag/Gag-Pol ratio is important for human immunodeficiency virus type 1 RNA dimerization and viral infectivity. *Journal of virology.* 2001;75(4):1834-1841.

143. Hunter E, Swanstrom R. Retrovirus envelope glycoproteins. In: *Retroviruses.* Springer; 1990:187-253.

144. McCune JM, Rabin LB, Feinberg MB, et al. Endoproteolytic cleavage of gp160 is required for the activation of human immunodeficiency virus. *Cell.* 1988;53(1):55-67.

145. Hallenberger S, Bosch V, Angliker H, Shaw E, Klenk H-D, Garten W. Inhibition of furin-mediated cleavage activation of HIV-1 glycoprotein gpl60. *Nature.* 1992;360(6402):358-361.

146. Doores KJ, Bonomelli C, Harvey DJ, et al. Envelope glycans of immunodeficiency virions are almost entirely oligomannose antigens. *Proceedings of the National Academy of Sciences.* 2010;107(31):13800-13805.

147. Bernstein HB, Tucker SP, Hunter E, Schutzbach JS, Compans RW. Human immunodeficiency virus type 1 envelope glycoprotein is modified by O-linked oligosaccharides. *Journal of virology.* 1994;68(1):463-468.

148. Allan J, Coligan J, Barin F, et al. Major glycoprotein antigens that induce antibodies in AIDS patients are encoded by HTLV-III. *Science.* 1985;228(4703):1091-1094.

149. Leonard CK, Spellman MW, Riddle L, Harris RJ, Thomas JN, Gregory T. Assignment of intrachain disulfide bonds and characterization of potential glycosylation sites of the type 1 recombinant human immunodeficiency virus envelope glycoprotein (gp120) expressed in Chinese hamster ovary cells. *Journal of Biological Chemistry.* 1990;265(18):10373-10382.

150. Wang W, Nie J, Prochnow C, et al. A systematic study of the N-glycosylation sites of HIV-1 envelope protein on infectivity and antibody-mediated neutralization. *Retrovirology.* 2013;10(1):14.

151. Wei X, Decker JM, Wang S, et al. Antibody neutralization and escape by HIV-1. *Nature.* 2003;422(6929):307-312.

152. Stewart-Jones GB, Soto C, Lemmin T, et al. Trimeric HIV-1-Env structures define glycan shields from clades A, B, and G. *Cell.* 2016;165(4):813-826.

153. Reitter JN, Means RE, Desrosiers RC. A role for carbohydrates in immune evasion in AIDS. *Nature medicine.* 1998;4(6):679-684.

154. Simmonds P, Balfe P, Ludlam C, Bishop J, Brown A. Analysis of sequence diversity in hypervariable regions of the external glycoprotein of human immunodeficiency virus type 1. *Journal of virology.* 1990;64(12):5840-5850.

155. Shioda T, Levy JA, Cheng-Mayer C. Small amino acid changes in the V3 hypervariable region of gp120 can affect the T-cell-line and macrophage tropism of human immunodeficiency virus type 1. *Proceedings of the National Academy of Sciences.* 1992;89(20):9434-9438.

156. Freed EO, Myers DJ, Risser R. Characterization of the fusion domain of the human immunodeficiency virus type 1 envelope glycoprotein gp41. *Proceedings of the National Academy of Sciences.* 1990;87(12):4650-4654.

157. Pinter A, Honnen WJ, Tilley SA, et al. Oligomeric structure of gp41, the transmembrane protein of human immunodeficiency virus type 1. *Journal of virology.* 1989;63(6):2674-2679.

158. Göttlinger HG. The HIV-1 assembly machine. *Aids.* 2001;15:S13-S20.

159. Callahan EM, Wills JW. Repositioning basic residues in the M domain of the Rous sarcoma virus gag protein. *Journal of Virology.* 2000;74(23):11222-11229.

160. Zhou W, Parent LJ, Wills JW, Resh MD. Identification of a membrane-binding domain within the amino-terminal region of human immunodeficiency virus type 1

Gag protein which interacts with acidic phospholipids. *Journal of virology.* 1994;68(4):2556-2569.

161. Göttlinger HG, Sodroski JG, Haseltine WA. Role of capsid precursor processing and myristoylation in morphogenesis and infectivity of human immunodeficiency virus type 1. *Proceedings of the National Academy of Sciences.* 1989;86(15):5781-5785.

162. Saad JS, Miller J, Tai J, Kim A, Ghanam RH, Summers MF. Structural basis for targeting HIV-1 Gag proteins to the plasma membrane for virus assembly. *Proceedings of the National Academy of Sciences.* 2006;103(30):11364-11369.

163. Ono A, Ablan SD, Lockett SJ, Nagashima K, Freed EO. Phosphatidylinositol (4, 5) bisphosphate regulates HIV-1 Gag targeting to the plasma membrane. *Proceedings of the National Academy of Sciences.* 2004;101(41):14889-14894.

164. Ono A, Freed EO. Plasma membrane rafts play a critical role in HIV-1 assembly and release. *Proceedings of the National Academy of Sciences.* 2001;98(24):13925-13930.

165. Puryear WB, Yu X, Ramirez NP, Reinhard BM, Gummuluru S. HIV-1 incorporation of host-cell–derived glycosphingolipid GM3 allows for capture by mature dendritic cells. *Proceedings of the National Academy of Sciences.* 2012;109(19):7475-7480.

166. Izquierdo-Useros N, Lorizate M, Puertas MC, et al. Siglec-1 is a novel dendritic cell receptor that mediates HIV-1 trans-infection through recognition of viral membrane gangliosides. *PLoS Biol.* 2012;10(12):e1001448.

167. Puryear WB, Akiyama H, Geer SD, et al. Interferon-inducible mechanism of dendritic cell-mediated HIV-1 dissemination is dependent on Siglec-1/CD169. *PLoS Pathog.* 2013;9(4):e1003291.

168. Hatch SC, Archer J, Gummuluru S. Glycosphingolipid composition of human immunodeficiency virus type 1 (HIV-1) particles is a crucial determinant for dendritic cell-mediated HIV-1 trans-infection. *Journal of virology.* 2009;83(8):3496-3506.

169. Akiyama H, Miller C, Patel HV, et al. Virus particle release from glycosphingolipid-enriched microdomains is essential for dendritic cell-mediated capture and transfer of HIV-1 and henipavirus. *Journal of virology.* 2014;88(16):8813-8825.

170. Accola MA, Höglund S, Göttlinger HG. A putative α-helical structure which overlaps the capsid-p2 boundary in the human immunodeficiency virus type 1 Gag precursor is crucial for viral particle assembly. *Journal of Virology.* 1998;72(3):2072-2078.

171. Yu X, Yuan X, Matsuda Z, Lee TH, Essex M. The matrix protein of human immunodeficiency virus type 1 is required for incorporation of viral envelope protein into mature virions. *Journal of virology.* 1992;66(8):4966-4971.

172. Yu X, Yuan X, Mclane MF, Lee TH, Essex M. Mutations in the cytoplasmic domain of human immunodeficiency virus type 1 transmembrane protein impair the incorporation of Env proteins into mature virions. *Journal of virology.* 1993;67(1):213-221.

173. Freed EO, Martin MA. Domains of the human immunodeficiency virus type 1 matrix and gp41 cytoplasmic tail required for envelope incorporation into virions. *Journal of virology.* 1996;70(1):341-351.

174. Lee Y-M, Tang X-B, Cimakasky LM, Hildreth J, Yu X-F. Mutations in the matrix protein of human immunodeficiency virus type 1 inhibit surface expression and virion incorporation of viral envelope glycoproteins in CD4+ T lymphocytes. *Journal of virology.* 1997;71(2):1443-1452.

175. Wyma DJ, Kotov A, Aiken C. Evidence for a stable interaction of gp41 with Pr55Gag in immature human immunodeficiency virus type 1 particles. *Journal of virology.* 2000;74(20):9381-9387.

176. Mammano F, Kondo E, Sodroski J, Bukovsky A, Göttlinger H. Rescue of human immunodeficiency virus type 1 matrix protein mutants by envelope glycoproteins with short cytoplasmic domains. *Journal of virology.* 1995;69(6):3824-3830.

177. Paxton W, Connor R, Landau N. Incorporation of Vpr into human immunodeficiency virus type 1 virions: requirement for the p6 region of gag and mutational analysis. *Journal of virology.* 1993;67(12):7229-7237.

178. Yu X-F, Matsuda M, Essex M, Lee TH. Open reading frame vpr of simian immunodeficiency virus encodes a virion-associated protein. *Journal of virology.* 1990;64(11):5688-5693.

179. Cohen EA, Dehni G, Sodroski JG, Haseltine WA. Human immunodeficiency virus vpr product is a virion-associated regulatory protein. *Journal of virology.* 1990;64(6):3097-3099.

180. Tremblay MJ, Fortin J-F, Cantin R. The acquisition of host-encoded proteins by nascent HIV-1. *Immunology today.* 1998;19(8):346-351.

181. Franke EK, Yuan HEH, Luban J. Specific incorporation of cyclophilin A into HIV-1 virions. *Nature.* 1994;372(6504):359-362.

182. Luban J. Absconding with the chaperone: essential cyclophilin–Gag interaction in HIV-1 virions. *Cell.* 1996;87(7):1157-1159.

183. Lu M, Hou G, Zhang H, et al. Dynamic allostery governs cyclophilin A–HIV capsid interplay. *Proceedings of the National Academy of Sciences.* 2015;112(47):14617-14622.

184. Thali M, Bukovsky A, Kondo E, et al. Functional association of cyclophilin A with HIV-1 virions. *Nature.* 1994;372(6504):363-365.

185. D'Souza V, Summers MF. How retroviruses select their genomes. *Nature Reviews Microbiology.* 2005;3(8):643-655.

186. Paillart J-C, Shehu-Xhilaga M, Marquet R, Mak J. Dimerization of retroviral RNA genomes: an inseparable pair. *Nature Reviews Microbiology.* 2004;2(6):461-472.

187. Harrison GP, Lever A. The human immunodeficiency virus type 1 packaging signal and major splice donor region have a conserved stable secondary structure. *Journal of virology.* 1992;66(7):4144-4153.

188. Berkowitz RD, Ohagen A, Höglund S, Goff SP. Retroviral nucleocapsid domains mediate the specific recognition of genomic viral RNAs by chimeric Gag polyproteins during RNA packaging in vivo. *Journal of virology.* 1995;69(10):6445-6456.

189. De Guzman RN, Wu ZR, Stalling CC, Pappalardo L, Borer PN, Summers MF. Structure of the HIV-1 nucleocapsid protein bound to the SL3 Ψ-RNA recognition element. *Science.* 1998;279(5349):384-388.

190. Clever JL, Parslow TG. Mutant human immunodeficiency virus type 1 genomes with defects in RNA dimerization or encapsidation. *Journal of virology.* 1997;71(5):3407-3414.

191. McBride MS, Panganiban AT. The human immunodeficiency virus type 1 encapsidation site is a multipartite RNA element composed of functional hairpin structures. *Journal of virology.* 1996;70(5):2963-2973.

192. Berkhout B, Van Wamel J. Role of the DIS hairpin in replication of human immunodeficiency virus type 1. *Journal of Virology.* 1996;70(10):6723-6732.

193. Paillart J-C, Skripkin E, Ehresmann B, Ehresmann C, Marquet R. A loop-loop" kissing" complex is the essential part of the dimer linkage of genomic HIV-1 RNA. *Proceedings of the National Academy of Sciences.* 1996;93(11):5572-5577.

194. Skripkin E, Paillart J-C, Marquet R, Ehresmann B, Ehresmann C. Identification of the primary site of the human immunodeficiency virus type 1 RNA dimerization in vitro. *Proceedings of the National Academy of Sciences.* 1994;91(11):4945-4949.

195. Abbink TE, Berkhout B. A novel long distance base-pairing interaction in human immunodeficiency virus type 1 RNA occludes the Gag start codon. *Journal of Biological Chemistry.* 2003;278(13):11601-11611.

196. Huthoff H, Berkhout B. Two alternating structures of the HIV-1 leader RNA. *Rna.* 2001;7(1):143-157.

197. Huthoff H, Berkhout B. Mutations in the TAR hairpin affect the equilibrium between alternative conformations of the HIV-1 leader RNA. *Nucleic acids research.* 2001;29(12):2594-2600.

198. Berkhout B, Ooms M, Beerens N, Huthoff H, Southern E, Verhoef K. In vitro evidence that the untranslated leader of the HIV-1 genome is an RNA checkpoint that regulates multiple functions through conformational changes. *Journal of Biological Chemistry.* 2002;277(22):19967-19975.

199. Cimarelli A, Sandin S, Höglund S, Luban J. Basic residues in human immunodeficiency virus type 1 nucleocapsid promote virion assembly via interaction with RNA. *Journal of virology.* 2000;74(7):3046-3057.

200. Rein A, Henderson LE, Levin JG. Nucleic-acid-chaperone activity of retroviral nucleocapsid proteins: significance for viral replication. *Trends in biochemical sciences.* 1998;23(8):297-301.

201. Wang H, Norris KM, Mansky LM. Involvement of the matrix and nucleocapsid domains of the bovine leukemia virus Gag polyprotein precursor in viral RNA packaging. *Journal of virology.* 2003;77(17):9431-9438.

202. Poon DT, Li G, Aldovini A. Nucleocapsid and matrix protein contributions to selective human immunodeficiency virus type 1 genomic RNA packaging. *Journal of Virology.* 1998;72(3):1983-1993.

203. Lodmell JS, Ehresmann C, Ehresmann B, Marquet R. Convergence of natural and artificial evolution on an RNA loop-loop interaction: the HIV-1 dimerization initiation site. *Rna.* 2000;6(9):1267-1276.

204. Fu W, Rein A. Maturation of dimeric viral RNA of Moloney murine leukemia virus. *Journal of Virology.* 1993;67(9):5443-5449.

205. Fu W, Gorelick RJ, Rein A. Characterization of human immunodeficiency virus type 1 dimeric RNA from wild-type and protease-defective virions. *Journal of Virology.* 1994;68(8):5013-5018.

206. Cromer D, Grimm AJ, Schlub TE, Mak J, Davenport MP. Estimating the in-vivo HIV template switching and recombination rate. *Aids.* 2016;30(2):185-192.

207. Levy DN, Aldrovandi GM, Kutsch O, Shaw GM. Dynamics of HIV-1 recombination in its natural target cells. *Proceedings of the National Academy of Sciences.* 2004;101(12):4204-4209.

208. Zhuang J, Jetzt AE, Sun G, et al. Human immunodeficiency virus type 1 recombination: rate, fidelity, and putative hot spots. *Journal of virology.* 2002;76(22):11273-11282.

209. Burke DS. Recombination in HIV: an important viral evolutionary strategy. *Emerging infectious diseases.* 1997;3(3):253.

210. Göttlinger HG, Dorfman T, Sodroski JG, Haseltine WA. Effect of mutations affecting the p6 gag protein on human immunodeficiency virus particle release. *Proceedings of the National Academy of Sciences.* 1991;88(8):3195-3199.

211. Strack B, Calistri A, Craig S, Popova E, Göttlinger HG. AIP1/ALIX is a binding partner for HIV-1 p6 and EIAV p9 functioning in virus budding. *Cell.* 2003;114(6):689-699.

212. Usami Y, Popov S, Popova E, Inoue M, Weissenhorn W, G Göttlinger H. The ESCRT pathway and HIV-1 budding. *Biochemical Society Transactions.* 2009;37(1):181-184.

213. Popov S, Popova E, Inoue M, Göttlinger HG. Human immunodeficiency virus type 1 Gag engages the Bro1 domain of ALIX/AIP1 through the nucleocapsid. *Journal of virology.* 2008;82(3):1389-1398.

214. Hurley JH, Hanson PI. Membrane budding and scission by the ESCRT machinery: it's all in the neck. *Nature reviews Molecular cell biology.* 2010;11(8):556-566.

215. Carlton JG, Agromayor M, Martin-Serrano J. Differential requirements for Alix and ESCRT-III in cytokinesis and HIV-1 release. *Proceedings of the National Academy of Sciences.* 2008;105(30):10541-10546.

216. Baumgärtel V, Ivanchenko S, Dupont A, et al. Live-cell visualization of dynamics of HIV budding site interactions with an ESCRT component. *Nature cell biology.* 2011;13(4):469-474.

217. Loeb D, Hutchison C, Edgell M, Farmerie W, Swanstrom R. Mutational analysis of human immunodeficiency virus type 1 protease suggests functional homology with aspartic proteinases. *Journal of virology.* 1989;63(1):111-121.

218. Meek TD, Dayton BD, Metcalf BW, et al. Human immunodeficiency virus 1 protease expressed in Escherichia coli behaves as a dimeric aspartic protease. *Proceedings of the National Academy of Sciences.* 1989;86(6):1841-1845.

219. Pettit SC, Sheng N, Tritch R, Erickson-Viitanen S, Swanstrom R. The regulation of sequential processing of HIV-1 Gag by the viral protease. In: *Aspartic Proteinases.* Springer; 1998:15-25.

220. ERICKSON-VIITANEN S, MANFREDI J, VIITANEN P, et al. Cleavage of HIV-1 gag polyprotein synthesized in vitro: sequential cleavage by the viral protease. *AIDS research and human retroviruses.* 1989;5(6):577-591.

221. Witte ON, Baltimore D. Relationship of retrovirus polyprotein cleavages to virion maturation studied with temperature-sensitive murine leukemia virus mutants. *Journal of virology.* 1978;26(3):750-761.

222. Tritel M, Resh MD. Kinetic analysis of human immunodeficiency virus type 1 assembly reveals the presence of sequential intermediates. *Journal of Virology.* 2000;74(13):5845-5855.

223. Peng C, Ho B, Chang T, Chang NT. Role of human immunodeficiency virus type 1-specific protease in core protein maturation and viral infectivity. *Journal of virology.* 1989;63(6):2550-2556.

224. Kohl NE, Emini EA, Schleif WA, et al. Active human immunodeficiency virus protease is required for viral infectivity. *Proceedings of the National Academy of Sciences.* 1988;85(13):4686-4690.

225. Crawford S, Goff SP. A deletion mutation in the 5'part of the pol gene of Moloney murine leukemia virus blocks proteolytic processing of the gag and pol polyproteins. *Journal of virology.* 1985;53(3):899-907.

226. Wills JW, Craven RC. Form, function, and use of retroviral gag proteins. *Aids.* 1991;5(6):639-654.

227. von Schwedler UK, Stemmler TL, Klishko VY, et al. Proteolytic refolding of the HIV-1 capsid protein amino-terminus facilitates viral core assembly. *The EMBO journal.* 1998;17(6):1555-1568.

228. Summers MF, Henderson LE, Chance MR, et al. Nucleocapsid zinc fingers detected in retroviruses: EXAFS studies of intact viruses and the solution-state structure of the nucleocapsid protein from HIV-1. *Protein Science.* 1992;1(5):563-574.

229. South TL, Blake PR, Sowder III RC, Arthur LO, Henderson LE, Summers MF. The nucleocapsid protein isolated from HIV-1 particles binds zinc and forms retroviral-type zinc fingers. *Biochemistry.* 1990;29(34):7786-7789.

230. Méric C, Darlix J-L, Spahr P-F. It is Rous sarcoma virus protein P12 and not P19 that binds tightly to Rous sarcoma virus RNA. *Journal of molecular biology.* 1984;173(4):531-538.

231. Vogt VM, Simon MN. Mass determination of Rous sarcoma virus virions by scanning transmission electron microscopy. *Journal of virology.* 1999;73(8):7050-7055.

232. Urbaneja MaA, Kane BP, Johnson DG, Gorelick RJ, Henderson LE, Casas-Finet JR. Binding properties of the human immunodeficiency virus type 1 nucleocapsid protein p7 to a model RNA: elucidation of the structural determinants for function. *Journal of molecular biology.* 1999;287(1):59-75.

233. Levin JG, Guo J, Rouzina I, Musier-Forsyth K. Nucleic acid chaperone activity of HIV-1 nucleocapsid protein: Critical role in reverse transcription and molecular mechanism. *Progress in nucleic acid research and molecular biology.* 2005;80:217-286.

234. Karpel R, Henderson LE, Oroszlan S. Interactions of retroviral structural proteins with single-stranded nucleic acids. *Journal of Biological Chemistry.* 1987;262(11):4961-4967.

235. Fisher RJ, Rein A, Fivash M, et al. Sequence-specific binding of human immunodeficiency virus type 1 nucleocapsid protein to short oligonucleotides. *Journal of virology.* 1998;72(3):1902-1909.

236. Chertova E, Chertov O, Coren LV, et al. Proteomic and biochemical analysis of purified human immunodeficiency virus type 1 produced from infected monocyte-derived macrophages. *Journal of virology.* 2006;80(18):9039-9052.

237. Levin JG, Mitra M, Mascarenhas A, Musier-Forsyth K. Role of HIV-1 nucleocapsid protein in HIV-1 reverse transcription. *RNA biology.* 2010;7(6):754-774.

238. Hargittai MR, Gorelick RJ, Rouzina I, Musier-Forsyth K. Mechanistic insights into the kinetics of HIV-1 nucleocapsid protein-facilitated tRNA annealing to the primer binding site. *Journal of molecular biology.* 2004;337(4):951-968.

239. Feng Y-X, Campbell S, Harvin D, Ehresmann B, Ehresmann C, Rein A. The human immunodeficiency virus type 1 Gag polyprotein has nucleic acid chaperone activity: possible role in dimerization of genomic RNA and placement of tRNA on the primer binding site. *Journal of Virology.* 1999;73(5):4251-4256.

240. Cen S, Huang Y, Khorchid A, Darlix J-L, Wainberg MA, Kleiman L. The role of Pr55 gag in the annealing of tRNA3 Lys to human immunodeficiency virus type 1 genomic RNA. *Journal of Virology.* 1999;73(5):4485-4488.

241. Simon V, Bloch N, Landau NR. Intrinsic host restrictions to HIV-1 and mechanisms of viral escape. *Nature immunology.* 2015;16(6):546-553.

242. Malim MH, Emerman M. HIV-1 accessory proteins—ensuring viral survival in a hostile environment. *Cell host & microbe.* 2008;3(6):388-398.

243. Malim MH, Bieniasz PD. HIV restriction factors and mechanisms of evasion. *Cold Spring Harbor perspectives in medicine.* 2012;2(5):a006940.

244. Soros VB, Yonemoto W, Greene WC. Newly synthesized APOBEC3G is incorporated into HIV virions, inhibited by HIV RNA, and subsequently activated by RNase H. *PLoS Pathog.* 2007;3(2):e15.

245. Bogerd HP, Cullen BR. Single-stranded RNA facilitates nucleocapsid: APOBEC3G complex formation. *Rna.* 2008;14(6):1228-1236.

246. Sheehy AM, Gaddis NC, Choi JD, Malim MH. Isolation of a human gene that inhibits HIV-1 infection and is suppressed by the viral Vif protein. *Nature.* 2002;418(6898):646-650.

247. Strebel K, Daugherty D, Clouse K, Cohen D, Folks T, Martin MA. The HIV A (sor) gene product is essential for virus infectivity. *Nature.* 1987;328(6132):728-730.

248. Sawyer SL, Emerman M, Malik HS. Ancient adaptive evolution of the primate antiviral DNA-editing enzyme APOBEC3G. *PLoS Biol.* 2004;2(9):e275.

249. Jarmuz A, Chester A, Bayliss J, et al. An anthropoid-specific locus of orphan C to U RNA-editing enzymes on chromosome 22. *Genomics.* 2002;79(3):285-296.

250. Zhang H, Yang B, Pomerantz RJ, Zhang C, Arunachalam SC, Gao L. The cytidine deaminase CEM15 induces hypermutation in newly synthesized HIV-1 DNA. *Nature.* 2003;424(6944):94-98.

251. Yu Q, König R, Pillai S, et al. Single-strand specificity of APOBEC3G accounts for minus-strand deamination of the HIV genome. *Nature structural & molecular biology.* 2004;11(5):435-442.

252. Mangeat B, Turelli P, Caron G, Friedli M, Perrin L, Trono D. Broad antiretroviral defence by human APOBEC3G through lethal editing of nascent reverse transcripts. *Nature.* 2003;424(6944):99-103.

253. Refsland EW, Stenglein MD, Shindo K, Albin JS, Brown WL, Harris RS. Quantitative profiling of the full APOBEC3 mRNA repertoire in lymphocytes and

tissues: implications for HIV-1 restriction. *Nucleic acids research.* 2010;38(13):4274-4284.

254. Hu C, Saenz DT, Fadel HJ, Walker W, Peretz M, Poeschla EM. The HIV-1 central polypurine tract functions as a second line of defense against APOBEC3G/F. *Journal of virology.* 2010;84(22):11981-11993.

255. Yu X, Yu Y, Liu B, et al. Induction of APOBEC3G ubiquitination and degradation by an HIV-1 Vif-Cul5-SCF complex. *Science.* 2003;302(5647):1056-1060.

256. Mehle A, Goncalves J, Santa-Marta M, McPike M, Gabuzda D. Phosphorylation of a novel SOCS-box regulates assembly of the HIV-1 Vif-Cul5 complex that promotes APOBEC3G degradation. *Genes & development.* 2004;18(23):2861-2866.

257. Mariani R, Chen D, Schröfelbauer B, et al. Species-specific exclusion of APOBEC3G from HIV-1 virions by Vif. *Cell.* 2003;114(1):21-31.

258. Gao D, Wu J, Wu Y-T, et al. Cyclic GMP-AMP synthase is an innate immune sensor of HIV and other retroviruses. *Science.* 2013;341(6148):903-906.

259. Yan N, Regalado-Magdos AD, Stiggelbout B, Lee-Kirsch MA, Lieberman J. The cytosolic exonuclease TREX1 inhibits the innate immune response to human immunodeficiency virus type 1. *Nature immunology.* 2010;11(11):1005-1013.

260. Stetson DB, Ko JS, Heidmann T, Medzhitov R. Trex1 prevents cell-intrinsic initiation of autoimmunity. *Cell.* 2008;134(4):587-598.

261. Unterholzner L, Keating SE, Baran M, et al. IFI16 is an innate immune sensor for intracellular DNA. *Nature immunology.* 2010;11(11):997-1004.

262. Monroe KM, Yang Z, Johnson JR, et al. IFI16 DNA sensor is required for death of lymphoid CD4 T cells abortively infected with HIV. *Science.* 2014;343(6169):428-432.

263. Doitsh G, Galloway NL, Geng X, et al. Cell death by pyroptosis drives CD4 T-cell depletion in HIV-1 infection. *Nature.* 2014;505(7484):509-514.

264. Lahouassa H, Daddacha W, Hofmann H, et al. SAMHD1 restricts the replication of human immunodeficiency virus type 1 by depleting the intracellular pool of deoxynucleoside triphosphates. *Nature immunology.* 2012;13(3):223-228.

265. Kim B, Nguyen LA, Daddacha W, Hollenbaugh JA. Tight interplay among SAMHD1 protein level, cellular dNTP levels, and HIV-1 proviral DNA synthesis kinetics in human primary monocyte-derived macrophages. *Journal of Biological Chemistry.* 2012;287(26):21570-21574.

266. Hrecka K, Hao C, Gierszewska M, et al. Vpx relieves inhibition of HIV-1 infection of macrophages mediated by the SAMHD1 protein. *Nature.* 2011;474(7353):658-661.

267. Laguette N, Sobhian B, Casartelli N, et al. SAMHD1 is the dendritic-and myeloid-cell-specific HIV-1 restriction factor counteracted by Vpx. *Nature.* 2011;474(7353):654-657.

268. St Gelais C, de Silva S, Amie SM, et al. SAMHD1 restricts HIV-1 infection in dendritic cells (DCs) by dNTP depletion, but its expression in DCs and primary CD4+ T-lymphocytes cannot be upregulated by interferons. *Retrovirology.* 2012;9(1):105.

269. Baldauf H-M, Pan X, Erikson E, et al. SAMHD1 restricts HIV-1 infection in resting CD4+ T cells. *Nature medicine.* 2012;18(11):1682-1688.

270. Usami Y, Wu Y, Göttlinger HG. SERINC3 and SERINC5 restrict HIV-1 infectivity and are counteracted by Nef. *Nature.* 2015;526(7572):218-223.
271. Dai W, Usami Y, Wu Y, Göttlinger H. A long cytoplasmic loop governs the sensitivity of the anti-viral host protein SERINC5 to HIV-1 Nef. *Cell reports.* 2018;22(4):869-875.
272. Shi J, Xiong R, Zhou T, et al. HIV-1 Nef antagonizes SERINC5 restriction by downregulation of SERINC5 via the endosome/lysosome system. *Journal of virology.* 2018;92(11):e00196-00118.
273. Roeth JF, Williams M, Kasper MR, Filzen TM, Collins KL. HIV-1 Nef disrupts MHC-I trafficking by recruiting AP-1 to the MHC-I cytoplasmic tail. *J Cell Biol.* 2004;167(5):903-913.
274. Wonderlich ER, Williams M, Collins KL. The tyrosine binding pocket in the adaptor protein 1 (AP-1) mu1 subunit is necessary for Nef to recruit AP-1 to the major histocompatibility complex class I cytoplasmic tail. *The Journal of biological chemistry.* 2008;283(6):3011-3022.
275. Wonderlich ER, Leonard JA, Kulpa DA, Leopold KE, Norman JM, Collins KL. ADP ribosylation factor 1 activity is required to recruit AP-1 to the major histocompatibility complex class I (MHC-I) cytoplasmic tail and disrupt MHC-I trafficking in HIV-1-infected primary T cells. *Journal of virology.* 2011;85(23):12216-12226.
276. Schaefer MR, Wonderlich ER, Roeth JF, Leonard JA, Collins KL. HIV-1 Nef targets MHC-I and CD4 for degradation via a final common beta-COP-dependent pathway in T cells. *PLoS Pathog.* 2008;4(8):e1000131.
277. Collins KL, Chen BK, Kalams SA, Walker BD, Baltimore D. HIV-1 Nef protein protects infected primary cells against killing by cytotoxic T lymphocytes. *Nature.* 1998;391(6665):397-401.
278. Jin YJ, Cai CY, Zhang X, Zhang HT, Hirst JA, Burakoff SJ. HIV Nef-mediated CD4 down-regulation is adaptor protein complex 2 dependent. *J Immunol.* 2005;175(5):3157-3164.
279. Stremlau M, Owens CM, Perron MJ, Kiessling M, Autissier P, Sodroski J. The cytoplasmic body component TRIM5α restricts HIV-1 infection in Old World monkeys. *Nature.* 2004;427(6977):848-853.
280. Perron MJ, Stremlau M, Song B, Ulm W, Mulligan RC, Sodroski J. TRIM5α mediates the postentry block to N-tropic murine leukemia viruses in human cells. *Proceedings of the National Academy of Sciences.* 2004;101(32):11827-11832.
281. Keckesova Z, Ylinen LM, Towers GJ. The human and African green monkey TRIM5α genes encode Ref1 and Lv1 retroviral restriction factor activities. *Proceedings of the National Academy of Sciences.* 2004;101(29):10780-10785.
282. Hatziioannou T, Perez-Caballero D, Yang A, Cowan S, Bieniasz PD. Retrovirus resistance factors Ref1 and Lv1 are species-specific variants of TRIM5α. *Proceedings of the National Academy of Sciences.* 2004;101(29):10774-10779.
283. Stremlau M, Perron M, Lee M, et al. Specific recognition and accelerated uncoating of retroviral capsids by the TRIM5α restriction factor. *Proceedings of the National Academy of Sciences.* 2006;103(14):5514-5519.
284. Hatziioannou T, Princiotta M, Piatak M, et al. Generation of simian-tropic HIV-1 by restriction factor evasion. *Science.* 2006;314(5796):95-95.

285. Van Damme N, Goff D, Katsura C, et al. The interferon-induced protein BST-2 restricts HIV-1 release and is downregulated from the cell surface by the viral Vpu protein. *Cell host & microbe.* 2008;3(4):245-252.

286. Neil SJ, Zang T, Bieniasz PD. Tetherin inhibits retrovirus release and is antagonized by HIV-1 Vpu. *Nature.* 2008;451(7177):425-430.

287. Neil SJ, Sandrin V, Sundquist WI, Bieniasz PD. An interferon-α-induced tethering mechanism inhibits HIV-1 and Ebola virus particle release but is counteracted by the HIV-1 Vpu protein. *Cell host & microbe.* 2007;2(3):193-203.

288. Neil SJ, Eastman SW, Jouvenet N, Bieniasz PD. HIV-1 Vpu promotes release and prevents endocytosis of nascent retrovirus particles from the plasma membrane. *PLoS Pathog.* 2006;2(5):e39.

289. Zhang F, Wilson SJ, Landford WC, et al. Nef proteins from simian immunodeficiency viruses are tetherin antagonists. *Cell host & microbe.* 2009;6(1):54-67.

290. Jia B, Serra-Moreno R, Neidermyer Jr W, et al. Species-specific activity of SIV Nef and HIV-1 Vpu in overcoming restriction by tetherin/BST2. *PLoS Pathog.* 2009;5(5):e1000429.

291. Le Tortorec A, Neil SJ. Antagonism to and intracellular sequestration of human tetherin by the human immunodeficiency virus type 2 envelope glycoprotein. *Journal of virology.* 2009;83(22):11966-11978.

292. Gupta RK, Mlcochova P, Pelchen-Matthews A, et al. Simian immunodeficiency virus envelope glycoprotein counteracts tetherin/BST-2/CD317 by intracellular sequestration. *Proceedings of the National Academy of Sciences.* 2009;106(49):20889-20894.

293. Miles RJ, Kerridge C, Hilditch L, Monit C, Jacques DA, Towers GJ. MxB sensitivity of HIV-1 is determined by a highly variable and dynamic capsid surface. *Elife.* 2020;9:e56910.

294. Kane M, Yadav SS, Bitzegeio J, et al. MX2 is an interferon-induced inhibitor of HIV-1 infection. *Nature.* 2013;502(7472):563-566.

295. Fricke T, White TE, Schulte B, et al. MxB binds to the HIV-1 core and prevents the uncoating process of HIV-1. *Retrovirology.* 2014;11(1):68.

296. Alvarez FJ, He S, Perilla JR, et al. CryoEM structure of MxB reveals a novel oligomerization interface critical for HIV restriction. *Science advances.* 2017;3(9):e1701264.

297. Lu J, Pan Q, Rong L, Liu S-L, Liang C. The IFITM proteins inhibit HIV-1 infection. *Journal of virology.* 2011;85(5):2126-2137.

298. Takata MA, Gonçalves-Carneiro D, Zang TM, et al. CG dinucleotide suppression enables antiviral defence targeting non-self RNA. *Nature.* 2017;550(7674):124-127.

299. Control CfD. Pneumocystis pneumonia Los Angeles. *MMWR.* 1981;30:250-252.

300. Barré-Sinoussi F, Chermann J-C, Rey F, et al. Isolation of a T-lymphotropic retrovirus from a patient at risk for acquired immune deficiency syndrome (AIDS). *Science.* 1983;220(4599):868-871.

301. Levy JA, Hoffman AD, Kramer SM, Landis JA, Shimabukuro JM, Oshiro LS. Isolation of lymphocytopathic retroviruses from San Francisco patients with AIDS. *Science.* 1984;225(4664):840-842.

302. Popovic M, Sarngadharan MG, Read E, Gallo RC. Detection, isolation, and continuous production of cytopathic retroviruses (HTLV-III) from patients with AIDS and pre-AIDS. *Science.* 1984;224(4648):497-500.
303. Sarngadharan MG, Popovic M, Bruch L, Schupbach J, Gallo RC. Antibodies reactive with human T-lymphotropic retroviruses (HTLV-III) in the serum of patients with AIDS. *Science.* 1984;224(4648):506-508.
304. Coffin J, Haase A, Levy JA, et al. Human immunodeficiency viruses. *Science.* 1986;232(4751):697-697.
305. Kappes JC, Morrow CD, Lee S-W, et al. Identification of a novel retroviral gene unique to human immunodeficiency virus type 2 and simian immunodeficiency virus SIVMAC. *Journal of virology.* 1988;62(9):3501-3505.
306. Cohen EA, Terwilliger EF, Sodroski JG, Haseltine WA. Identification of a protein encoded by the vpu gene of HIV-1. *Nature.* 1988;334(6182):532-534.
307. Robertson DL, Anderson J, Bradac J, et al. HIV-1 nomenclature proposal. *Science.* 2000;288(5463):55-55.
308. Foley BT, Leitner T, Paraskevis D, Peeters M. Primate immunodeficiency virus classification and nomenclature. *Infection, Genetics and Evolution.* 2016;46:150-158.
309. Royce RA, Sena A, Cates Jr W, Cohen MS. Sexual transmission of HIV. *New England Journal of Medicine.* 1997;336(15):1072-1078.
310. Shaw GM, Hunter E. HIV transmission. *Cold Spring Harbor perspectives in medicine.* 2012;2(11):a006965.
311. Fowler MG, Simonds R, Roongpisuthipong A. Update on perinatal HIV transmission. *Pediatric Clinics of North America.* 2000;47(1):21-38.
312. Hecht FM, Busch MP, Rawal B, et al. Use of laboratory tests and clinical symptoms for identification of primary HIV infection. *Aids.* 2002;16(8):1119-1129.
313. Hoenigl M, Green N, Camacho M, et al. Signs or symptoms of acute HIV infection in a cohort undergoing community-based screening. *Emerging infectious diseases.* 2016;22(3):532.
314. Chouquet C, Autran B, Gomard E, et al. Correlation between breadth of memory HIV-specific cytotoxic T cells, viral load and disease progression in HIV infection. *Aids.* 2002;16(18):2399-2407.
315. Musey L, Hughes J, Schacker T, Shea T, Corey L, Mcelrath MJ. Cytotoxic-T-cell responses, viral load, and disease progression in early human immunodeficiency virus type 1 infection. *New England Journal of Medicine.* 1997;337(18):1267-1274.
316. Saag MS, Holodniy M, Kuritzkes D, et al. HIV viral load markers in clinical practice. *Nature medicine.* 1996;2(6):625-629.
317. Ndhlovu ZM, Kamya P, Mewalal N, et al. Magnitude and kinetics of CD8+ T cell activation during hyperacute HIV infection impact viral set point. *Immunity.* 2015;43(3):591-604.
318. Wei X, Ghosh SK, Taylor ME, et al. Viral dynamics in human immunodeficiency virus type 1 infection. *Nature.* 1995;373(6510):117-122.
319. Perelson AS, Neumann AU, Markowitz M, Leonard JM, Ho DD. HIV-1 dynamics in vivo: virion clearance rate, infected cell life-span, and viral generation time. *Science.* 1996;271(5255):1582-1586.

320. Ho DD, Neumann AU, Perelson AS, Chen W, Leonard JM, Markowitz M. Rapid turnover of plasma virions and CD4 lymphocytes in HIV-1 infection. *Nature.* 1995;373(6510):123-126.

321. Dalgleish AG, Beverley PC, Clapham PR, Crawford DH, Greaves MF, Weiss RA. The CD4 (T4) antigen is an essential component of the receptor for the AIDS retrovirus. *Nature.* 1984;312(5996):763-767.

322. Klatzmann D, Champagne E, Chamaret S, et al. T-lymphocyte T4 molecule behaves as the receptor for human retrovirus LAV. *Nature.* 1984;312(5996):767-768.

323. Alkhatib G, Combadiere C, Broder CC, et al. CC CKR5: a RANTES, MIP-1α, MIP-1β receptor as a fusion cofactor for macrophage-tropic HIV-1. *Science.* 1996;272(5270):1955-1958.

324. Choe H, Farzan M, Sun Y, et al. The β-chemokine receptors CCR3 and CCR5 facilitate infection by primary HIV-1 isolates. *Cell.* 1996;85(7):1135-1148.

325. Deng H, Liu R, Ellmeier W, et al. Identification of a major co-receptor for primary isolates of HIV-1. *Nature.* 1996;381(6584):661-666.

326. Doranz BJ, Rucker J, Yi Y, et al. A dual-tropic primary HIV-1 isolate that uses fusin and the β-chemokine receptors CKR-5, CKR-3, and CKR-2b as fusion cofactors. *Cell.* 1996;85(7):1149-1158.

327. Dragic T, Litwin V, Allaway GP, et al. HIV-1 entry into CD4+ cells is mediated by the chemokine receptor CC-CKR-5. *Nature.* 1996;381(6584):667-673.

328. Koenig S, Gendelman HE, Orenstein JM, et al. Detection of AIDS virus in macrophages in brain tissue from AIDS patients with encephalopathy. *Science.* 1986;233(4768):1089-1093.

329. Ganor Y, Real F, Sennepin A, et al. HIV-1 reservoirs in urethral macrophages of patients under suppressive antiretroviral therapy. *Nature microbiology.* 2019;4(4):633-644.

330. Zaikos TD, Terry VH, Kettinger NTS, et al. Hematopoietic stem and progenitor cells are a distinct HIV reservoir that contributes to persistent viremia in suppressed patients. *Cell Reports.* 2018;25(13):3759-3773. e3759.

331. Miedema F, Tersmette M, van Lier RW. AIDS pathogenesis: a dynamic interaction between HIV and the immune system. *Immunology today.* 1990;11:293-297.

332. Gougeon M-L, Lecoeur H, Dulioust A, et al. Programmed cell death in peripheral lymphocytes from HIV-infected persons: increased susceptibility to apoptosis of CD4 and CD8 T cells correlates with lymphocyte activation and with disease progression. *The Journal of Immunology.* 1996;156(9):3509-3520.

333. Geijtenbeek TB, Kwon DS, Torensma R, et al. DC-SIGN, a dendritic cell–specific HIV-1-binding protein that enhances trans-infection of T cells. *Cell.* 2000;100(5):587-597.

334. Boggiano C, Manel N, Littman DR. Dendritic cell-mediated trans-enhancement of human immunodeficiency virus type 1 infectivity is independent of DC-SIGN. *Journal of virology.* 2007;81(5):2519-2523.

335. Maelfait J, Bridgeman A, Benlahrech A, Cursi C, Rehwinkel J. Restriction by SAMHD1 limits cGAS/STING-dependent innate and adaptive immune responses to HIV-1. *Cell reports.* 2016;16(6):1492-1501.

336. Meyerhans A, Cheynier R, Albert J, et al. Temporal fluctuations in HIV quasispecies in vivo are not reflected by sequential HIV isolations. *Cell.* 1989;58(5):901-910.

337. Starcich BR, Hahn BH, Shaw GM, et al. Identification and characterization of conserved and variable regions in the envelope gene of HTLV-III/LAV, the retrovirus of AIDS. *Cell.* 1986;45(5):637-648.

338. Willey RL, Rutledge RA, Dias S, et al. Identification of conserved and divergent domains within the envelope gene of the acquired immunodeficiency syndrome retrovirus. *Proceedings of the National Academy of Sciences.* 1986;83(14):5038-5042.

339. Tomaras GD, Yates NL, Liu P, et al. Initial B-cell responses to transmitted human immunodeficiency virus type 1: virion-binding immunoglobulin M (IgM) and IgG antibodies followed by plasma anti-gp41 antibodies with ineffective control of initial viremia. *Journal of virology.* 2008;82(24):12449-12463.

340. Albert J, Abrahamsson B, Nagy K, et al. Rapid development of isolate-specific neutralizing antibodies and consequent emergence of virus variants which resist neutralization by autologous sera. *AIDS.* 1990;4(107-112):22J.

341. Moore JP, Cao Y, Ho DD, Koup RA. Development of the anti-gp120 antibody response during seroconversion to human immunodeficiency virus type 1. *Journal of Virology.* 1994;68(8):5142-5155.

342. Qiao X, He B, Chiu A, Knowles DM, Chadburn A, Cerutti A. Human immunodeficiency virus 1 Nef suppresses CD40-dependent immunoglobulin class switching in bystander B cells. *Nature immunology.* 2006;7(3):302-310.

343. Moog C, Fleury H, Pellegrin I, Kirn A, Aubertin AM. Autologous and heterologous neutralizing antibody responses following initial seroconversion in human immunodeficiency virus type 1-infected individuals. *Journal of virology.* 1997;71(5):3734-3741.

344. Richman DD, Wrin T, Little SJ, Petropoulos CJ. Rapid evolution of the neutralizing antibody response to HIV type 1 infection. *Proceedings of the National Academy of Sciences.* 2003;100(7):4144-4149.

345. Horwitz JA, Bar-On Y, Lu C-L, et al. Non-neutralizing antibodies alter the course of HIV-1 infection in vivo. *Cell.* 2017;170(4):637-648. e610.

346. Sok D, Burton DR. Recent progress in broadly neutralizing antibodies to HIV. *Nature immunology.* 2018;19(11):1179-1188.

347. Moran MJ, Andris JS, Matsumato Y-i, Capra JD, Hersh EM. Variable region genes of anti-HIV human monoclonal antibodies: non-restricted use of the V gene repertoire and extensive somatic mutation. *Molecular immunology.* 1993;30(16):1543-1551.

348. Klein F, Diskin R, Scheid JF, et al. Somatic mutations of the immunoglobulin framework are generally required for broad and potent HIV-1 neutralization. *Cell.* 2013;153(1):126-138.

349. Andris JS, Johnson S, Zolla-Pazner S, Capra JD. Molecular characterization of five human anti-human immunodeficiency virus type 1 antibody heavy chains reveals extensive somatic mutation typical of an antigen-driven immune response. *Proceedings of the National Academy of Sciences.* 1991;88(17):7783-7787.

350. Gautam R, Nishimura Y, Pegu A, et al. A single injection of anti-HIV-1 antibodies protects against repeated SHIV challenges. *Nature.* 2016;533(7601):105-109.
351. Caskey M, Schoofs T, Gruell H, et al. Antibody 10-1074 suppresses viremia in HIV-1-infected individuals. *Nature medicine.* 2017;23(2):185-191.
352. Caskey M, Klein F, Lorenzi JC, et al. Viraemia suppressed in HIV-1-infected humans by broadly neutralizing antibody 3BNC117. *Nature.* 2015;522(7557):487-491.
353. Scheid JF, Horwitz JA, Bar-On Y, et al. HIV-1 antibody 3BNC117 suppresses viral rebound in humans during treatment interruption. *Nature.* 2016;535(7613):556-560.
354. Wang Q, Zhang L. Broadly neutralizing antibodies and vaccine design against HIV-1 infection. *Frontiers of medicine.* 2020;14(1):30-42.
355. Simonich CA, Williams KL, Verkerke HP, et al. HIV-1 neutralizing antibodies with limited hypermutation from an infant. *Cell.* 2016;166(1):77-87.
356. Koup R, Safrit JT, Cao Y, et al. Temporal association of cellular immune responses with the initial control of viremia in primary human immunodeficiency virus type 1 syndrome. *Journal of virology.* 1994;68(7):4650-4655.
357. Borrow P, Lewicki H, Wei X, et al. Antiviral pressure exerted by HIV-l-specific cytotoxic T lymphocytes (CTLs) during primary infection demonstrated by rapid selection of CTL escape virus. *Nature medicine.* 1997;3(2):205.
358. Pollack RA, Jones RB, Pertea M, et al. Defective HIV-1 proviruses are expressed and can be recognized by cytotoxic T lymphocytes, which shape the proviral landscape. *Cell host & microbe.* 2017;21(4):494-506. e494.
359. Leslie A, Pfafferott K, Chetty P, et al. HIV evolution: CTL escape mutation and reversion after transmission. *Nature medicine.* 2004;10(3):282-289.
360. Goulder PJ, Brander C, Tang Y, et al. Evolution and transmission of stable CTL escape mutations in HIV infection. *Nature.* 2001;412(6844):334-338.
361. Zhang J-Y, Zhang Z, Wang X, et al. PD-1 up-regulation is correlated with HIV-specific memory CD8+ T-cell exhaustion in typical progressors but not in long-term nonprogressors. *Blood.* 2007;109(11):4671-4678.
362. Day CL, Kaufmann DE, Kiepiela P, et al. PD-1 expression on HIV-specific T cells is associated with T-cell exhaustion and disease progression. *Nature.* 2006;443(7109):350-354.
363. Said EA, Dupuy FP, Trautmann L, et al. Programmed death-1–induced interleukin-10 production by monocytes impairs CD4+ T cell activation during HIV infection. *Nature medicine.* 2010;16(4):452-459.
364. Rodríguez-García M, Porichis F, de Jong OG, et al. Expression of PD-L1 and PD-L2 on human macrophages is up-regulated by HIV-1 and differentially modulated by IL-10. *Journal of leukocyte biology.* 2011;89(4):507-515.
365. Akhmetzyanova I, Drabczyk M, Neff CP, et al. PD-L1 expression on retrovirus-infected cells mediates immune escape from CD8+ T cell killing. *PLoS Pathog.* 2015;11(10):e1005224.
366. Collins KL, Chen BK, Kalams SA, Walker BD, Baltimore D. HIV-1 Nef protein protects infected primary cells against killing by cytotoxic T lymphocytes. *Nature.* 1998;391(6665):397.

367. Zinkernagel RM, Doherty PC. MHC-restricted cytotoxic T cells: studies on the biological role of polymorphic major transplantation antigens determining T-cell restriction-specificity, function, and responsiveness. In: *Advances in immunology.* Vol 27. Elsevier; 1979:51-177.

368. Moran AE, Hogquist KA. T-cell receptor affinity in thymic development. *Immunology.* 2012;135(4):261-267.

369. Grakoui A, Bromley SK, Sumen C, et al. The immunological synapse: a molecular machine controlling T cell activation. *Science.* 1999;285(5425):221-227.

370. Darmon AJ, Nicholson DW, Bleackley RC. Activation of the apoptotic protease CPP32 by cytotoxic T-cell-derived granzyme B. *Nature.* 1995;377(6548):446-448.

371. Henkart PA, Millard PJ, Reynolds CW, Henkart MP. Cytolytic activity of purified cytoplasmic granules from cytotoxic rat large granular lymphocyte tumors. *The Journal of experimental medicine.* 1984;160(1):75-93.

372. Peters PJ, Borst J, Oorschot V, et al. Cytotoxic T lymphocyte granules are secretory lysosomes, containing both perforin and granzymes. *The Journal of experimental medicine.* 1991;173(5):1099-1109.

373. Podack ER, Young J, Cohn ZA. Isolation and biochemical and functional characterization of perforin 1 from cytolytic T-cell granules. *Proceedings of the National Academy of Sciences.* 1985;82(24):8629-8633.

374. Lowin B, Hahne M, Mattmann C, Tschopp J. Cytolytic T-cell cytotoxicity is mediated through perforin and Fas lytic pathways. *Nature.* 1994;370(6491):650.

375. Robinson J, Halliwell JA, Hayhurst JD, Flicek P, Parham P, Marsh SG. The IPD and IMGT/HLA database: allele variant databases. *Nucleic acids research.* 2014;43(D1):D423-D431.

376. Apps R, Meng Z, Del Prete GQ, Lifson JD, Zhou M, Carrington M. Relative expression levels of the HLA class-I proteins in normal and HIV-infected cells. *The Journal of Immunology.* 2015;194(8):3594-3600.

377. Matthews PC, Prendergast A, Leslie A, et al. Central role of reverting mutations in HLA associations with human immunodeficiency virus set point. *Journal of virology.* 2008;82(17):8548-8559.

378. Neisig A, Melief CJ, Neefjes J. Reduced cell surface expression of HLA-C molecules correlates with restricted peptide binding and stable TAP interaction. *The Journal of Immunology.* 1998;160(1):171-179.

379. Mkhwanazi N, Thobakgale CF, van der Stok M, et al. Immunodominant HIV-1-specific HLA-B-and HLA-C-restricted CD8+ T cells do not differ in polyfunctionality. *Virology.* 2010;405(2):483-491.

380. Makadzange AT, Gillespie G, Dong T, et al. Characterization of an HLA-C-restricted CTL response in chronic HIV infection. *European journal of immunology.* 2010;40(4):1036-1041.

381. Leslie A, Matthews PC, Listgarten J, et al. Additive contribution of HLA class I alleles in the immune control of HIV-1 infection. *Journal of virology.* 2010;84(19):9879-9888.

382. Parham P, Ohta T. Population biology of antigen presentation by MHC class I molecules. *Science.* 1996;272(5258):67-74.

383. Fan QR, Long EO, Wiley DC. Crystal structure of the human natural killer cell inhibitory receptor KIR2DL1–HLA-Cw4 complex. *Nature immunology.* 2001;2(5):452-460.

384. Braud VM, Allan DS, O'Callaghan CA, et al. HLA-E binds to natural killer cell receptors CD94/NKG2A, B and C. *Nature.* 1998;391(6669):795-799.

385. Rouas-Freiss N, Marchal RE, Kirszenbaum M, Dausset J, Carosella ED. The α1 domain of HLA-G1 and HLA-G2 inhibits cytotoxicity induced by natural killer cells: is HLA-G the public ligand for natural killer cell inhibitory receptors? *Proceedings of the National Academy of Sciences.* 1997;94(10):5249-5254.

386. Parham P. MHC class I molecules and KIRs in human history, health and survival. *Nature reviews immunology.* 2005;5(3):201.

387. Champsaur M, Lanier LL. Effect of NKG2D ligand expression on host immune responses. *Immunological reviews.* 2010;235(1):267-285.

388. Betts MR, Nason MC, West SM, et al. HIV nonprogressors preferentially maintain highly functional HIV-specific CD8+ T cells. *Blood.* 2006;107(12):4781-4789.

389. Migueles SA, Laborico AC, Shupert WL, et al. HIV-specific CD8+ T cell proliferation is coupled to perforin expression and is maintained in nonprogressors. *Nature immunology.* 2002;3(11):1061.

390. Sáez-Cirión A, Lacabaratz C, Lambotte O, et al. HIV controllers exhibit potent CD8 T cell capacity to suppress HIV infection ex vivo and peculiar cytotoxic T lymphocyte activation phenotype. *Proceedings of the National Academy of Sciences.* 2007;104(16):6776-6781.

391. Gaiha GD, Rossin EJ, Urbach J, et al. Structural topology defines protective CD8+ T cell epitopes in the HIV proteome. *Science.* 2019;364(6439):480-484.

392. Carrington M, O'Brien SJ. The influence of HLA genotype on AIDS. *Annual review of medicine.* 2003;54(1):535-551.

393. Kaslow RA, Carrington M, Apple R, et al. Influence of combinations of human major histocompatibility complex genes on the course of HIV–1 infection. *Nature medicine.* 1996;2(4):405.

394. Study IHC. The major genetic determinants of HIV-1 control affect HLA class I peptide presentation. *Science.* 2010;330(6010):1551-1557.

395. Noyan K, Nguyen S, Betts MR, Sönnerborg A, Buggert M. Human immunodeficiency virus type-1 elite controllers maintain low co-expression of inhibitory receptors on CD4+ T cells. *Frontiers in immunology.* 2018;9:19.

396. Jiang C, Lian X, Gao C, et al. Distinct viral reservoirs in individuals with spontaneous control of HIV-1. *Nature.* 2020;585(7824):261-267.

397. Kumar BV, Ma W, Miron M, et al. Human tissue-resident memory T cells are defined by core transcriptional and functional signatures in lymphoid and mucosal sites. *Cell reports.* 2017;20(12):2921-2934.

398. Wong MT, Ong DEH, Lim FSH, et al. A high-dimensional atlas of human T cell diversity reveals tissue-specific trafficking and cytokine signatures. *Immunity.* 2016;45(2):442-456.

399. Buggert M, Nguyen S, de Oca GS-M, et al. Identification and characterization of HIV-specific resident memory CD8+ T cells in human lymphoid tissue. *Science immunology.* 2018;3(24).

400. Nguyen S, Deleage C, Darko S, et al. Elite control of HIV is associated with distinct functional and transcriptional signatures in lymphoid tissue CD8+ T cells. *Science translational medicine.* 2019;11(523).
401. Chevalier MF, Weiss L. The split personality of regulatory T cells in HIV infection. *Blood, The Journal of the American Society of Hematology.* 2013;121(1):29-37.
402. Nilsson J, Boasso A, Velilla PA, et al. HIV-1–driven regulatory T-cell accumulation in lymphoid tissues is associated with disease progression in HIV/AIDS. *Blood.* 2006;108(12):3808-3817.
403. Elahi S, Dinges WL, Lejarcegui N, et al. Protective HIV-specific CD8+ T cells evade T reg cell suppression. *Nature medicine.* 2011;17(8):989-995.
404. Arts EJ, Hazuda DJ. HIV-1 antiretroviral drug therapy. *Cold Spring Harb Perspect Med.* 2012;2(4):a007161.
405. Broder S. The development of antiretroviral therapy and its impact on the HIV-1/AIDS pandemic. *Antiviral research.* 2010;85(1):1-18.
406. Larder BA, Kemp SD. Multiple mutations in HIV-1 reverse transcriptase confer high-level resistance to zidovudine (AZT). *Science.* 1989;246(4934):1155-1158.
407. Lewden C, Chêne G, Morlat P, et al. HIV-infected adults with a CD4 cell count greater than 500 cells/mm3 on long-term combination antiretroviral therapy reach same mortality rates as the general population. *JAIDS Journal of Acquired Immune Deficiency Syndromes.* 2007;46(1):72-77.
408. Hammer SM, Squires KE, Hughes MD, et al. A controlled trial of two nucleoside analogues plus indinavir in persons with human immunodeficiency virus infection and CD4 cell counts of 200 per cubic millimeter or less. *New England Journal of Medicine.* 1997;337(11):725-733.
409. Gulick RM, Mellors JW, Havlir D, et al. Treatment with indinavir, zidovudine, and lamivudine in adults with human immunodeficiency virus infection and prior antiretroviral therapy. *New England Journal of Medicine.* 1997;337(11):734-739.
410. Dragic T, Trkola A, Thompson DA, et al. A binding pocket for a small molecule inhibitor of HIV-1 entry within the transmembrane helices of CCR5. *Proceedings of the National Academy of Sciences.* 2000;97(10):5639-5644.
411. Tsamis F, Gavrilov S, Kajumo F, et al. Analysis of the mechanism by which the small-molecule CCR5 antagonists SCH-351125 and SCH-350581 inhibit human immunodeficiency virus type 1 entry. *Journal of virology.* 2003;77(9):5201-5208.
412. Kilby JM, Hopkins S, Venetta TM, et al. Potent suppression of HIV-1 replication in humans by T-20, a peptide inhibitor of gp41-mediated virus entry. *Nature medicine.* 1998;4(11):1302-1307.
413. Cheng Y, Dutschman GE, Bastow KF, Sarngadharan M, Ting R. Human immunodeficiency virus reverse transcriptase. General properties and its interactions with nucleoside triphosphate analogs. *Journal of Biological Chemistry.* 1987;262(5):2187-2189.
414. Balzarini J, Herdewijn P, De Clercq E. Differential patterns of intracellular metabolism of 2', 3'-didehydro-2', 3'-dideoxythymidine and 3'-azido-2', 3'-dideoxythymidine, two potent anti-human immunodeficiency virus compounds. *Journal of Biological Chemistry.* 1989;264(11):6127-6133.
415. Arion D, Kaushik N, McCormick S, Borkow G, Parniak MA. Phenotypic mechanism of HIV-1 resistance to 3 '-azido-3 '-deoxythymidine (AZT): Increased

polymerization processivity and enhanced sensitivity to pyrophosphate of the mutant viral reverse transcriptase. *Biochemistry.* 1998;37(45):15908-15917.

416. Boyer PL, Sarafianos SG, Arnold E, Hughes SH. Selective excision of AZTMP by drug-resistant human immunodeficiency virus reverse transcriptase. *Journal of virology.* 2001;75(10):4832-4842.

417. Meyer PR, Matsuura SE, Mian AM, So AG, Scott WA. A mechanism of AZT resistance: an increase in nucleotide-dependent primer unblocking by mutant HIV-1 reverse transcriptase. *Molecular cell.* 1999;4(1):35-43.

418. García-Lerma JG, MacInnes H, Bennett D, et al. A novel genetic pathway of human immunodeficiency virus type 1 resistance to stavudine mediated by the K65R mutation. *Journal of virology.* 2003;77(10):5685-5693.

419. Schinazi RF, Lloyd R, Nguyen M-H, et al. Characterization of human immunodeficiency viruses resistant to oxathiolane-cytosine nucleosides. *Antimicrobial agents and chemotherapy.* 1993;37(4):875-881.

420. Spence RA, Kati WM, Anderson KS, Johnson KA. Mechanism of inhibition of HIV-1 reverse transcriptase by nonnucleoside inhibitors. *Science.* 1995;267(5200):988-993.

421. Tantillo C, Ding J, Jacobo-Molina A, et al. Locations of anti-AIDS drug binding sites and resistance mutations in the three-dimensional structure of HIV-1 reverse transcriptase: implications for mechanisms of drug inhibition and resistance. *Journal of molecular biology.* 1994;243(3):369-387.

422. Tebit DM, Lobritz M, Lalonde M, et al. Divergent evolution in reverse transcriptase (RT) of HIV-1 group O and M lineages: impact on structure, fitness, and sensitivity to nonnucleoside RT inhibitors. *Journal of virology.* 2010;84(19):9817-9830.

423. Descamps D, Collin G, Letourneur F, et al. Susceptibility of human immunodeficiency virus type 1 group O isolates to antiretroviral agents: in vitro phenotypic and genotypic analyses. *Journal of virology.* 1997;71(11):8893-8898.

424. Ren J, Bird L, Chamberlain P, Stewart-Jones G, Stuart D, Stammers D. Structure of HIV-2 reverse transcriptase at 2.35-Å resolution and the mechanism of resistance to non-nucleoside inhibitors. *Proceedings of the National Academy of Sciences.* 2002;99(22):14410-14415.

425. Deeks SG. Nonnucleoside reverse transcriptase inhibitor resistance. *JAIDS Journal of Acquired Immune Deficiency Syndromes.* 2001;26:S25-S33.

426. Dykes C, Fox K, Lloyd A, Chiulli M, Morse E, Demeter LM. Impact of clinical reverse transcriptase sequences on the replication capacity of HIV-1 drug-resistant mutants. *Virology.* 2001;285(2):193-203.

427. Espeseth AS, Felock P, Wolfe A, et al. HIV-1 integrase inhibitors that compete with the target DNA substrate define a unique strand transfer conformation for integrase. *Proceedings of the National Academy of Sciences.* 2000;97(21):11244-11249.

428. Shimura K, Kodama E, Sakagami Y, et al. Broad antiretroviral activity and resistance profile of the novel human immunodeficiency virus integrase inhibitor elvitegravir (JTK-303/GS-9137). *Journal of virology.* 2008;82(2):764-774.

429. Van Baelen K, Van Eygen V, Rondelez E, Stuyver LJ. Clade-specific HIV-1 integrase polymorphisms do not reduce raltegravir and elvitegravir phenotypic susceptibility. *Aids.* 2008;22(14):1877-1880.

430. Flexner C. HIV-protease inhibitors. *New England Journal of Medicine.* 1998;338(18):1281-1293.
431. Yant SR, Mulato A, Hansen D, et al. A highly potent long-acting small-molecule HIV-1 capsid inhibitor with efficacy in a humanized mouse model. *Nature medicine.* 2019;25(9):1377-1384.
432. Bester SM, Wei G, Zhao H, et al. Structural and mechanistic bases for a potent HIV-1 capsid inhibitor. *Science.* 2020;370(6514):360-364.
433. Chun T-W, Carruth L, Finzi D, et al. Quantification of latent tissue reservoirs and total body viral load in HIV-1 infection. *Nature.* 1997;387(6629):183-188.
434. Finzi D, Hermankova M, Pierson T, et al. Identification of a reservoir for HIV-1 in patients on highly active antiretroviral therapy. *Science.* 1997;278(5341):1295-1300.
435. Abrahams M-R, Joseph SB, Garrett N, et al. The replication-competent HIV-1 latent reservoir is primarily established near the time of therapy initiation. *Science translational medicine.* 2019;11(513).
436. Crooks AM, Bateson R, Cope AB, et al. Precise quantitation of the latent HIV-1 reservoir: implications for eradication strategies. *The Journal of infectious diseases.* 2015;212(9):1361-1365.
437. Chun T-W, Engel D, Berrey MM, Shea T, Corey L, Fauci AS. Early establishment of a pool of latently infected, resting CD4+ T cells during primary HIV-1 infection. *Proceedings of the National Academy of Sciences.* 1998;95(15):8869-8873.
438. Schacker T, Little S, Connick E, et al. Rapid accumulation of human immunodeficiency virus (HIV) in lymphatic tissue reservoirs during acute and early HIV infection: implications for timing of antiretroviral therapy. *The Journal of infectious diseases.* 2000;181(1):354-357.
439. Barouch DH, Ghneim K, Bosche WJ, et al. Rapid inflammasome activation following mucosal SIV infection of rhesus monkeys. *Cell.* 2016;165(3):656-667.
440. Henrich TJ, Hatano H, Bacon O, et al. HIV-1 persistence following extremely early initiation of antiretroviral therapy (ART) during acute HIV-1 infection: An observational study. *PLoS medicine.* 2017;14(11):e1002417.
441. Jain V, Hartogensis W, Bacchetti P, et al. Antiretroviral therapy initiated within 6 months of HIV infection is associated with lower T-cell activation and smaller HIV reservoir size. *The Journal of infectious diseases.* 2013;208(8):1202-1211.
442. Persaud D, Gay H, Ziemniak C, et al. Absence of detectable HIV-1 viremia after treatment cessation in an infant. *New England Journal of Medicine.* 2013;369(19):1828-1835.
443. Sáez-Cirión A, Bacchus C, Hocqueloux L, et al. Post-treatment HIV-1 controllers with a long-term virological remission after the interruption of early initiated antiretroviral therapy ANRS VISCONTI Study. *PLoS Pathog.* 2013;9(3):e1003211.
444. Ndhlovu ZM, Kazer SW, Nkosi T, et al. Augmentation of HIV-specific T cell function by immediate treatment of hyperacute HIV-1 infection. *Science translational medicine.* 2019;11(493):eaau0528.
445. de Souza MS, Group RSS, Pinyakorn S, et al. Initiation of antiretroviral therapy during acute HIV-1 infection leads to a high rate of nonreactive HIV serology. *Reviews of Infectious Diseases.* 2016;63(4):555-561.

446. Bruner KM, Wang Z, Simonetti FR, et al. A quantitative approach for measuring the reservoir of latent HIV-1 proviruses. *Nature.* 2019;566(7742):120-125.

447. Bruner KM, Murray AJ, Pollack RA, et al. Defective proviruses rapidly accumulate during acute HIV-1 infection. *Nature medicine.* 2016;22(9):1043-1049.

448. Ho Y-C, Shan L, Hosmane NN, et al. Replication-competent noninduced proviruses in the latent reservoir increase barrier to HIV-1 cure. *Cell.* 2013;155(3):540-551.

449. Finzi D, Blankson J, Siliciano JD, et al. Latent infection of CD4+ T cells provides a mechanism for lifelong persistence of HIV-1, even in patients on effective combination therapy. *Nature medicine.* 1999;5(5):512-517.

450. Chomont N, El-Far M, Ancuta P, et al. HIV reservoir size and persistence are driven by T cell survival and homeostatic proliferation. *Nature medicine.* 2009;15(8):893-900.

451. Bosque A, Famiglietti M, Weyrich AS, Goulston C, Planelles V. Homeostatic proliferation fails to efficiently reactivate HIV-1 latently infected central memory CD4+ T cells. *PLoS Pathog.* 2011;7(10):e1002288.

452. Dobrowolski C, Valadkhan S, Graham AC, et al. Entry of polarized effector cells into quiescence forces HIV latency. *MBio.* 2019;10(2).

453. Kim M, Hosmane NN, Bullen CK, et al. A primary CD4+ T cell model of HIV-1 latency established after activation through the T cell receptor and subsequent return to quiescence. *nature protocols.* 2014;9(12):2755.

454. Brooks DG, Kitchen SG, Kitchen CM, Scripture-Adams DD, Zack JA. Generation of HIV latency during thymopoiesis. *Nat Med.* 2001;7(4):459-464.

455. Hiener B, Horsburgh BA, Eden J-S, et al. Identification of genetically intact HIV-1 proviruses in specific CD4+ T cells from effectively treated participants. *Cell reports.* 2017;21(3):813-822.

456. Estes JD, Kityo C, Ssali F, et al. Defining total-body AIDS-virus burden with implications for curative strategies. *Nature medicine.* 2017;23(11):1271.

457. Cantero-Pérez J, Grau-Expósito J, Serra-Peinado C, et al. Resident memory T cells are a cellular reservoir for HIV in the cervical mucosa. *Nature communications.* 2019;10(1):1-16.

458. Yukl SA, Shergill AK, Ho T, et al. The distribution of HIV DNA and RNA in cell subsets differs in gut and blood of HIV-positive patients on ART: implications for viral persistence. *The Journal of infectious diseases.* 2013;208(8):1212-1220.

459. Ananworanich J, Schuetz A, Vandergeeten C, et al. Impact of multi-targeted antiretroviral treatment on gut T cell depletion and HIV reservoir seeding during acute HIV infection. *PloS one.* 2012;7(3):e33948.

460. Gras G, Kaul M. Molecular mechanisms of neuroinvasion by monocytes-macrophages in HIV-1 infection. *Retrovirology.* 2010;7(1):1-11.

461. Coombs RW, Reichelderfer PS, Landay AL. Recent observations on HIV type-1 infection in the genital tract of men and women. *Aids.* 2003;17(4):455-480.

462. Günthard HF, Havlir DV, Fiscus S, et al. Residual human immunodeficiency virus (HIV) Type 1 RNA and DNA in lymph nodes and HIV RNA in genital secretions and in cerebrospinal fluid after suppression of viremia for 2 years. *The Journal of infectious diseases.* 2001;183(9):1318-1327.

463. Connick E, Mattila T, Folkvord JM, et al. CTL fail to accumulate at sites of HIV-1 replication in lymphoid tissue. *The Journal of Immunology.* 2007;178(11):6975-6983.

464. Connick E, Folkvord JM, Lind KT, et al. Compartmentalization of simian immunodeficiency virus replication within secondary lymphoid tissues of rhesus macaques is linked to disease stage and inversely related to localization of virus-specific CTL. *The Journal of Immunology.* 2014;193(11):5613-5625.

465. Bronnimann MP, Skinner PJ, Connick E. The B-cell follicle in HIV infection: barrier to a cure. *Frontiers in immunology.* 2018;9:20.

466. Banga R, Procopio FA, Ruggiero A, et al. Blood CXCR3+ CD4 T cells are enriched in inducible replication competent HIV in aviremic antiretroviral therapy-treated individuals. *Frontiers in immunology.* 2018;9:144.

467. Banga R, Procopio FA, Noto A, et al. PD-1+ and follicular helper T cells are responsible for persistent HIV-1 transcription in treated aviremic individuals. *Nature medicine.* 2016;22(7):754-761.

468. Kumar A, Abbas W, Herbein G. HIV-1 latency in monocytes/macrophages. *Viruses.* 2014;6(4):1837-1860.

469. Honeycutt JB, Thayer WO, Baker CE, et al. HIV persistence in tissue macrophages of humanized myeloid-only mice during antiretroviral therapy. *Nature medicine.* 2017;23(5):638-643.

470. Brennan TP, Woods JO, Sedaghat AR, Siliciano JD, Siliciano RF, Wilke CO. Analysis of human immunodeficiency virus type 1 viremia and provirus in resting CD4+ T cells reveals a novel source of residual viremia in patients on antiretroviral therapy. *Journal of virology.* 2009;83(17):8470-8481.

471. Bailey JR, Sedaghat AR, Kieffer T, et al. Residual human immunodeficiency virus type 1 viremia in some patients on antiretroviral therapy is dominated by a small number of invariant clones rarely found in circulating CD4+ T cells. *Journal of virology.* 2006;80(13):6441-6457.

472. Lerner P, Guadalupe M, Donovan R, et al. The gut mucosal viral reservoir in HIV-infected patients is not the major source of rebound plasma viremia following interruption of highly active antiretroviral therapy. *Journal of virology.* 2011;85(10):4772-4782.

473. Arai F, Hirao A, Ohmura M, et al. Tie2/angiopoietin-1 signaling regulates hematopoietic stem cell quiescence in the bone marrow niche. *Cell.* 2004;118(2):149-161.

474. Cheng T, Rodrigues N, Shen H, et al. Hematopoietic stem cell quiescence maintained by p21cip1/waf1. *Science.* 2000;287(5459):1804-1808.

475. Doulatov S, Notta F, Eppert K, Nguyen LT, Ohashi PS, Dick JE. Revised map of the human progenitor hierarchy shows the origin of macrophages and dendritic cells in early lymphoid development. *Nature immunology.* 2010;11(7):585-593.

476. Josefsson L, Eriksson S, Sinclair E, et al. Hematopoietic precursor cells isolated from patients on long-term suppressive HIV therapy did not contain HIV-1 DNA. *The Journal of infectious diseases.* 2012;206(1):28-34.

477. Durand CM, Ghiaur G, Siliciano JD, et al. HIV-1 DNA is detected in bone marrow populations containing CD4+ T cells but is not found in purified CD34+

hematopoietic progenitor cells in most patients on antiretroviral therapy. *Journal of Infectious Diseases.* 2012;205(6):1014-1018.

478. Deeks SG. Shock and kill. *Nature.* 2012;487(7408):439-440.

479. Pardons M, Baxter AE, Massanella M, et al. Single-cell characterization and quantification of translation-competent viral reservoirs in treated and untreated HIV infection. *PLoS pathogens.* 2019;15(2):e1007619.

480. Spina CA, Anderson J, Archin NM, et al. An in-depth comparison of latent HIV-1 reactivation in multiple cell model systems and resting CD4+ T cells from aviremic patients. *PLoS Pathog.* 2013;9(12):e1003834.

481. Ait-Ammar A, Kula A, Darcis G, et al. Current Status of Latency Reversing Agents Facing the Heterogeneity of HIV-1 Cellular and Tissue Reservoirs. *Frontiers in microbiology.* 2019;10.

482. Kauder SE, Bosque A, Lindqvist A, Planelles V, Verdin E. Epigenetic regulation of HIV-1 latency by cytosine methylation. *PLoS Pathog.* 2009;5(6):e1000495.

483. Blazkova J, Trejbalova K, Gondois-Rey F, et al. CpG methylation controls reactivation of HIV from latency. *PLoS Pathog.* 2009;5(8):e1000554.

484. Zaikos TD, Painter MM, Kettinger NTS, Terry VH, Collins KL. Class 1-selective histone deacetylase (HDAC) inhibitors enhance HIV latency reversal while preserving the activity of HDAC isoforms necessary for maximal HIV gene expression. *Journal of virology.* 2018;92(6):e02110-02117.

485. Lusic M, Marcello A, Cereseto A, Giacca M. Regulation of HIV-1 gene expression by histone acetylation and factor recruitment at the LTR promoter. *The EMBO journal.* 2003;22(24):6550-6561.

486. Jiang G, Espeseth A, Hazuda DJ, Margolis DM. c-Myc and Sp1 contribute to proviral latency by recruiting histone deacetylase 1 to the human immunodeficiency virus type 1 promoter. *Journal of virology.* 2007;81(20):10914-10923.

487. Contreras X, Schweneker M, Chen C-S, et al. Suberoylanilide hydroxamic acid reactivates HIV from latently infected cells. *Journal of Biological Chemistry.* 2009;284(11):6782-6789.

488. Archin NM, Espeseth A, Parker D, Cheema M, Hazuda D, Margolis DM. Expression of latent HIV induced by the potent HDAC inhibitor suberoylanilide hydroxamic acid. *AIDS research and human retroviruses.* 2009;25(2):207-212.

489. Wei DG, Chiang V, Fyne E, et al. Histone deacetylase inhibitor romidepsin induces HIV expression in CD4 T cells from patients on suppressive antiretroviral therapy at concentrations achieved by clinical dosing. *PLoS Pathog.* 2014;10(4):e1004071.

490. Huber K, Doyon G, Plaks J, Fyne E, Mellors JW, Sluis-Cremer N. Inhibitors of histone deacetylases correlation between isoform specificity and reactivation of HIV Type 1 (HIV-1) from latently infected cells. *Journal of Biological Chemistry.* 2011;286(25):22211-22218.

491. Keedy KS, Archin NM, Gates AT, Espeseth A, Hazuda DJ, Margolis DM. A limited group of class I histone deacetylases acts to repress human immunodeficiency virus type 1 expression. *Journal of virology.* 2009;83(10):4749-4756.

492. Søgaard OS, Graversen ME, Leth S, et al. The depsipeptide romidepsin reverses HIV-1 latency in vivo. *PLoS Pathog.* 2015;11(9):e1005142.

493. Rasmussen TA, Tolstrup M, Brinkmann CR, et al. Panobinostat, a histone deacetylase inhibitor, for latent-virus reactivation in HIV-infected patients on suppressive antiretroviral therapy: a phase 1/2, single group, clinical trial. *The lancet HIV.* 2014;1(1):e13-e21.

494. Archin NM, Kirchherr JL, Sung JA, et al. Interval dosing with the HDAC inhibitor vorinostat effectively reverses HIV latency. *The Journal of clinical investigation.* 2017;127(8):3126-3135.

495. Sun S-C. Non-canonical NF-κB signaling pathway. *Cell research.* 2011;21(1):71-85.

496. Mehla R, Bivalkar-Mehla S, Zhang R, et al. Bryostatin modulates latent HIV-1 infection via PKC and AMPK signaling but inhibits acute infection in a receptor independent manner. *PloS one.* 2010;5(6):e11160.

497. Jiang G, Mendes EA, Kaiser P, et al. Synergistic reactivation of latent HIV expression by ingenol-3-angelate, PEP005, targeted NF-kB signaling in combination with JQ1 induced p-TEFb activation. *PLoS Pathog.* 2015;11(7):e1005066.

498. Bullen CK, Laird GM, Durand CM, Siliciano JD, Siliciano RF. New ex vivo approaches distinguish effective and ineffective single agents for reversing HIV-1 latency in vivo. *Nature medicine.* 2014;20(4):425-429.

499. Gutiérrez C, Serrano-Villar S, Madrid-Elena N, et al. Bryostatin-1 for latent virus reactivation in HIV-infected patients on antiretroviral therapy. *Aids.* 2016;30(9):1385-1392.

500. Pache L, Dutra MS, Spivak AM, et al. BIRC2/cIAP1 is a negative regulator of HIV-1 transcription and can be targeted by Smac mimetics to promote reversal of viral latency. *Cell host & microbe.* 2015;18(3):345-353.

501. Pache L, Marsden MD, Teriete P, et al. Pharmacological Activation of Non-canonical NF-κB Signaling Activates Latent HIV-1 Reservoirs In Vivo. *Cell Reports Medicine.* 2020;1(3):100037.

502. Zhu Y, Pe'ery T, Peng J, et al. Transcription elongation factor P-TEFb is required for HIV-1 tat transactivation in vitro. *Genes & development.* 1997;11(20):2622-2632.

503. Budhiraja S, Famiglietti M, Bosque A, Planelles V, Rice AP. Cyclin T1 and CDK9 T-loop phosphorylation are downregulated during establishment of HIV-1 latency in primary resting memory CD4+ T cells. *Journal of virology.* 2013;87(2):1211-1220.

504. Yang Z, Zhu Q, Luo K, Zhou Q. The 7SK small nuclear RNA inhibits the CDK9/cyclin T1 kinase to control transcription. *Nature.* 2001;414(6861):317-322.

505. Kiss T, Michels AA, Bensaude O. 7SK small nuclear RNA binds to and inhibits the activity of CDK9/cyclin T complexes. *Nature.* 2001;414(6861):322-325.

506. Contreras X, Barboric M, Lenasi T, Peterlin BM. HMBA releases P-TEFb from HEXIM1 and 7SK snRNA via PI3K/Akt and activates HIV transcription. *PLoS Pathog.* 2007;3(10):e146.

507. Reuse S, Calao M, Kabeya K, et al. Synergistic activation of HIV-1 expression by deacetylase inhibitors and prostratin: implications for treatment of latent infection. *PloS one.* 2009;4(6):e6093.

508. Laird GM, Bullen CK, Rosenbloom DI, et al. Ex vivo analysis identifies effective HIV-1 latency–reversing drug combinations. *The Journal of clinical investigation.* 2015;125(5):1901-1912.

509. Darcis G, Kula A, Bouchat S, et al. An in-depth comparison of latency-reversing agent combinations in various in vitro and ex vivo HIV-1 latency models identified bryostatin-1+ JQ1 and ingenol-B+ JQ1 to potently reactivate viral gene expression. *PLoS Pathog.* 2015;11(7):e1005063.

510. Archin NM, Bateson R, Tripathy M, et al. HIV-1 expression within resting CD4 T-cells following multiple doses of vorinostat. *Journal of Infectious Diseases.* 2014;jiu155.

511. Prins JM, Jurriaans S, van Praag RM, et al. Immuno-activation with anti-CD3 and recombinant human IL-2 in HIV-1-infected patients on potent antiretroviral therapy. *Aids.* 1999;13(17):2405-2410.

512. Cillo AR, Sobolewski MD, Bosch RJ, et al. Quantification of HIV-1 latency reversal in resting CD4+ T cells from patients on suppressive antiretroviral therapy. *Proceedings of the National Academy of Sciences.* 2014;111(19):7078-7083.

513. Richman DD, Margolis DM, Delaney M, Greene WC, Hazuda D, Pomerantz RJ. The challenge of finding a cure for HIV infection. *Science.* 2009;323(5919):1304-1307.

514. Lehrman G, Hogue IB, Palmer S, et al. Depletion of latent HIV-1 infection in vivo: a proof-of-concept study. *Lancet.* 2005;366(9485):549-555.

515. Contreras X, Schweneker M, Chen CS, et al. Suberoylanilide hydroxamic acid reactivates HIV from latently infected cells. *The Journal of biological chemistry.* 2009;284(11):6782-6789.

516. Archin NM, Liberty AL, Kashuba AD, et al. Administration of vorinostat disrupts HIV-1 latency in patients on antiretroviral therapy. *Nature.* 2012;487(7408):482-485.

517. Irvine DJ, Purbhoo MA, Krogsgaard M, Davis MM. Direct observation of ligand recognition by T cells. *Nature.* 2002;419(6909):845.

518. Sykulev Y, Joo M, Vturina I, Tsomides TJ, Eisen HN. Evidence that a single peptide–MHC complex on a target cell can elicit a cytolytic T cell response. *Immunity.* 1996;4(6):565-571.

519. Anmole G, Kuang XT, Toyoda M, et al. A robust and scalable TCR-based reporter cell assay to measure HIV-1 Nef-mediated T cell immune evasion. *Journal of immunological methods.* 2015;426:104-113.

520. Stevanovic S, Schild H. Quantitative aspects of T cell activation—peptide generation and editing by MHC class I molecules. Paper presented at: Seminars in immunology1999.

521. Christinck ER, Luscher MA, Barber BH, Williams DB. Peptide binding to class I MHC on living cells and quantitation of complexes required for CTL lysis. *Nature.* 1991;352(6330):67.

522. Brower R, England R, Takeshita T, et al. Minimal requirements for peptide mediated activation of CD8+ CTL. *Molecular immunology.* 1994;31(16):1285-1293.

523. Valitutti S, Müller S, Cella M, Padovan E, Lanzavecchia A. Serial triggering of many T-cell receptors by a few peptide–MHC complexes. *Nature.* 1995;375(6527):148.

524. Donaldson JG, Williams DB. Intracellular assembly and trafficking of MHC class I molecules. *Traffic.* 2009;10(12):1745-1752.

525. Kasper MR, Roeth JF, Williams M, Filzen TM, Fleis RI, Collins KL. HIV-1 Nef disrupts antigen presentation early in the secretory pathway. *Journal of Biological Chemistry.* 2005;280(13):12840-12848.

526. Robinson MS. Adaptable adaptors for coated vesicles. *Trends in cell biology.* 2004;14(4):167-174.

527. Schwartz O, Maréchal V, Le Gall S, Lemonnier F, Heard J-M. Endocytosis of major histocompatibility complex class I molecules is induced by the HIV–1 Nef protein. *Nature medicine.* 1996;2(3):338.

528. Blagoveshchenskaya AD, Thomas L, Feliciangeli SF, Hung C-H, Thomas G. HIV-1 Nef downregulates MHC-I by a PACS-1-and PI3K-regulated ARF6 endocytic pathway. *Cell.* 2002;111(6):853-866.

529. Lubben NB, Sahlender DA, Motley AM, Lehner PJ, Benaroch P, Robinson MS. HIV-1 Nef-induced down-regulation of MHC class I requires AP-1 and clathrin but not PACS-1 and is impeded by AP-2. *Molecular biology of the cell.* 2007;18(9):3351-3365.

530. Jia X, Singh R, Homann S, Yang H, Guatelli J, Xiong Y. Structural basis of evasion of cellular adaptive immunity by HIV-1 Nef. *Nature structural & molecular biology.* 2012;19(7):701-706.

531. Shen QT, Ren X, Zhang R, Lee IH, Hurley JH. HIV-1 Nef hijacks clathrin coats by stabilizing AP-1:Arf1 polygons. *Science.* 2015;350(6259):aac5137.

532. Buffalo CZ, Iwamoto Y, Hurley JH, Ren X. How HIV Nef Proteins Hijack Membrane Traffic to Promote Infection. *Journal of Virology.* 2019:JVI. 01322-01319.

533. Mellman I, Fuchs R, Helenius A. Acidification of the endocytic and exocytic pathways. *Annual review of biochemistry.* 1986;55(1):663-700.

534. Nishi T, Forgac M. The vacuolar (H+)-ATPases—nature's most versatile proton pumps. *Nature reviews Molecular cell biology.* 2002;3(2):94.

535. Kirchhoff F, Schindler M, Specht A, Arhel N, Münch J. Role of Nef in primate lentiviral immunopathogenesis. *Cellular and molecular life sciences.* 2008;65(17):2621.

536. Geyer M, Munte CE, Schorr J, Kellner R, Kalbitzer HR. Structure of the anchor-domain of myristoylated and non-myristoylated HIV-1 Nef protein. *Journal of molecular biology.* 1999;289(1):123-138.

537. Bentham M, Mazaleyrat S, Harris M. Role of myristoylation and N-terminal basic residues in membrane association of the human immunodeficiency virus type 1 Nef protein. *Journal of general virology.* 2006;87(3):563-571.

538. Breuer S, Gerlach H, Kolaric B, Urbanke C, Opitz N, Geyer M. Biochemical indication for myristoylation-dependent conformational changes in HIV-1 Nef. *Biochemistry.* 2006;45(7):2339-2349.

539. Liu LX, Heveker N, Fackler OT, et al. Mutation of a conserved residue (D123) required for oligomerization of human immunodeficiency virus type 1 Nef protein abolishes interaction with human thioesterase and results in impairment of Nef biological functions. *Journal of Virology.* 2000;74(11):5310-5319.

540. Peng B, Robert-Guroff M. Deletion of N-terminal myristoylation site of HIV Nef abrogates both MHC-1 and CD4 down-regulation. *Immunology letters.* 2001;78(3):195-200.

541. Niederman TM, Hastings WR, Ratner L. Myristoylation-Enhanced Binding of the HIV-1 Net Protein to T Cell Skeletal Matrix. *Virology.* 1993;197(1):420-425.

542. Kaminchik J, Margalit R, Yaish S, et al. Cellular distribution of HIV type 1 Nef protein: identification of domains in Nef required for association with membrane and detergent-insoluble cellular matrix. *AIDS research and human retroviruses.* 1994;10(8):1003-1010.

543. Macrae D, Bruss V, Ganem D, et al. The role of myristoylation in the interactions between human immunodeficiency virus type I Nef and cellular proteins. *Virology.* 1983;181:359-363.

544. Garcia JV, Miller AD. Serine phosphorylation-independent downregulation of cell-surface CD4 by nef. *Nature.* 1991;350(6318):508-511.

545. Greenberg ME, Bronson S, Lock M, Neumann M, Pavlakis GN, Skowronski J. Co-localization of HIV-1 Nef with the AP-2 adaptor protein complex correlates with Nef-induced CD4 down-regulation. *Embo J.* 1997;16(23):6964-6976.

546. Coleman SH, Van Damme N, Day JR, et al. Leucine-specific, functional interactions between human immunodeficiency virus type 1 Nef and adaptor protein complexes. *J Virol.* 2005;79(4):2066-2078.

547. Michel N, Allespach I, Venzke S, Fackler OT, Keppler OT. The Nef protein of human immunodeficiency virus establishes superinfection immunity by a dual strategy to downregulate cell-surface CCR5 and CD4. *Current Biology.* 2005;15(8):714-723.

548. Veillette M, Désormeaux A, Medjahed H, et al. Interaction with cellular CD4 exposes HIV-1 envelope epitopes targeted by antibody-dependent cell-mediated cytotoxicity. *Journal of virology.* 2014;88(5):2633-2644.

549. Veillette M, Coutu M, Richard J, et al. The HIV-1 gp120 CD4-bound conformation is preferentially targeted by antibody-dependent cellular cytotoxicity-mediating antibodies in sera from HIV-1-infected individuals. *Journal of virology.* 2015;89(1):545-551.

550. Prévost J, Richard J, Medjahed H, et al. Incomplete downregulation of CD4 expression affects HIV-1 Env conformation and antibody-dependent cellular cytotoxicity responses. *Journal of virology.* 2018;92(13).

551. Miller MD, Warmerdam MT, Gaston I, Greene WC, Feinberg MB. The human immunodeficiency virus-1 nef gene product: a positive factor for viral infection and replication in primary lymphocytes and macrophages. *The Journal of experimental medicine.* 1994;179(1):101-113.

552. Chowers MY, Spina CA, Kwoh TJ, Fitch N, Richman DD, Guatelli JC. Optimal infectivity in vitro of human immunodeficiency virus type 1 requires an intact nef gene. *Journal of virology.* 1994;68(5):2906-2914.

553. Bell I, Schaefer TM, Trible RP, Amedee A, Reinhart TA. Down-modulation of the costimulatory molecule, CD28, is a conserved activity of multiple SIV Nefs and is dependent on histidine 196 of Nef. *Virology.* 2001;283(1):148-158.

554. Saksela K, Cheng G, Baltimore D. Proline-rich (PxxP) motifs in HIV-1 Nef bind to SH3 domains of a subset of Src kinases and are required for the enhanced growth

of Nef+ viruses but not for down-regulation of CD4. *The EMBO journal.* 1995;14(3):484-491.

555. Simmons A, Aluvihare V, McMichael A. Nef triggers a transcriptional program in T cells imitating single-signal T cell activation and inducing HIV virulence mediators. *Immunity.* 2001;14(6):763-777.

556. Alexander L, Du Z, Rosenzweig M, Jung JU, Desrosiers RC. A role for natural simian immunodeficiency virus and human immunodeficiency virus type 1 nef alleles in lymphocyte activation. *Journal of virology.* 1997;71(8):6094-6099.

557. Schrager JA, Marsh JW. HIV-1 Nef increases T cell activation in a stimulus-dependent manner. *Proceedings of the National Academy of Sciences.* 1999;96(14):8167-8172.

558. Wolf D, Witte V, Laffert B, et al. HIV-1 Nef associated PAK and PI3-kinases stimulate Akt-independent Bad-phosphorylation to induce anti-apoptotic signals. *Nature medicine.* 2001;7(11):1217-1224.

559. Cohen GB, Gandhi RT, Davis DM, et al. The selective downregulation of class I major histocompatibility complex proteins by HIV-1 protects HIV-infected cells from NK cells. *Immunity.* 1999;10(6):661-671.

560. Williams M, Roeth JF, Kasper MR, Fleis RI, Przybycin CG, Collins KL. Direct binding of human immunodeficiency virus type 1 Nef to the major histocompatibility complex class I (MHC-I) cytoplasmic tail disrupts MHC-I trafficking. *J Virol.* 2002;76(23):12173-12184.

561. Specht A, DeGottardi MQ, Schindler M, Hahn B, Evans DT, Kirchhoff F. Selective downmodulation of HLA-A and-B by Nef alleles from different groups of primate lentiviruses. *Virology.* 2008;373(1):229-237.

562. Hopfensperger K, Richard J, Stürzel CM, et al. Convergent Evolution of HLA-C Downmodulation in HIV-1 and HIV-2. *Mbio.* 2020;11(4).

563. Bachtel ND, Umviligihozo G, Pickering S, et al. HLA-C downregulation by HIV-1 adapts to host HLA genotype. *PLoS pathogens.* 2018;14(9):e1007257.

564. Apps R, Del Prete GQ, Chatterjee P, et al. HIV-1 vpu mediates HLA-C downregulation. *Cell host & microbe.* 2016;19(5):686-695.

565. Körner C, Simoneau CR, Schommers P, et al. HIV-1-mediated downmodulation of HLA-C impacts target cell recognition and antiviral activity of NK cells. *Cell host & microbe.* 2017;22(1):111-119. e114.

566. Emert-Sedlak LA, Narute P, Shu ST, et al. Effector kinase coupling enables high-throughput screens for direct HIV-1 Nef antagonists with antiretroviral activity. *Chemistry & biology.* 2013;20(1):82-91.

567. Mujib S, Saiyed A, Fadel S, et al. Pharmacologic HIV-1 Nef blockade promotes CD8 T cell-mediated elimination of latently HIV-1-infected cells in vitro. *JCI Insight.* 2017;2(17).

568. Shu ST, Emert-Sedlak LA, Smithgall TE. Cell-based fluorescence complementation reveals a role for HIV-1 nef protein dimerization in AP-2 adaptor recruitment and CD4 co-receptor down-regulation. *Journal of Biological Chemistry.* 2017;292(7):2670-2678.

569. Liu B, Zhang X, Zhang W, et al. Lovastatin inhibits HIV-1-induced MHC-I downregulation by targeting Nef–AP-1 complex formation: A new strategy to boost

immune eradication of HIV-1 infected cells. *Frontiers in Immunology.* 2019;10:2151.

570. Butler MS, Robertson AA, Cooper MA. Natural product and natural product derived drugs in clinical trials. *Natural product reports.* 2014;31(11):1612-1661.

571. Chater KF. Streptomyces inside-out: a new perspective on the bacteria that provide us with antibiotics. *Philosophical Transactions of the Royal Society B: Biological Sciences.* 2006;361(1469):761-768.

572. Berdy J. Bioactive microbial metabolites. *The Journal of antibiotics.* 2005;58(1):1.

573. Scherlach K, Hertweck C. Triggering cryptic natural product biosynthesis in microorganisms. *Organic & biomolecular chemistry.* 2009;7(9):1753-1760.

574. Newman DJ, Cragg GM. Natural products as sources of new drugs from 1981 to 2014. *Journal of natural products.* 2016;79(3):629-661.

575. Hupfeld J, Efferth T. Drug resistance of human immunodeficiency virus and overcoming it by natural products. *In vivo.* 2009;23(1):1-6.

576. Richard K, Williams D, de Silva E, et al. Identification of novel HIV-1 latency-reversing agents from a library of marine natural products. *Viruses.* 2018;10(7):348.

577. Cary DC, Peterlin BM. Natural products and HIV/AIDS. *AIDS research and human retroviruses.* 2018;34(1):31-38.

CHAPTER 2

Quiescence Promotes Latent HIV Infection and Resistance to Reactivation From Latency With Histone Deacetylase Inhibitors[3]

Abstract

Human immunodeficiency virus type-1 (HIV-1) establishes transcriptionally silent latent infections in many cell types, including resting memory T cells and hematopoietic stem and progenitor cells (HSPCs), which allow the virus to persist in infected individuals despite antiretroviral therapy. Developing *in vitro* models of HIV-1 latency that recapitulate the characteristics of latently infected cells *in vivo* is crucial to identifying and developing effective latency-reversing therapies. HSPCs exist in a quiescent state *in vivo*, and quiescence is correlated with latent infections in T cells. However, current models for culturing HSPCs and for infecting T cells *in vitro* require that they be maintained in an actively proliferating state. Here, we describe a novel culture system in which primary human HSPCs cultured under hypothermic conditions are maintained in a quiescent state. We show that these quiescent HSPCs are susceptible to predominantly latent

infection with HIV-1, while actively-proliferating and differentiating HSPCs obtain predominantly active infections. Furthermore, we demonstrate that the most primitive quiescent HSPCs are more resistant to spontaneous reactivation from latency than more differentiated HSPCs, and that quiescent HSPCs are resistant to reactivation by histone deacetylase inhibitors or P-TEFb activation but are susceptible to reactivation by PKC agonists. We also demonstrate that inhibition of HSP90, a known regulator of HIV transcription, recapitulates the quiescence and latency phenotypes of hypothermia, suggesting that hypothermia and HSP90 inhibition may regulate these processes by similar mechanisms. In summary, these studies describe a novel model for studying HIV-1 latency in human primary cells maintained in a quiescent state.

Introduction

Human immunodeficiency virus type-1 (HIV-1) is known to establish a latent infection in some cells, in which the viral genome is integrated into the host cell genome but remains as a transcriptionally silent provirus[1,2]. Such latent infections are believed to contribute to the phenomenon in which HIV-1 infections in individuals treated with antiretroviral therapy that suppresses plasma viral load below detectable levels will rebound if therapy is interrupted[1,3]. The primary cellular target of HIV-1 is CD4^{+} T cells, and the most abundant reservoir of latent HIV proviruses is also likely to reside in these cells[1,3]. Notably, latency in CD4^{+} T cells is observed most frequently in quiescent resting memory T cells, and quiescence has been shown to correlate with HIV latency[4,5]. While T cells are the primary target of HIV-1 infection, other cell types have also been shown to

91

be infected, including macrophages and hematopoietic stem and progenitor cells (HSPCs), and non-T cell sources of residual viremia in treated patients have been described[6-13].

Reactivation of transcriptionally silent proviruses and subsequent killing of cells harboring these proviruses by immune-mediated clearance or viral cytopathic effect is one approach to eliminating the residual virus present in individuals receiving antiretroviral therapy. Expression of HIV-1 genes is known to be regulated by a number of mechanisms that can be targeted for reactivation *in vitro*. NFκB is essential to efficient transcription from the HIV LTR[14], and NFκB signaling can be induced by TNFα stimulation[12] or protein kinase C (PKC) activation with agonists such as bryostatin[15]. In addition to NFκB, P-TEFb, which is composed of cyclin T1 and CDK9, acts with HIV Tat to promote RNA polymerase elongation during HIV-1 gene transcription[16,17]. P-TEFb is held in an inactive state by 7SK snRNP, but can be released from this complex and activated following treatment with HMBA[18]. Thus TNFα, bryostatin, and HMBA each have the potential to reactivate latent HIV-1 infections, as has been demonstrated previously[12,19]. Other latency-reversing agents have also been proposed, including histone deacetylase (HDAC) inhibitors, such as vorinostat[20,21] and romidepsin[22-24], which are believed to achieve reactivation through chromatin remodeling.

Heat shock protein 90 (HSP90), a molecular chaperone of the heat shock family of proteins, is a known positive regulator of HIV-1 transcription. A growing body of literature supports the role of HSP90 in regulating HIV-1 gene expression, and the mechanisms of this effect are likely pleiotropic. HSP90 has been implicated in the activation of the NFκB pathway[25], the formation of stable P-TEFb complexes[26,27], and the

92

formation of RNA Pol II complexes in the cytoplasm[28]. Hyperthermia has been shown to increase HIV-1 gene expression in persistently-infected cell lines in an HSP90-dependent manner, increasing the colocalization of HSP90 with the HIV-1 promoter[29-32]. Inhibition of HSP90 with the specific inhibitor 17-AAG can prevent viral rebound in an HIV-1-infected humanized mouse model[30], and HSP90 inhibition is also linked with cell cycle arrest, similar to that which occurs in quiescent cells[33,34]. Thus, emerging evidence suggests that HSP90 may be a useful target in strategies to eliminate the latent reservoir of HIV-1.

To determine which reactivation strategies are most likely to be successful *in vivo*, it is important to develop *in vitro* models of HIV-1 latent infection. These *in vitro* systems must recapitulate the *in vivo* nature of the latent HIV-1 reservoir, including the diverse cell types that can harbor latent infections and the quiescent state of many cells that contain transcriptionally silent proviruses. While latent HIV-1 infection has been observed in several *in vitro* systems[19], there is notable absence of primary cell models in which HIV-1 preferentially establishes a latent infection in quiescent cells. Furthermore, treatments that were effective in many of these models have failed to reduce the viral reservoir *in vivo*[35-40].

HSPCs reside in the bone marrow and are responsible for generating the hematopoietic cell compartment throughout the life of an individual. While both active and latent HIV-1 infection of HSPCs *in vitro* and from patient bone marrow have been described by some investigators[10-13], others have been unable to detect HIV-1 provirus in HSPCs from optimally treated HIV-infected donors[41,42]. Helping to resolve this apparent discrepancy, a recent publication by Sebastian et al. demonstrated that the frequency of HIV genomes in HSPCs from people is significantly lower than in T cells and that prior

negative studies lacked the necessary statistical power for reliable detection. Additionally, Sebastian et al. provided clear *in vivo* examples of infected HSPCs passing clonal defective genomes to differentiated progeny. Because the clonal genomes were defective, this observation could not have been attributed to coincident infection.[43]. Thus, there is evidence supporting the possibility that HSPCs form a reservoir of HIV in vivo.

The most primitive HSPCs, hematopoietic stem cells (HSCs), exist in a quiescent state and are long-lived and capable of self-renewal[44,45]. HSCs differentiate into more mature progenitor cells, which in turn continue to differentiate and give rise to the entire repertoire of mature hematopoietic cells[46]. Differentiation from the most primitive to more mature HSPCs can be determined by expression of cell surface antigens, including CD133 and CD34[47-49]. In HSPCs purified from human cord blood, the most primitive progenitors, including most stem cells, express both CD133 and CD34, whereas intermediate progenitors, such as CMPs and MEPs, express reduced levels of CD133 but remain CD34+, making these surface markers a suitable choice to assess HSPC differentiation[43].

HSPCs cultured *in vitro* differ from those *in vivo* in that the viability of the cells is dependent on the presence of growth factors in the culture medium. For this reason, previous work investigating latent infection of primary human HSPCs *in vitro* has been performed with cells cultured at 37°C in the presence of growth factors including thrombopoietin, stem cell factor, insulin-like growth factor-1, and FLT3L[12,50]. Here, we demonstrate that cells cultured under these conditions are actively proliferating and differentiating, and thus do not recapitulate the quiescent state of HSPCs *in vivo*. Furthermore, we show that while latent infections are observed, these cells are

susceptible to predominantly active infections with HIV-1. In contrast, we show that cells cultured in the presence of the same growth factors at 30°C are maintained in a quiescent state with no loss in viability, and these cells harbor predominantly latent HIV-1 infections. Additionally, we demonstrate that latent infections in the most primitive quiescent HSPCs are resistant to spontaneous reactivation and remain in a latent state for extended periods in culture. We further demonstrate that differentiation to more mature progenitors correlates with spontaneous reactivation from latency, and some stimuli that are sufficient for reactivation from latency in proliferating and differentiating HSPCS are not effective in quiescent HSPCs. Latency in this system is dependent on the active maintenance of latently infected cells in a quiescent state and is regulated post-integration. We have also shown that inhibition of HSP90 at standard temperatures recapitulates the quiescence and latency phenotypes observed under hypothermic conditions. In all, we identify and characterized two distinct models of HIV-1 latency using primary human HSPCs maintained in a quiescent state *in vitro*. We further implicate HSP90 as an important modulator of HIV latency, and we provide evidence to suggest that quiescent cells may be more resistant to reactivation than previously believed.

Results

HSPCs cultured at hypothermic conditions maintain a quiescent state

To develop conditions that simulate the quiescent state typical of HPSCs in vivo, we examined the effect of hypothermic culturing conditions, which we hypothesized could slow cellular proliferation and differentiation. Cellular proliferation was measured using

PKH26, a membrane-binding dye that is diluted with each cell division, as depicted in Fig. 2.1A. We found that HSPCs cultured at 37°C proliferated at a significantly higher rate than those cultured at 30°C (Fig. 2.1B and C). Cells initially maintained at 37°C and switched to 30°C also proliferated consistently less than those maintained at 37°C throughout the 6 days in culture, suggesting that switching to 30°C after initial culture at 37°C could halt proliferation (Fig. 2.1B and C). Furthermore, cell counts were also measured after 3 days of culture at 37°C and 30°C, and the cells expanded significantly more at 37°C (4.6-fold) than at 30°C (1.5-fold), reflecting what was observed with PKH26 staining (Fig. 2.1D, $p<0.0001$, Wilcoxon signed-rank test). Thus, HSPCs cultured at 30°C are maintained in a more quiescent state in which proliferation and expansion in culture are dramatically reduced, with no loss in viability (Fig. 2.1E).

HSPC proliferation is often linked to differentiation. To determine whether hypothermia also maintains HSPCs in an undifferentiated state, we stained cells for the HSPC markers CD133 and CD34. As HSPCs differentiate and become more mature progenitors, expression of CD133 is lost, followed by loss of CD34 expression in the most mature cells[43]. We found that HSPCs maintained at 30°C from the time of isolation remained undifferentiated based on expression of both CD133 and CD34 (Fig. 2.1F and G). In contrast, HSPCs cultured at 37°C for as little as 2 days began to lose expression of CD133, and by day 6 post-isolation approximately half of the cells no longer expressed CD133 (Fig. 2.1F and G). Thus, reduced proliferation and expansion of HSPCs at 30°C is also accompanied by reduced differentiation.
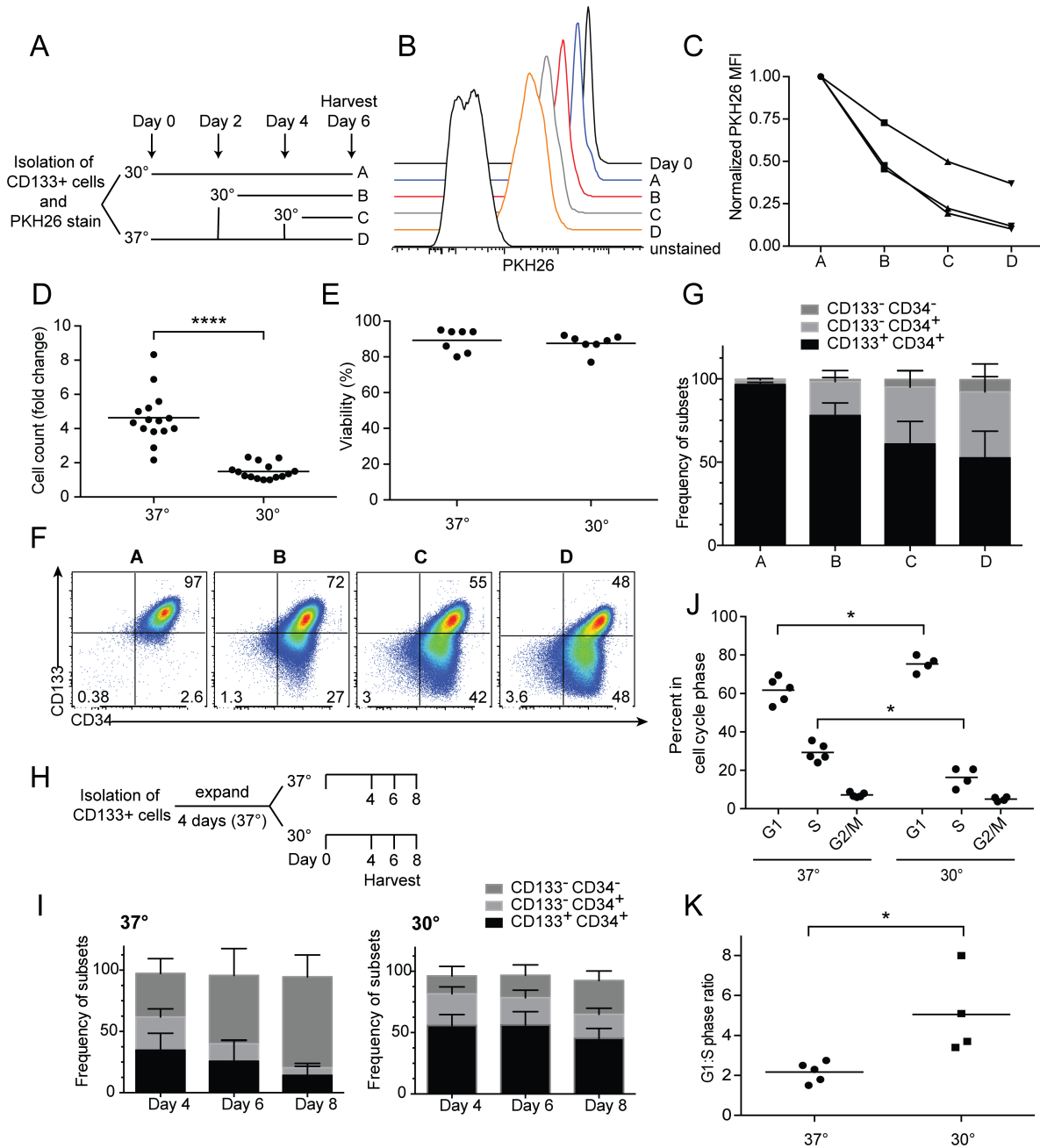
Fig. 2.1: HSPCs cultured in vitro under hypothermic conditions are maintained in a quiescent state.
(A) Schematic demonstrating the experimental process for (B,C F and G). (B) Representative histogram from one donor demonstrating the intensity of PKH26 staining in HSPCs following 6 days of culture as assessed by flow cytometry, where dilution of the PKH26 stain represents proliferation. Day 0 = cells harvested immediately following PKH26 stain prior to any dilution. Unstained = cells never stained with PKH26 and harvested 6 days post-isolation. (C) Summary graph of flow cytometric data from 3 independent experiments as in (B) where the median fluorescence intensity of PKH26 is normalized to that of condition A. (D) Summary graph depicting the fold-change in cell number at each temperature over a three-day culture period (**** = $p<0.0001$, Wilcoxon signed-rank test). (E) Summary graph depicting viability of HSPCs calculated as percent of events falling within both FSC/SSC and 7-AAD viability gates following 6 days of

97

culture at the respective temperatures. (F) Representative flow cytometric analysis of HSPCs cultured as in (A) and stained for the indicated surface markers. (G) Summary graph of flow cytometric data from 3 experiments as in (F), demonstrating the frequency of each of the indicated cellular subsets in the whole population. Mean values are shown with error bars indicating standard deviation. (H) Schematic demonstrating experimental process for (I-K). (I) Summary graph of flow cytometric data from 3 experiments, demonstrating the frequency of each of the indicated cellular subsets in the whole population of HSPCs cultured at 30°C or 37°C post-expansion. Mean values are shown with error bars indicating standard deviation. (J) Summary graph of flow cytometric data from HSPCs cultured as in (H) and harvested on day 4. HSPCs were stained with DAPI and the frequency of each cell cycle phase was determined using FlowJo software (* = $p<0.05$, Mann-Whitney tests). Each symbol represents an independent experiment using cells from a unique donor. (K) Summary graph of normalized flow cytometric data from (J) displaying the ratio of cells in G1:S phase of the cell cycle (* = $p<0.05$, Mann-Whitney test).

Only a small number of CD133$^+$CD34$^+$ cells can be isolated from a single donation of human cord blood, requiring an initial expansion of the cells to acquire sufficient cell numbers for downstream experiments. To verify that a quiescent state could be induced after HSPCs had been actively expanding, we performed a temperature shift experiment in which cells initially cultured at 37°C were shifted to the lower temperature (Fig. 2.1H). We found that switching HSPCs to 30°C after initially expanding them at 37°C effectively halted differentiation at the time of the switch (Fig. 2.1I). In contrast, HSPCs maintained at 37°C continued to differentiate; the frequency of CD133$^-$ CD34$^-$ cells was significantly higher than at 30°C (Fig. 2.1I, Day 4 $p<0.05$, Day 6 $p<0.01$, Day 8 $p<0.01$, Mann-Whitney tests) and the frequency of CD133$^+$ CD34$^+$ cells was significantly lower than at 30°C (Day 4 $p<0.05$, Day 6 $p<0.05$, Day 8 $p<0.01$, Mann-Whitney tests). These data support the conclusion that HSPCs cultured at 37°C will continue to differentiate and proliferate, while HSPCs cultured at 30°C will enter a sustained quiescent state even after 4 days of expansion. Thus, this expansion phase was employed for the remainder of the manuscript, as it allowed us to acquire sufficient cell numbers for downstream analyses.

To further characterize the quiescent state of HSPCs cultured at 30°C *in vitro*, we asked whether hypothermia led to arrest at a specific stage of the cell cycle. We found

that HSPCs cultured at 37°C had significantly fewer cells in G1 phase and significantly more cells in S phase than HSPCs cultured at 30°C (Fig. 2.1J, $p<0.05$, Mann-Whitney tests). After normalization, the ratio of G1:S phase cells is 2.2-fold higher in HSPCs cultured at 30°C than at 37°C (Fig. 2.1K, $p<0.05$, Mann-Whitney test). Taken together, these data demonstrate that primary human HSPCs cultured at 30°C *in vitro* are maintained in a quiescent state with minimal proliferation, differentiation, and cell cycle progression.

Quiescence promotes HIV-1 latency in HSPCs

To determine whether quiescence affected the frequency of active and latent infection with HIV-1, we used a previously-published system that efficiently detects the rate of latent infection in HSPCs established with a single round GFP reporter virus (Fig. 2.2A)[12]. In this assay system, infected cells expressing viral proteins are detectable by expression of a GFP-envelope fusion protein, while uninfected or latently infected cells remain GFP-negative. At the time of infection, HSPCs were split to 37°C or 30°C as in Fig. 2.2B, and 3 days post-infection actively infected, GFP$^+$ cells were removed by FACS. The integrase inhibitor raltegravir was added immediately after FACS sorting to prevent *de novo* integration. 24 hours post-sort, cells were harvested, and the frequency of inducible latent infection was determined by subtracting the frequency of GFP$^+$ cells in the raltegravir-only sample, defined as spontaneous reactivation, from the frequency of GFP$^+$ cells in a TNFα-stimulated condition (Fig. 2.2B and 2C). To ensure that reactivation was truly the result of integrated genomes that were not producing viral proteins 3 days

post-infection, we verified that raltegravir was indeed capable of completely blocking infection of HSPCs at both 37°C and 30°C (Fig. 2.2D).
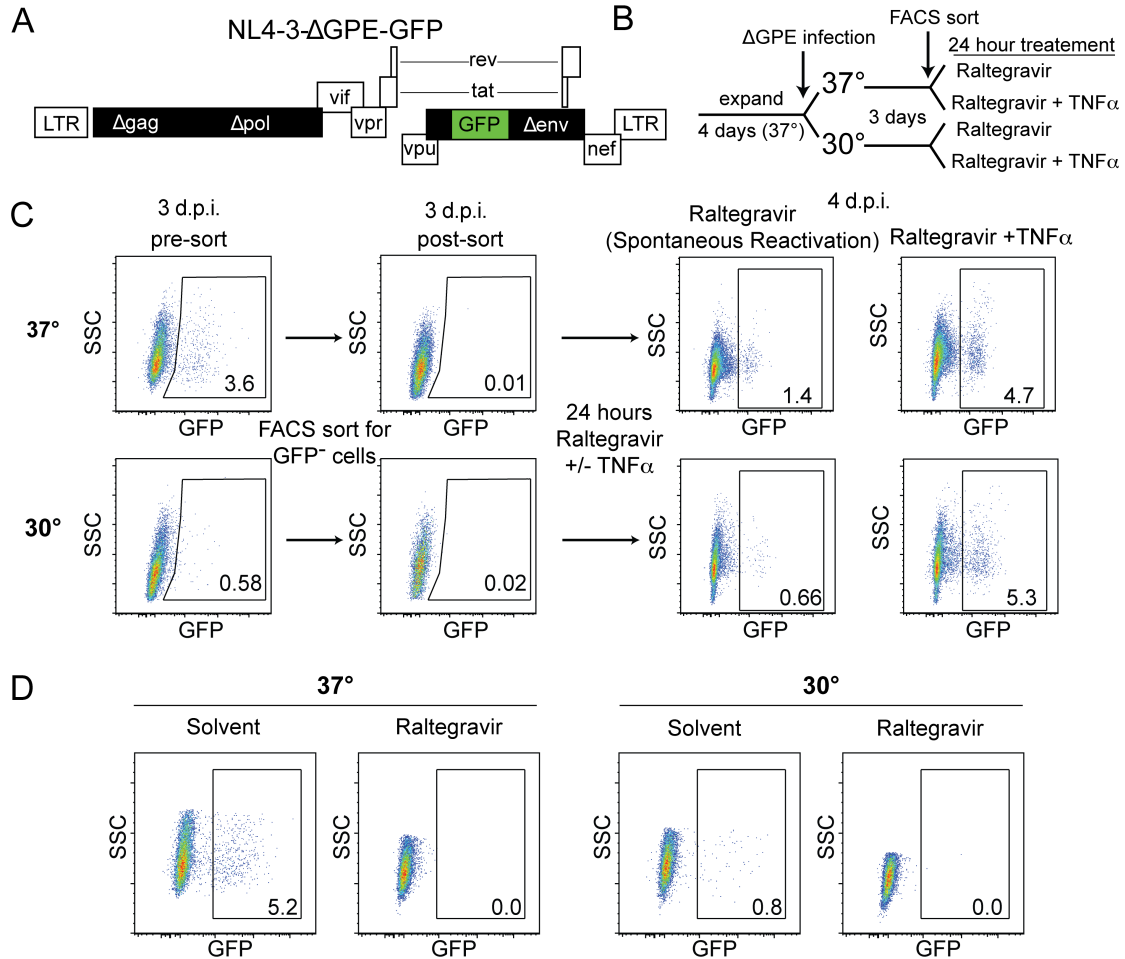
Fig. 2.2: Assessing post-integration latency in HSPCs. (A) Schematic depicting the NL4-3-ΔGPE-E-GFP HIV-1 viral construct expressing GFP in the *env* open reading frame. (B) Schematic of experimental setup for Fig. 2.3. (C) Representative flow cytometric plots of the latency reactivation assay used in Fig. 2.3 in which HSPCs infected at the indicated temperature were sorted to remove actively infected cells and treated with TNFα or a solvent control in the presence of raltegravir to ensure the assay exclusively measures post-integration latency reactivation. (D) Representative flow cytometric plots from HSPCs infected as in (B) with addition of raltegravir at the time of infection. Numbers in lower right-hand corner represent frequency of GFP+ cells 3 days post-infection.

We found that HSPCs cultured at 30°C had a significantly lower frequency of active infection than inducible latent infection (Fig. 2.3A; 5.4-fold, *p*<0.0001, Wilcoxon signed-rank test) whereas the reverse was true for cells cultured at 37°C (Fig. 2.3A, *p*<0.001,

Wilcoxon signed-rank test). Correspondingly, the frequency of active infection was significantly higher at 37°C than at 30°C (Fig. 2.3B; 4.9-fold, $p<0.0001$, Wilcoxon signed-rank test), and the frequency of inducible latent infection was significantly higher at 30°C than at 37°C (Fig. 2.3B; 1.8-fold, $p<0.0001$, Wilcoxon signed-rank test). Thus, hypothermia promotes latent HIV infection in HSPCs.

To further define the latency observed in HSPCs cultured at 30°C, we compared the frequency of spontaneous reactivation from latency that occurs in the absence of additional stimuli under these two conditions. To facilitate comparison across multiple experiments, these results were normalized to the maximal reactivation induced by TNFα. At 37°C, 42% of the reactivation that can be induced with TNFα reactivated spontaneously within 24 hours. Notably, at 30°C, only 15% of inducible proviruses reactivate spontaneously within 24 hours (Fig. 2.3C, $p<0.0001$, Wilcoxon signed-rank test).
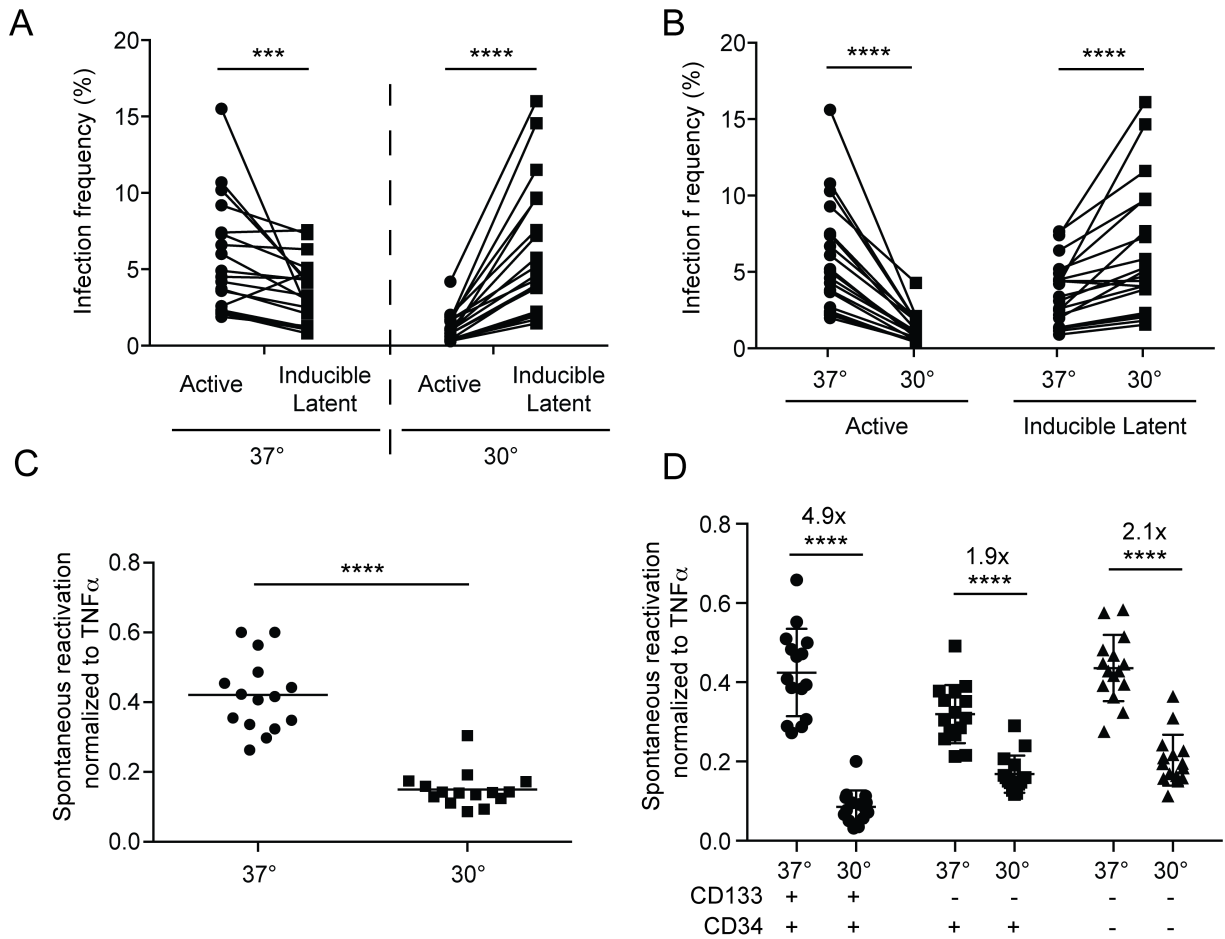
Fig. 2.3: Quiescent HSPCs are susceptible to predominantly latent HIV-1 infections in vitro. (A) Summary graph of flow cytometric data from 15 experiments as in Fig. 2.2, where active infection is the frequency of GFP$^+$ cells 3 d.p.i. and inducible latent infection is the frequency of GFP$^+$ cells 4 d.p.i. following 24 hours of TNFα and raltegravir treatment. For this analysis, the frequency of spontaneous reactivation occurring in control cells treated with raltegravir and run in parallel was subtracted. (*** = $p<0.001$, **** = $p<0.0001$, Wilcoxon signed-rank test). (B) Summary graph of flow cytometric data as in Fig. 2.2 comparing total frequency of active and inducible latent infection in HSPCs cultured at the indicated temperature (**** = $p<0.0001$, Wilcoxon signed-rank test). (C) Summary graph depicting the frequency of spontaneous reactivation in raltegravir-only samples normalized to the frequency of inducible infection resulting from 24 hours of TNFα stimulation (**** = $p<0.0001$, Wilcoxon signed-rank test). (D) Summary graph showing spontaneous reactivation normalized as in (C) in each subset of HSPCs at the indicated temperature. Numbers above the symbols indicate fold reduction in spontaneous reactivation frequency (**** = $p<0.0001$, Wilcoxon signed-rank test). N = 15 for (D-G).

Differentiation is associated with spontaneous reactivation from latency

Although increased latency was observed in HSPCs maintained at 30°C, it is important to note that this represents a heterogeneous population of various hematopoietic progenitor cells, which can be identified as primitive or mature based on

102

expression of the surface markers CD133 and CD34[43]. To determine whether the differentiation state of the cell influenced active versus latent infection, we analyzed cells infected and sorted as in Fig. 2.2B and compared the frequency of spontaneous reactivation for each differentiation subset. To facilitate comparison across independent experiments, the frequency of spontaneous reactivation was normalized to the frequency of TNFα-inducible infection in a sample treated in parallel. This analysis revealed that in each subset, proviruses in HSPCs maintained in hypothermic conditions were significantly less likely to reactivate spontaneously than those in actively proliferating HSPCs maintained at 37°C (Fig. 2.3D; $p<0.0001$ for each, Wilcoxon signed-rank tests). However, we also observed that amongst those cells cultured at reduced temperature, not all differentiation subsets were equally susceptible to spontaneous reactivation. The most undifferentiated progenitors (CD133$^+$ CD34$^+$) were almost 5-fold less likely to reactivate spontaneously at 30°C than at 37°C, while more differentiated progenitors were about 2-fold less-likely to reactivate spontaneously. These data show that the most primitive progenitors harbor the latent proviruses that are least likely to reactivate in quiescent cells absent additional stimulation.

Resistance to reactivation is reversible with temperature shift

Resistance of latent infection to spontaneous reactivation in quiescent HSPCs could be the result of permanent differences established during integration in quiescent or proliferating cells, such as a preference for different integration sites in the different populations. However, it is also possible that latency is maintained by differences in quiescent and proliferating cells post-integration, and thus can easily be reversed when

103

a cell exits a quiescent state. To determine which of these possibilities contributed to the differences in latency observed in quiescent HSPCs compared to proliferating HSPCs, we performed a series of temperature shifts (Fig. 2.4A). After performing a FACS sort to isolate latently infected GFP⁻ cells, cells were split to 37°C or 30°C for reactivation. As demonstrated previously, cells maintained at 37°C had a higher frequency of spontaneous reactivation than cells maintained at 30°C (Fig. 2.4B, *p*<0.01, Mann-Whitney test). Cells infected at 37°C and switched to 30°C for reactivation, however, had a significantly reduced frequency of spontaneous reactivation compared to cells maintained at 37°C throughout, suggesting that a more stable form of latency could be established by allowing the cells to enter a quiescent state (Fig. 2.4B, *p*<0.01, Mann-Whitney test). Conversely, cells infected in a quiescent state at 30°C and subsequently switched to a proliferating state at 37°C had dramatically higher spontaneous reactivation frequencies, which were not significantly different from cells infected and reactivated at 37°C. Thus, under the conditions of our assay, the relative frequency of spontaneous reactivation is determined, at least in part, by post-integration cellular conditions that are readily reversible.
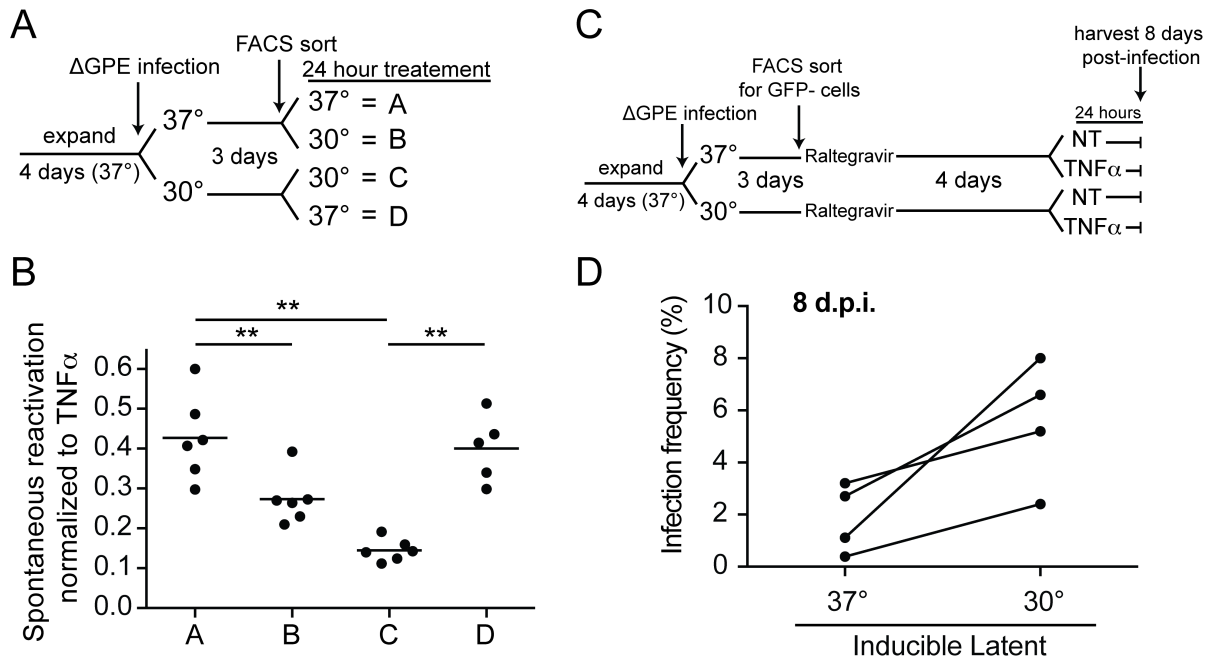
Fig. 2.4: Post-integration latency in quiescent cells is sustained for extended culture periods but easily reversible with removal from the quiescent state. (A) Schematic representation of experimental workflow for (B). (B) Summary graph of the frequency of spontaneous reactivation 24 hours after isolating GFP- cells by FACS normalized to TNFα-inducible reactivation run in parallel as shown in (A) (n=5-6 distinct donors, ** = $p<0.01$, Mann-Whitney tests). (C) Schematic representation of experimental workflow for (D). (D) Summary graph depicting frequency of inducible latent infection in HSPCs treated as in (C). For this analysis, the frequency of spontaneous reactivation occurring in control cells treated with raltegravir (NT, no treatment) and run in parallel was subtracted.

Latency in quiescent cells persists for extended culture periods

To assess whether the increased latent infection observed in HSPCs at 30°C is stable over longer culture periods, latently infected cells were maintained at their respective temperatures in the presence of raltegravir until 7 days post-infection, at which point some were stimulated for 24 hours with TNFα (Fig. 2.4C). Indeed, we found that hypothermia-induced latency continued to be detectable at a higher frequency than when infected cells were cultured under standard conditions even at this extended time point in four of four donors (Fig. 2.4D). These data suggest that proviruses in quiescent cells will

maintain latency for extended periods, but will readily produce viral proteins upon stimulation with TNFα or removal of the quiescent state.

Preferential establishment of latency under hypothermic conditions is not due to deficient expression of NFκB

Given that TNFα is a potent reactivator of latent proviruses in HSPCs and acts by activating NFκB, we asked whether a deficiency in steady-state NFκB expression could explain the reduced HIV protein expression in HSPCs at 30°C. However, we found that expression and nuclear localization of NFκB p65 were identical in HSPCs as assessed by western blot following culture at 37°C or 30°C as in Fig. 2.1H, harvesting at day 4 following the temperature split (Fig. 2.5A, quantified in Fig. 2.5E). Additionally, HSPCs at 37°C and 30°C showed no differences in steady-state activity or responsiveness to TNFα by p65 DNA-binding ELISA (Fig. 2.5B). This suggests that baseline levels of NFκB activity and responsiveness of the NFκB signaling pathway to activation are identical in HSPCs cultured at 30°C and 37°C. Taken together, these data suggest that while NFκB activation is sufficient for reactivation from latency, differences in NFκB expression, DNA-binding capacity, and nuclear localization are not responsible for the increased susceptibility to latent infection in quiescent HSPCs.
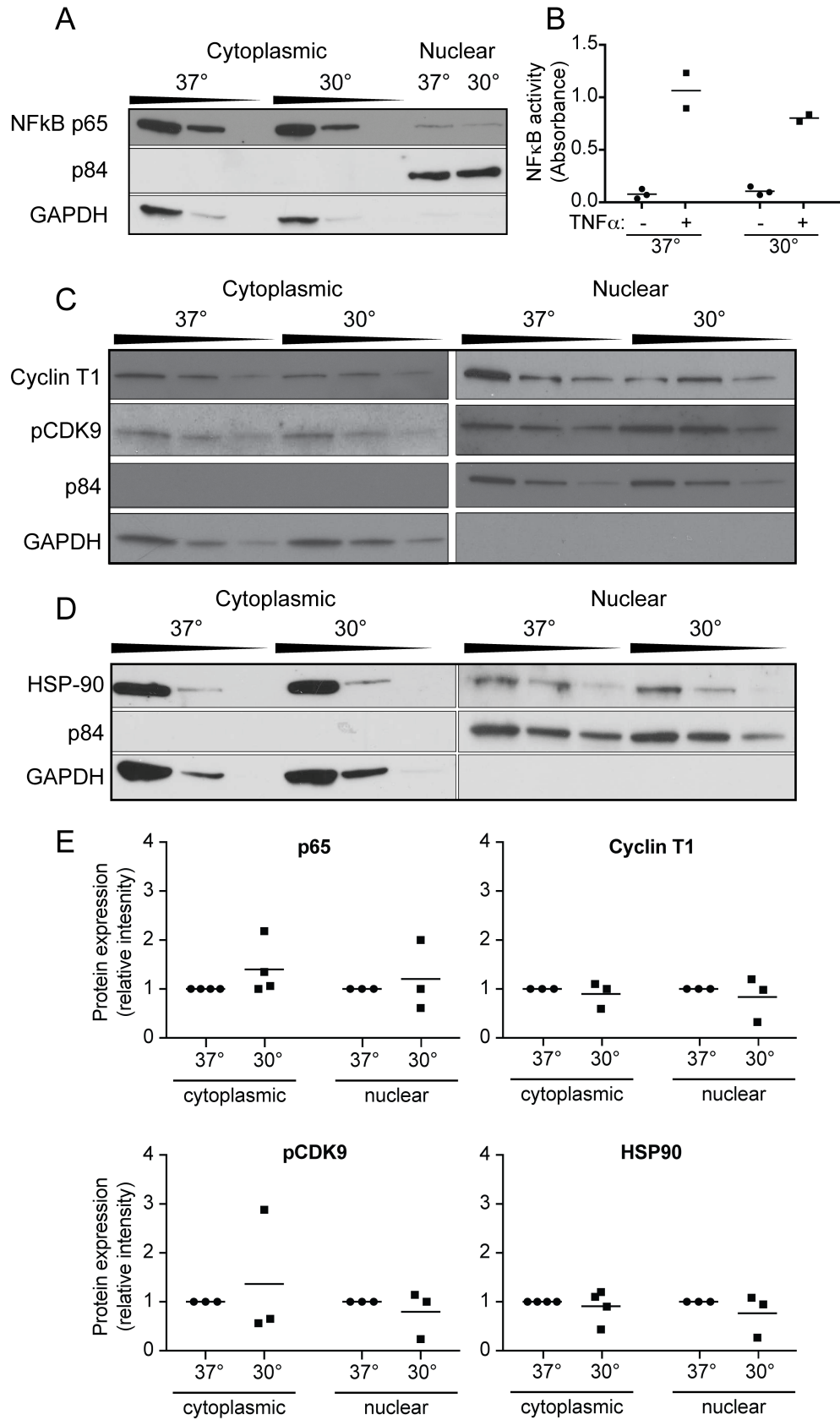
Fig. 2.5: Expression and cellular localization of P-TEFb, NF B, and HSP90 fail to explain latency in quiescent HSPCs in vitro.[4] (A, C and D) Representative western blots of lysates from HSPCs cultured at the indicated temperatures for 4 days post-expansion. The antibody to pCDK9 recognizes the activating phosphorylation at Thr 186 (n=4, distinct donors in separate experiments). p84 and GAPDH serve as controls for separation of the nuclear and cytoplasmic fractions, respectively. Where indicated, fractions were loaded as a serial dilution for enhanced comparison. (B) Summary data from NFκB p65 DNA-binding ELISA using whole cell lysates from HSPCs cultured at the indicated temperature for 4 days post expansion receiving no treatment (NT) or stimulated with TNFα for 6 hours (n=2-3). Each symbol represents an independent experiment using cells from a unique donor. (E) Summary graphs of western blot band intensity quantifications from western blots as in (A, C, and D). The average pixel density of the band was normalized to the pixel density of the loading control for that sample, and subsequently normalized to the relative intensity of the 37°C condition. Each symbol within a condition represents a band from a different gel from a distinct donor (n=3-4 donors).

Preferential establishment of latency under hypothermic conditions is not due to deficient expression of P-TEFb

P-TEFb, composed of CDK9 and cyclin T1, also plays an important role in expression of HIV genes through regulation of transcriptional elongation by RNA polymerase II[16,17]. However, no differences in the level of expression or cellular localization of cyclin T1 and an activated phosphorylated form of CDK9 (Thr 186) were observed in HSPCs cultured at 37°C or 30°C (Fig. 2.5C, quantified in Fig. 2.5E). These data suggest that a deficiency in P-TEFb is not responsible for regulating the increased susceptibility of quiescent HSPCs to latent infection with HIV-1.

HSP90 protein expression is unchanged in hypothermic HSPCs

Heat shock protein 90 (HSP90) is a heat-sensitive chaperone that is known to promote HIV gene transcription. This effect is likely pleiotropic, as several mechanisms for this activity have been described, including via activation of the NFκB pathway, stabilization of the P-TEFb complex, or formation of the RNA Pol II complex in the cytoplasm[26-31,33,34]. In response to the growing body of literature supporting the role of

---

[4] Zaikos TD contributed to generating the data in Fig. 2.5B.

HSP90 in promoting HIV gene transcription, we hypothesized that diminished HSP90 activity in response to hypothermia may be regulating quiescence and latency in this model. As an initial assessment, we measured HSP90 protein expression in cytoplasmic and nuclear fractions of HSPCs cultured at 37°C or 30°C and observed no significant difference (Fig. 2.5D, quantified in Fig. 2.5E). This result, however, did not exclude the possibility that HSP90 activity was reduced at the lower temperature despite similar abundance of HSP90 protein.

Inhibition of HSP90 recapitulates hypothermia-induced quiescence

Despite the lack of change in HSP90 protein levels, it remained possible that hypothermia reduced HSP90 functional activity. Thus, we asked whether inhibition of HSP90 with 17-AAG (tanespimycin) recapitulated the effects of hypothermia on the quiescent cell state of HSPCs. Remarkably when we assessed the effect of HSP90 inhibition on cellular proliferation, differentiation and viability, we found that 17-AAG treatment achieved a similar degree of quiescence in HSPCs at 37°C as in HSPCs at 30°C. Inhibition of HSP90 reduced proliferation as assessed by PKH26 dilution after 2 and 4 days of culture (Fig. 2.6A, upper panels). These results were significant when compiled across three independent experiments (Fig. 2.6A, lower panels, $p<0.05$ for all comparisons, Mann-Whitney tests). Moreover, inhibition of HSP90 with 17-AAG limited the expansion of cells in culture to a similar degree as hypothermia; HSPCs cultured at 37°C in the absence of 17-AAG expanded dramatically, and this expansion was significantly greater than that observed in the presence of 17-AAG or under hypothermic conditions (Fig. 2.6B, $p<0.001$ for each, Mann-Whitney tests).
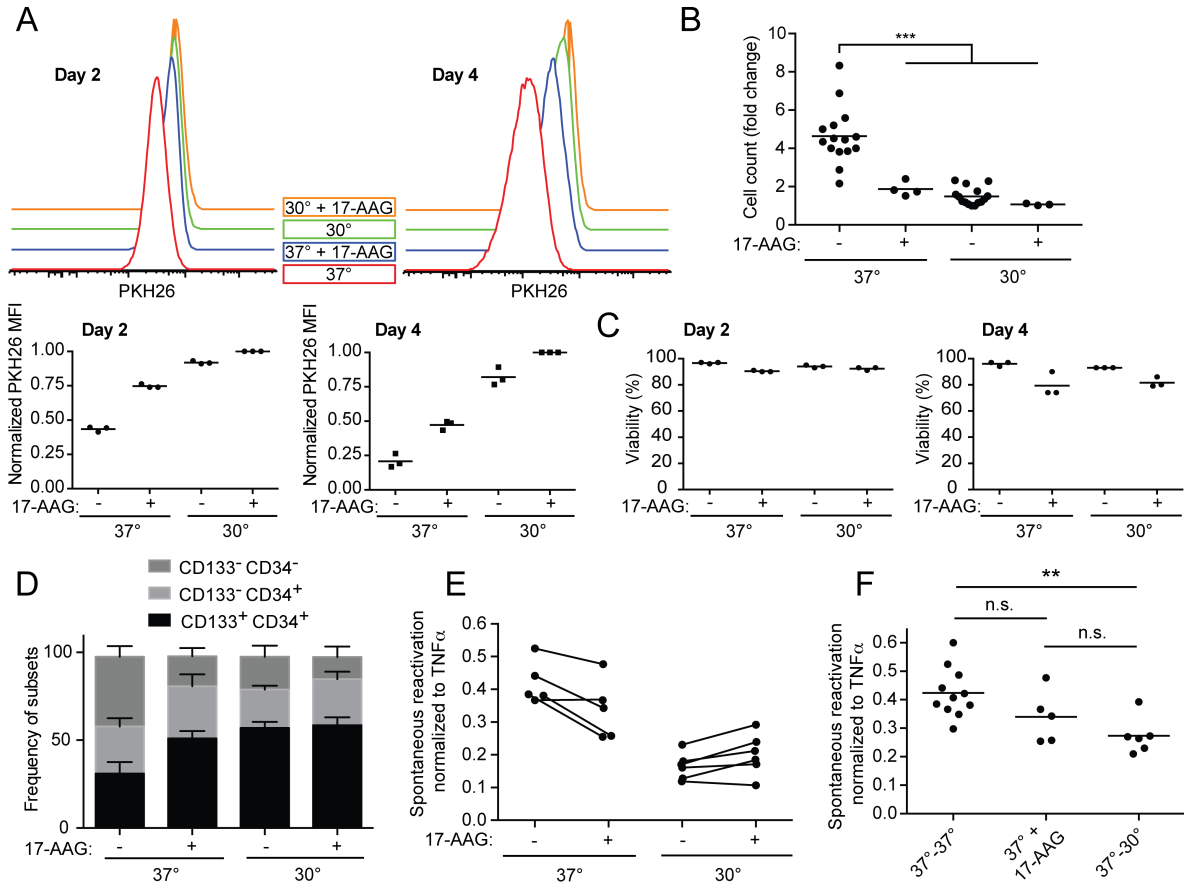
Fig. 2.6: Inhibition of HSP90 with 17-AAG recapitulates latency and quiescence phenotypes of hypothermia. (A) Representative flow plots (upper panel) and summary graphs (lower panel) of PKH26 staining following 2 (left) or 4 (right) days of culture at the indicated temperature plus or minus 17-AAG as indicated. For the summary graph, values were normalized to the 30°C, plus 17-AAG condition ($p<0.05$ for all comparisons, Mann-Whitney tests, MFI = median fluorescence intensity). (B) Summary graph depicting the fold-change in cell number at each condition over a three-day culture period (*** = $p<0.001$, Mann-Whitney tests). (C) Summary plots of flow cytometric data depicting frequency of viable cells after 2 or 4 days at each condition based on inclusion in both a FSC/SSC and a 7-AAD viability gate. Each symbol represents an independent experiment using cells from a unique donor. (D) Summary graph of flow cytometric data from 3 experiments demonstrating the frequency of each of the indicated cellular subsets in the whole population after 3 days at the corresponding conditions. Mean values are shown with error bars indicating standard deviation. (E-F) Summary graphs of frequency of spontaneous reactivation for cells cultured at the indicated temperature for three days and treated for 24 hours as indicated. Values were normalized to the amount of inducible infection by dividing the frequency of GFP+ cells in solvent control by the frequency in TNFα-stimulated cells run in parallel. (E) Connecting lines indicate samples from the same donor (*n*=5-6). (F) Comparison of the effect of 24-hour treatment with 17-AAG or hypothermia on spontaneous reactivation. Temperature switch performed as in Fig. 2.4A (n.s. = not significant, ** = $p<0.01$, Mann-Whitney tests).

Importantly, we demonstrated that treatment with 17-AAG was minimally toxic over the course of 4 days (Fig. 2.6C). In addition, we found that inhibition of HSP90 activity

resembled the effect of hypothermia in that it slowed differentiation of HSPCs at 37°C, leading to a significant increase in the proportion of the most undifferentiated progenitors (CD133$^+$ CD34$^+$) and a significant decrease in the proportion of the most differentiated progenitors (CD133$^-$ CD34$^-$) after 3 days (Fig. 2.6D, $p<0.01$, Wilcoxon signed-rank test). Taken together, these data suggest that inhibition of HSP90 at standard temperatures is sufficient to recapitulate the quiescence observed in HSPCs cultured at hypothermic temperatures.

Inhibition of HSP90 suppresses spontaneous but not TNF-induced reactivation from latency

Having determined that HSP90 inhibition was sufficient to recapitulate the quiescent cellular state observed in hypothermic HSPCs, we asked whether this correlated with reduced spontaneous reactivation from latency. We found that, similar to what was observed under hypothermic conditions, 17-AAG reduced spontaneous reactivation from latency in 4 of 5 donors at 37°C, although this trend was not statistically significant (Fig. 2.6E, $p=0.07$). Consistent with hypothermia and 17-AAG acting on the same factor, we found that spontaneous reactivation from latency at 30°C remained low and was not significantly affected by inhibiting HSP90 (Fig. 2.6E). While the frequency of spontaneous reactivation was higher at 37°C with HSP90 inhibition than at 30°C, it was not significantly different from that observed in cells infected at 37°C and shifted to 30°C for the 24 hour reactivation period, as in Fig. 2.4A (Fig. 2.6F, $p=0.42$), suggesting that quiescence following inhibition of HSP90 is similar to hypothermia in suppressing post-integration spontaneous reactivation of latent proviral genomes.

Latently infected quiescent HSPCs are resistant to reactivation from latency by Histone deacetylase inhibitors (HDACi) and HMBA

As latently infected cells likely exist in a quiescent state *in vivo*, it was important to assess whether quiescent cells differed from actively-proliferating cells in their sensitivity to reactivation by chemical latency reactivators currently being used in therapeutic trials. Indeed, we observed minimal reactivation by the HDACi vorinostat and romidepsin and by the P-TEFb activator HMBA under hypothermic conditions, whereas there was potent reactivation with these compounds at 37°C (Fig. 2.7A). In a compiled analysis of data from multiple independent experiments, vorinostat, romidepsin and HMBA were inefficient at reactivating latency at 30°C. Indeed, romidepsin and HMBA did not significantly reactivate above the solvent control at 30°C despite potent activity at 37°C (Fig. 2.7B). (To facilitate comparison across multiple experiments, the frequency of inducible genomes (GFP$^+$ cells) observed under each condition was normalized to the frequency of TNFα–inducible proviruses observed in paired samples. For this analysis, the frequency of spontaneous reactivation observed in a paired solvent control sample was subtracted prior to normalization.) These results suggest that latent genomes in quiescent cells differ dramatically from those in proliferating cells in their ability to respond to HDACi and P-TEFb stimulation.
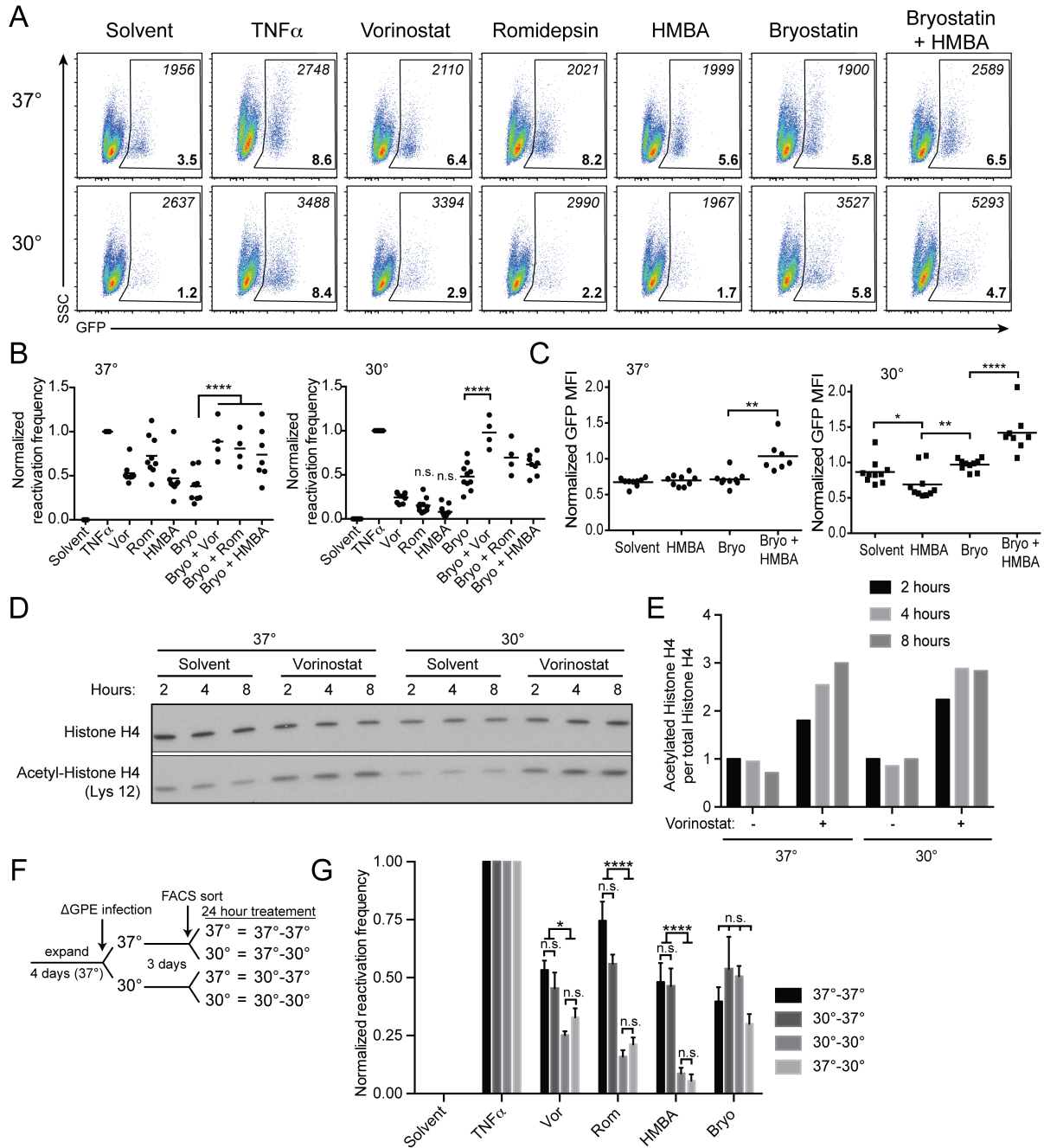
Fig. 2.7: Latent HIV-1 infections in quiescent HSPCs are resistant to reactivation by HDAC inhibitors and HMBA but can be reactivated with bryostatin. (A) Representative flow cytometric plots of latently infected HSPCs treated for 24 hours with the indicated latency-reversing compounds as in Fig. 2.2. Frequency of GFP+ HSPCs is depicted in bold in the bottom-right of each plot, with mean fluorescence intensity (MFI) of GFP in the GFP+ cells shown below in italics in the top-right (*n* = at least 4 experiments). (B) Summary graphs of flow cytometric data as in (A). Spontaneous reactivation as assessed by the frequency of GFP+ cells in the solvent control was subtracted prior to normalization to the frequency of GFP+ cells in the TNFα-stimulated sample (n.s. = not significantly different from solvent control, **** = *p*<0.0001, Mann-Whitney tests). (C) Summary graphs of flow cytometric data as in (A) depicting the GFP MFI in the indicated GFP+ gate for each condition normalized to that of TNFα-stimulated HSPCs (* = p<0.05,

** = p<0.01, **** = p,0.0001, Mann-Whitney tests). (D) Western blot of lysates from HSPCs cultured at the indicated temperatures for 3 days post-expansion and treated with DMSO (solvent) or vorinostat and lysed at the indicated time post-treatment. (E) Quantification of bands in (D) by measuring the pixel density of each band for acetylated Histone H4 and dividing by that of total Histone H4 for each sample. Data are normalized to the baseline proportion of acetylated Histone H4 2 hours post-treatment with solvent control for the respective temperature. (F) Schematic of experimental setup used for (G). (G) Summary graph of flow cytometric data from cells treated as in (F) and stimulated with the indicated reactivation regimen for 24 hours, adjusted for spontaneous reactivation and normalized as in (B). Columns indicate means, and error bars indicate standard deviation (*n*=at least 4, n.s. = not significant, * = *p*<0.05, **** = *p*<0.0001, Mann-Whitney tests). Solvent = matched DMSO.

In contrast, bryostatin, which acts by activating PKC and subsequently NFκB, was effective under both conditions. Additionally, while HDACi and HMBA were not sufficient for reactivation from latency in quiescent HSPCs, they were still capable of enhancing reactivation frequency in combination with bryostatin, suggesting that the drugs are functional at 30°C (Fig. 2.7A and B).

The median fluorescence intensity (MFI) of GFP in GFP⁺ cells was also measured and normalized to that in TNFα-treated cells to determine the level of HIV protein expression in reactivated cells. This measurement reflects the amount of the protein expressed on a per cell basis. Although most treatments had no appreciable effect on GFP MFI (Fig. 2.7A, compiled data not shown), we observed that HMBA increased GFP expression in combination with bryostatin over that observed with bryostatin or HMBA alone, even at 30°C where HMBA alone had no positive effect on reactivation (Fig. 2.7C). These data demonstrate that while HMBA was not sufficient for enhancement of protein expression in quiescent HSPCs, it was still capable of this activity in combination with bryostatin, indicating that the drug had activity at this temperature but was ineffective in the absence of additional stimulation.

Similarly, the failure of vorinostat to reactivate latent genomes in quiescent cells was not due to a loss of activity under hypothermic conditions, as treatment of HSPCs

114

with the HDACi vorinostat efficiently induced Histone H4 acetylation with similar kinetics in HSPCs at both temperatures (Fig. 2.7D and E). No changes in acetylation were observed following treatment with solvent control, confirming that the increased acetylation was due to vorinostat HDAC inhibitory activity and verifying that the drug was capable of inducing chromatin remodeling at 30°C. Taken together, these data suggest that HDACi and HMBA are active at hypothermic temperatures in HSPCs, but their activity is not sufficient to induce reactivation from latency in quiescent cells without additional stimulation.

To determine whether the reduced ability of HDACi and HMBA to reactivate post-integration latency under hypothermic conditions was reversible, we performed temperature shift experiments as depicted in Fig. 2.7F. We observed that cells reactivated for 24 hours at 30°C responded similarly regardless of whether they were infected at 37°C or 30°C, with low responsiveness to HDAC inhibitors or HMBA and high responsiveness to bryostatin. In comparison, cells reactivated at 37°C in a proliferative state were responsive to all reactivation treatments, regardless of whether they were infected at 37°C or 30°C (Fig. 2.7G). These data suggest that mechanisms preventing reactivation with HDACi or HMBA in quiescent cells respond rapidly to changes in the quiescent state of the cell and are regulated post-integration.

Quiescence mediated by HSP90 inhibition also prevents reactivation with HDACi and HMBA

We further hypothesized that quiescence induced by inhibition of HSP90 at 37°C would recapitulate the reactivation profile of hypothermia-induced quiescence. Indeed,

HSPCs reactivated with these approaches in combination with 17-AAG yielded a similar reactivation profile to that at 30°C (Fig. 2.8). Addition of 17-AAG significantly reduced the effects of vorinostat, romidepsin, and HMBA at 37°C, but had no effect on reactivation with bryostatin (Fig. 2.8, *p*<0.01, Mann-Whitney). In contrast, addition of 17-AAG to HSPCs infected and reactivated at 30°C had no significant effect, maintaining the decreased responsiveness to vorinostat, romidepsin, and HMBA compared to HSPCs at 37°C without affecting reactivation with bryostatin (Fig. 2.8, *p*<0.01, Mann-Whitney tests). Inhibition of HSP90 can therefore recapitulate the reduced frequency of spontaneous reactivation and reduced susceptibility to certain reactivation approaches observed for latent HIV-1 proviruses at 30°C, supporting the hypothesis that quiescence leads to greater resistance to reactivation from latency.
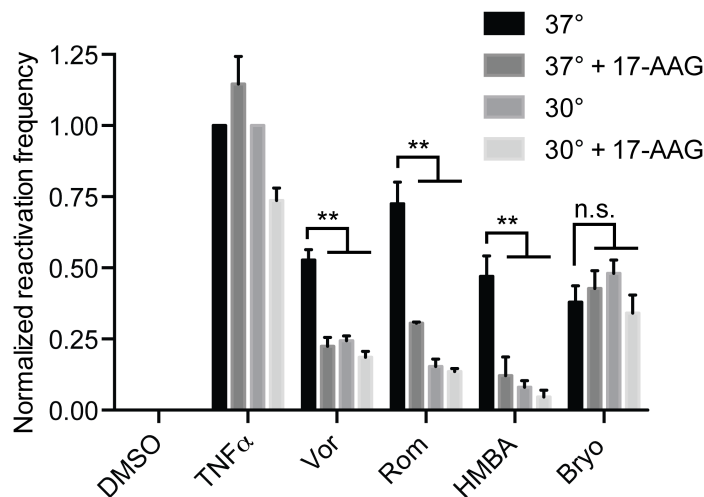
Fig. 2.8: Quiescence following inhibition of HSP90 restricts reactivation in the same way as hypothermia-induced quiescence. Summary graph of flow cytometric data from cells cultured at the indicated temperature for three days and treated with the indicated latency reactivator for 24 hours as in Fig. 2.2. Background reactivation in the DMSO solvent control was subtracted from each sample prior to normalization to the frequency of GFP⁺ cells in the TNFα-stimulated control. Columns indicate means, and error bars indicate standard deviation (*n*=at least 3, n.s. = not significant, ** = *p*<0.01, Mann-Whitney tests).

Discussion

Here we have demonstrated that culturing primary human HSPCs at 30°C maintains these cells in a quiescent state characterized by lower rates of proliferation, differentiation, and progression beyond the G1 phase of the cell cycle. Furthermore, we show that these quiescent HSPCs are susceptible to infection with HIV-1 that is predominantly latent, while proliferating and differentiating HSPCs are susceptible to predominantly active infections. Thus, culturing HSPCs at 30°C as a means of inducing quiescence represents a novel *in vitro* model of HIV-1 latency using primary human cells. We have further shown that latency in this model system is maintained for extended periods in culture, is resistant to spontaneous reactivation, and can be reactivated by NFκB activation in response to TNFα stimulation. In addition, the most undifferentiated progenitor cells found in this model were the most resistant to spontaneous reactivation, while differentiation to more mature progenitors correlated with viral protein expression. This suggests that primitive HSPCs maintained in a quiescent state without undergoing differentiation could harbor latent HIV proviruses for long periods of time. Furthermore, the fact that quiescence-induced latency is reversible in this model of post-integration latency means that our results can't be explained by integration site differences. Instead, our results support the hypothesis that quiescence-induced latency is maintained by an unknown factor with activity that is modulated by the cellular state.

In an effort to determine the mechanisms regulating the latency observed in this model, we have demonstrated that differences in NFκB and P-TEFb expression, activation, and cellular localization were not responsible for the increased frequency of

117

latent infection at 30°C. Interestingly, we found that HMBA treatment, which presumably activates P-TEFb, and chromatin remodeling with HDAC inhibitors only enhanced viral protein expression in quiescent HSPCs when used in combination with bryostatin, a PKC agonist, although they are functional in the absence of bryostatin in proliferating cells. These data suggest that either a factor downstream of PKC stimulation or a deficiency of some factor that can be overcome with PKC stimulation is responsible for maintaining latency in quiescent HSPCs, but is functional at some level in the absence of PKC activation in proliferating HSPCs. Although NFκB would seem to be a likely candidate, we have found no differences in NFκB expression, localization, or activity in HSPCS at 37°C or 30°C. Future studies will be needed to confirm the existence and identity of such a factor and clearly define the mechanism promoting latency in this model. The determination of this mechanism may shed light on the factors regulating whether a particular cell will maintain a latent infection *in vivo* and guide the development of targeted therapies for inducing HIV gene expression from latent proviruses.

The observation that quiescent HSPCs are resistant to reactivation by previously described latency reversing agents that are effective in actively-proliferating HSPCs calls into question whether these therapies will be effective at reactivating latent reservoirs of virus in HSPCs *in vivo*, where the cells harboring latent proviruses tend to be maintained in a quiescent state. This model system may allow for more informative testing of latency reversing agents *in vitro* by establishing a higher threshold for reactivation. In fact, the reactivation profile observed in hypothermic HSPCs closely resembles that of the Greene and Planelles models of HIV latency, which use T cells maintained in a relatively quiescent state, while other models behave more similarly to proliferating HSPCs[19].

Notably, previous clinical trials with HDAC inhibitors vorinostat and romidepsin failed to reduce the size of the HIV-1 latent reservoir *in vivo,* consistent with the inability of these compounds to induce reactivation in quiescent HSPCs[35,36]. Further studies will be needed to determine whether the requirements for reactivation in this quiescent model of latency more accurately reflect those observed *in vivo* than other model systems, including those using actively proliferating HSPCs cultured at 37°C.

We also showed that inhibition of HSP90 is sufficient to induce quiescence and regulates HIV-1 latency similarly to hypothermia in this model. While differences in HSP90 protein expression were not observed, it is still possible that a deficiency in HSP90 activity in hypothermic conditions is responsible for the observations we have described. HSP90 has been shown as a positive regulator of HIV gene expression in numerous studies[26-34], and the mechanism of this activity is likely pleiotropic. Our findings further implicate HSP90 as potentially playing an important role in regulating HIV-1 latency, drawing a novel connection between quiescence-induced latency and HSP90 inhibition. Determining the mechanisms modulating latency downstream of hypothermia and HSP90 inhibition, which may be identical based on their numerous similarities, warrants further investigation. It will be important to determine if these mechanisms are also involved in maintaining latency in quiescent resting memory T cells, which would enhance their utility as targets for reactivation of the latent reservoir in HIV-infected individuals.

We observed that latent proviruses in the least differentiated HSPCs at 30°C were unlikely to reactivate spontaneously, and that spontaneous reactivation correlated with differentiation to more mature progenitors. HSCs are long-lived and are capable of self-renewal. This leads to speculation that a quiescent HSC *in vivo* could be infected with

HIV-1 and maintain the provirus in a latent state. This latent provirus could remain stable without reactivating spontaneously for long periods of time, only reactivating upon differentiation into more mature progenitor cells. As primitive HSCs persist without differentiating throughout the life of an individual, it is possible that these cells could represent a long-lived reservoir of latent HIV-1 infection that is resistant to spontaneous reactivation but continues to contribute to the pool of replicating virus as HSC progeny differentiate and undergo spontaneous reactivation. The possible existence of HSCs as a reservoir of latent virus in HIV-1-infected individuals would represent an additional barrier to the development of a cure for HIV, as reactivation-based approaches would be required to reactivate latent proviruses in both T cells and quiescent HSCs. While the existence of such a reservoir of latent HIV-1 proviruses in HSPCs has been controversial, a recent publication from Sebastian et al.[43] has provided compelling evidence supporting the existence of rare proviruses in bone marrow HSPCs from optimally-treated donors that cannot be attributed to T cell contamination. Furthermore, the low rate of infection observed explains prior negative studies, which lacked statistical power to reliably detect the low frequency of latently infected HSPCs.

Several future lines of investigation will be of interest to expand on the findings presented here. While we used HIV virions pseudotyped with VSV-G to infect HSPCs in this study, characterizing the infection of quiescent HSPCs with full-length, wild-type HIV-1 will be important to better assess how infection of these cells proceeds *in vivo*. Furthermore, while HSPCs likely contribute to the latent reservoir of HIV-1, the major reservoir is in resting memory T cells. Determining whether hypothermia or the underlying mechanisms regulating latency in quiescent HSPCs can be used to enhance T cell

models of HIV-1 latency warrants further investigation. Initial attempts suggest that differences in the cell biology of T cells cause them to respond poorly to hypothermia (data not shown). The model system described here, in combination with improving models of T cell latency, can serve as an important tool to identify effective therapies and gain a deeper understanding of the mechanisms regulating the establishment and maintenance of latency in quiescent cells.

Materials and Methods

Ethics statement

Anonymized whole umbilical cord blood (CB) from uninfected donors was obtained from the New York Blood Center.

Isolation and culturing of HSPCs from human cord blood

HSPCs were isolated from whole umbilical cord blood (New York Blood Center) as previously described[12]. Briefly, cord blood mononuclear cells (CBMCs) were isolated from cord blood by Ficoll-Paque (GE Healthcare) density gradient centrifugation and either frozen in BSA (7.5% in PBS; Gibco) and DMSO (10%; Sigma-Aldrich) in liquid nitrogen or used immediately. CBMCs were then adherence depleted in Stemspan II medium for 2 hours, and non-adherent cells were purified for CD133$^+$ cells by magnetic sort using a CD133 Microbead Kit (Miltenyi Biotech) according to the manufacturer's protocol, with the modification that 1.5X the recommended number of beads were added to increase the purity of the sort. Purity following the magnetic sort was greater than 92% CD133$^+$ cells,

which were also unanimously positive for CD34 expression. Purified HSPCs were then maintained in Stemspan II medium supplemented with 100ng/mL stem cell factor, 100ng/mL thrombopoietin, 100ng/mL Flt3 ligand (all from STEMCELL Technologies), and 100ng/mL insulin-like growth factor binding protein 2 (R&D Systems), termed STIF medium, at 37°C or 30°C with 5% CO_2.

Flow cytometry surface staining

Antibodies with binding specificity for the following surface antigens were used for flow cytometry: CD133 (phycoerythrin [PE] conjugated; Miltenyi Biotec), and CD34 (fluorescein isothiocyanate [FITC] or allophycocyanin [APC] conjugated; Miltenyi Biotec). Cells were stained with 2μg/mL 7-aminoactinomycin D (7-AAD; Calbiochem) to exclude dead cells. For staining of surface proteins, cells were suspended in FACS buffer (2% FBS, 1% human serum, 2mM HEPES, 0.025% sodium azide in PBS) with 7-AAD and antibodies (CD34, CD133), incubated on ice for 15 minutes, washed, and then fixed in 2% paraformaldehyde in PBS. Flow cytometry data were collected with a BD FACS Canto cytometer or a BD FACScan cytometer with Cytek 6-color upgrade and analyzed with FlowJo software.

PKH26 proliferation assay

HSPCs were stained with PKH26 cell membrane-binding dye (Sigma-Aldrich) according to the manufacturer's protocol immediately following isolation of CD133+ cells. HSPCs were maintained as described above, and intensity of PKH26 staining was assessed by

flow cytometry using a BD FACS Canto cytometer. Histograms were generated and median fluorescence intensity of PKH26 was calculated using FlowJo software.

DAPI cell cycle analysis

Total cellular DNA content was assessed by staining HSPCs with DAPI (Thermo Scientific) and determining the intensity of DAPI staining by flow cytometry. HSPCs were harvested, washed twice with PBS, fixed on ice in 70% ethanol in PBS, washed with PBS, permeabilized and stained with 1μg/mL DAPI in 0.1% Triton X 100 (Fisher Biotech) in PBS for 30 minutes on ice. Data for the intensity of DAPI staining were collected using a BD FACS Canto cytometer, and cell cycle analysis was performed using FlowJo software. Following doublet exclusion, DAPI signal intensity was plotted on a linear scale and the proportion of singlets in G1, S, or G2/M phase was determined by averaging the results from the Watson (pragmatic) and Dean-Jett-Fox models, with the G2 coefficient of variation (CV) set to equal the CV of G1.

Viral constructs and HIV-1 infection of HSPCs

HSPCs were infected with HIV-1 construct NL4-3-ΔGPE-E-GFP[12] after 4 days of expansion at 37°C following isolation of CD133^{+} cells. Infectious viral supernatants were produced by transfection of the proviral NL4-3-ΔGPE-E-GFP plasmid into 293T cells using polyethylenimine. Proviral plasmid was co-transfected with a plasmid containing vesicular stomatitis virus glycoprotein (VSV-G) to generate VSV-G-pseudotyped viral particles and a helper plasmid (p-CMV-HIV), which encodes the necessary structural proteins for virion formation that are absent in NL4-3-ΔGPE-E-GFP. Culture supernatants

from these 293T cells were collected 48 to 72 hours post-transfection, filtered through a 0.4μm syringe filter (GE Healthcare), and frozen at -80°C. 293T cells were cultured in Dulbecco's modified Eagle medium (DMEM; Gibco) supplemented with 10% fetal bovine serum (FBS; Gibco), 1 U/ml penicillin, 1 μg/ml streptomycin, 292 μg/ml glutamine (Gibco), and 56μg/mL plasmocin (Invivogen), termed D10 medium.

HSPCs were infected by spin inoculation at 1,049 x g for 2 hours at room temperature. Mock infected controls were treated with D10 culture medium. Following spin inoculation, the viral supernatants were removed and HSPCs were resuspended in STIF medium. Cells were then split and maintained at 37°C or 30°C in STIF immediately post-infection.

FACS sort and reactivation studies

HSPCs infected with NL4-3-ΔGPE-E-GFP were sorted for GFP$^-$ cells by fluorescence-activated cell sorting (FACS) using a FACSAria III (BD Biosciences) cytometer to remove GFP$^+$ (actively infected) cells and obtain a pure population of GFP$^-$ (uninfected or latently infected) cells. GFP$^+$ and GFP$^-$ populations were defined using mock-infected HSPCs.

Following isolation of GFP$^-$ HSPCs, 70,000-100,000 cells were immediately resuspended in 200μL Stemspan II medium supplemented with 8μM Raltegravir (Selleck Chemicals) in all experiments, along with one of the following treatment conditions: 3ng/mL tumor necrosis factor alpha (TNFα; R&D Chemicals), 1μM vorinostat (Vor, Cayman Chemical), 25nM romidepsin (Rom, Selleck Chemicals), 10mM Hexamethylene bisacetamide (HMBA, Sigma-Aldrich), 2.5nM bryostatin-1 (Bryo, Sigma-Aldrich), or 750nM 17-N-

allylamino-17-demethoxygeldanamycin (17-AAG, Selleck Chemicals). Combination treatments used the same concentrations of each compound as individual treatments. Solvent controls were performed with cells cultured in Stemspan II supplemented with raltegravir and either water or DMSO matched to the concentration in the treated samples. Reactivation observed in solvent controls was termed *spontaneous reactivation* and was subtracted from calculations of the frequency of *inducible latent infection* or frequency of reactivated cells with different treatments. Treatments were performed immediately following the FACS sort, and cells were harvested for flow cytometric analysis after 24 hours.

HSPCs cultured for extended periods following the FACS sort were cultured in STIF supplemented with $8\mu M$ Raltegravir until 7 d.p.i., at which point cells were resuspended in Stemspan II supplemented with $8\mu M$ Raltegravir and stimulated with TNFα or solvent control for 24 hours as described above.

Nuclear and cytoplasmic fractionation and Western blotting

HSPCs were expanded for 4 days at 37°C, then split to 37°C or 30°C for 4 additional days. Cells were harvested and nuclear and cytoplasmic fractions were isolated using a Nuclear Extract Kit (Active Motif) according to the manufacturer's protocol. Nuclear and Cytoplasmic extracts were loaded into wells of a polyacrylamide gel for Western blot at serial dilutions to enhance comparisons of protein expression levels. Western blotting was performed using antibodies directed against the following proteins: NFκB p65 (clone 572, Invitrogen), pCDK9 (activating phosphorylation on Thr186; Cell Signaling

Technology), cyclin T1 (Santa Cruz Biotechnology), GAPDH (Abnova) and p84 (Abcam) as cytoplasmic and nuclear protein controls, respectively. HRP-conjugated secondary antibodies were used (Invitrogen), and signal was detected using Pierce ECL (Thermo Scientific) or Amersham ECL Prime (GE Healthcare).

For acetylated Histone H4 western blots as in Fig. 2.7D-E, whole cell lysates were obtained using Blue Loading Buffer (Cell Signaling Technology, 7722S) according to manufacturer's protocol and membranes were probed with primary antibodies against the following proteins: Histone H4, pantropic (Millipore, 04-858) and acetyl-Histone H4 (Lys 12) (Millipore, 04-119). Secondary antibodies and detection reagents were as above.

NFκB p65 ELISA

Whole cell lysates were obtained from HSPCs after 8 days in culture using a TransAM NFκB Kit (Active Motif) according to the manufacturer's protocol. Protein concentrations were determined by Bradford assay, and equal protein amounts were loaded into each ELISA reaction. ELISA was performed according to the manufacturer's protocol in the TransAM NFκB Kit (Active Motif) kit.

Cell counts

For cell counting experiments, CD133$^+$ HSPCs were isolated as described and expanded for 4 days in STIF culture medium at 37°C. Cells were then split to 37°C or 30°C, with or without 17-AAG (750nM, Selleck Chemicals) added to the STIF culture medium. Cells

were sampled two, three, and four days after splitting to these conditions and live cells were counted with a hemoctyometer following Trypan Blue (Gibco) staining.

Quantification of Western blots

Western blotting results were quantified using Photoshop by determining the average pixel density in a box of equal size overlayed with each band from a single, unedited film displaying a single gel. No quantification comparisons were made from bands on different films or gels at any point.

Statistical analyses

All statistical analyses were performed using GraphPad Prism software as described in the figure legends for each experiment.

Acknowledgments

like to express our gratitude toward S.-J.-K. Yee (City of Hope National Medical Center) for providing pCMV-HIV-1.

References

1. Chun T-W, Carruth L, Finzi D, et al. Quantification of latent tissue reservoirs and total body viral load in HIV-1 infection. *Nature.* 1997;387(6629):183-188.
2. Finzi D, Hermankova M, Pierson T, et al. Identification of a reservoir for HIV-1 in patients on highly active antiretroviral therapy. *Science.* 1997;278(5341):1295-1300.
3. Finzi D, Blankson J, Siliciano JD, et al. Latent infection of CD4+ T cells provides a mechanism for lifelong persistence of HIV-1, even in patients on effective combination therapy. *Nature medicine.* 1999;5(5):512-517.
4. Zack JA, Arrigo SJ, Weitsman SR, Go AS, Haislip A, Chen IS. HIV-1 entry into quiescent primary lymphocytes: molecular analysis reveals a labile, latent viral structure. *Cell.* 1990;61(2):213-222.
5. Brooks DG, Kitchen SG, Kitchen CM, Scripture-Adams DD, Zack JA. Generation of HIV latency during thymopoiesis. *Nat Med.* 2001;7(4):459-464.
6. Brennan TP, Woods JO, Sedaghat AR, Siliciano JD, Siliciano RF, Wilke CO. Analysis of human immunodeficiency virus type 1 viremia and provirus in resting CD4+ T cells reveals a novel source of residual viremia in patients on antiretroviral therapy. *Journal of virology.* 2009;83(17):8470-8481.
7. Bailey JR, Sedaghat AR, Kieffer T, et al. Residual human immunodeficiency virus type 1 viremia in some patients on antiretroviral therapy is dominated by a small number of invariant clones rarely found in circulating CD4+ T cells. *Journal of virology.* 2006;80(13):6441-6457.
8. Embretson J, Zupancic M, Ribas JL, et al. Massive covert infection of helper T lymphocytes and macrophages by HIV during the incubation period of AIDS. *Nature.* 1993;362(6418):359.
9. Koenig S, Fauci AS. Detection of AIDS virus in macrophages in brain tissue from AIDS patients with encephalopathy. *Science.* 1986;233:1089-1094.
10. Carter CC, Onafuwa-Nuga A, McNamara LA, et al. HIV-1 infects multipotent progenitor cells causing cell death and establishing latent cellular reservoirs. *Nature medicine.* 2010;16(4):446-451.
11. McNamara LA, Onafuwa-Nuga A, Sebastian NT, Riddell J, Bixby D, Collins KL. CD133+ hematopoietic progenitor cells harbor HIV genomes in a subset of optimally treated people with long-term viral suppression. *Journal of Infectious Diseases.* 2013:jit118.
12. McNamara LA, Ganesh JA, Collins KL. Latent HIV-1 infection occurs in multiple subsets of hematopoietic progenitor cells and is reversed by NF-kappaB activation. *J Virol.* 2012;86(17):9337-9350.
13. Redd AD, Avalos A, Essex M. Infection of hematopoietic progenitor cells by HIV-1 subtype C, and its association with anemia in southern Africa. *Blood.* 2007;110(9):3143-3149.
14. Nabel G, Baltimore D. An inducible transcription factor activates expression of human immunodeficiency virus in T cells. *Nature.* 1987;326(6114):711-713.

15. Mehla R, Bivalkar-Mehla S, Zhang R, et al. Bryostatin modulates latent HIV-1 infection via PKC and AMPK signaling but inhibits acute infection in a receptor independent manner. *PloS one.* 2010;5(6):e11160.

16. Wei P, Garber ME, Fang S-M, Fischer WH, Jones KA. A novel CDK9-associated C-type cyclin interacts directly with HIV-1 Tat and mediates its high-affinity, loop-specific binding to TAR RNA. *Cell.* 1998;92(4):451-462.

17. Zhu Y, Pe'ery T, Peng J, et al. Transcription elongation factor P-TEFb is required for HIV-1 tat transactivation in vitro. *Genes & development.* 1997;11(20):2622-2632.

18. Contreras X, Barboric M, Lenasi T, Peterlin BM. HMBA releases P-TEFb from HEXIM1 and 7SK snRNA via PI3K/Akt and activates HIV transcription. *PLoS Pathog.* 2007;3(10):e146.

19. Spina CA, Anderson J, Archin NM, et al. An in-depth comparison of latent HIV-1 reactivation in multiple cell model systems and resting CD4+ T cells from aviremic patients. *PLoS Pathog.* 2013;9(12):e1003834.

20. Contreras X, Schweneker M, Chen C-S, et al. Suberoylanilide hydroxamic acid reactivates HIV from latently infected cells. *Journal of Biological Chemistry.* 2009;284(11):6782-6789.

21. Archin NM, Espeseth A, Parker D, Cheema M, Hazuda D, Margolis DM. Expression of latent HIV induced by the potent HDAC inhibitor suberoylanilide hydroxamic acid. *AIDS research and human retroviruses.* 2009;25(2):207-212.

22. Wei DG, Chiang V, Fyne E, et al. Histone deacetylase inhibitor romidepsin induces HIV expression in CD4 T cells from patients on suppressive antiretroviral therapy at concentrations achieved by clinical dosing. *PLoS Pathog.* 2014;10(4):e1004071.

23. Huber K, Doyon G, Plaks J, Fyne E, Mellors JW, Sluis-Cremer N. Inhibitors of histone deacetylases correlation between isoform specificity and reactivation of HIV Type 1 (HIV-1) from latently infected cells. *Journal of Biological Chemistry.* 2011;286(25):22211-22218.

24. Keedy KS, Archin NM, Gates AT, Espeseth A, Hazuda DJ, Margolis DM. A limited group of class I histone deacetylases acts to repress human immunodeficiency virus type 1 expression. *Journal of virology.* 2009;83(10):4749-4756.

25. Pittet J-F, Lee H, Pespeni M, O'Mahony A, Roux J, Welch WJ. Stress-induced inhibition of the NF-κB signaling pathway results from the insolubilization of the IκB kinase complex following its dissociation from heat shock protein 90. *The journal of Immunology.* 2005;174(1):384-394.

26. O'Keeffe B, Fong Y, Chen D, Zhou S, Zhou Q. Requirement for a kinase-specific chaperone pathway in the production of a Cdk9/cyclin T1 heterodimer responsible for P-TEFb-mediated tat stimulation of HIV-1 transcription. *Journal of Biological Chemistry.* 2000;275(1):279-287.

27. Pan X-Y, Zhao W, Wang C-Y, et al. Heat shock protein 90 facilitates latent HIV reactivation through maintaining the function of positive transcriptional elongation factor b (p-TEFb) under proteasome inhibition. *Journal of Biological Chemistry.* 2016;291(50):26177-26187.

28.	Boulon S, Pradet-Balade B, Verheggen C, et al. HSP90 and its R2TP/Prefoldin-like cochaperone are involved in the cytoplasmic assembly of RNA polymerase II. *Molecular cell.* 2010;39(6):912-924.

29.	Roesch F, Meziane O, Kula A, et al. Hyperthermia stimulates HIV-1 replication. *PLoS Pathog.* 2012;8(7):e1002792.

30.	Joshi P, Maidji E, Stoddart CA. Inhibition of heat shock protein 90 prevents HIV rebound. *Journal of Biological Chemistry.* 2016;291(19):10332-10346.

31.	Vozzolo L, Loh B, Gane PJ, et al. Gyrase B inhibitor impairs HIV-1 replication by targeting Hsp90 and the capsid protein. *Journal of Biological Chemistry.* 2010;285(50):39314-39328.

32.	Joshi P, Sloan B, Torbett BE, Stoddart CA. Heat shock protein 90AB1 and hyperthermia rescue infectivity of HIV with defective cores. *Virology.* 2013;436(1):162-172.

33.	Bedin M, Gaben AM, Saucier C, Mester J. Geldanamycin, an inhibitor of the chaperone activity of HSP90, induces MAPK-independent cell cycle arrest. *International journal of cancer.* 2004;109(5):643-652.

34.	Burrows F, Zhang H, Kamal A. Hsp90 activation and cell cycle regulation. *Cell cycle.* 2004;3(12):1530-1536.

35.	Archin NM, Bateson R, Tripathy M, et al. HIV-1 expression within resting CD4 T-cells following multiple doses of vorinostat. *Journal of Infectious Diseases.* 2014:jiu155.

36.	Søgaard OS, Graversen ME, Leth S, et al. The depsipeptide romidepsin reverses HIV-1 latency in vivo. *PLoS Pathog.* 2015;11(9):e1005142.

37.	Rasmussen TA, Tolstrup M, Brinkmann CR, et al. Panobinostat, a histone deacetylase inhibitor, for latent-virus reactivation in HIV-infected patients on suppressive antiretroviral therapy: a phase 1/2, single group, clinical trial. *The Lancet HIV.* 2014;1(1):e13-e21.

38.	Prins JM, Jurriaans S, van Praag RM, et al. Immuno-activation with anti-CD3 and recombinant human IL-2 in HIV-1-infected patients on potent antiretroviral therapy. *Aids.* 1999;13(17):2405-2410.

39.	Bullen CK, Laird GM, Durand CM, Siliciano JD, Siliciano RF. New ex vivo approaches distinguish effective and ineffective single agents for reversing HIV-1 latency in vivo. *Nature medicine.* 2014;20(4):425-429.

40.	Cillo AR, Sobolewski MD, Bosch RJ, et al. Quantification of HIV-1 latency reversal in resting CD4+ T cells from patients on suppressive antiretroviral therapy. *Proceedings of the National Academy of Sciences.* 2014;111(19):7078-7083.

41.	Josefsson L, Eriksson S, Sinclair E, et al. Hematopoietic precursor cells isolated from patients on long-term suppressive HIV therapy did not contain HIV-1 DNA. *The Journal of infectious diseases.* 2012;206(1):28-34.

42.	Durand CM, Ghiaur G, Siliciano JD, et al. HIV-1 DNA is detected in bone marrow populations containing CD4+ T cells but is not found in purified CD34+ hematopoietic progenitor cells in most patients on antiretroviral therapy. *Journal of Infectious Diseases.* 2012;205(6):1014-1018.

43.	Sebastian NT, Zaikos TD, Terry V, et al. CD4 is expressed on a heterogeneous subset of hematopoietic progenitors, which persistently harbor CXCR4 and CCR5-tropic HIV proviral genomes in vivo. *PLoS Pathogens.* 2017;13(7):e1006509.

44. Arai F, Hirao A, Ohmura M, et al. Tie2/angiopoietin-1 signaling regulates hematopoietic stem cell quiescence in the bone marrow niche. *Cell.* 2004;118(2):149-161.
45. Cheng T, Rodrigues N, Shen H, et al. Hematopoietic stem cell quiescence maintained by p21cip1/waf1. *Science.* 2000;287(5459):1804-1808.
46. Doulatov S, Notta F, Eppert K, Nguyen LT, Ohashi PS, Dick JE. Revised map of the human progenitor hierarchy shows the origin of macrophages and dendritic cells in early lymphoid development. *Nature immunology.* 2010;11(7):585-593.
47. Goussetis E, Theodosaki M, Paterakis G, et al. A functional hierarchy among the CD34+ hematopoietic cells based on in vitro proliferative and differentiative potential of AC133+ CD34bright and AC133dim/-CD34+ human cord blood cells. *Journal of hematotherapy & stem cell research.* 2000;9(6):827-840.
48. Freund D, Oswald J, Feldmann S, Ehninger G, Corbeil D, Bornhäuser M. Comparative analysis of proliferative potential and clonogenicity of MACS-immunomagnetic isolated CD34+ and CD133+ blood stem cells derived from a single donor. *Cell proliferation.* 2006;39(4):325-332.
49. Matsumoto K, Yasui K, Yamashita N, et al. In vitro proliferation potential of AC133 positive cells in peripheral blood. *Stem Cells.* 2000;18(3):196-203.
50. Carter CC, McNamara LA, Onafuwa-Nuga A, et al. HIV-1 utilizes the CXCR4 chemokine receptor to infect multipotent hematopoietic stem and progenitor cells. *Cell host & microbe.* 2011;9(3):223-234.

CHAPTER 3

Concanamycin A Counteracts HIV-1 Nef to Enhance Immune Clearance of Infected Primary Cells by Cytotoxic T Lymphocytes[5]

Abstract

Nef is a human immunodeficiency virus (HIV)-encoded accessory protein that enhances pathogenicity by downregulating major histocompatibility class I (MHC-I) expression to evade killing by cytotoxic T lymphocytes (CTLs). A potent Nef inhibitor that restores MHC-I is needed to promote immune-mediated clearance of HIV-infected cells. We discovered that the plecomacrolide family of natural products restored MHC-I to the surface of Nef-expressing primary cells with variable potency. Concanamycin A (CMA) counteracted Nef at sub-nanomolar concentrations that did not interfere with lysosomal acidification or degradation and were non-toxic in primary cell cultures. CMA specifically reversed Nef-mediated downregulation of MHC-I, but not CD4, and cells treated with CMA showed reduced formation of the AP-1:Nef:MHC-I complex required for MHC-I downregulation.

---

[5] Portions of this chapter were published previously:

CMA restored expression of diverse allotypes of MHC-I in Nef-expressing cells and inhibited Nef alleles from divergent clades of HIV and SIV, including from primary patient isolates. Lastly, we found that restoration of MHC-I in HIV-infected cells was accompanied by enhanced CTL-mediated clearance of infected cells comparable to genetic deletion of Nef. Thus, we propose CMA as a lead compound for therapeutic inhibition of Nef to enhance immune-mediated clearance of HIV-infected cells.

Introduction

The development of combination antiretroviral therapy (ART) has drastically altered the course of the HIV epidemic, yet HIV infection remains a lifelong condition for which there is no cure. The virus persists despite the presence of HIV-specific cytotoxic T lymphocytes (CTLs), the main effectors of cellular adaptive immunity responsible for clearing viral infections[1,2]. While rare elite controllers with particularly potent CTLs or CTLs targeting vulnerable antigens can spontaneously suppress the virus, even these individuals fail to clear the infection[3-5]. In controllers or ART-treated patients with suppressed viral loads, HIV persists in long-lived latent reservoirs of virus. Approaches to clear these reservoirs by reactivating latent viruses have provided evidence that latency can be reversed *in vivo*, but this alone is unlikely to eliminate infected cells[6-9]. Thus, new strategies are needed to enhance the clearance of infected cells following latency reversal.

CTLs recognize peptide antigens presented in the context of major histocompatibility complex class-I (MHC-I) on the surface of infected cells, mediating

death of the target cell through perforin and Fas lytic pathways[10]. MHC-I is both polygenic, with genes encoding HLA-A, -B, -C, -E, -F, and -G, and polymorphic, with remarkable allelic variation particularly in HLA-A, -B, and -C[11]. Polygeny allows for functional separation, as HLA-A and -B, and to a lesser extent -C, are responsible for presenting peptides to CTLs, which recognize non-self-antigens expressed by intracellular pathogens. HLA-C, -E, and -G are predominantly responsible for inhibiting the responsiveness of natural killer (NK) cells, which recognize cells with low MHC-I[12] and elevated natural killer cell activating ligands[13]. Allelic variation in the antigen-presenting forms of MHC-I yields alleles that are optimized for presentation of diverse peptides[14]. Some alleles of HLA-B, in particular, are associated with rapid or delayed progression of HIV disease, and this may be attributable to whether the optimal peptide repertoire for an allele includes vulnerable regions in the HIV genome[5,15,16].

MHC-I is loaded with peptides in the endoplasmic reticulum and proceeds through the secretory pathway to reach the cell surface[17]. The HIV accessory protein Nef alters MHC-I trafficking by binding to the cytoplasmic tail of MHC-I early in the secretory pathway, stabilizing an interaction between a tyrosine residue in the MHC-I cytoplasmic tail and the tyrosine-binding pocket in the μ subunit of clathrin adaptor protein 1 (AP-1)[18,19]. Formation of the AP-1:Nef:MHC-I complex mediates the redirection of MHC-I into the endolysosomal trafficking pathway in an ADP-ribosylation factor-1 (ARF-1)-dependent manner, where it is degraded in the lysosome[20,21]. Lysosomal acidification, which is required for the function of lysosomal proteases responsible for this degradation, is maintained by the vacuolar H^+-ATPase (V-ATPase), a rotary proton-pumping motor[22]. X-ray crystallography[23] and cryo-electron microscopy analyses[24] have confirmed the

direct contacts between Nef, MHC-I, AP-1, and ARF-1 and described the structural basis for these interactions[25].

As a result of these interactions, HIV-infected cells expressing Nef experience a loss of cell-surface MHC-I, which protects them from being killed by HIV-specific CTLs[26]. Nef binds specifically to the cytoplasmic domains of HLA-A and -B, but not HLA-C and -E. Because of their different functional roles, this differentiation optimizes evasion of both CTL and NK cell responses and is conserved across primate lentiviruses[27-29]. The identification of a potent inhibitor of Nef that restores MHC-I to the surface of HIV-infected cells therefore represents an important and perhaps essential step toward the goal of efficiently clearing HIV reservoirs following therapeutic latency reversal. Here we describe a novel function for the plecomacrolide family of natural products, in particular concanamycin A, which potently counteracts Nef downregulation of MHC-I to enhance CTL-mediated clearance of HIV-infected primary lymphocytes.

Results

Screening for natural-product inhibitors of HIV Nef

To identify a Nef inhibitor capable of reversing MHC-I downmodulation in HIV-infected cells, we performed a high-throughput flow cytometric screen for compounds that increased expression of recombinant HLA-A2 in a CEM T cell line (CEM-A2) expressing Nef from a gutted adenoviral vector (Appendix, Fig. 3.S1A)[30]. HLA-A2 was chosen as a representative allele of MHC-I because HLA-A allotypes are strongly targeted by Nef for downregulation[27], HLA-A2 is abundant in diverse ethnic groups[31], and a high-affinity

monoclonal antibody selective for HLA-A2 (BB7.2) is available[32]. Initial screening of over 200,000 small molecules failed to identify convincing hits. Screening of over 20,000 natural product extracts[33] identified 37 that were positive in the primary screen and negative in the counter screen. A secondary screen using CEM-A2 cells infected with a VSV-G pseudotyped single-round reporter virus derived from the HIV NL4-3 molecular clone (NL4-3-ΔGPE-EGFP, ΔGPE, Fig. 3.1A) confirmed that extracts from 11 strains inhibit Nef in the context of HIV infection (Appendix, Fig. 3.S1B-C).

Natural product Nef inhibitors are plecomacrolides

Natural product metabolites with anti-Nef activity analyzed by NMR and mass spectrometry were identified as members of the bafilomycin (Baf) plecomacrolide family of natural products (Figs. S2A-C and S3A)[34]. Baf A1 and C1 purified from our natural product extracts by standard fractionation procedures had near identical activity to commercial sources of these compounds (Appendix, Fig. 3.S3B-C). Baf A1 dramatically increased cell-surface HLA-A2 in CEM-A2 cells expressing Nef from the cytomegalovirus promoter in the context of an adenoviral delivery vector (Appendix, Fig. 3.S4A-B) and the HIV LTR using ΔGPE (Appendix, Fig. 3.S4C-D). Nef-dependent HLA-A2 downmodulation was reduced by over ten-fold in CEM-A2 cells (Appendix, Fig. 3.S4C-D) and by 18-fold in primary T cells transduced with ΔGPE (Fig. 3.1B).

Plecomacrolides have diverse Nef inhibitory potencies and achieve superior restoration of MHC-I compared to recently identified Nef Inhibitors B9 and Lovastatin

The plecomacrolide family includes the bafilomycins, which have a characteristic 16-member ring, and the concanamycins, which have an 18-member ring (Appendix, Fig. 3.S3A). We exposed HIV-infected primary CD4$^+$ T cells to plecomacrolide family members and determined that each restored MHC-I to similar levels, but with variable potencies (Fig. 3.1C-D). CMA counteracted Nef at the lowest concentrations (EC_{50} = 0.07nM), while Baf C1 was most potent among the bafilomycins (EC_{50} = 0.4nM, Baf B1 = 1.6nM, Baf A1 = 2.8nM, Baf D = 380nM). We further confirmed that the effects of CMA on Nef activity could not be attributed to a reduction in viral gene expression (Appendix, Fig. 3.S5).

For comparison, we also tested recently identified Nef inhibitors B9 and lovastatin. Both B9[35,36] and lovastatin[37] have been reported to impair multiple Nef functions, with the effects of lovastatin evident only at supratherapeutic concentrations. We observed no effect of B9 on Nef-dependent MHC-I downmodulation across a wide range of concentrations, including those that had been previously reported to inhibit Nef in cells (Appendix, Fig. 3.S4A-F)[35,36]. For lovastatin, we observed little restoration of MHC-I at 24 hours post-treatment, but did confirm that lovastatin partially restored MHC-I to the surface of Nef-expressing cells after 48 hours of exposure. However, restoration of MHC-I by lovastatin required 2,000-fold higher concentrations than CMA and failed to achieve comparable levels (Appendix, Fig. 3.S4G-H). To confirm that the negative results achieved with B9 were not due to receipt of the wrong compound, we independently validated that the purchased material matched the published structure of B9 by ^{1}H NMR (Appendix, Fig. 3.S6) and mass spectrometry (Appendix, Fig. 3.S7) analysis. Based on

these results, we conclude that CMA achieves the greatest magnitude of MHC-I restoration and is the most potent Nef inhibitor yet described.

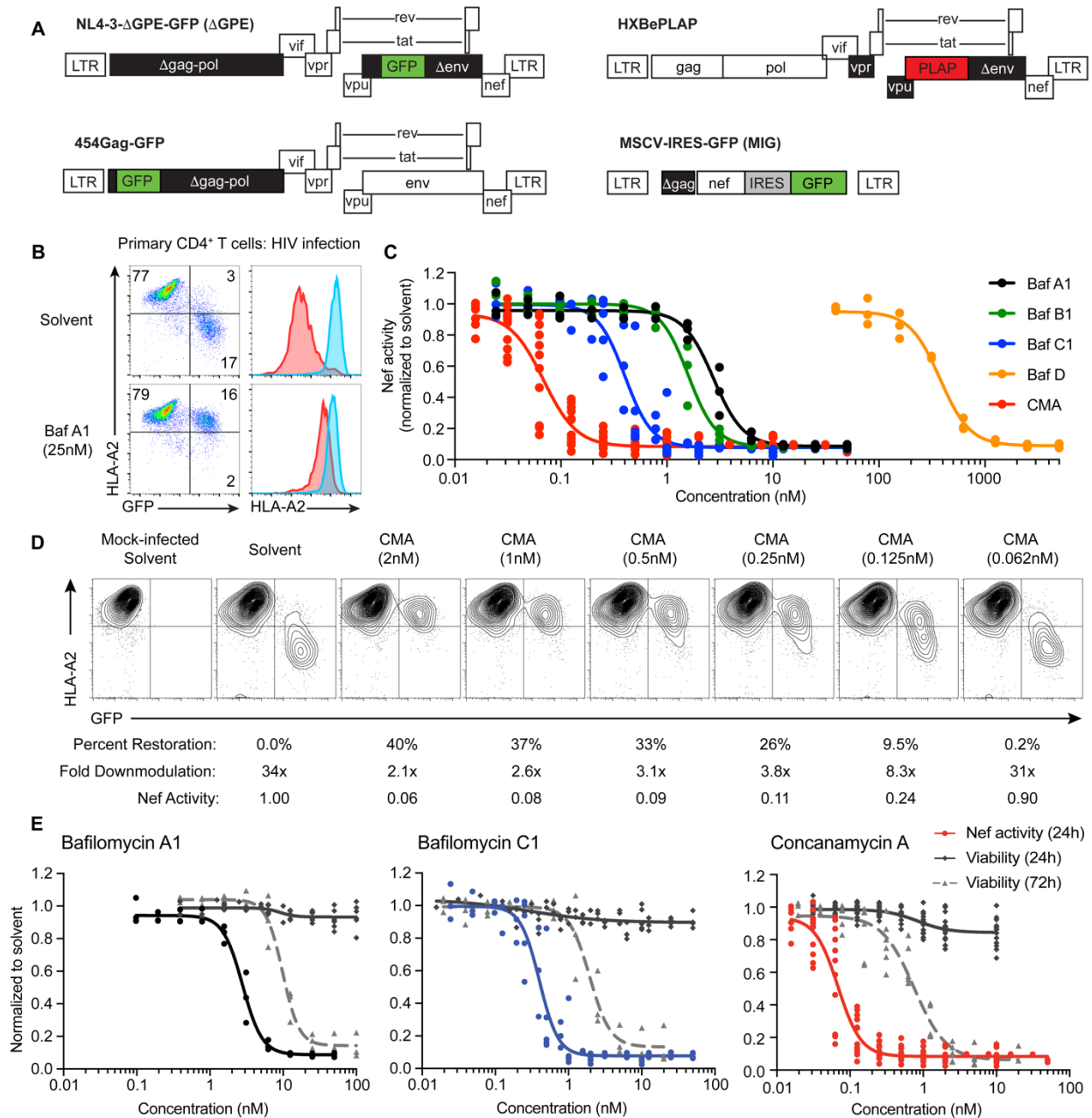**Fig. 3.1: Plecomacrolides possess distinct potencies for Nef inhibition and cellular toxicity, which are separable for CMA[6].** (A) Schematic representations of viral genomes used throughout the manuscript. Deleted genes are in black. (B) Representative flow cytometry plots (n=3) from primary CD4+ T cells

---

[6] Zimmerman GE contributed to data in Fig. 3.1C and 3.1E. Merlino MS contributed to data in Fig. 3.1E.

infected with HIV ΔGPE and treated with Baf A1 as in Appendix, Fig. 3.S1B. Blue histograms are from GFP⁻ cells, red histograms are from infected GFP⁺ cells. Compiled data are in C. (C) Summary graph of flow cytometric data from primary CD4⁺ T cells infected as in B and treated with the indicated plecomacrolides (n=3 for Baf A1, B1 and D, n=8 for Baf C1, n=12 for CMA). Nef activity is the fold downmodulation of Nef normalized to solvent control as shown in D. (D) Representative flow cytometric plots from experiments summarized in C, shown from the donor with results closest to the mean among 12 donors tested. Percent restoration, fold downmodulation, and Nef activity were calculated as described in Materials and Methods. (E) Summary graph comparing Nef activity as in D after 24 hours (n=3 for Baf A1, n=8 for BafC1, n=12 for CMA) and viability as in Appendix, Fig. 3.S8A after 24 hours (n=7 for Baf A1, n=8 for Baf C1, n=15 for CMA) and 72 hours of plecomacrolide exposure(n=3 for Baf A1 and Baf C1, n=6 for CMA). Solvent control is DMSO. Extra sum-of-squares F test used to compare IC_{50} values of curves.

CMA restores MHC-I at concentrations that are non-toxic to primary cells

High-dose plecomacrolide treatment is toxic to cells, and questions remain over the safety and utility of plecomacrolides in clinical applications targeting V-ATPase activity[38-40]. We did not observe any notable toxicity with 24-hour exposure to plecomacrolides in the above or any subsequent experiments (Fig. 3.1E). However, in agreement with published reports, we observed toxicity when primary cells were exposed to plecomacrolides at high concentrations for extended periods[41,42]. Nevertheless, based on MTT and flow cytometric viability assays (Appendix, Fig. 3.S8A-B), inhibition of Nef in CD4⁺ primary T cells occurred at concentrations that were non-toxic even with 72 hours of direct exposure (Fig. 3.1E). For CMA there was an 11-fold difference between the 50% effective and toxic concentrations (EC_{50} and TC_{50}). This compared with 3.5-fold and 4.8-fold differences for Baf A1 and C1, respectively (Fig. 3.1E). For subsequent experiments in primary CD4⁺ T cells, we utilized 24-hour incubations with 0.5nM CMA, which suppressed Nef activity by 10-fold and maintained 95% viability (Fig. 3.1E).

We also found that G0/G1 cell cycle arrest, a reported effect of plecomacrolide exposure, was minimal even at concentrations well above the EC_{50} for Nef inhibition (Appendix, Fig. 3.S8C)[43]. CD4⁺ T cells treated with 0.5nM CMA showed a 1.15-fold increase in the proportion of cells in S phase compared to the solvent control, but the

corresponding decrease in cells in G2/M was not statistically significant. Given the small

magnitude of these changes, it is unlikely that cell cycle arrest meaningfully contributes

to toxicity in cells treated with 0.5nM CMA. Thus, plecomacrolides, and particularly CMA,

may be promising lead compounds for therapeutic Nef inhibition.

Plecomacrolides have distinct Nef inhibitory and lysosome neutralization potencies

The toxicity associated with plecomacrolide treatment likely results from their

inhibition of V-ATPase, which is responsible for many cellular processes, including

lysosomal acidification[44]. To determine whether inhibition of lysosomal pH might be

responsible for reversal of MHC-I downmodulation in Nef-expressing cells, we adapted a

previously-described method to measure the pH of the lysosome of primary human

monocyte-derive macrophages (MDMs) by measuring ratiometric fluorescence of an

endocytosed dextran[45] (Appendix, Fig. 3.S9A). We first confirmed that Baf A1 completely

neutralized lysosomal pH (Appendix, Fig. 3.S9B-C). We then tested each of the

plecomacrolides over a range of concentrations. Interestingly, the most potent inhibitor of

Nef, CMA, was not the most potent inhibitor of V-ATPase. Instead, Baf C1 (EC_{50} = 7.3nM)

neutralized lysosomes more potently than CMA (EC_{50} = 12.7nM, $p<0.0001$), which had

comparable potency to Baf A1 (EC_{50} = 18.5nM, $p=0.06$). (Fig. 3.2A). This evidence

indicated a qualitative separation between plecomacrolide inhibition of Nef in primary T

cells and V-ATPase-mediated acidification in MDMs.

Because CD4$^+$ T cells did not efficiently endocytose dextran, we assessed

lysosomal neutralization in these cells with Lysotracker Red dye, which freely crosses cell

membranes until it reaches an acidic compartment, where it is protonated and retained. As measured by flow cytometry (Fig. 3.2B-C) and confocal microscopy (Appendix, Fig. 3.S9D), the EC_{50} for lysosome neutralization by CMA in primary $CD4^+$ T cells (EC_{50} = 1.9nM) was significantly higher than the EC_{50} for Nef inhibition (EC_{50} = 0.07 nM, 27-fold difference, $p<0.0001$). Taken together, these results indicate that CMA counteracted Nef in primary human $CD4^+$ T cells at concentrations that were non-toxic and did not alter lysosomal pH.

CMA restores cell-surface MHC-I, but not CD4, in Nef-expressing cells

Both MHC-I and CD4 are targeted to the lysosome by Nef, but by distinct mechanisms. MHC-I is redirected from the trans-Golgi network to the lysosome via the AP-1 adaptor complex[18,19], while CD4 is internalized from the cell surface and trafficked to the lysosome in an AP-2-dependent manner[46]. Based on the above data, we hypothesized that surface restoration of MHC-I was not simply secondary to lysosome dysregulation. To explore this hypothesis, we treated pure populations of HIV-infected primary cells with a high dose of CMA that neutralizes the lysosome (2.5nM) or a low dose that leaves acidic compartments intact (0.5nM). We found that neither dose of CMA reversed Nef-dependent downregulation of cell-surface CD4, while downregulation of surface MHC-I was reversed equally in both conditions (Fig. 3.2D). This indicated that CMA specifically redirects MHC-I, and not all proteins targeted to the lysosome by Nef, to the cell surface.

CMA restores MHC-I in Nef-expressing cells with functional lysosomal protein degradation

We then sought to confirm that CMA restores MHC-I by a mechanism independent of its effects on lysosomal degradation by directly observing Nef-mediated lysosomal degradation. As expected, both MHC-I and CD4 were degraded in Nef-expressing cells (Fig. 3.2E, left). A high dose of CMA, which neutralized the lysosome (Figs. 2B-C, S9D), inhibited Nef-mediated degradation of both HLA-A2 and CD4 (Fig. 3.2E, center). Notably, high-dose CMA also increased MHC-I expression in uninfected cells, consistent with disruption of the steady-state turnover of MHC-I in the lysosome. Low-dose CMA, however, did not prevent degradation of CD4 and did not increase steady-state levels of MHC-I, indicating that the lysosome was functional for protein degradation. Despite this, MHC-I was not degraded in Nef-expressing cells (Fig. 3.2E, right). Thus, low-dose CMA treatment selectively alters the transport of MHC-I in HIV-infected primary cells, preventing redirection to the lysosome and restoring MHC-I to the cell surface.

To validate these results, we performed immunofluorescence microscopy on pure populations of HIV-infected primary CD4$^+$ T cells. Cells infected with Nef-expressing HIV had a dramatic reduction in cell surface and total expression of HLA-A2 compared to uninfected cells or cells infected with Nef-deficient HIV (Fig. 3.2F). Exposure to 0.5nM CMA restored the appearance of MHC-I staining to that observed in the absence of Nef (Fig. 3.2F). High doses (2.5nM) of CMA caused accumulation of HLA-A2 in intracellular compartments, consistent with inhibition of lysosomal degradation. Taken together, these experiments confirmed that low doses of CMA that do not disrupt lysosomal function specifically restore MHC-I to the surface of Nef-expressing HIV-infected CD4+ T cells.

These results strongly suggest a role for CMA in this process that is independent of its effects on lysosomal pH through its known target, V-ATPase.
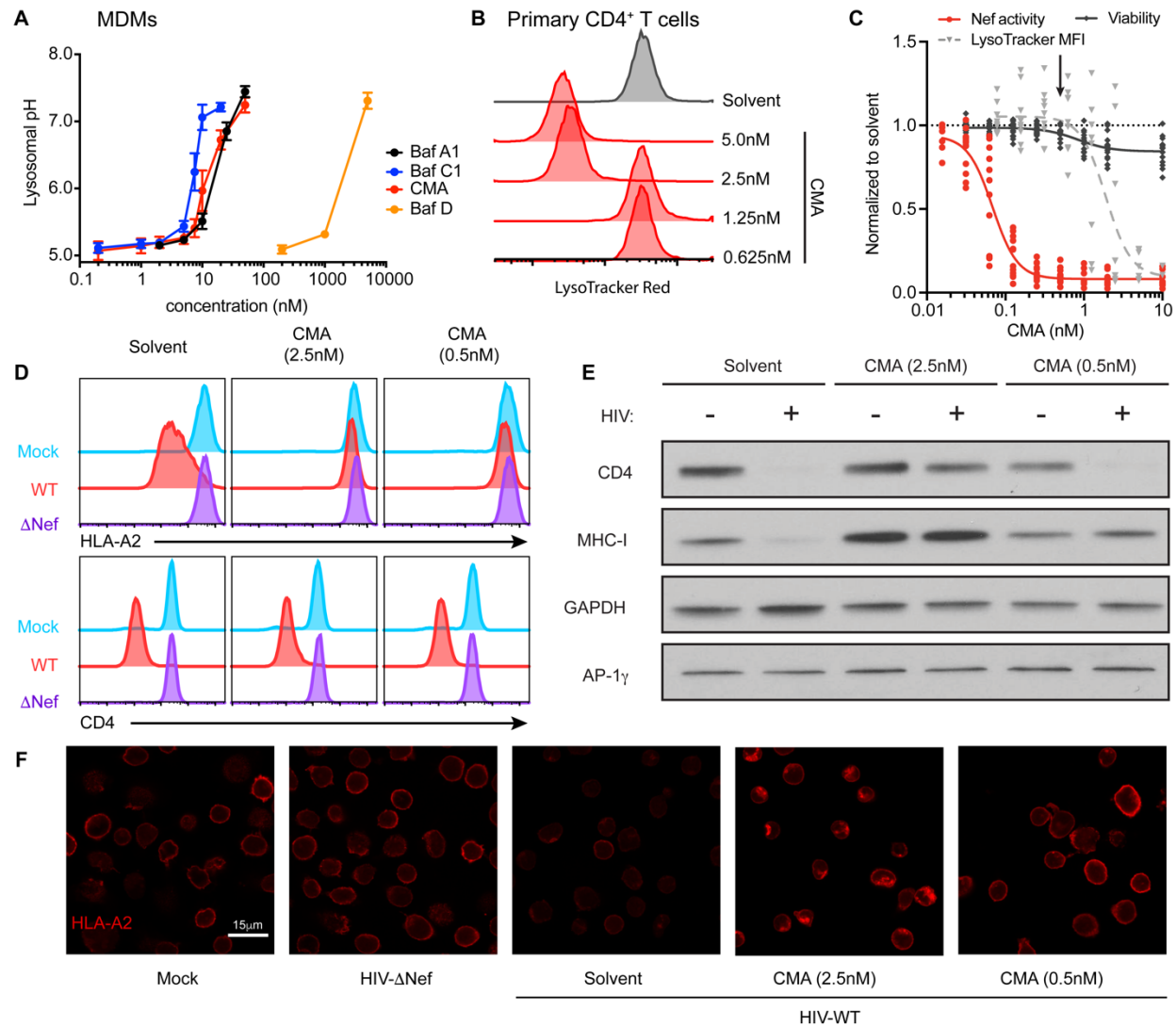
Fig. 3.2: Lysosome function and acidification remain intact at concentrations of CMA that restore MHC-I.[7] (A) Summary graph of flow cytometric data from MDMs as in S9A-C, treated with plecomacrolides for 1 hour as indicated (n=8 for Baf A1 and Baf C1, n=2 for Baf D, n=6 for CMA). (B) Representative flow cytometry histograms of primary activated CD4^{+} T cells treated for 24 hours with CMA as indicated and incubated with Lysotracker Red for 1 hour. (C) Summary graph of flow cytometric data from B comparing the normalized median fluorescence intensity (MFI) of Lysotracker Red (n =9) with the normalized Nef activity (n=12) and viability (n=15) from Fig. 3.1E in primary CD4^{+} T cells treated with CMA at the indicated concentrations. Arrow indicates concentration of CMA used in primary cells in Fig. 3.4-3.5. (D) Representative flow cytometry histograms from primary activated CD4^{+} T cells infected with HXBePLAP (Fig. 3.1A) for 72 hours, sorted for PLAP^{+} cells, and treated with CMA as indicated for 24 hours. Blue histograms represent mock-infected cells, red histograms represent sorted PLAP^{+} cells infected with

---

[7] Lubow J contributed to experiments in Fig. 3.2A. Zimmerman GE performed experiments and generated Fig. 3.2B, 3.2C, and 3.2F.

HXBePLAP (WT), and purple histograms represent sorted PLAP$^+$ cells infected with HXBePLAP in which Nef was deleted (ΔNef, representative of 3 independent experiments). (E) Western blot of whole cell lysates from CD4$^+$ T cells prepared as described for (D) (representative of 4 independent experiments). (F) Representative confocal microscopy images of primary activated CD4$^+$ T cells prepared as described in D, stained for HLA-A2. Mock cells are uninfected. All images were captured with identical microscope settings. Solvent control is DMSO. Extra sum-of-squares F test used to compare IC$_{50}$ values of curves.

CMA reduces the association of Nef and AP-1 with MHC-I

The observation that CMA selectively affects MHC-I and not CD4 degradation suggests that CMA disrupts the formation of the AP-1:Nef:MHC-I complex. To test this directly, we used CEM-A2 cells transduced with an adenoviral vector expressing Nef. This system has been used to study the formation of the AP-1:Nef:MHC-I complex under conditions where ammonium chloride (NH$_4$Cl) prevents lysosomal degradation[18]. Higher concentrations of CMA were required for reversal of Nef activity in CEM cells than in primary CD4$^+$ T cells. However, we identified 1.25nM CMA as a non-toxic concentration that inhibited Nef without significantly altering intracellular acidification (Fig. 3.3A). Thus, we consider this to be functionally similar to 0.5nM CMA treatment in primary CD4$^+$ T cells.

Because both NH$_4$Cl and CMA stabilized HLA-A2 expression to similar levels, we were able to compare whether CMA specifically resulted in a reduction in the abundance of the AP-1:Nef:MHC-I relative to what is observed under conditions of lysosomal neutralization. We found that CMA treatment led to a reproducible reduction in the abundance of Nef, AP-1γ, and AP-1μ1 subunits associating with HLA-A2 compared to cells treated with NH$_4$Cl (Fig. 3.3B). These effects were highly significant when compiled across multiple experiments (Fig. 3.3C, p < 0.0001). Control experiments confirmed the specificity of the assay, as detection of AP-1γ, and AP-1μ1 in pulldowns required both HLA-A2 and Nef (Fig. 3.3B, leftmost lanes). In addition, we confirmed that the complex

145

could not reliably be observed in the absence of NH$_4$Cl due to robust HLA-A2 degradation

and minimal HLA-A2 recovery in the presence of Nef (Fig. 3.3B, leftmost lanes).
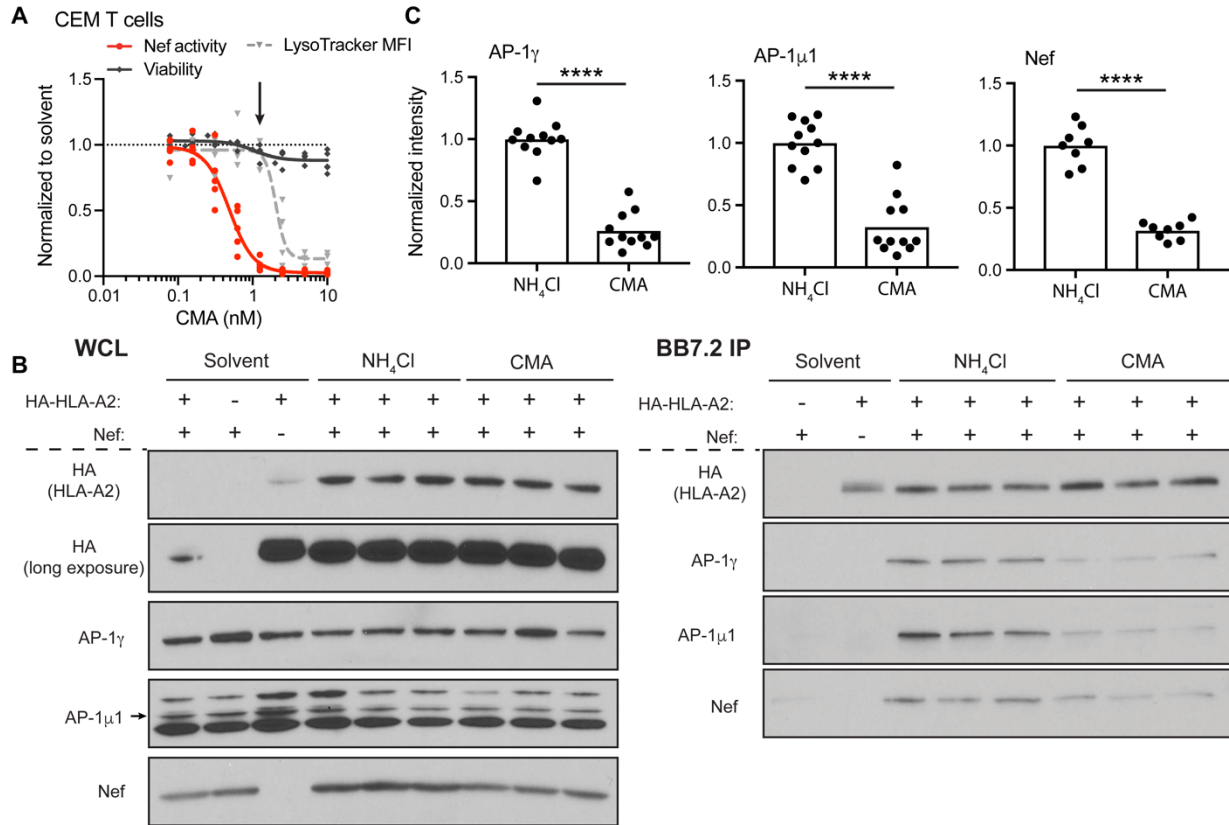
Fig. 3.3: CMA reduces the abundance of AP-1:Nef:MHC-I complexes. (A) Summary graph of flow cytometric data comparing the normalized median fluorescence intensity (MFI) of Lysotracker Red (n =4) with the normalized Nef activity following ΔGPE infection as in Appendix, Fig. 3.S1B (n=5) and viability as in Fig. 3.S8A (n=5) in CEM-A2 cells treated with a range of CMA concentrations for 24 hours. Arrow indicates the concentration of CMA used in remaining experiments with CEM cells. (B) Representative western blot depicting three experimental replicates (of 11 total replicates) of whole cell lysates before (left panel) or matched samples after (right panel) immunoprecipitation using BB7.2-conjugated beads (specific for HLA-A2) from CEM-SS or CEM-A2 cells transduced with Nef-expressing adenoviral vector construct or the control vector lacking Nef. NH$_4$Cl = 35mM NH$_4$Cl. CMA = 1.25nM CMA. (C) Summary graphs quantifying experimental replicates of western blots for AP-1 subunits (n=11) and Nef (n=8) as in B. Band intensities were recorded for each protein from a single exposure in which all bands were visible but none were saturated. Band intensity was normalized to the intensity of HLA-A2 for each sample to account for differences in HLA-A2 recovery. Results were normalized to NH$_4$Cl, and the mean of NH$_4$Cl values was used where multiple replicates were run simultaneously as in B. **** = $p < 0.0001$, unpaired two-tailed t-tests.

To determine whether CMA directly binds to components of the AP-1:Nef:MHC-I

complex, we performed differential scanning fluorimetry thermal stability assays using a

146

comprehensive panel of purified components of the AP-1:Nef:MHC-I complex (Appendix, Fig. 3.S10A) including the AP-1 μ1-C-terminal domain, the MHC-I tail fused with HIV-1 NL4-3 Nef, the μ1-CTD:MHC-NL4-3 Nef complex, the AP-1 core, the AP-1 trimer containing AP-1 core:Arf1-GTP: MHC-NL4-3 Nef complex, and NL4-3 Nef alone (Appendix, Fig. 3.S10B-G). No significant changes in T_m were observed with 1-hour incubation of any of the samples with CMA compared to solvent control, indicating that CMA does not bind directly to any of these members of the ARF-1:AP-1:Nef:MHC-I complex *in vitro*. Furthermore, when GST-tagged MHC-I cytoplasmic tail was immobilized on resin, the presence of CMA did not alter pulldown of NL4-3 Nef, SIV Nef, or the AP-1 μ1-CTD (Appendix, Fig. 3.S10H). In summary, these results demonstrate that CMA impairs the formation of the AP-1:Nef:MHC-I complex in cells. However, we did not observe direct binding of CMA to known protein components of the complex, implicating the existence of an alternative target necessary for Nef-specific MHC-I trafficking.

CMA enhances CTL-mediated clearance of HIV-infected cells comparably to genetic deletion of *nef*

There is a large body of literature indicating that increases in cell-surface MHC-I on target cells yield proportional increases in CTL-mediated clearance of target cells[47-50]. Given that Nef-expressing CD4^{+} T cells treated with 0.5nM CMA have near normal surface expression of HLA-A2 (Fig. 3.2D), we hypothesized that CMA would eliminate Nef-mediated protection of HIV-infected cells from HIV-specific CTLs. To test this directly, we performed *in vitro* flow cytometric CTL killing assays (Appendix, Fig. 3.S11A) with two HLA-A2-restricted CTL clones expressing T cell receptors specific for HLA-A2 presenting

the Gag SL9 epitope, which is expressed in the HIV molecular clone HXBePLAP (Fig. 3.1A)[26].

As previously observed[26], PLAP+ primary cells infected with a Nef-deleted virus were efficiently eliminated by CTLs (Fig. 3.4A, top row). In contrast, CTL-mediated elimination of cells infected with a Nef-competent virus was notably reduced at every effector:target (E:T) ratio. Importantly, there was no further elimination of PLAP+ cells when the E:T ratio was increased from 5:1 to 10:1, indicating that there was a residual population of Nef-expressing cells that were highly resistant to clearance even by a large excess of potent HIV-specific CTLs (Fig. 3.4A, middle row). Cells infected with Nef-competent virus and treated with 0.5nM CMA, however, had restored HLA-A2 expression, and the PLAP+ subset was efficiently eliminated by CTLs (Fig. 3.4A, bottom row). The effect of CMA on CTL killing of HIV-infected cells was indistinguishable from genetic deletion of Nef and was Nef-dependent, as there was no increase in clearance of cells infected with Nef-deleted virus (Fig. 3.4B). Importantly, when target cells from a donor lacking HLA-A2 were co-cultured with CTLs, there was no reduction in PLAP+ target cells regardless of whether they were treated with CMA (Appendix, Fig. 3.S11B), validating the specificity of the CTLs and demonstrating that CMA only enhances clearance of HIV-infected cells in the presence of both Nef and specific anti-HIV CTL responses. Nef-dependent increases in killing of CMA-treated cells were statistically significant for both CTL clones tested ($p<0.0001$, Appendix, Fig. 3.S11C). These observations confirm that low-dose CMA treatment of Nef-expressing cells restores HLA-A2 that is properly loaded with an HIV-derived peptide that can be successfully presented to CTLs without impairing responsiveness to CTL-derived lytic signals.

Previous reports have indicated that concentrations of CMA greater than 1nM could inhibit the effector functions of CTLs, but no such effect was observed at 0.5nM CMA[51,52]. We confirmed these published results using our anti-HIV CTLs. We observed no change in the clearance of SL9 peptide-pulsed target cells in the presence of 0.5nM CMA (Fig. 3.S11D).
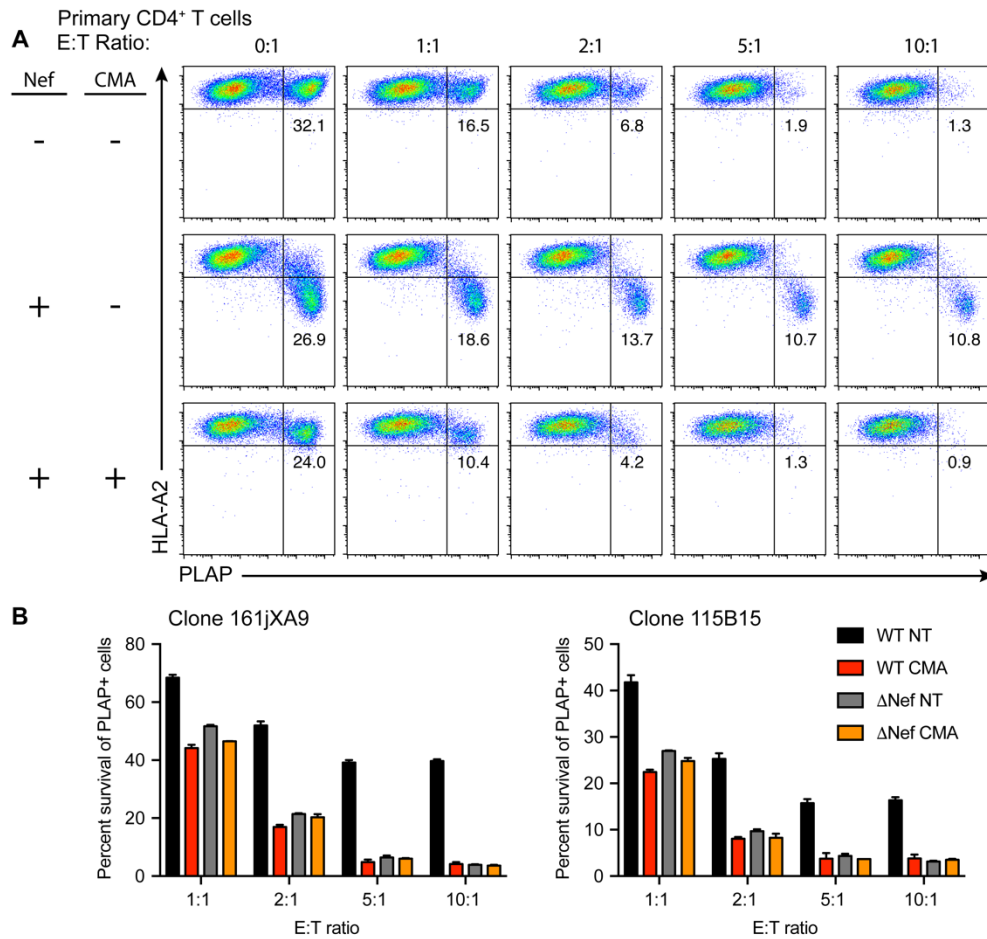
Fig. 3.4: CMA enhances clearance of HIV-infected cells by HIV-specific CTLs.[8] (A) Representative flow cytometry plots depicting CTL-mediated killing of primary CD4+ T cells infected with HXBePLAP plus or minus Nef (Fig. 3.1A) for 72 hours and treated for 24 hours with 0.5nM CMA or matched DMSO solvent control prior to 4-hour co-culture with CTLs. Cells were gated for CD4$^+$ T cell targets as in Appendix, Fig. 3.S11A. (B) Summary graph of results from A in two independent experiments using two distinct CTL clones. Each condition was performed in duplicate, and survival of PLAP$^+$ cells was determined by normalizing to the mean of quadruplicate 0:1 samples. Error bars represent standard deviation. WT,

---

[8] Terry VH contributed to experiments in Fig. 3.4.

HXBePLAP wild-type; ΔNef, HXBePLAP in which Nef was deleted; E:T, effector:target ratio, indicates the number of anti-HIV CTLs present in the 4-hour co-culture per CD4^{+} T cell target cell.

CMA reverses Nef-mediated downregulation of HLA-B in primary cells

Nef downregulates both HLA-A and HLA-B allotypes, and many patients possess robust HLA-B-restricted, HIV-specific CTLs[53-55]. Thus, we sought to determine whether CMA would restore HLA-B expression in HIV-infected cells. Sequence differences in HLA-B allotypes classify them as either HLA-Bw4 or HLA-Bw6 serotypes. Each serotype can be detected with monoclonal antibodies, but these antibodies are cross-reactive with some HLA-A (Bw4) and HLA-C (Bw6) allotypes[56]. As previously reported, we identified a donor that was heterozygous for Bw4 (B*51:01) and Bw6 (B*07:02) with no cross-reactive HLA-A alleles and minimal cross-reactivity from HLA-C, allowing us to reliably measure expression of two HLA-B alleles (Appendix, Fig. 3.S12A)[56]. We observed significant downmodulation of both HLA-B*51:01 and HLA-B*07:02 in cells infected with ΔGPE, which was consistently counteracted by CMA (Fig. 3.5A-C). The effects of Nef and CMA on both HLA-B alleles in this donor were similar in magnitude to those observed for HLA-A*02 in an array of donors (Fig. 3.5B). Thus, we conclude that CMA can potently counteract Nef-mediated downregulation of both HLA-A and HLA-B allotypes in primary CD4^{+} T cells.

A primary HIV isolate from an optimally-treated patient downregulates MHC-I and is inhibited by CMA

Enhancing the clearance of latent reservoirs of virus that persist in optimally-treated patients, likely following therapeutic reactivation from latency, is an important clinical application for a Nef inhibitor. We previously isolated a full-length provirus that

was expressed as residual plasma virus in an optimally-treated patient and was further shown to be infectious[57]. We deleted Gag-Pol and introduced GFP, allowing identification of infected cells in a single round infection while preserving Nef from the original isolate (454-Gag-GFP, Fig. 3.1A). Primary CD4$^+$ T cells infected with 454-Gag-GFP demonstrated downregulation of HLA-A*02:01, HLA-B*51:01, and HLA-B*07:02, which was Nef-dependent (Figs. 5D and S12B). CMA restored expression of all three allotypes of MHC-I in the context of infection with the primary isolate virus (Fig. 3.5D), and this result was confirmed in two additional donors for HLA-A*02 (Appendix, Fig. 3.S12C). Thus, we have demonstrated that sub-nanomolar concentrations of CMA can potently restore MHC-I to the surface of primary cells expressing Nef from a virus isolated from an optimally-treated patient.
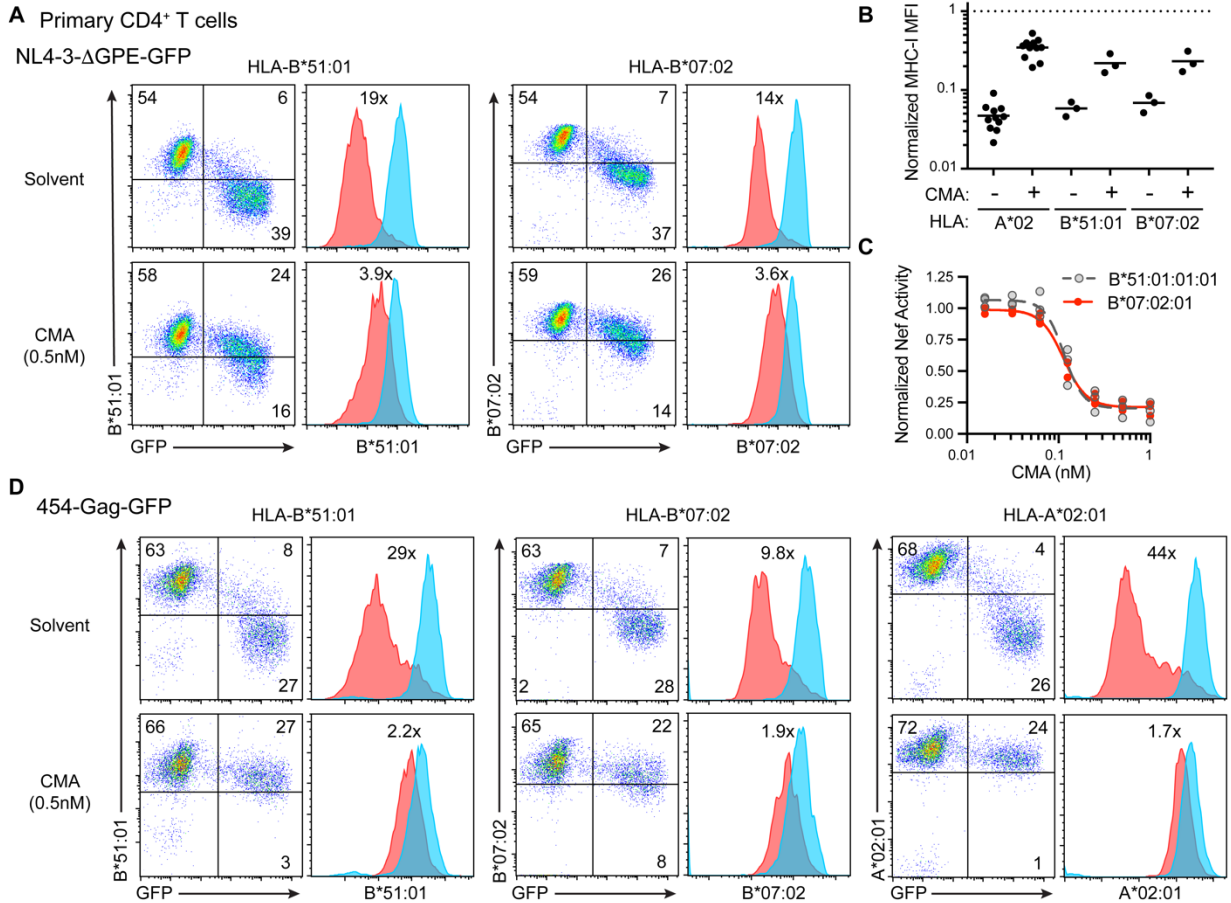
Fig. 3.5: CMA counteracts Nef-mediated HLA-B downregulation in primary cells, including those expressing Nef from a primary isolate of HIV.[9] (A) Representative flow cytometry plots (n=3 independent replicates from a single donor) from primary CD4+ T cells infected with NL4-3-ΔGPE for 48 hours, treated with 0.5nM CMA for 24 hours, and stained with monoclonal antibodies to Bw4 (B*51:01) and Bw6 (B*07:02). Blue histograms are from GFP- cells, red histograms are from infected GFP+ cells. (B) Summary graph of data from A plotting the MHC-I MFI from infected GFP+ cells normalized to that in uninfected cells treated with solvent control. Data for HLA-A*02 are from independent experiments with 11 different donors, data for HLA-B*51:01 and HLAB*07:02 are from 3 independent experiments with a single donor. (C) Summary graph of data from A depicting the relative Nef activity against the indicated HLA-B allotypes in cells treated with a range of CMA concentrations (n=3). (D) Flow cytometry plots from CD4+ T cells infected with 454-Gag-GFP (Fig. 3.1A) and treated and stained as in A (n=1 for HLA-B allotypes, n=3 for HLA-A*02). Solvent control is DMSO.

CMA broadly inhibits *nef* alleles from diverse clades of HIV and SIV targeting a range of MHC-I alleles

---

[9] Zimmerman GE and Olson E contributed to experiments in Fig. 3.5.

152

Globally, HIV possesses remarkable genetic diversity. To this point, we had only investigated the inhibitory activity of plecomacrolides against Nef alleles from NL4-3, HXB and the 454 patient molecular clones, all of which are clade B viruses. To determine whether plecomacrolides offer broad therapeutic promise against a diverse range of Nef sequences, we tested *nef* alleles from HIV clades A, B, C, D, F, and F/B, as well as one from simian immunodeficiency virus (SIV) (Fig. 3.6A) cloned into the MSCV-IRES-GFP vector (Fig. 3.1A)[58]. We observed that CMA restored expression of HLA-A2 in cells expressing each *nef* allele, indicating that plecomacrolides broadly inhibit *nef* alleles from genetically diverse HIV isolates (Fig. 3.6B-D, red bars), and the potency of CMA was comparable for each allele (Fig. 3.6C). CMA was able to restore HLA-A2 expression more completely for *nef* alleles that downregulate HLA-A2 to a lesser extent but had the most dramatic effect on HLA-A2 expression in cells expressing the most potent *nef* alleles (Fig. 3.6D). Similarly, CMA restored surface expression of HA-tagged MHC-I allotypes HLA-A*02, HLA-B*08, HLA-B*27, and HLA-B*57 expressed in CEM cells. Each allele of Nef downregulated each allele of MHC-I, with varying magnitudes, and CMA restored MHC-I surface expression in every context (Fig. 3.6E-H). These observations support the hypothesis that CMA can enhance cellular adaptive immunity regardless of the initial degree of impairment and may provide therapeutic benefit despite HLA and viral diversity.
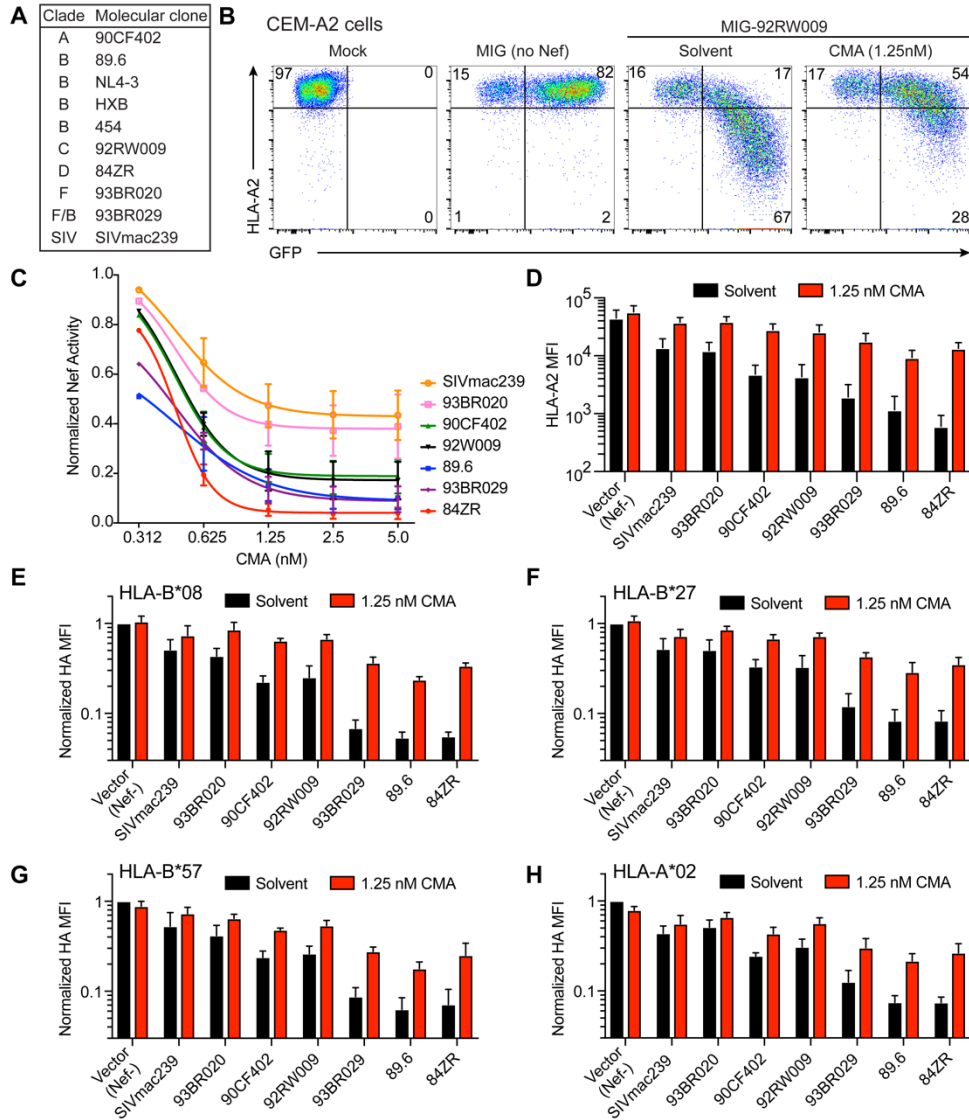
Fig. 3.6: CMA inhibits Nef alleles from diverse clades of HIV and SIV targeting diverse alleles of MHC-I.[10] (A) Summary of Nef alleles tested and clade of HIV or SIV to which the isolate belongs. (B) Representative flow cytometry plots depicting CEM-A2 cells infected with MSCV-IRES-GFP (MIG) alone or expressing the Nef allele from clade C HIV isolate 92RW009, the median Nef allele from C, and treated for 24 hours with 1.25nM CMA. (C) Summary graph of data from B, showing the relative Nef activity of each Nef allele after treatment with varying concentrations of CMA (n=3). (D) Summary graph of HLA-A2 MFI from experiments shown in B-C. (E-H) Summary graphs of flow cytometric data from CEM cells expressing the indicated HA-tagged MHC-I alleles treated as in D. Cell surface MHC-I expression was assessed by staining for HA, and the median fluorescence intensity in GFP$^+$ cells was normalized to vector control for each cell line. (E-F) n=4; (G-H) n=3.

Discussion

---

[10] Zimmerman GE performed all experiments in Fig. 3.6. McLeod MR contributed to the design of Fig. 3.6A.

In summary, we have identified plecomacrolides as potent inhibitors of HIV Nef-mediated downregulation of MHC-I. Inhibition of Nef by CMA, in particular, occurs at concentrations that are non-toxic to primary T cells and that do not inhibit lysosome function. Restoration of cell-surface MHC-I in HIV-infected cells enhances their clearance by CTLs comparably to genetic deletion of Nef, confirming that the restored MHC-I is functional for presentation of viral antigens. We further demonstrated that CMA inhibits *nef* alleles isolated from diverse clades of HIV, an allele of SIV *nef,* and an allele of HIV *nef* from an optimally-treated patient. Additionally, we found that CMA restored diverse allotypes of MHC-I in HIV-infected cells, and that CMA treatment enhanced antigen presentation for all combinations of *nef* alleles and MHC-I alleles tested. These results provide evidence that inhibition of Nef by this mechanism could have broad clinical utility.

The identification of plecomacrolides as inhibitors of HIV Nef may seem intuitive, given that Nef redirects many of its targets for lysosomal degradation and plecomacrolides lead to potent lysosomal neutralization and loss of degradative capacities[59-64]. Yet, we determined that CMA restored MHC-I in Nef-expressing primary CD4$^+$ T cells at concentrations that were non-toxic and did not alter the function of the lysosome or reduce the abundance of acidified intracellular compartments. Thus, we propose that CMA specifically alters a step prior to lysosomal degradation. This may be an unrecognized activity of the known target, V-ATPase, or the activity of a novel non-V-ATPase target, although our data suggest this target is unlikely to be a component of the AP-1:Nef:MHC-I:ARF-1 complex itself. Inhibition of this putative target activity reduces the capacity of Nef to interact with MHC-I and AP-1 in CMA-treated cells but does not alter the ability of Nef

to downregulate and degrade CD4. The fact that Nef-MHC-I-AP1 complex formation in cells is CMA-sensitive suggests that there may be more subtle pH-dependent steps that are unrelated to lysosomal function. Plecomacrolides have previously been shown to alter intracellular trafficking, but generally with the effect of reducing the expression of cell-surface markers rather than increasing them[65,66]. A subunit of V-ATPase has been reported to form a complex with Nef and CD4 to promote endocytosis[67-69]. However, this subunit has not been implicated in Nef-dependent MHC-I trafficking, which occurs by a different mechanism that begins in the Golgi rather than at the cell surface[18,70]. Other explanations are also possible. For example, there may be an as yet unidentified target of CMA that is required for Nef activity against MHC-I.

In addition, we demonstrated that the potency of CMA is greater than previously published Nef inhibitors, including B9 and lovastatin. B9 failed to restore MHC-I to the surface of Nef-expressing cells in any of the assays employed, while lovastatin was able to restore MHC-I to a fraction of the levels achieved by CMA with prolonged incubations and supratherapeutic concentrations. The explanation for the negative result obtained with B9 is unclear. A recent paper showed small but statistically significant effects of B9 on CTL clearance and the authors claimed these effects were mediated through reversal of Nef-dependent MHC-I downregulation[36]. Because of these reports, we confirmed the structure of the commercially-obtained B9 to rule out the possibility that we had received the wrong compound. Our results clearly demonstrated that any potential effect of B9 on MHC-I downregulation in cells is not biologically meaningful under the conditions of our assays.

In short-term co-cultures with HIV-specific CTLs, primary CD4^{+} T cells infected with Nef-expressing HIV revealed a residual population of infected cells that could not be cleared from the culture, regardless of how many CTLs were present. If the cells were treated with CMA or Nef was genetically removed from the virus, this population was virtually non-existent. This raises the possibility that Nef activity in a subset of HIV-infected cells *in vivo* renders those cells refractory to killing even by highly responsive CTLs. Following therapeutic reactivation in a "shock and kill" effort to eliminate the HIV reservoir, such cells could escape CTL killing long enough to proliferate and return to latency, re-seeding the reservoir with clonally-expanded sequences expressing potent alleles of *nef*. Thus, our co-culture assays demonstrate proof-of-concept that therapeutic Nef inhibition with low-dose CMA is sufficient to dramatically enhance the clearance of previously hard-to-kill cells when effective CTLs are present.

The CTL response *in vivo* is polyclonal, with CTLs responding to a diverse array of HIV antigens presented predominantly by HLA-A and HLA-B. Furthermore, MHC-I is remarkably polymorphic and HIV sequences are tremendously diverse both within and between infected individuals. A CTL-based therapeutic intervention will therefore need to function in a wide range of immune contexts. CTL responses restricted to HLA-B are predominant in HIV infection, and many MHC-I genes associated with HIV control are HLA-B alleles[53-55]. We observed reversal of Nef downregulation of HLA-A and HLA-B allotypes following CMA treatment. Restoration was particularly dramatic when MHC-I was targeted most strongly by Nef. Therefore, CMA could facilitate the elimination of resistant reservoirs of virus by enhancing the efficiency of both already-effective HLA-B-restricted and previously-suboptimal HLA-A-restricted CTL responses. In the absence of

Nef-mediated protection and in combination with vaccination strategies to increase the abundance and breadth of HIV-specific CTLs, antigens that had not experienced strong selective pressure to generate CTL-escape mutants prior to the initiation of ART could become vulnerable targets for immune-mediated clearance of HIV reservoirs.

Despite the promising nature of these results, several limitations warrant further investigation. CMA restores expression of diverse MHC-I allotypes in HIV-infected primary T lymphocytes, but CTL killing was only confirmed for a single MHC-I allotype. In addition, we report an 11-fold window between EC_{50} and TC_{50} for CMA in primary cells, which is encouraging for a lead compound. However, chemical modifications that further separate toxicity and activity will likely be necessary for clinical utility. Moreover, additional research using animal models is needed to determine the toxicity, accessibility, and efficacy of CMA *in vivo*. Lastly, Nef inhibition alone is unlikely to achieve a cure for HIV, as latent reservoirs of virus express neither Nef nor viral-derived peptide antigens. Thus, the parallel development of improved latency-reversal agents will be needed to achieve a cure.

In summary, we demonstrated that CMA potently counteracts HIV Nef at sub-nanomolar concentrations to restore immune-mediated clearance of HIV-infected cells. This approach has the potential to broadly enhance anti-HIV immunity in diverse immune contexts. Thus, we propose CMA as a lead compound for further development as a therapeutic inhibitor of Nef, a crucial addition to current efforts to cure HIV by eradicating residual viral reservoirs.

Materials and Methods

158

Ethics statement

Anonymized leukocytes isolated by apheresis from healthy donors were obtained from the New York Blood Center.

For experiments for which the HLA genotype was determined, blood was collected in Ann Arbor, MI, USA, with informed consent from healthy donors in accordance with a University of Michigan IRB approved protocol (HUM00071750).

Nef inhibitory compounds

The following compounds were used as described below; B9 (Calbiochem, MilliporeSigma, 500653), Lovastatin (MilliporeSigma, PHR1285), Baf A1 (Cayman Chemical, 11038), Baf B1 (Cayman, 14005), Baf C1 (Cayman, 19624), Baf D (Cayman, 19438), CMA (Fermentek, 80890-47-7; Cayman, 11050)

Preparation of primary CD4⁺ T lymphocytes and monocyte-derived macrophages

Anonymized leukocytes isolated by apheresis were obtained from the New York Blood Center, and peripheral blood mononuclear cells (PBMCs) were isolated by Ficoll-Paque Plus (GE Healthcare, 17144002) centrifugation using SepMate tubes (Stemcell Technologies, 85450) according to manufacturer's protocol. CD8⁺ lymphocytes were depleted with Dynabeads according to manufacturer's protocol (Invitrogen, 11147D), and the remaining cells were incubated at a density of 2×10^6 cells/mL in R10 medium and stimulated with 10µg/ml phytohemagglutinin (PHA-L, EMD/Millipore Sigma, 431784). 16-

24 hours post-PHA activation, cells were cultured in R10-50. Primary CD4^{+} T cells were infected via spinoculation or treated for other experiments 48 hours after IL-2 addition.

Genotyping of donor PBMCs was performed as previously described[56].

Primary monocyte-derived macrophages (MDMs) were isolated with a CD14 positive isolation kit (StemCell Technologies, 17858), stimulated with 50ng/mL each of M-CSF and GM-CSF (R&D Systems, 216-MC-025/CF and 215-GM-050), and cultured as previously described[71]. MDMs were used for lysosomal pH measurements 7-10 days post-isolation.

Viral constructs and infections

Infectious supernatants for HIV constructs were prepared by co-transfection of 293T cells using polyethylenimine (PEI) as previously described[72] with each viral construct, the HIV packaging plasmid pCMV-HIV, and pHCMV-G at a mass ratio of 1:1:1. Infections were performed by spinoculation. Murine stem cell virus internal ribosome entry site GFP (pMIG) constructs containing various *nef* alleles were generated as previously described[58]. Nef-expressing and control adenoviral vectors were obtained from the University of Michigan Gene Vector Core as previously described[30].

Flow cytometry surface staining

Detailed methodology can be found in the Appendix. In all experiments, cells were gated sequentially by forward scatter vs. side scatter for cells, doublet exclusion (forward scatter area vs. height) for singlets, and exclusion of viability dye for viable cells.

Lysosensor Yellow/Blue dextran analysis of lysosomal pH

To measure the lysosomal pH in human monocyte-derive macrophages (MDMs), MDMs adhered to 24-well plates were exposed to 500μg/mL Lysosensor Yellow/Blue dextran, 10,000 MW (Invitrogen, L22460) in R10 for 24 hours. MDMs were then exposed to plecomacrolides for 1 hour and harvested with 0.05% Trypsin-EDTA (Gibco, 25300054). Cells were washed twice in FACS buffer, and analyzed on a MoFlo Astrios flow cytometer, with blue signal excited from a 354nm laser and yellow signal excited from a 405nm laser. A standard curve was generated by resuspending MDMs in equilibration buffers of known pH as previously described[45]. The ratio of blue:yellow fluorescence intensity was calculated for each cell, the median blue:yellow ratio for the cell population for each condition was obtained, and the lysosomal pH in MDMs was calculated for each condition using the standard curve.

Lysotracker flow cytometry assay

Cells were treated with plecomacrolides at a density of 1×10^6 cells/mL for 24 hours, then treated with 100nM LysoTracker Red DND-99 (Invitrogen, L7528) in PBS at a density of 1×10^6 cells/mL for 1 hour at 37°C, washed twice in PBS, and fixed in 2% PFA before flow cytometric analysis on a BioRad Ze5 flow cytometer.

Western Blotting

Detailed methodology can be found in the Appendix. Briefly, sorted PLAP^{+} CD4^{+} T cells isolated as previously described[73] were pelleted and lysed, sonicated, separated by gel electrophoresis, and transferred onto PVDF membrane. Membranes were blocked in 5% milk prior to probing with target-specific antibodies. Western blotting results were quantified using Photoshop by determining the mean pixel density in a box of equal size over each band from a single, unedited film displaying a single gel. Background pixel density was subtracted. No quantification comparisons were made from bands on different films or gels at any point.

Confocal Immunofluorescence microscopy

For HLA-A2 staining, sorted PLAP^{+} primary CD4^{+} T cells isolated as previously described[73] were attached to Poly-L-lysine (Sigma Aldrich, P4707) coated chambered slides (Fisher, 154534), fixed in PBS + 2% PFA and permeabilized in PBS + 0.2% Tween 20. Staining was performed as previously described[18] with primary antibody against HLA-A2 (BB7.2, 2 μg/mL) and secondary goat anti-mouse IgG2b-AF546 (Invitrogen, A21143, 1:250). Slides were coated with ProLong Gold Antifade Mountant (Invitrogen, P36930), coverslips were added, and images were collected on a Leica SP5 Confocal microscope using identical instrument settings for each sample.

HLA-A2 coimmunoprecipitation

Immunoprecipitation of CEM cell lysates with BB7.2-conjugated beads was performed as previously described[20]. Briefly, 25×10^6 CEM-A2 cells were transduced with Nef-

expressing or control adenoviral vectors. 48 hours post-infection, cells were counted and resuspended at a density of 1x10^6 cells/mL R10 supplemented with 35mM NH$_4$Cl, 1.25nM CMA, or solvent control for 24 hours. Cells were pelleted, washed twice in PBS, and lysed in 1% digitonin lysis buffer (1% digitonin (Wako, 043-21371), 100 mM NaCl, 50 mM Tris, pH 7.0, 1 mM CaCl$_2$, and 1 mM MgCl$_2$) as previously described[19]. 1% of the lysate was removed for input controls. After overnight pre-clear with isotype control antibody and protein A/G agarose (EMD Bioscience, IP-10), lysates were immunoprecipitated overnight with protein A/G agarose cross-linked to BB7.2. After pulldown, resin was washed five times in 0.1% digitonin wash buffer, and proteins were eluted by incubating in 150mM dithiothreitol (Invitrogen) for 30 minutes at 37°C and analyzed by western blot.

Flow cytometric CTL killing assays

CTL elimination assays were performed as previously described[26] with the following modifications: 72 hours post-infection primary CD4$^+$ T cells (target cells) were stained with CellTracker Green CMFDA (Fisher, C7025) according to manufacturer's protocol and treated with 0.5nM CMA or solvent control for 24 hours. For each condition, 50,000 target cells were resuspended in fresh R10/50 without CMA with the corresponding number of effector CTLs to achieve the desired E:T ratio. Following the 4 hours of co-culture, the cells were stained with DAPI as a viability dye in addition to anti-PLAP and BB7.2 antibodies. Viable target cells were separated by gating for cells that were CellTracker Green-positive and excluded DAPI. The proportion of PLAP$^+$ cells present in each condition was divided by that in the mean of target cells-only conditions (E:T = 0:1) to report the proportion of PLAP$^+$ cells surviving in the presence of CTLs. All samples were

performed in experimental duplicates, except the target cells-only conditions (E:T = 0:1), which were performed in quadruplicate. Flow cytometry data were collected on a Bio-Rad Ze5 cytometer.

Calculations

$$MFI = median\ fluorescence\ intensity\ of\ MHC\text{-}I$$

$$Fold\ downmodulation = \frac{MFI_{uninfected}}{MFI_{infected}}$$

$$Normalized\ Nef\ activity = \frac{Fold\ downmodulation\ MHC\text{-}I_{sample}}{Fold\ downmodulation\ MHC\text{-}I_{solvent}}$$

$$Percent\ restoration = \left(\frac{MFI_{infected,sample} - MFI_{infected,solvent}}{MFI_{uninfected,solvent} - MFI_{infected,solvent}}\right) * 100$$

Statistical Analysis

All statistical analyses were performed using GraphPad Prism software as described in the Fig. 3.legends for each experiment. Curves were generated using GraphPad Prism software using [Inhibitor] vs. response with variable slope (four parameters), and the extra sum-of-squares F test was used to compare the EC_{50} for different curves.

Supplementary Materials and Methods

Cell Culture

All cell cultures were maintained at 37°C in 5% CO_2 humidified atmosphere. Virus producer cells (293T and BOSC cells[74]) were maintained in D10 medium [DMEM medium

(Gibco) supplemented with 100 U/mL penicillin, 100 μg/mL streptomycin, 2 mM glutamine (Pen-Strep-Glutamine, Invitrogen), 10 mM HEPES (Invitrogen), 10% fetal bovine serum (Sigma, Invitrogen), and 0.022% plasmocin (Invivogen)]. All other cells were maintained in R10 medium [RPMI-1640 medium (Gibco) supplemented as D10]. Primary T cells were cultured in R10-50 [R10 plus 50IU/mL interleukin-2 (IL-2, Fisher 202IL010)]. CEM cell lines expressing recombinant, HA-tagged MHC-I molecules[18,75] were maintained in R10 supplemented with 1mg/mL geneticin (Gibco).

Viral constructs and infections

(i) HIV constructs: NL4-3-ΔGPE-GFP (ΔGPE) wild type and HXBePLAP wild type and *nef* mutants have been described previously[26,76]. 454-Gag-GFP was constructed from a molecular clone isolated from a donor who was treated with combination ART and had undetectable plasma viral levels[57]. Briefly, we utilized 454-LTR-GFP, created as previously described[57], in which *gfp* was inserted by gene synthesis in frame at position 809, which corresponded to position 19 in the *gag* open reading frame and created a Gag-GFP fusion protein when expressed. To reconstruct the remainder of the genome, we used PCR to generate donor derived sequence from position 4761 in *pol* through the XhoI site at 9255 in *nef* using the re-constructed near full length 454 genome as a template. The PCR product, which contained 11-15 base pair overlaps with 454-LTR-GFP, was inserted using the GeneArt Seamless Cloning Enzyme Mix (Thermo Fisher A14606). Nef mutations were introduced into ΔGPE and 454-Gag-GFP by filling in a unique Xho I site using klenow and re-ligating.

(ii) HIV infections: Infectious supernatants were prepared by co-transfection of 293T cells using polyethylenimine (PEI) as previously described[72] with each viral construct, the HIV packaging plasmid pCMV-HIV, and pHCMV-G at a mass ratio of 1:1:1. 293T cells were maintained and transfected in D10 medium. Infections were performed by spinoculation at 1,050xg for 2 hours at room temperature at a density of 1.0x10^6 cells/mL. Primary cells were spinoculated in undiluted infectious supernatants supplemented with 4μg/mL hexadimethrine bromide (polybrene, Sigma-Aldrich, H9268). Cell lines were spinoculated with infectious supernatants diluted in D10 to achieve the desired MOI (approximately 50% infection) in the absence of polybrene. Following spinoculation, infectious supernatants were replaced with the appropriate culture medium for the infected cell type.

(iii) MSCV: Murine stem cell virus internal ribosome entry site GFP (pMIG) constructs containing various *nef* alleles were generated as previously described[58]. Retroviral supernatants were prepared using BOSC cells transfected with the pMIG constructs (5.5μg), the retrovirus packaging vector pCL-Eco (4.0μg)[77] and pHCMV-G (0.5μg) using PEI as for HIV. Viral supernatants were collected 48 hours post-transfection, clarified by centrifugation, stored at -80°C, and transductions were performed as described for HIV constructs.

(iv) Adenoviral vectors: Nef-expressing and control adenoviral vectors were obtained from the University of Michigan Gene Vector Core (vector clone: Ad-Ef1a.dIE3 #6, Nef clone: Ad-EF1 Nef.dIE3 #2) as previously described[30]. CEM-A2 cells were transduced in serum-

free R10 medium for 6 hours at a concentration of 1.0×10^6 cells/mL, then R10 with 20% FBS was added to achieve a density of 5.0×10^5 cells/mL in R10.

Flow cytometry surface staining

All flow cytometry stains were performed on ice in FACS buffer (2% fetal bovine serum, 1% human AB serum (Fisher, BP2525), 2 mM HEPES, 0.025% sodium azide (Sigma) in PBS). Briefly, cells were resuspended in primary antibody diluted in FACS buffer for 20 min., washed once in FACS buffer, resuspended in secondary antibody diluted in FACS buffer for 15 min., washed once in FACS buffer, and fixed in 2% paraformaldehyde. Primary antibodies against the following proteins were used: HLA-A2 (BB7.2 from HB-82 hybridoma as previously described[70], 0.5μg/mL), Bw4 (Bw4-PE (Miltenyi Biotec, 130-103-847, 1:50), Bw6 (Bw6-APC (Miltenyi Biotec, 130-099-845, 1:50)), pan MHC (w6/32 (Fisher, MA1-70111, 1:1000), PLAP (PLAP-647 (Santa Cruz Biotechnology, clone 8B6, sc47691, 1:1000), CD4 (BD Bioscience, 555344, 1:1000), and HA (HA.11, clone 16B12, Covance, MMS-101R 1:100).

Secondary antibody for BB7.2 was goat anti-mouse IgG2b-AF647 or -AF546 (Invitrogen, 1:2000), secondary antibody for w6/32 was goat anti-mouse IgG2a-PeCy7 (Abcam, 1:1000), secondary antibody for CD4 was goat anti-mouse IgG1-PE (Invitrogen, 1:1000), secondary antibody for HA.11 was goat anti-mouse IgG1-AF647 (Invitrogen, 1:1000).

2μg/mL 7-aminoactinomycin D (7-AAD; Calbiochem) or 4ng/mL DAPI (4′,6-diamidino-2-phenylindole; Thermo Scientific) viability dyes were included with secondary antibodies

in staining protocols. In all experiments, cells were gated sequentially by forward scatter vs. side scatter for cells, doublet exclusion (forward scatter area vs. height) for singlets, and exclusion of viability dye for viable cells. Flow cytometry data were collected with a BioRad Ze5 cytometer, a MoFlo Astrios cytometer (Beckman Coulter), or a BD FACScan cytometer with Cytek 6-color upgrade, and all flow cytometry data were analyzed with FlowJo software.

Primary screen and counter-screen

CEM-A2 cells were transduced with an adenoviral vector expressing Nef derived from NL4-3 driven from the Ef1α promoter at the minimal multiplicity of infection that demonstrated downmodulation of HLA-A2 in at least 90% of cells as assessed by flow cytometry, which was determined for each viral prep. Cells were incubated for 48 hours, then counted and re-suspended in R10 with only 0.2% FBS at a density of 2.0×10^6 cells/mL. Experimental plates were prepared separately using robotic equipment provided by the University of Michigan Life Sciences Institute Center for Chemical Genomics by delivering 4µL of PBS into each well on a 384 well plate followed by Natural Product Extracts (NPEs). CEM T cells transduced with adenoviral vector were then dispensed into experimental plates (4µL/well) and incubated overnight at 37°C and 5% CO_2. 2µL of a 5x antibody solution of 7-AAD and BB7.2-AF488 in 5x FACS buffer (10% FBS, 5% Human A/B serum, 5% HEPES and 0.025% sodium azide in PBS) was added directly to the cells and culture medium per well and incubated at 4°C for 30 minutes. Each sample was then diluted and fixed with 20µL of 1.5% paraformaldehyde (Sigma-Aldrich) in 1x FACS buffer (2% FBS, 1% Human A/B serum, 1% HEPES ad 0.025%

sodium azide in PBS). After fixation, plates were read on an Accuri C6 flow cytometer (BD Biosciences, San Jose, CA) within one week. The counter screen was performed exactly as the primary screen but with parental CEM-SS T cells that do not express HA-HLA-A2.

Relative activity among the averaged control samples was set to 100% for control-vector-transduced cells, and 0% for Nef-transduced cells. Activity was defined as an increase in HLA-A2 cell surface expression greater than three standard deviations above the negative control samples for each plate, within the entire assay, or greater than 25% activity. Wells in which fewer than 25 live cell events were recorded were discarded, interpreted as cytotoxic, or considered worthy of re-testing due to potential sampling error. Only compounds which tested as hits in a minimum of 2 of 3 replicate wells were counted as confirmed hits. Hits from the primary screen were then subjected to the counter screen. Any compound that registered as a hit in the counter screen using the same criteria was eliminated as a false positive.

Initial screening was performed on the Spectrum library of FDA-approved compounds, Chembridge and Maybridge collections of drug-like compounds, and the ChemDiv 100,000 library of small molecules. We subsequently screened the natural product extract library housed in the Natural Products Discovery Core (NPDC) at the University of Michigan. This library consists of over 40,000 natural product extracts and over 8,000 microorganisms from a variety of locations worldwide. Hits that were deemed to be confirmed positives in the counter screen were then subjected to secondary screening

using NL4-3-ΔGPE-GFP-transduced CEM-A2 T cells. Activity was defined as percent inhibition of MHC-I fold downmodulation.

Secondary screen

CEM-A2 cells were infected with ΔGPE and maintained in R10 for 48 hours post-infection. Cells were counted, re-suspended and plated in a 96-well flat-bottom plate at 1×10^5 cells/100μL in R10 with only 0.1% FBS, supplemented with hits from the primary screen. After 24 hours, downregulation of HLA-A2 was assessed by BB7.2 staining of viable cells, comparing the MFI of HLA-A2 in GFP$^+$ infected cells to that in uninfected GFP$^-$ cells to obtain the fold inhibition of Nef.

Flow cytometric viability assay

Primary, PHA-activated CD4$^+$ T cells were treated as in the MTT assay prior to harvest after 72 hours of exposure to plecomacrolides. Cells were pelleted and incubated on ice in FACS buffer with 2μg/mL 7-AAD for 15 minutes, washed once in FACS buffer, and fixed in 2% paraformaldehyde. The frequency of cells excluding the 7-AAD vital dye was assessed using a BD FACScan cytometer with Cytek 6-color upgrade and analyzed with FlowJo software.

MTT assay

CD4$^+$ T cells were plated at a density of 1×10^5 cells in 200μL R10-50 in flat-bottom 96-well plates 4 days post-stimulation with PHA. Cells were exposed to titrations of plecomacrolides or solvent controls for 72 hours in culture, at which point viability was

assessed relative to solvent by MTT assay in experimental duplicates. Equal volumes of cell culture medium containing CD4$^+$ T cells were pelleted in 96-well round-bottom plates and incubated in 4.5mg/mL MTT (3-(4,5-Dimethylthiazol-2-yl)-2,5-Diphenyltetrazolium Bromide, Fisher, M6494) in R10 with no Phenol Red at 37°C until the purple formazan signal was clearly visible. The absorbance of cell pellets resuspended in DMSO was measured at 595nm on a Molecular Devices Emax precision microplate reader and compared a standard curve of known viable cell numbers to ensure the experimental samples fell within the linear range of the assay.

DAPI cell cycle analysis

DAPI cell cycle analysis was performed as previously described[78], and data were collected on a BioRad Ze5 cytometer and analyzed with FlowJo software.

LysoTracker fluorescence microscopy

CD4$^+$ T cells were treated at a density of 1x10^6 cells/mL in R-10/50 for 24 hours, at which point 500,000 CD4$^+$ T cells were incubated in 500 µL of PBS containing 100 nM LysoTracker Red DND-99 and 5 µg/mL Hoechst 33342 (Invitrogen, H3570) on a Poly-L-lysine (Sigma Aldrich) coated chambered slide (ThermoFisher, 154534) for 1 hour at 37°C. Slides were then fixed in PBS + 2% PFA for 20 minutes at room temperature and washed once in PBS. ProLong Gold Antifade Mountant (Invitrogen, P36930) was applied before adding coverslips. Images were acquired on a Leica SP5 confocal microscope using identical instrument settings for each sample, and maximum projections were created using ImageJ.

Western blotting

Sorted PLAP^{+} CD4^{+} T cells isolated as previously described[73] were pelleted and lysed in Blue Loading Buffer (Cell Signaling Technology, 56036S) with DTT according to manufacturer's protocol. Lysates were sonicated with a Misonix Sonicator (QSonica) at 100 amps for four minutes, boiled at 95°C prior to loading onto Criterion Tris-HCl gels (Bio-Rad Laboratories, Hercules CA), and separated by gel electrophoresis. Gels were transferred onto PVDF transfer membrane (MilliporeSigma, IPVH00010) for 90 minutes at 350 mA. Membranes were blocked in 5% milk (LabScientific Inc., Highlands, NJ) in TBS-T (0.05% Tween 20, 0.15M NaCl, 0.01M Tris pH 8.0) for 1 hour. Antibodies against the following proteins were used for western blotting: clathrin adaptor protein AP-1 γ (Fisher, 610386, 1:100); Nef (2949, AIDS Research and Reference Reagent Program, Division of AIDS, National Institute of Allergy and Infectious Diseases, NIH, Ron Swanstrom, 1:500); MHC-I heavy chain (HC.10, prepared as described[79]); CD4 (Abcam, 133616, 1:1000); HA (HA.11, Covance), glyceraldehyde-3-phosphate dehydrogenase (Abnova, clone 32C, H00002597) and AP-1 μ1 (RY/1, Dr. Linton Traub, University of Pittsburgh). The secondary antibody for GAPDH and HA.11 was Rat anti-Mouse IgG1-horesradish peroxidase (Invitrogen, 18401582). The secondary antibody used for Nef 2949, CD4, and RY/1 was Goat anti-Rabbit IgG-HRP (Invitrogen, 656120). The secondary antibody used for AP-1 γ was Goat anti-Mouse IgG1-HRP (Zymed Laboratories Inc.). The secondary for HC.10 was Rat anti-Mouse IgG2a-HRP (Invitrogen, 046220).

Western blotting results were quantified using Photoshop by determining the mean pixel density in a box of equal size over each band from a single, unedited film displaying a single gel. Background pixel density was subtracted. No quantification comparisons were made from bands on different films or gels at any point.

***In vitro* investigations of AP-1:Nef:MHC-I complexes**

Recombinant protein expression and purification

The His6- and GST-tagged AP-1 core, mouse AP1μ1 (157-423) (referred as μ1-CTD), human Arf1 (17-181)-Q71L, human MHC-I (338-365)-NL4-3 Nef, HIV-1 NL4-3 Nef constructs and protein purification were previously described [24,80]. For the GST pull down assay, codon-optimized human MHC-I (338-365) was subcloned into pGST parallel2 vector using BamHI/XhoI sites, and fused to an N-terminal GST tag and a TEV cleavage site[81]. PCR encoding HIV-1 Nef or SIVsmm Nef fused with GFP was subcloned into LIC 2BT vector (Macrolab) and expressed as a TEV-cleavable N-terminal His6 tag and C-terminal uncleavable GFP tag.

His-NL4-3 Nef-GFP or His-SIVsmm Nef-GFP constructs were expressed in BL21 (DE3) star cells (Life technologies, Grand Island, NY), induced with 0.3mM IPTG at 25°C overnight. The purification was carried out using Ni-NTA resin. The eluate was subjected to a HiLoad 16/60 Superdex 75 column in the buffer of 20mM Tris pH 8, 300mM NaCl, 0.1mM TCEP.

His-MBP tagged µ1-CTD was expressed in BL21 (DE3) star cells and induced with 0.3mM IPTG at 20°C overnight. The clarified lysate was purified by Ni-NTA resin. The protein was eluted with 0.1 M imidazole in 50mM Tris pH 8, 300mM NaCl, followed by TEV cleavage at 4°C overnight. The sample was then diluted 2 times by SP buffer A (30mM Tris pH 8), and then loaded onto a HiTrap SP HP 5mL column (GE healthcare). The SP column elution was performed with a 10 CV linear gradient from 0-1 M NaCl in SP buffer A. The sample fractions were pooled together and subjected to a 16/60 Superdex 75 column in 20mM Tris pH 8, 300mM NaCl, 0.1mM TCEP.

GST tagged MHC-I tail was expressed in BL21 (DE3) star cells by induction at 20ºC overnight. The purification was carried out using glutathione-Sepharose 4B resin, the elution was then subjected to a HiLoad 16/60 Superdex 75 column in 20mM Tris pH 8, 150mM NaCl, 0.1mM TCEP.

AP-1:Arf1: MHC-I-Nef complex assembly

Recombinant AP-1 core was mixed with Arf1-GTP and MHC-I-Nef at a molar ratio of 1:4:6, then incubated at 4ºC overnight. The mixture was then subjected to a Superose6 10/100GL column in 20mM Tris pH 8.0, 150mM NaCl, 5mM $MgCl_2$, 0.3mM TCEP. The early eluted peak, corresponding to AP-1 trimer assembly, was pooled together and concentrated to 25µM. Each AP-1 trimer complex consists of three AP-1 core, three MHC-I-Nef, and six Arf1-GTP molecules.

Differential Scanning Fluorimetry (DSF) assay

DSF assays were performed using a Stratagene Mx3000P RT-PCR machine (Stratagene, La Jolla, CA) to monitor protein unfolding by the florescence increasing of SYPRO Orange (Invitrogen, Carlsbad, CA). SYPRO Orange (5000x concentration in DMSO) was first diluted to 1000x using DMSO, then diluted to 100x using the assay buffer. The final volume of the reaction was 20 µl. Protein samples with CMA (6 or 12µM) or with the DMSO control were first incubated at 4 ºC for one hour, then mixed with SYPRO Orange dye in a 96-well polypropylene plate (Agilent Technologies, Santa Clara, CA). DMSO concentration in each well was fixed at 5% (v/v). Final concentrations of the proteins were 6µM in the assay buffer (20mM HEPES pH 7.5, 200mM NaCl, 1mM TCEP), and the final dye concentration was 8x. The fluorescence intensity was measured using the SYBR green filter over the temperature range of 25 to 90ºC in 1 degree/min increments. After subtracting fluorescence from the DMSO control reaction without protein, the average fluorescence intensities were plotted as a function of temperature. Measurements were repeated three times and the data were processed using Origin software (OriginLab, Northampton, MA). The fluorescence intensity (before post-peak region) was fitted to Boltzmann equation to obtain melting temperature (Tm).

GST pull down assay

35 µg of recombinant GST-MHC-I tail proteins were incubated with His-MBP tagged µ1-CTD and HIV-1 NL4-3 Nef-GFP or SIVsmm Nef-GFP proteins (10 µM each), with or without CMA (40 µM) at 4°C overnight in 20 mM Tris pH 8, 150 mM NaCl, 0.1 mM TCEP. DMSO concentration in each tube was fixed at 2.5%. 30 µl glutathione-Sepharose 4B resin was then added into the mixture, which was rocked at 4°C for 2 hours. The beads

were washed 4 times, mixed with 60 µl of 2x lithium dodecylsulfate (LDS)/ βME buffer and heated at 90°C for 3 min. 28 µl of each sample and 1 µg inputs were subjected to SDS/PAGE gel and stained with Coomassie blue.

CTL clones

CTL clones were isolated by limiting dilution from HIV-1 infected individuals. Clonality of the line was established by demonstration of unique T cell receptor usage. The CTL clones were maintained in culture with periodic re-stimulation as previously described[82,83] except for the following changes; CTL clones were stimulated with anti-CD3 clone 12F6 (NIH AIDS Reagent Program) and cultured with IL-2 (NIH AIDS Reagent Program, Hoffman-La Roche, 136). Peripheral blood mononuclear feeder cells were isolated from leukopaks (New York Blood Center) and X-irradiated with 30 cGy in R10 medium. Irradiations were performed using a Kimtron IC 225 (Kimtron Medical) at a dose rate of approximately 2 Gy/min in the University of Michigan Comprehensive Cancer Center Experimental Irradiation Core (Ann Arbor, MI). CTL clones 115B15 and 161JXA14 both recognize HIV gag amino acids 77–85; SLYNTVATL presented by MHC-I HLA-A2[84].

CTL killing of peptide-pulsed JY cells

The HLA-A2 expressing B-cell line JY was maintained in R10 medium. Non-peptide pulsed cells were labeled with 1µM CellTrace Violet (Invitrogen, C34557) according to the manufacturer's protocol. Cells for gag SL9 peptide loading were labelled with 0.5µM CellTracker Green CMFDA (Invitrogen, C7025) in R10 medium for 15 min at 37°C and quenched with 5 volumes warm R10 medium. Peptide loading was performed in 10µg/mL

gag SL9 peptide in R10 medium for 1 h. Unbound peptide was removed with 3 washes of cold R10 medium. Violet (no peptide) and green (peptide-pulsed) cells were combined 1:1 and 20,000 cells per well were added to CTLs at 5:1 and 10:1 effector:target ratios in duplicate. CMA assays included solvent (DMSO, Sigma) or 0.5nM CMA (Cayman Chemical). Target cells were gated by light scatter and viability dye exclusion, then plotted by violet and green fluorescence to distinguish peptide loaded and peptide negative cells. Specific killing was calculated by dividing the percent of viable target cells that were green in the sample by the percent observed in the control wells lacking CTLs and subtracting from 1.

Natural Product extraction and purification

***Streptomyces* sp. (39098-H2N) Fermentation and Extraction**

Streptomyces sp. (39098-H2N) was cultured on R2YE agar[85] for 3-5 days until sporulation occurred. A 1 x 1 cm^2 lawn was inoculated into 2 L of ISP2 (0.4% yeast extract, 1% malt extract, 0.4% dextrose, 3% NaCl), and incubated at 28 °C with agitation (175 RPM) for 48-72 h. Using this growth, nutrient poor media for marine bacteria (0.025% yeast extract, 0.064% malt extract, 0.025% dextrose, 3% NaCl) was then inoculated with 3% (v/v) seed culture. Growths were performed in 50 L batches (300 L total) in baffled 2.8 L Fernbach flasks containing 1 L of media per flask, or 10-15 L bioreactors with agitation (175 RPM) and filtered air bubbled through solution. All growths were performed at 28 °C for 10 days. Completed growths were passed through coffee filters to remove the majority of bacteria and cell debris. MeOH-activated Amberlite XAD16N absorbent resin (20% w/v) was added to the clarified broth and stirred at room temperature for 24 h. The resin was filtered

from the solution and washed with copious amounts of H_2O (~80 L). Material was eluted

by washing with methanol (3 × 3 L), followed by acetonitrile (3 × 3 L). Organic extracts

were dried via rotary evaporation. Dry material was dissolved in minimal HPLC grade

methanol and filtered to remove any insoluble material. This solution was subsequentially

dried yielding 1.573 g of crude extract from 300 L of fermentation.

Streptomyces sp. (39098-H2N) fractionation and dereplication

The sample was dissolved in a minimal volume of methanol, loaded onto C18

resin, and dried *in vacuo*. Flash chromatography was performed using an Isolera One

(Biotage®) utilizing a pre-packed SiliCycle® reversed-phase C18 column (40 g). Material

was eluted with a flow rate of 50 mL/min collecting 120 mL fractions. Material was eluted

using a three-solvent gradient system, consisting of H_2O (solvent A), methanol (solvent

B) and acetonitrile (solvent C). The column was first washed with 10% methanol in H_2O

for 1 CV, followed by a linear increasing gradient from 10% to 95% methanol in H_2O over

12 CV. An isocratic gradient of 95% methanol in H_2O was then applied for 5 CV, followed

finally by an additional isocratic gradient of 95% acetonitrile in H_2O for 5CV. Fractions

were dried into pre-weighed vials using a V10-touch evaporator (Biotage®) coupled with

a Gilson GX-271 liquid handler. Samples were analyzed in the secondary screen for Nef

activity. Active fractions (F6-F9) were combined (92.5 mg) for further HPLC purification.

Purification of active metabolites was accomplished utilizing preparative HPLC

(Shimadzu LC-20AT), using a reversed-phase Phenomenex Luna 5 μm Phenyl-Hexyl

100 Å column (250 × 10.00 mm) run at a flow rate of 4 mL/min. Compound elution was

monitored using a Shimadzu diode array detector (SPD-M20A). The sample was brought

up in 1 mL of HPLC grade MeOH (~100 mgmL^{-1}) and injected in 100 µL aliquots (using a 200 µL loop). Elution was accomplished using H_2O + 0.1% formic acid (solvent A) and acetonitrile (solvent B). The gradient involved an initial isocratic step of 15% acetonitrile for 2 min. This was followed by a linear increasing gradient from 15% to 95% acetonitrile over 38 min (40 min total). The column was washed with an isocratic gradient of 95% acetonitrile for an additional 10 min (50 min total), finally followed by an isocratic equilibration step of 15% acetonitrile for 10 min (60 min total). From this nine peaks with similar UV-profiles were collected and immediately dried using the V10-touch evaporator. All fractions were identified as active in the Nef inhibition assay. Samples were analyzed by HRESIMS and screened against the Antibase 2017 database[86], identifying a series of ions related to the bafilomycin family of natural products. Ions of interest include: F3 *m/z* 667.4085 [M – H + FA]$^-$ (bafilomycin A1); F4 *m/z* 764.4253 [M – H + FA] (bafilomycin C1); F5 *m/z* 814.4410 [M – H]$^-$ (bafilomycin B1); F6 *m/z* 719.4054 [M – H]$^-$ (bafilomycin C1); F7 *m/z* 719.4054 [M – H]$^-$ (bafilomycin C1); F8 *m/z* 814.4404 [M – H]$^-$ (bafilomycin B1); F9 *m/z* 828.4561 [M – H]$^-$ (bafilomycin B2). Preliminary NMR data coupled with MS-dereplication, strongly suggested the active metabolites to be the bafilomycin family of natural products. Due to low yields from *Streptomyces* sp. (39098-H2N) and access to a higher producing strain within the Sherman laboratory, efforts towards isolation of bafilomycin analogs shifted to *Streptomyces lohii* Δ*bafY*.

Streptomyces lohii Δ*bafY* fermentation and extraction

Streptomyces lohii Δ*bafY* was cultured on R2YE agar for 3-5 days until sporulation occurred. A 1 x 1 cm^2 lawn was inoculated into 1 L of 2× YT media (1.6% tryptone, 1%

yeast extract, 0.5% NaCl), and incubated at 28 °C with agitation (175 RPM) for 48-72 h. Bafilomycin production media[87] was then inoculated with 3% (v/v) seed culture. Growths were performed on 10 L scale in baffled 2.8 L Fernbach flasks containing 1 L of bafilomycin production media per flask. Fermentations were conducted at 28 °C with agitation (175 RPM) for 7 days. Upon completion of the growth, cells were pelleted via centrifugation at 5500 RPM (4°C) for 45 min. The supernatant (containing both aqueous and oil layers) was removed from the cell pellet and stored for workup, as described below. The cell pellets were combined and extracted into acetone (10 L) for 24 h. Cell debris was removed via filtration through coffee filters, and reextracted with acetone (5 L). Cell debris was removed again via filtration through coffee filters. The acetone layers were combined and dried via rotary evaporation until only water remained. Residual oil that separated as the acetone was dried off, separated from the final aqueous layer using a separatory funnel, and combined with the oil layer from the supernatant produced via centrifugation as described above. This aqueous solution was then extracted 3X with equal volumes of ethyl acetate, followed by a fourth extraction of an equal volume of dichloromethane. The organic layers were combined, dried over anhydrous Na_2SO_4, filtered, and dried via rotary evaporators yielding a viscous, yellow-brown oil.

The supernatant, containing the mixture of oil and aqueous broth generated from centrifugation, was separated using a separatory funnel. The aqueous broth was discarded, and the combined oil layers were extracted 3X with equal volumes of methanol. The methanol extracts were combined and dried immediately via rotary evaporation to minimize any degradation. This yielded a viscous, yellow-brown oil that was combined with the cell extract sample described above, yielding ~6 g of material.

***Streptomyces lohii* Δ*bafY*: Bafilomycin A1 and C1 purification**

The extract was diluted with an equal volume of acetone and loaded onto minimal silica. The loaded silica was dried via rotary evaporation and separated into 4 equal aliquots. Aliquots were loaded into separate dry load vessels and run individually. Flash chromatography was performed using an Isolera One (Biotage®) utilizing pre-packed SiliCycle® normal phase silica columns (40 g). Material was eluted with a flow rate of 50 mL/min collecting 27 mL fractions. Purification was accomplished using a four-solvent gradient system, consisting of hexanes (solvent A), ethyl acetate (solvent B), dichloromethane (solvent C), and methanol (solvent D). Initially, the column was washed with 1 CV of 5% ethyl acetate in hexanes, followed by a linear increasing gradient of 5% to 60% ethyl acetate in hexanes over 13 CV. This was followed by an isocratic gradient of 60% ethyl acetate in hexanes over 6 CV. Bafilomycin A1 eluted at approximately 13-15 CV as a broad peak absorbing at λ = 235 and 285 nm. To purify bafilomycin C1, the gradient was switched to dichloromethane and methanol. Material was eluted starting with an isocratic gradient of 10% methanol in dichloromethane for 5 CV, followed by a final wash of 20% methanol in dichloromethane for 5 CV. Bafilomycin C1 eluted at approximately 27-28 CV within the 20% methanol in dichloromethane step as a broad peak absorbing at λ = 235 and 285 nm. Fractions were checked by TLC for purity and combined yielding bafilomycin A1 and C1 as impure yellow oils.

Final purification of bafilomycin A1 was accomplished utilizing preparative HPLC (Shimadzu LC-20AT), using a reversed-phase Phenomenex Luna 5 μm C18(2) 100 Å column (250 × 10.00 mm) run at a flow rate of 4 mL/min. Elution was monitored at 235

and 285 nm using a Shimadzu diode array detector (SPD-M20A). The sample was dissolved in HPLC grade acetone to a final concentration of 100 mgmL^{-1}. Purification was accomplished by injecting 100-180 μL aliquots of this solution (using a 200 μL loop). Material was eluted using H_2O (solvent A) and acetonitrile (solvent B). The gradient used an initial isocratic step of 60% acetonitrile for 2 min. This was followed by a linear increasing gradient from 60% to 95% acetonitrile over 38 min (40 min total). The column was washed with an isocratic gradient of 95% acetonitrile for an additional 20 min (60 min total), finally followed by an isocratic equilibration step of 60% acetonitrile in water for 10 min (70 min total). Bafilomycin A$_1$ eluted at 28.1 min. All fractions containing the purified bafilomycin A1 were combined and dried immediately using a V10-touch evaporator (Biotage®). Material was lyophilized for 24 hours yielding 48.7 mg of bafilomycin A1 as a white powder; HRESIMS m/z 667.4085 [M − H + FA]$^-$ (expected m/z 667.4063). Mass spec, elution time and NMR all matched commercial standard.

Final purification of bafilomycin C1 was accomplished utilizing preparative HPLC (Shimadzu LC-20AT), using a reversed-phase Phenomenex Luna 5 μm C18(2) 100 Å column (250 × 10.00 mm) run at a flow rate of 4 mL/min. Elution was monitored at 235 and 285 nm using a Shimadzu diode array detector (SPD-M20A). The sample was dissolved in HPLC grade methanol to a final concentration of 100 mgmL^{-1}. Purification was accomplished by injecting 250-450 μL aliquots of this solution (using a 500 μL loop). Material was eluted using H_2O + 0.1% (v/v) formic acid (solvent A) and acetonitrile (solvent B) following the same gradient described for bafilomycin A1. Due to instability of the bafilomycins in acidic conditions, material was collected into test tubes containing 5 mL of phosphate buffered saline (pH 7.5). Bafilomycin C1 eluted at 25.1 min. Fractions

were combined and the acetonitrile was removed via rotary evaporation. The buffered aqueous layer was then extracted 3X with equal volumes of ethyl acetate. The organic layers were combined and dried *in vacuo*, then lyophilized for 24 hours, yielding 6.7 mg of bafilomycin C1 as a white powder; HRESIMS *m/z* 719.4053 [M − H]$^-$ (expected *m/z* 719.4012). Mass spec, elution time and NMR all matched commercial standards.

Global Natural Products Social Molecular Networking (GNPS)

The strains *Streptomyces sp. (34893-N3I), Streptomyces sp. (54875-N1N), Streptomyces sp. (5736-A1I),* and *Streptomyces sp. (39098-H2N)* were cultivated in liquid medium and subsequently extracted to be analyzed with HPLC coupled with HRMS and automated fragmentation. The resulting MS^2 data were factored with media blank and analyzed using GNPS[34] to generate respective molecular networks consisting of multiple nodes, with precursor mass tolerance of 2.0 Da and fragment ion mass tolerance of 0.5 Da. The obtained data was then visualized and interpreted using Cytoscape 3.6.1. High-resolution mass spectrometry provided a [M+ Na]$^+$ ion peak at 645.3988 m/z, from which the molecular formula of $C_{35}H_{58}O_9$, containing seven degrees of unsaturation, was deduced. H^1 and C^{13}-NMR comparison along with co-elution LCMS experiment using Baf A1 standard confirmed the identity as bafilomycin A1.

Acknowledgments

References

1. Borrow P, Lewicki H, Wei X, et al. Antiviral pressure exerted by HIV-I-specific cytotoxic T lymphocytes (CTLs) during primary infection demonstrated by rapid selection of CTL escape virus. *Nature medicine.* 1997;3(2):205.
2. Ndhlovu ZM, Kamya P, Mewalal N, et al. Magnitude and kinetics of CD8+ T cell activation during hyperacute HIV infection impact viral set point. *Immunity.* 2015;43(3):591-604.
3. Migueles SA, Laborico AC, Shupert WL, et al. HIV-specific CD8+ T cell proliferation is coupled to perforin expression and is maintained in nonprogressors. *Nature immunology.* 2002;3(11):1061.
4. Sáez-Cirión A, Lacabaratz C, Lambotte O, et al. HIV controllers exhibit potent CD8 T cell capacity to suppress HIV infection ex vivo and peculiar cytotoxic T lymphocyte activation phenotype. *Proceedings of the National Academy of Sciences.* 2007;104(16):6776-6781.
5. Gaiha GD, Rossin EJ, Urbach J, et al. Structural topology defines protective CD8+ T cell epitopes in the HIV proteome. *Science.* 2019;364(6439):480-484.
6. Lehrman G, Hogue IB, Palmer S, et al. Depletion of latent HIV-1 infection in vivo: a proof-of-concept study. *Lancet.* 2005;366(9485):549-555.
7. Shan L, Deng K, Shroff NS, et al. Stimulation of HIV-1-specific cytolytic T lymphocytes facilitates elimination of latent viral reservoir after virus reactivation. *Immunity.* 2012;36(3):491-501.
8. Archin NM, Liberty AL, Kashuba AD, et al. Administration of vorinostat disrupts HIV-1 latency in patients on antiretroviral therapy. *Nature.* 2012;487(7408):482-485.
9. Deng K, Pertea M, Rongvaux A, et al. Broad CTL response is required to clear latent HIV-1 due to dominance of escape mutations. *Nature.* 2015;517(7534):381.
10. Lowin B, Hahne M, Mattmann C, Tschopp J. Cytolytic T-cell cytotoxicity is mediated through perforin and Fas lytic pathways. *Nature.* 1994;370(6491):650.
11. Robinson J, Halliwell JA, Hayhurst JD, Flicek P, Parham P, Marsh SG. The IPD and IMGT/HLA database: allele variant databases. *Nucleic acids research.* 2014;43(D1):D423-D431.
12. Parham P. MHC class I molecules and KIRs in human history, health and survival. *Nature reviews immunology.* 2005;5(3):201.
13. Champsaur M, Lanier LL. Effect of NKG2D ligand expression on host immune responses. *Immunological reviews.* 2010;235(1):267-285.
14. Parham P, Ohta T. Population biology of antigen presentation by MHC class I molecules. *Science.* 1996;272(5258):67-74.
15. Study TIHC. The major genetic determinants of HIV-1 control affect HLA class I peptide presentation. *Science (New York, NY).* 2010;330(6010):1551.
16. Kaslow RA, Carrington M, Apple R, et al. Influence of combinations of human major histocompatibility complex genes on the course of HIV–1 infection. *Nature medicine.* 1996;2(4):405.

17. Donaldson JG, Williams DB. Intracellular assembly and trafficking of MHC class I molecules. *Traffic.* 2009;10(12):1745-1752.

18. Roeth JF, Williams M, Kasper MR, Filzen TM, Collins KL. HIV-1 Nef disrupts MHC-I trafficking by recruiting AP-1 to the MHC-I cytoplasmic tail. *J Cell Biol.* 2004;167(5):903-913.

19. Wonderlich ER, Williams M, Collins KL. The tyrosine binding pocket in the adaptor protein 1 (AP-1) mu1 subunit is necessary for Nef to recruit AP-1 to the major histocompatibility complex class I cytoplasmic tail. *The Journal of biological chemistry.* 2008;283(6):3011-3022.

20. Wonderlich ER, Leonard JA, Kulpa DA, Leopold KE, Norman JM, Collins KL. ADP ribosylation factor 1 activity is required to recruit AP-1 to the major histocompatibility complex class I (MHC-I) cytoplasmic tail and disrupt MHC-I trafficking in HIV-1-infected primary T cells. *Journal of virology.* 2011;85(23):12216-12226.

21. Schaefer MR, Wonderlich ER, Roeth JF, Leonard JA, Collins KL. HIV-1 Nef targets MHC-I and CD4 for degradation via a final common beta-COP-dependent pathway in T cells. *PLoS Pathog.* 2008;4(8):e1000131.

22. Nishi T, Forgac M. The vacuolar (H+)-ATPases—nature's most versatile proton pumps. *Nature reviews Molecular cell biology.* 2002;3(2):94.

23. Jia X, Singh R, Homann S, Yang H, Guatelli J, Xiong Y. Structural basis of evasion of cellular adaptive immunity by HIV-1 Nef. *Nature structural & molecular biology.* 2012;19(7):701-706.

24. Shen QT, Ren X, Zhang R, Lee IH, Hurley JH. HIV-1 Nef hijacks clathrin coats by stabilizing AP-1:Arf1 polygons. *Science.* 2015;350(6259):aac5137.

25. Buffalo CZ, Iwamoto Y, Hurley JH, Ren X. How HIV Nef Proteins Hijack Membrane Traffic to Promote Infection. *Journal of Virology.* 2019:JVI. 01322-01319.

26. Collins KL, Chen BK, Kalams SA, Walker BD, Baltimore D. HIV-1 Nef protein protects infected primary cells against killing by cytotoxic T lymphocytes. *Nature.* 1998;391(6665):397-401.

27. Cohen GB, Gandhi RT, Davis DM, et al. The selective downregulation of class I major histocompatibility complex proteins by HIV-1 protects HIV-infected cells from NK cells. *Immunity.* 1999;10(6):661-671.

28. Williams M, Roeth JF, Kasper MR, Fleis RI, Przybycin CG, Collins KL. Direct binding of human immunodeficiency virus type 1 Nef to the major histocompatibility complex class I (MHC-I) cytoplasmic tail disrupts MHC-I trafficking. *J Virol.* 2002;76(23):12173-12184.

29. Specht A, DeGottardi MQ, Schindler M, Hahn B, Evans DT, Kirchhoff F. Selective downmodulation of HLA-A and-B by Nef alleles from different groups of primate lentiviruses. *Virology.* 2008;373(1):229-237.

30. Kasper MR, Collins KL. Nef-mediated disruption of HLA-A2 transport to the cell surface in T cells. *Journal of virology.* 2003;77(5):3041-3049.

31. Cao K, Hollenbach J, Shi X, Shi W, Chopek M, Fernández-Viña MA. Analysis of the frequencies of HLA-A, B, and C alleles and haplotypes in the five major ethnic groups of the United States reveals high levels of diversity in these loci and contrasting distribution patterns in these populations. *Human immunology.* 2001;62(9):1009-1030.

32. Hilton HG, Parham P. Direct binding to antigen-coated beads refines the specificity and cross-reactivity of four monoclonal antibodies that recognize polymorphic epitopes of HLA class I molecules. *Tissue antigens.* 2013;81(4):212-220.

33. Jacob RT, Larsen MJ, Larsen SD, Kirchhoff PD, Sherman DH, Neubig RR. MScreen: an integrated compound management and high-throughput screening data storage and analysis system. *Journal of biomolecular screening.* 2012;17(8):1080-1087.

34. Wang M, Carver JJ, Phelan VV, et al. Sharing and community curation of mass spectrometry data with Global Natural Products Social Molecular Networking. *Nature biotechnology.* 2016;34(8):828.

35. Emert-Sedlak LA, Narute P, Shu ST, et al. Effector kinase coupling enables high-throughput screens for direct HIV-1 Nef antagonists with antiretroviral activity. *Chemistry & biology.* 2013;20(1):82-91.

36. Mujib S, Saiyed A, Fadel S, et al. Pharmacologic HIV-1 Nef blockade promotes CD8 T cell-mediated elimination of latently HIV-1-infected cells in vitro. *JCI Insight.* 2017;2(17).

37. Liu B, Zhang X, Zhang W, et al. Lovastatin inhibits HIV-1-induced MHC-I downregulation by targeting Nef–AP-1 complex formation: A new strategy to boost immune eradication of HIV-1 infected cells. *Frontiers in Immunology.* 2019;10:2151.

38. Dröse S, Altendorf K. Bafilomycins and concanamycins as inhibitors of V-ATPases and P-ATPases. *J Exp Biol.* 1997;200(1):1-8.

39. KINASHI H, SOMENO K, SAKAGUCHI K. Isolation and characterization of concanamycins A, B and C. *The Journal of antibiotics.* 1984;37(11):1333-1343.

40. Pérez-Sayáns M, Somoza-Martín JM, Barros-Angueira F, Rey JMG, García-García A. V-ATPase inhibitors and implication in cancer treatment. *Cancer treatment reviews.* 2009;35(8):707-713.

41. Hall TJ. Cytotoxicity of vacuolar H+-ATPase inhibitors to UMR-106 rat osteoblasts: an effect on iron uptake into cells? *Cell biology international.* 1994;18(3):189-193.

42. Manabe T, Yoshimori T, Henomatsu N, Tashiro Y. Inhibitors of vacuolar-type H+-ATPase suppresses proliferation of cultured cells. *Journal of cellular physiology.* 1993;157(3):445-452.

43. Gao X, Han L, Ding N, et al. Bafilomycin C1 induces G0/G1 cell-cycle arrest and mitochondrial-mediated apoptosis in human hepatocellular cancer SMMC7721 cells. *The Journal of antibiotics.* 2018;71(9):808.

44. Beyenbach KW, Wieczorek H. The V-type H+ ATPase: molecular structure and function, physiological roles and regulation. *J Exp Biol.* 2006;209(4):577-589.

45. Yanagawa M, Tsukuba T, Nishioku T, et al. Cathepsin E deficiency induces a novel form of lysosomal storage disorder showing the accumulation of lysosomal membrane sialoglycoproteins and the elevation of lysosomal pH in macrophages. *Journal of Biological Chemistry.* 2007;282(3):1851-1862.

46. Jin YJ, Cai CY, Zhang X, Zhang HT, Hirst JA, Burakoff SJ. HIV Nef-mediated CD4 down-regulation is adaptor protein complex 2 dependent. *J Immunol.* 2005;175(5):3157-3164.

47. Sykulev Y, Joo M, Vturina I, Tsomides TJ, Eisen HN. Evidence that a single peptide–MHC complex on a target cell can elicit a cytolytic T cell response. *Immunity.* 1996;4(6):565-571.

48. Anmole G, Kuang XT, Toyoda M, et al. A robust and scalable TCR-based reporter cell assay to measure HIV-1 Nef-mediated T cell immune evasion. *Journal of immunological methods.* 2015;426:104-113.

49. Christinck ER, Luscher MA, Barber BH, Williams DB. Peptide binding to class I MHC on living cells and quantitation of complexes required for CTL lysis. *Nature.* 1991;352(6330):67.

50. Valitutti S, Müller S, Cella M, Padovan E, Lanzavecchia A. Serial triggering of many T-cell receptors by a few peptide–MHC complexes. *Nature.* 1995;375(6527):148.

51. Kataoka T, Shinohara N, Takayama H, et al. Concanamycin A, a powerful tool for characterization and estimation of contribution of perforin-and Fas-based lytic pathways in cell-mediated cytotoxicity. *The Journal of Immunology.* 1996;156(10):3678-3686.

52. Togashi K-i, Kataoka T, Nagai K. Characterization of a series of vacuolar type H+-ATPase inhibitors on CTL-mediated cytotoxicity. *Immunology letters.* 1997;55(3):139-144.

53. Kiepiela P, Leslie AJ, Honeyborne I, et al. Dominant influence of HLA-B in mediating the potential co-evolution of HIV and HLA. *Nature.* 2004;432(7018):769.

54. Apps R, Meng Z, Del Prete GQ, Lifson JD, Zhou M, Carrington M. Relative expression levels of the HLA class-I proteins in normal and HIV-infected cells. *The Journal of Immunology.* 2015;194(8):3594-3600.

55. Mwimanzi F, Toyoda M, Mahiti M, et al. Relative resistance of MHC-B to Nef-mediated downregulation is conserved among primate lentiviruses and influences antiviral T cell responses in HIV-1-infected individuals. *Journal of Virology.* 2017:JVI. 01409-01417.

56. Yarzabek B, Zaitouna AJ, Olson E, et al. Variations in HLA-B cell surface expression, half-life and extracellular antigen receptivity. *Elife.* 2018;7:e34961.

57. Zaikos TD, Terry VH, Kettinger NTS, et al. Hematopoietic stem and progenitor cells are a distinct HIV reservoir that contributes to persistent viremia in suppressed patients. *Cell reports.* 2018;25(13):3759-3773. e3759.

58. Leonard JA, Filzen T, Carter CC, Schaefer M, Collins KL. HIV-1 Nef disrupts intracellular trafficking of major histocompatibility complex class I, CD4, CD8, and CD28 by distinct pathways that share common elements. *J Virol.* 2011;85(14):6867-6881.

59. Schaefer MR, Wonderlich ER, Roeth JF, Leonard JA, Collins KL. HIV-1 Nef targets MHC-I and CD4 for degradation via a final common β-COP–dependent pathway in T cells. *PLoS pathogens.* 2008;4(8).

60. Shi J, Xiong R, Zhou T, et al. HIV-1 Nef antagonizes SERINC5 restriction by downregulation of SERINC5 via the endosome/lysosome system. *Journal of virology.* 2018;92(11):e00196-00118.

61. Luo T, Anderson SJ, Garcia JV. Inhibition of Nef-and phorbol ester-induced CD4 degradation by macrolide antibiotics. *Journal of virology.* 1996;70(3):1527-1534.

62.	Roeth JF, Williams M, Kasper MR, Filzen TM, Collins KL. HIV-1 Nef disrupts MHC-I trafficking by recruiting AP-1 to the MHC-I cytoplasmic tail. *The Journal of cell biology.* 2004;167(5):903-913.

63.	El-Far M, Isabelle C, Chomont N, et al. Down-regulation of CTLA-4 by HIV-1 Nef protein. *PLoS One.* 2013;8(1).

64.	Pawlak EN, Dirk BS, Jacob RA, Johnson AL, Dikeakos JD. The HIV-1 accessory proteins Nef and Vpu downregulate total and cell surface CD28 in CD4+ T cells. *Retrovirology.* 2018;15(1):6.

65.	Johnson LS, Dunn K, Pytowski B, McGraw TE. Endosome acidification and receptor trafficking: bafilomycin A1 slows receptor externalization by a mechanism involving the receptor's internalization motif. *Molecular biology of the cell.* 1993;4(12):1251-1266.

66.	Marshansky V, Futai M. The V-type H+-ATPase in vesicular trafficking: targeting, regulation and function. *Current opinion in cell biology.* 2008;20(4):415-426.

67.	Geyer M, Yu H, Mandic R, et al. Subunit H of the V-ATPase binds to the medium chain of adaptor protein complex 2 and connects Nef to the endocytic machinery. *Journal of Biological Chemistry.* 2002;277(32):28521-28529.

68.	Lu X, Yu H, Liu S-H, Brodsky FM, Peterlin BM. Interactions between HIV1 Nef and vacuolar ATPase facilitate the internalization of CD4. *Immunity.* 1998;8(5):647-656.

69.	Mandic R, Fackler OT, Geyer M, Linnemann T, Zheng Y-H, Peterlin BM. Negative factor from SIV binds to the catalytic subunit of the V-ATPase to internalize CD4 and to increase viral infectivity. *Molecular biology of the cell.* 2001;12(2):463-473.

70.	Kasper MR, Collins KL. Nef-mediated disruption of HLA-A2 transport to the cell surface in T cells. *J Virol.* 2003;77(5):3041-3049.

71.	Mashiba M, Collins DR, Terry VH, Collins KL. Vpr overcomes macrophage-specific restriction of HIV-1 Env expression and virion production. *Cell host & microbe.* 2014;16(6):722-735.

72.	Kuroda H, Kutner RH, Bazan NG, Reiser J. Simplified lentivirus vector production in protein-free media using polyethylenimine-mediated transfection. *Journal of virological methods.* 2009;157(2):113-121.

73.	Zaikos TD, Painter MM, Kettinger NTS, Terry VH, Collins KL. Class 1-selective histone deacetylase (HDAC) inhibitors enhance HIV latency reversal while preserving the activity of HDAC isoforms necessary for maximal HIV gene expression. *Journal of virology.* 2018;92(6):e02110-02117.

74.	Pear WS, Nolan GP, Scott ML, Baltimore D. Production of high-titer helper-free retroviruses by transient transfection. *Proceedings of the National Academy of Sciences.* 1993;90(18):8392-8396.

75.	Thammavongsa V, Schaefer M, Filzen T, et al. Assembly and intracellular trafficking of HLA-B* 3501 and HLA-B* 3503. *Immunogenetics.* 2009;61(11-12):703-716.

76.	McNamara LA, Ganesh JA, Collins KL. Latent HIV-1 infection occurs in multiple subsets of hematopoietic progenitor cells and is reversed by NF-kappaB activation. *J Virol.* 2012;86(17):9337-9350.

77.   Naviaux RK, Costanzi E, Haas M, Verma IM. The pCL vector system: rapid production of helper-free, high-titer, recombinant retroviruses. *Journal of virology.* 1996;70(8):5701-5705.

78.   Painter MM, Zaikos TD, Collins KL. Quiescence promotes latent HIV infection and resistance to reactivation from latency with histone deacetylase inhibitors. *Journal of virology.* 2017;91(24):e01080-01017.

79.   Kasper MR, Roeth JF, Williams M, Filzen TM, Fleis RI, Collins KL. HIV-1 Nef disrupts antigen presentation early in the secretory pathway. *Journal of Biological Chemistry.* 2005;280(13):12840-12848.

80.   Morris KL, Buffalo C, Ren X, Hurley JH. High Resolution cryo-EM Structure of a HIV Nef-Inhibited AP-1 Clathrin Adaptor Complex. *Biophysical Journal.* 2018;114(3):163a.

81.   Sheffield P, Garrard S, Derewenda Z. Overcoming expression and purification problems of RhoGDI using a family of "parallel" expression vectors. *Protein expression and purification.* 1999;15(1):34-39.

82.   Johnson RP, Trocha A, Yang L, et al. HIV-1 gag-specific cytotoxic T lymphocytes recognize multiple highly conserved epitopes. Fine specificity of the gag-specific response defined by using unstimulated peripheral blood mononuclear cells and cloned effector cells. *The Journal of Immunology.* 1991;147(5):1512-1521.

83.   Walker BD, Flexner C, Birch-Limberger K, et al. Long-term culture and fine specificity of human cytotoxic T-lymphocyte clones reactive with human immunodeficiency virus type 1. *Proceedings of the National Academy of Sciences.* 1989;86(23):9514-9518.

84.   Walter JB, Brander C, Mammen M, et al. Stimulation of human cytotoxic T cells with HIV-1-derived peptides presented by recombinant HLA-A2 peptide complexes. *International immunology.* 1997;9(3):451-459.

85.   Shepherd MD, Kharel MK, Bosserman MA, Rohr J. Laboratory maintenance of Streptomyces species. *Current protocols in microbiology.* 2010;18(1):10E. 11.11-10E. 11.18.

86.   Laatsch H. *AntiBase 2011: the natural compound identifier.* Wiley-Vch; 2011.

87.   Li Z, Du L, Zhang W, et al. Complete elucidation of the late steps of bafilomycin biosynthesis in Streptomyces lohii. *Journal of Biological Chemistry.* 2017;292(17):7095-7104.

Appendix
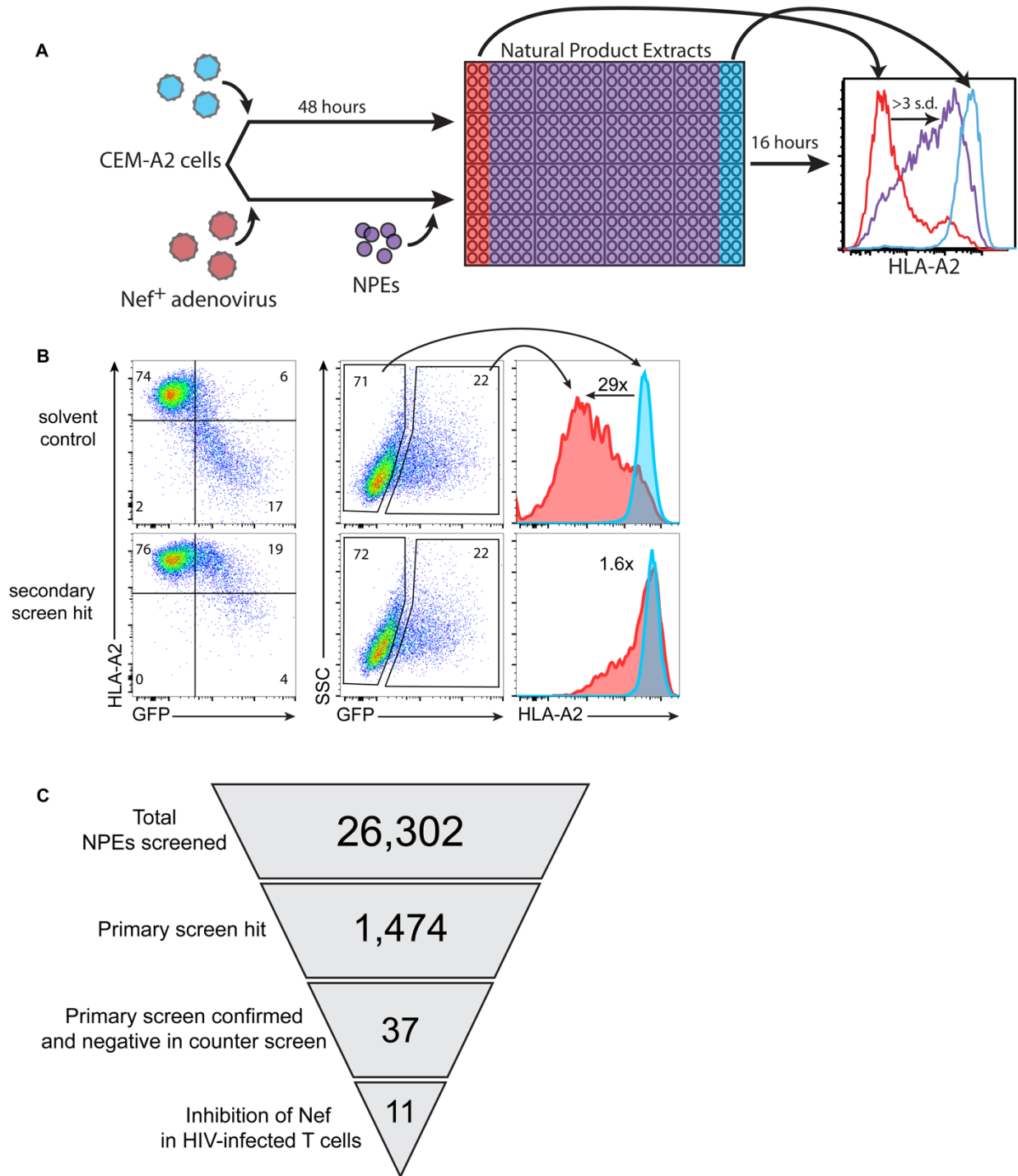
Fig. 3.S1: Screening of natural product extracts for inhibitors of HIV Nef.[11] (A) Schematic representation of primary screen assay. Blue histogram represents CEM-A2 cells transduced with Nef-negative adenoviral vector and treated with solvent control, red histogram represents cells transduced with Nef-expressing adenoviral vector and treated with solvent control, purple histogram represents cells transduced with Nef-expressing adenoviral vector and treated with a representative positive hit in the primary screen. (B) Representative flow cytometry plots from secondary screen assay showing the solvent control and a representative positive hit in the secondary screen. Blue histograms are from uninfected, GFP⁻ cells, red histograms are from infected, GFP⁺ cells. Numbers in histograms indicate the fold decrease in HLA-A2 MFI in infected cells relative to uninfected cells. (C) Summary of NPE screening results, yielding the identification of 11 microbial strains producing Nef inhibitory compounds for further purification.

---

[11] Zimmerman GE, Robertson, AW, McLeod MR, Gomez-Rodriguez L, Garcia KA, Leonard JA, Leopold KE, and Neevel AJ contributed to Fig. 3.S1.
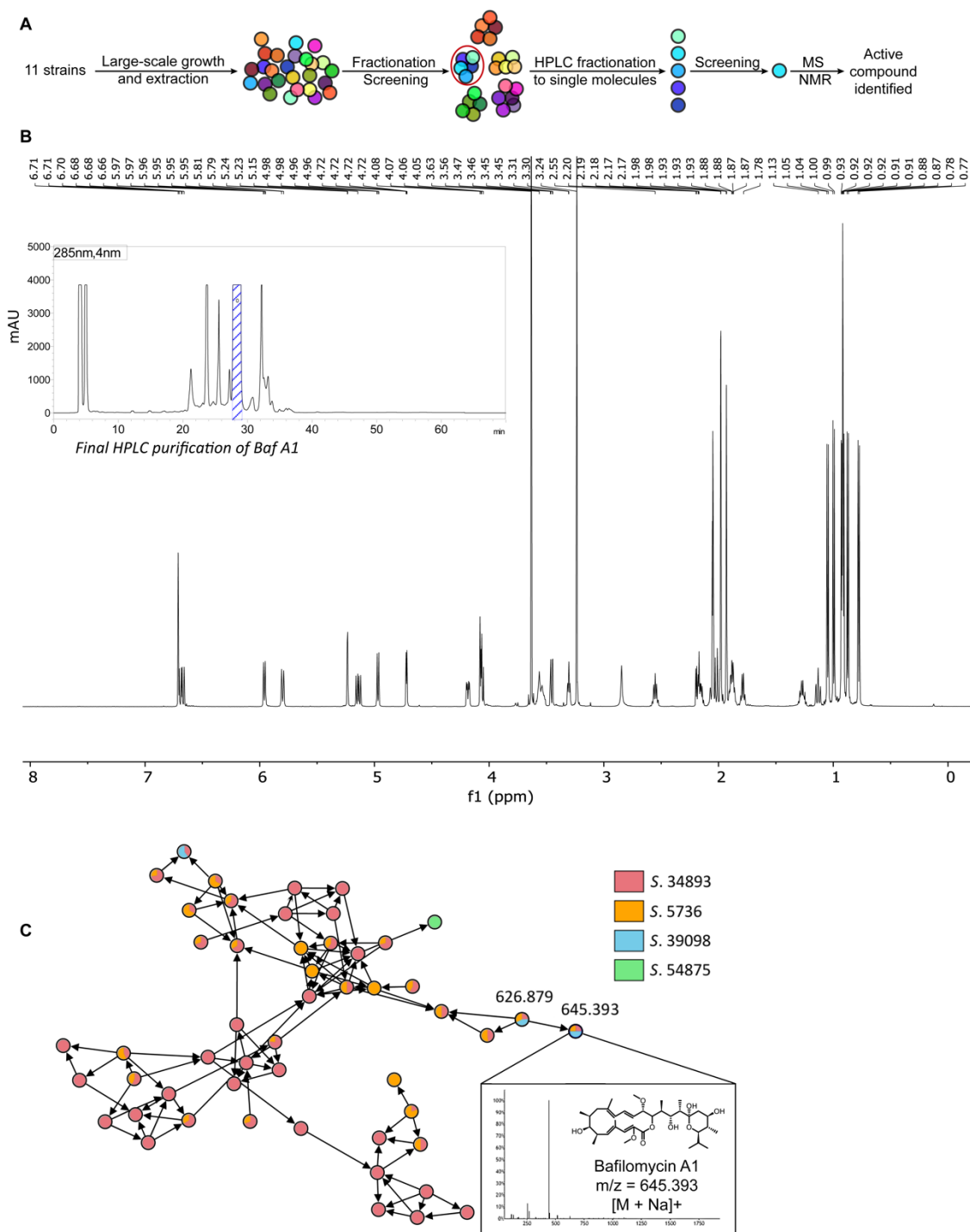
Fig. 3.S2: Plecomacrolides identified as Nef inhibitors in multiple NPE strains.[12] (A) Schematic representation of the isolation of a single active compound from a natural product extract by sequential fractionation and re-screening. (B) Fractionation from one strain yields a single HPLC peak that possesses activity, and NMR identifies Bafilomycin A1. (C) MS/MS molecular networking reveals Baf A1 in 3 of 4 lead candidate extracts.

---

[12] Robertson AW, Gomez-Rodriguez L, and Tripathi A contributed to Fig. 3.S2.
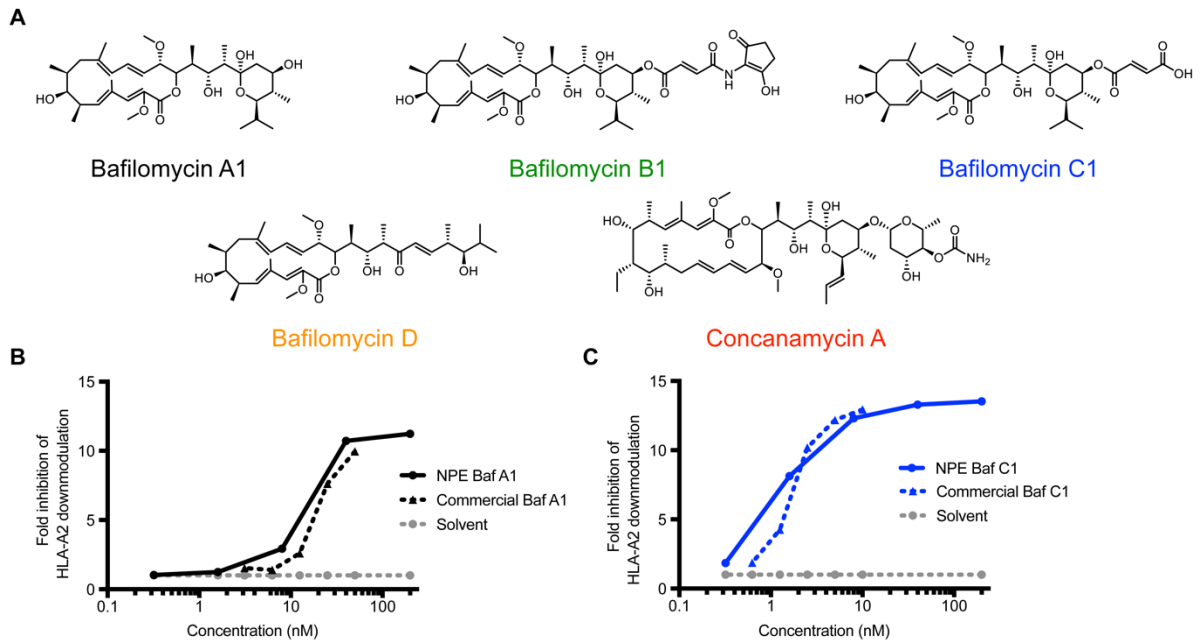
Fig. 3.S3: Natural product extract-derived plecomacrolides mirror commercially available compounds.[13] (A) Chemical structures of plecomacrolides. (B-C) Summary graphs of flow cytometric data from the secondary screen assay (as in Fig. 3.S1B) using the indicated compounds. NPE Bafs were isolated as in Fig. 3.S2 (n=1).

---

[13] Robertson AW generated Fig. 3.S3A. Robertson AW and Zimmerman GE contributed to Fig. 3.S3B-C.
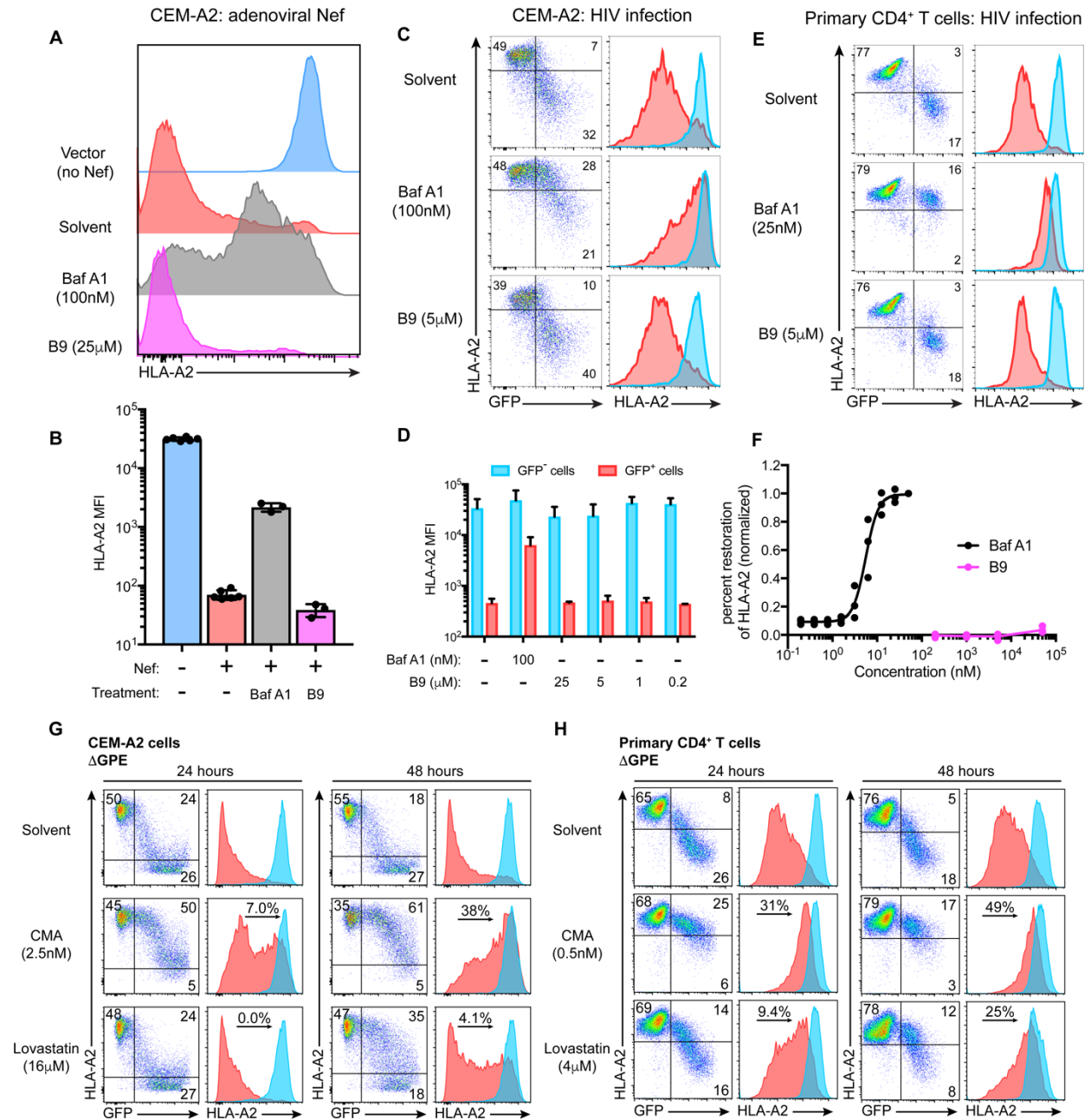
Fig. 3.S4: B9 fails to restore MHC-I in cell line screens and HIV-infected primary cells, while lovastatin restores less effectively than CMA. (A) Representative flow cytometry histograms and (B) summary graph (n=6 for controls, n=3 for experimental samples) from CEM-A2 cells treated with B9 and Baf A1 in the primary screen as in Fig. 3.S1A. (C) Representative flow cytometry plots and (D) summary graph (n=3) from CEM-A2 cells infected with ΔGPE and treated with B9 and Baf A1 in the secondary screen as in Fig. 3.S1B. Blue histograms are from GFP$^-$ cells, red histograms are from infected GFP$^+$ cells. (E) Representative flow cytometry plots from primary activated CD4$^+$ T cells infected with ΔGPE and analyzed as in the secondary screen in Fig. 3.S1B. Blue histograms are from GFP$^-$ cells, red histograms are from infected GFP$^+$ cells. (F) Summary graph of assays performed as in E using the indicated compound. Percent restoration of HLA-A2 is calculated as described in Materials and Methods and normalized to percent restoration achieved at 50nM Baf A1 (n=3). (G-H) Representative flow cytometry plots from ΔGPE-infected (G) CEM-A2 cells and (H) primary CD4$^+$ T cells, treated side-by-side with the indicated compound

196

for the indicated time. Numbers in histogram panels indicate percent restoration of HLA-A2 (n=3). Error bars indicate standard deviation, MFI = median fluorescence intensity. Solvent control is DMSO.
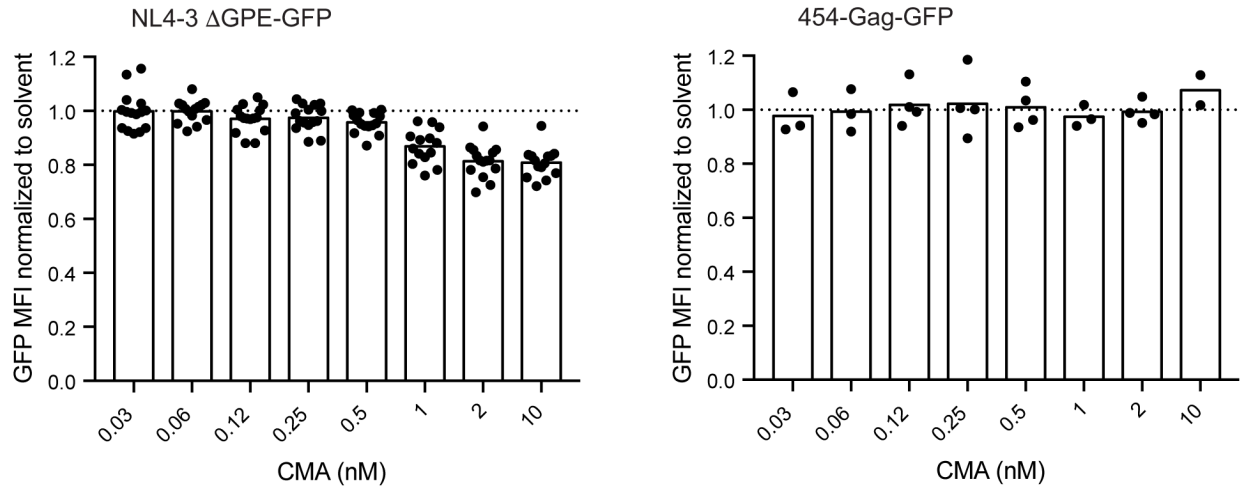
Fig. 3.S5: CMA does not counteract Nef by reducing HIV gene expression in primary CD4+ T cells.[14]
Summary graph of flow cytometric data analyzing the mean fluorescence intensity (MFI) of GFP in the GFP⁺ cells gate of CD4⁺ T cells infected with the indicated GFP-expressing viral constructs and treated with CMA as in Fig. 3.1. Dots represent biological replicates with independent donors.

---

[14] Zimmerman GE contributed to the data collection and analysis in Fig. 3.S5.
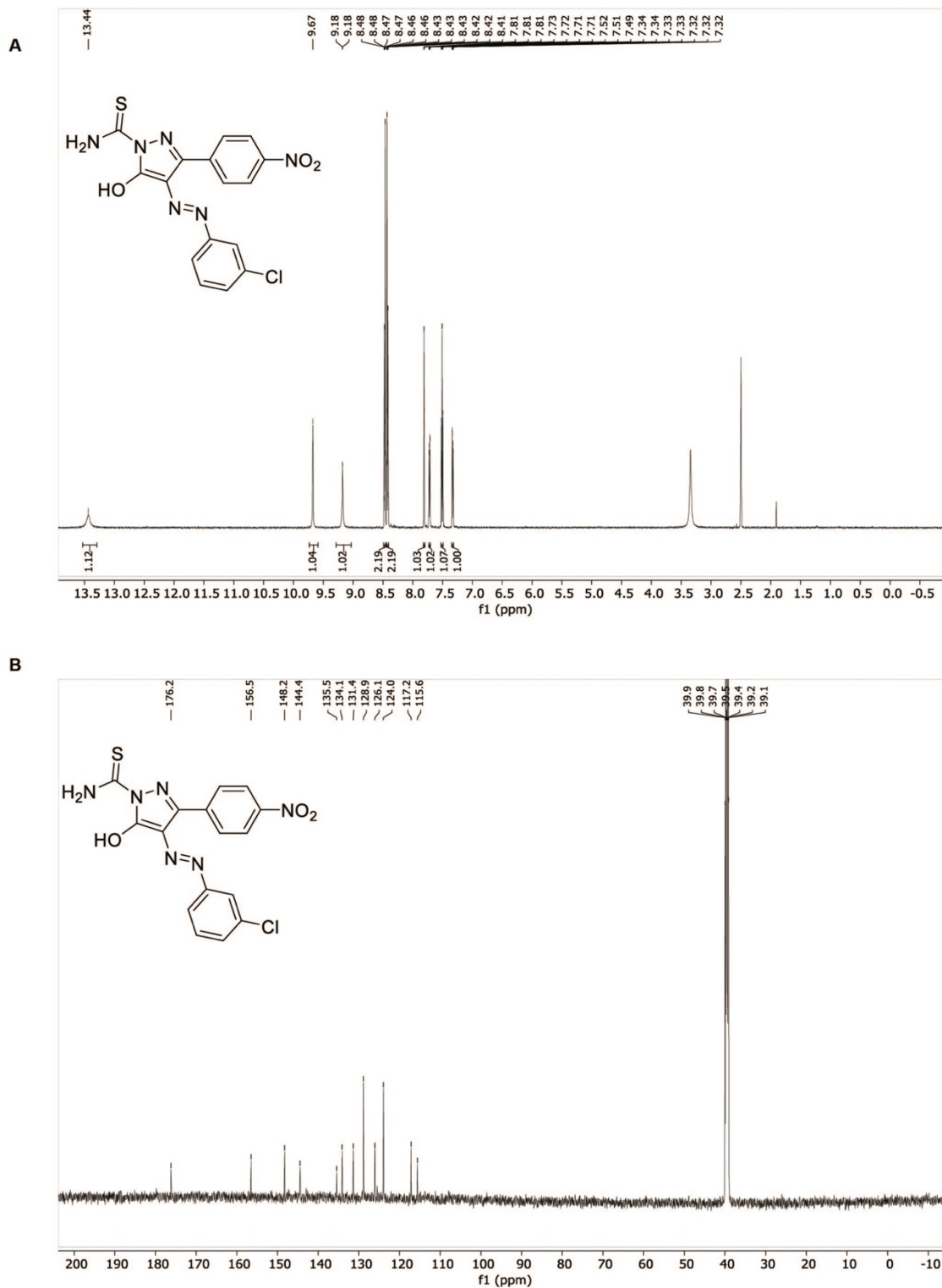
Fig. 3.S6: Confirmation of B9 structure.[15]
(A) 1H-NMR of B9 in DMSO-d$_6$ (600 MHz). (B) 13C-NMR of B9 in DMSO-d$_6$ (125 MHz).

---

[15] Robertson AW generated Fig. 3.S6.

A

B
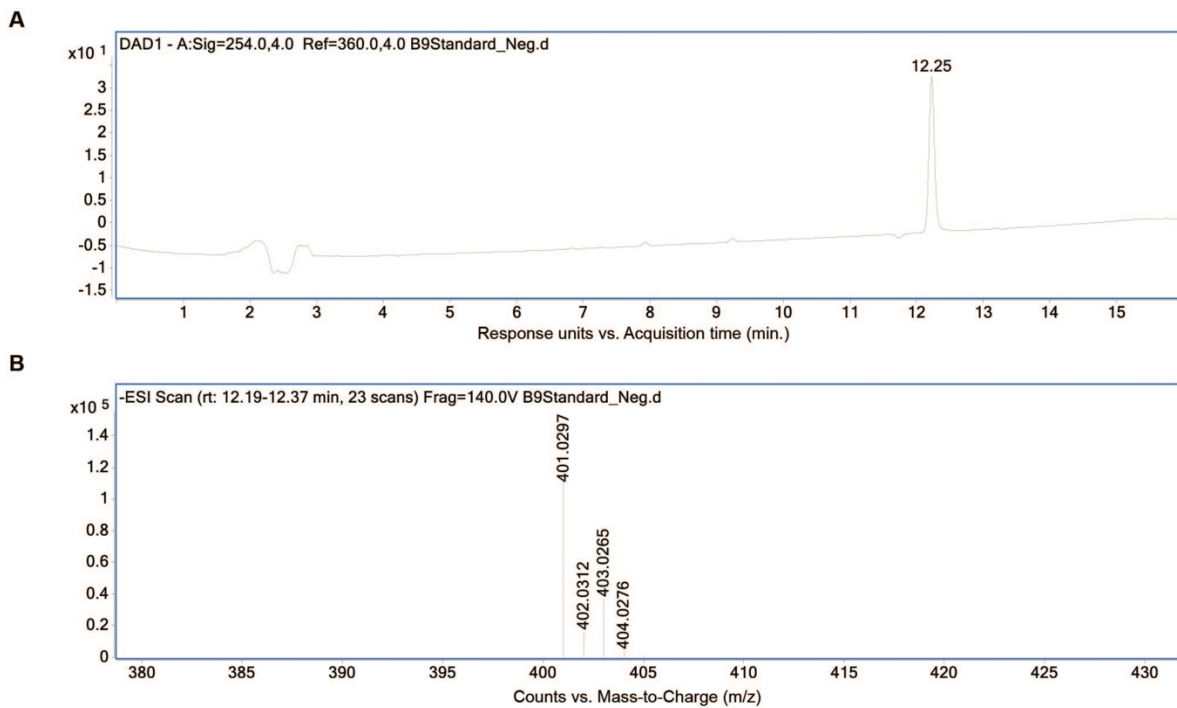
Fig. 3.S7: Confirmation of B9 structure, continued.[16]
LCMS trace of standard B9 illustrating (A) diode array detector (DAD) trace (Rt = 12.25 min) and (B) mass spectrum at 12.15 – 12.41 min. All confirm that the structure of commercially-acquired B9 matches the published structure.

---

[16] Robertson AW generated Fig. 3.S7.
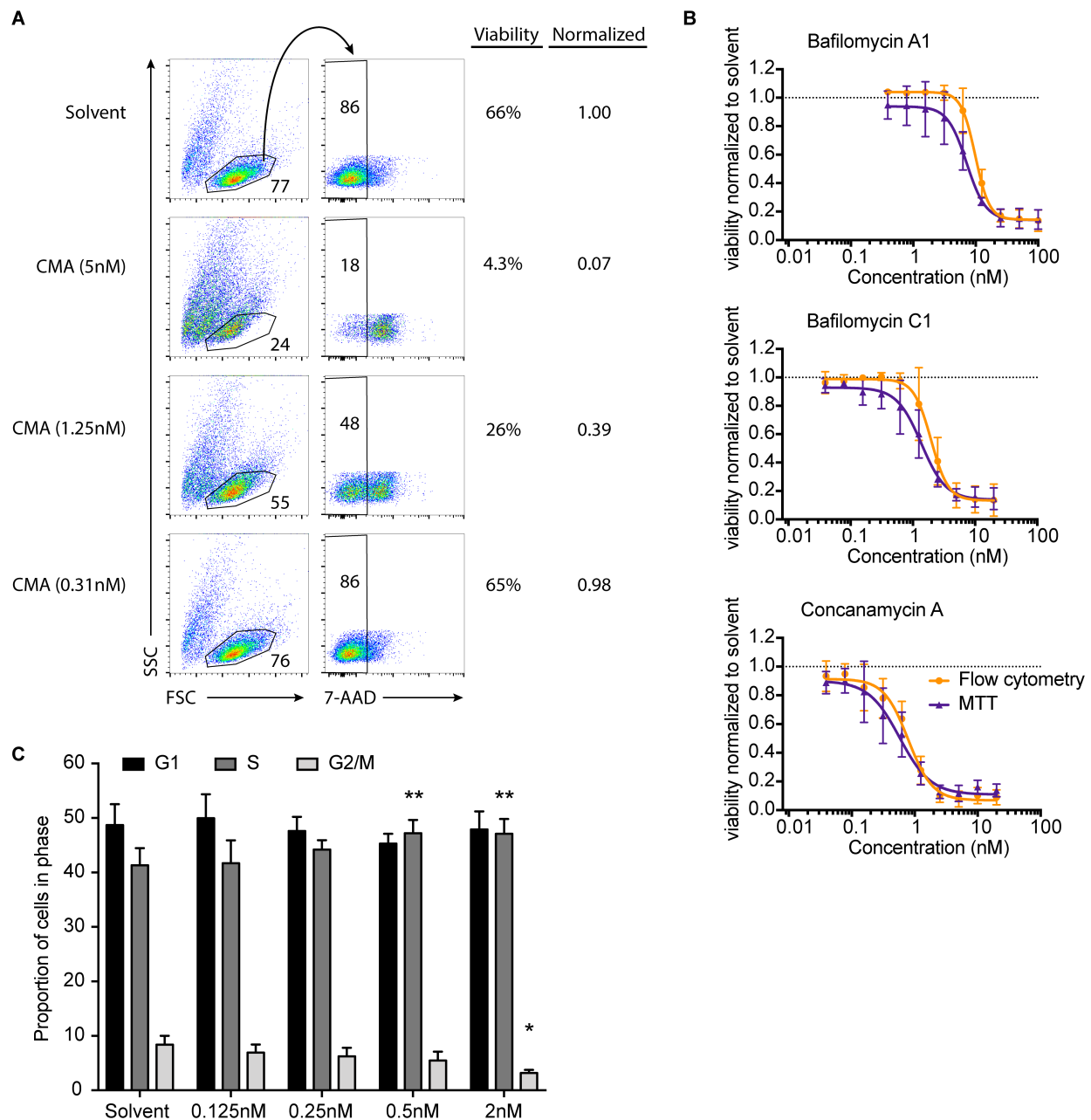
Fig. 3.S8: Plecomacrolide toxicity is consistent between assays and cell cycle arrest requires higher concentrations than Nef inhibition.[17] (A) Gating strategy and representative flow cytometric plots for data in Fig. 3.1E. (B) Comparison of MTT and flow cytometric viability assays, showing comparable results in primary CD4+ T cells incubated with the indicated compounds for 72 hours. Summary graph of data from flow cytometric (circles, orange, as in A) and MTT assay (triangles, purple) assessing the viability of CD4+ T cells treated with titrations of the indicated plecomacrolides for 72 hours (n=3 for Baf A1 and C1, n=6 for CMA). Data are normalized to viability of cells treated with matched DMSO solvent control. (C) Summary graph of DAPI flow cytometric cell cycle data from primary CD4+ T cells treated with CMA or matched

---

[17] Merlino MS contributed to generating data for Fig. 3.S8A-B.

201

DMSO solvent control for 24 hours as indicated (n=5). All error bars represent standard deviation. (** = p < 0.01, * = p < 0.05, Dunnett's multiple comparisons test, compared to solvent)
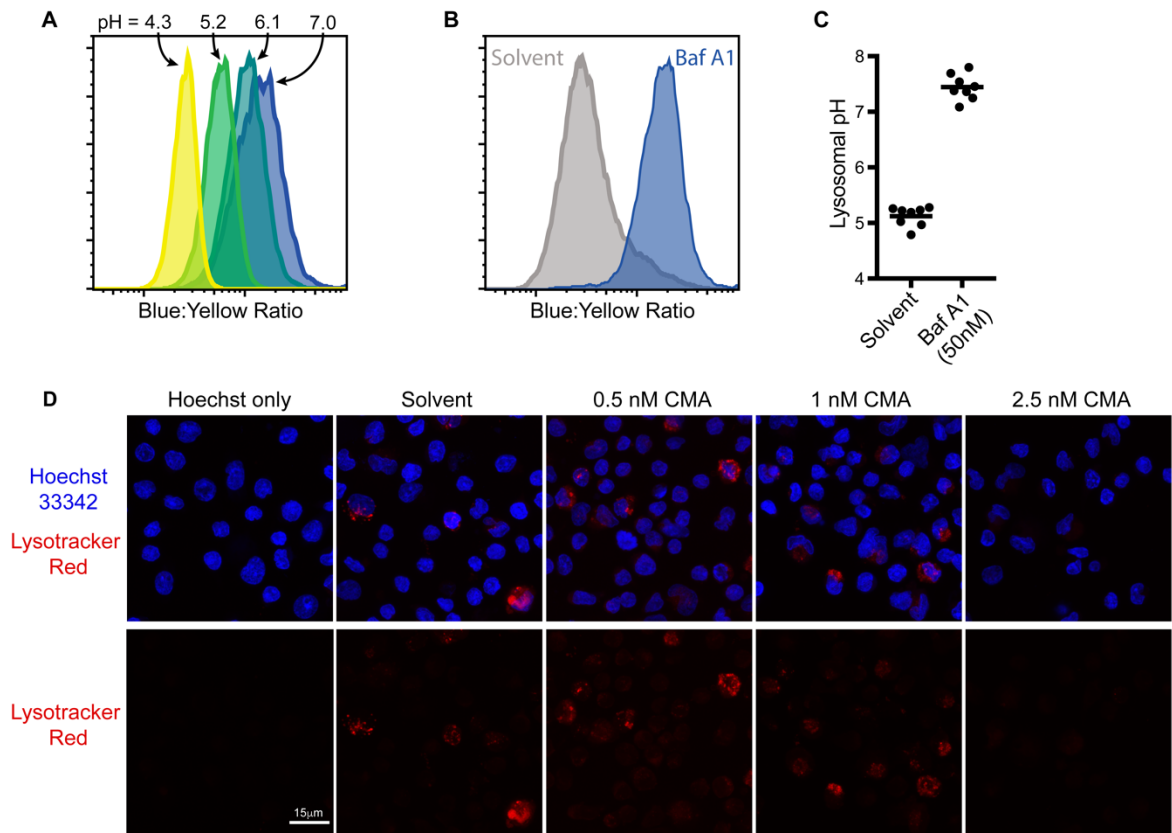
Fig. 3.S9: Supplement to lysosome and trafficking studies in Fig. 3.2.[18] (A) Flow cytometric data derived from primary monocyte-derived macrophages (MDM) incubated with Lysosensor Yellow/Blue dextran, 10,000 MW for 24 hours and analyzed in buffers of known pH as indicated. The ratio of blue:yellow fluorescence was calculated for each cell, and the median ratio for each sample was used to generate a standard curve to calculate lysosomal pH. (B-C) Representative flow cytometric plot (B) and summary graph (C) describing the lysosomal pH of primary monocyte-derived macrophages (MDM) treated with 50nM Baf A1 for 1 hour after incubation with Lysosensor Yellow/Blue dextran, 10,000 MW as in A (n=8). Lysosomal pH was calculated using a standard curve generated for each donor as in A. (D) Representative confocal microscopy max projections from multiple z-stack images of primary CD4$^+$ T cells treated for 24 hours with CMA as indicated and incubated with Lysotracker Red and Hoechst 3342 for 1 hour. All images were captured with identical microscope settings (representative from 3 independent experiments).

---

[18] Lubow J contributed to experiments in Fig. 3.S9A-C. Zimmerman GE performed experiments and generated Fig. 3.S9.
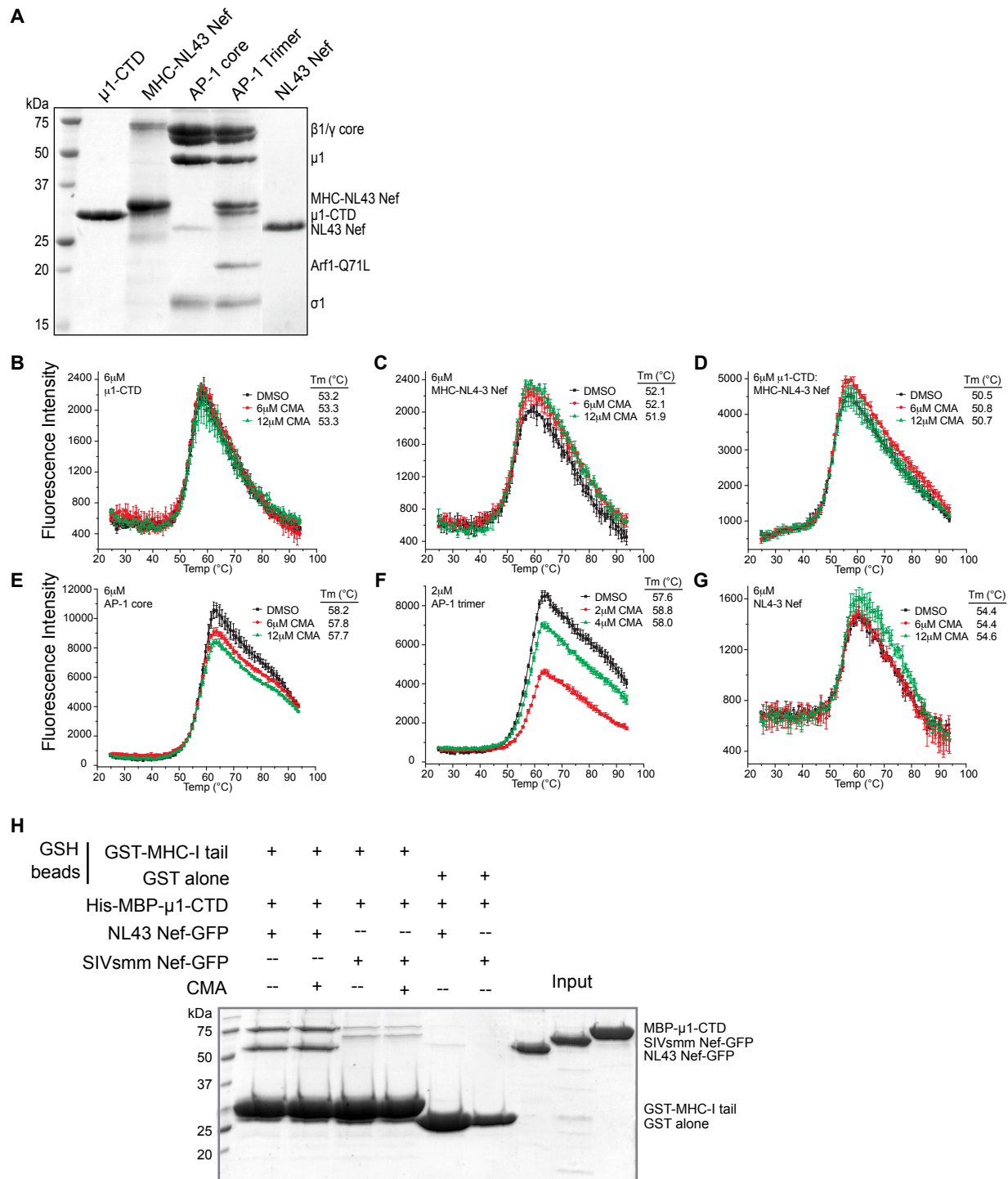
Fig. 3.S10: CMA does not directly alter the interaction between the MHC-I tail, AP-1, and Nef.[19] (A) SDS PAGE gel of protein samples used in DSF assay in Fig. 3.3D-I, which was visualized by Coomassie blue staining. (B-G) CMA does not affect the AP-1:Nef:MHC-I interaction in vitro. Differential scanning fluorimetry (DSF) plots of protein thermal stability with or without CMA treatment. Reaction mixtures contained SYPRO orange and 2-6 µM proteins in the presence or absence of 2-12 µM CMA. SYPRO orange fluorescence intensity was plotted as a function of temperature for (B) µ1-CTD domain, (C) MHC-I tail fused with HIV-1 NL4-3 Nef (MHC-NL43 Nef), (D) µ1-CTD: MHC-NL43 Nef, (E) AP-1 core, (F) AP-1

---

[19] Ren X generated Fig. 3.S10.

204

trimer containing AP-1 core: Arf1-GTP: MHC-NL43 Nef, and (G) NL43 Nef alone. DMSO concentration in each reaction was fixed at 5%. Measured fluorescence intensity (before post-peak region) was fitted to Boltzmann equation to obtain melting temperature (Tm). The error bars represent the corresponding standard deviation among three replicates. (H) The effect of CMA in μ1-CTD:MHC-I tail:Nef interaction analyzed by GST pull down assay. Glutathione sepharose beads were used to immobilize GST tagged MHC-I tail and subsequently pull down MBP tagged μ1-CTD and Nef-GFP in the presence or absence of 40μM CMA. The pull-down results were visualized by SDS-PAGE and Coomassie blue staining.
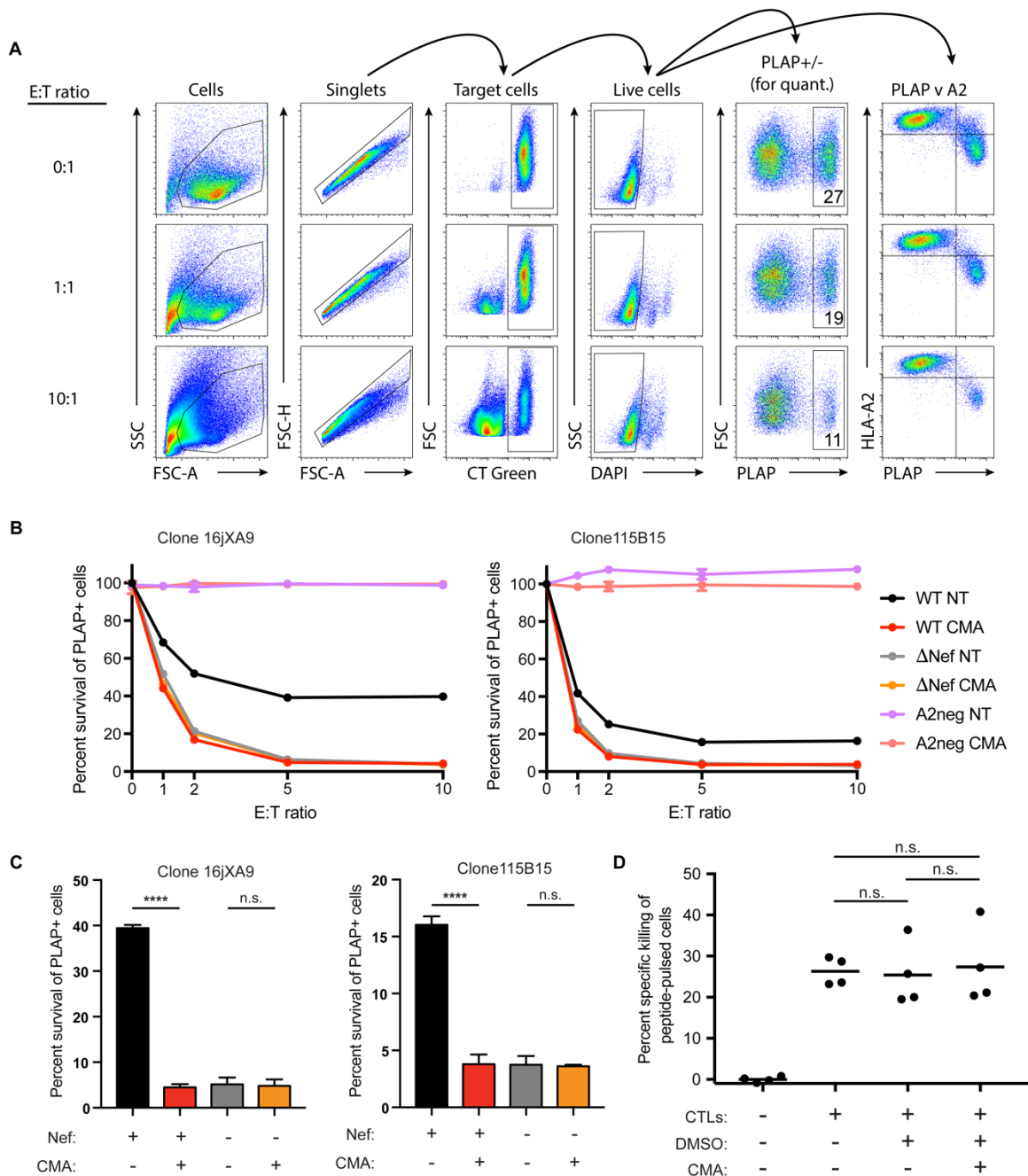
Fig. 3.S11: Supplement to CTL killing assay as in Fig. 3.4.[20] (A) Gating strategy for results in Fig. 3.4. Representative flow cytometric plots from CD4^{+} T cells infected with HXBePLAP (Fig. 3.1A) and co-cultured with increasing ratios of HIV-specific CTLs. CD4^{+} T cell target cells are stained with CellTracker Green dye (CT Green) 24 hours before co-culture to distinguish the CD4^{+} T cell targets from CTL effectors. DAPI is used as a viability dye, and PLAP marks infected cells. Data for summary graphs in B are generated from PLAP vs. FSC plots as indicated. (B) Summary graphs for assays described in Fig. 3.4A-B, where elimination of PLAP^{+} cells is only observed for HLA-A2^{+} target cells. WT = HXBePLAP, ΔNef = HXBePLAP with Nef deletion, A2neg = target cells derived from a donor lacking the HLA-A2 allele of MHC-I infected

---

[20] Terry VH contributed to all experiments in Fig. 3.S11 and generated all data for Fig. 3.S11D.

with HXBePLAP with Nef deleted, NT = no treatment (matched DMSO solvent control), CMA = 0.5nM CMA. (C) Summary graphs of flow cytometric data as in Fig. 3.4 in which the 5:1 and 10:1 E:T ratios were pooled into a single condition where CTL killing was saturated, yielding four individual replicates within each experiment (unpaired t test, **** = $p < 0.0001$, n.s. = not significant). (D) Summary graphs of flow cytometric data from co-culture experiments of CTL clones with Gag SL9 peptide-pulsed JY cells, reporting specific elimination of peptide-pulsed JY target cells relative to unpulsed target cells, which were differentially dyed. Co-cultures were performed in the presence or absence of 0.5nM CMA and the solvent DMSO. Viable cells were identified by light scatter and viability dye exclusion, and specific killing was calculated by dividing the frequency of viable cells that were peptide-pulsed observed in the sample by the frequency observed in the control and subtracting from 1. Individual points represent experimental duplicates from each of two independent biological replicates (unpaired t tests, n.s. = not significant).

A HLA genotypes for donor in Fig. 5

Locus	Allele	Reactivity
HLA-A	A*02:01:01:01	BB7.2
HLA-A	A*03:01:01:01	none
HLA-B	B*51:01:01:01	anti-Bw4
HLA-B	B*07:02:01	anti-Bw6
HLA-C	C*15:02:01:01	none
HLA-C	C*07:02:01:03	anti-Bw6

*note: HLA-C is reportedly expressed at 6-fold lower levels than HLA-B, so most anti-Bw6 signal is expected to come from B*07:02:01 for this donor
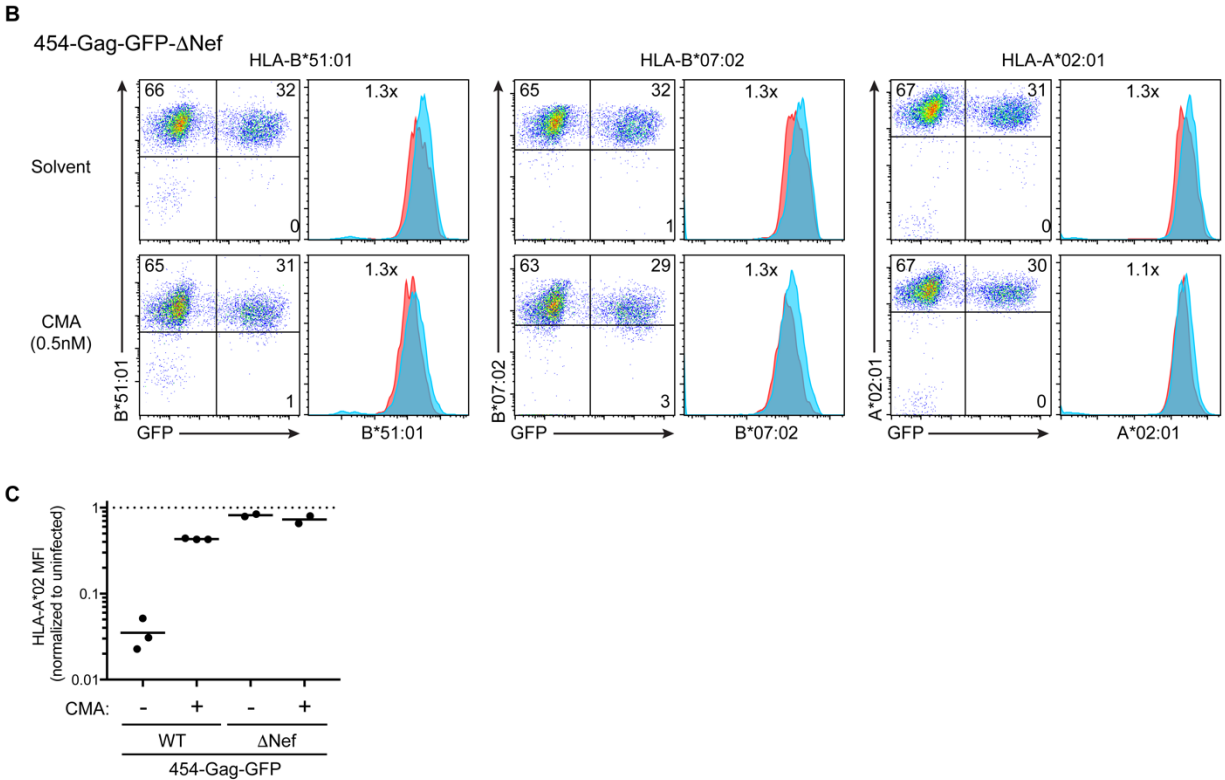
Fig. 3.S12: Supplemental information for primary cell experiments with HLA-B and 454-Gag-GFP.[21] (A) HLA genotypes for the donor used in Fig. 3.5. Only A*02:01:01:01 reacts with BB7.2. Only B*51:01:01:01 reacts with Bw4. Both B*07:02:01 and C*07:02:01:03 react with Bw6, although B*07:02:01 is expected to contribute the majority of the staining, since HLA-B is expressed at 6-fold higher levels than HLA-C[54]. (B) Representative flow cytometry plots (n=3 independent replicates from a single donor) from CD4^{+} T cells infected with Nef-deleted 454-Gag-GFP for 48 hours, treated with 0.5nM CMA for 24 hours, and stained with monoclonal antibodies to Bw4 (B*51:01) and Bw6 (B*07:02), and monoclonal antibody BB7.2 (HLA-A*02:01). Blue histograms are from GFP^{-} cells, red histograms are from infected GFP^{+} cells. (C) Summary graph of data from B and Fig. 3.5D plotting the HLA-A*02 MFI normalized to that in uninfected cells treated with solvent control. Data are from independent experiments with 3 donors for 454-Gag-GFP, 2 donors for 454-Gag-GFP-ΔNef.

---

[21] Zimmerman GE and Olson E contributed to Fig. 3.S12.

CHAPTER 4

Discussion and Future Directions

The findings presented in Chapters 2 and 3 represent meaningful advances in both arms of the "shock and kill" approach to an HIV cure. In order for this approach to be successful, the shock will need to potently reactivate every replication-competent provirus in every cell in the body, including those found in a multitude of cell types residing in diverse tissues. While resting CD4$^+$ T cells likely make up the majority of the replication-competent reservoir, hematopoietic stem and progenitor cells (HSPCs) also harbor replication-competent proviruses in optimally-treated individuals, and these may contribute disproportionally to residual viremia during ART. Even if all proviruses from CD4$^+$ T cells were eliminated, replication-competent viruses residing in HSPCs could likely re-establish infection, and thus the latent reservoir in HSPCs represents a critical barrier to an HIV cure. Understanding the mechanisms regulating latency in HSPCs is essential to developing effective latency reversing therapies targeting this critical reservoir. The discoveries detailed in Chapter 2 begin to characterize which latency reversal agents (LRAs) may be capable of reactivating quiescent HSPCs and provide a path forward to identify mechanisms contributing to latency and latency reversal in quiescent primary cells.

In the event that a potent shock or sequential shocks successfully induce HIV gene expression in every cell harboring a replication-competent provirus, these cells need to

be rapidly killed before the latent reservoir can be reseeded. While most HIV-infected individuals generate effective anti-HIV cytotoxic T lymphocytes (CTLs), the expression of Nef in reactivated cells will protect some cells harboring HIV from even the most effective CTLs. Thus, in addition to strategies to enhance the breadth of the CTL repertoire and increase cytolytic functionality, pharmacologic inhibition of Nef may be an essential step in pursuit of the elimination of the latent HIV reservoir. The identification of concanamycin A (CMA) as a potent inhibitor of HIV Nef, detailed in Chapter 3, represents a critical first step in the development of kill-enhancing therapeutics.

Latent HIV in Quiescent HSPCs: Barrier to a Cure

HSPCs reside in the bone marrow in a quiescent state, where they are long-lived, capable of self-renewal, and give rise to daughter cells that will differentiate to maintain the entire hematopoietic system through the life of an individual[1,2]. Quiescence is a key feature of HPSCs and other cells that comprise the latent reservoir of HIV, such as resting CD4^{+} T cells[3-5]. Thus, latency reversing agents (LRAs) will need to be effective in quiescent cells to achieve meaningful reactivation *in vivo*. Despite the urgent need, no *in vitro* models were known to keep primary cells in a quiescent state that maintained susceptibility to HIV infection or promoted HIV latency, as HIV infection of T cells *in vitro* requires that they be activated at the time of infection[4,6,7]. Chapter 2 described the simultaneous discovery that hypothermia, established by culturing cells at 30°C instead of 37°C, and pharmacologic inhibition of HSP90 by 17-AAG were both able to induce quiescence in HSPCs. Quiescence was associated with decreased proliferation based

on dilution of a membrane dye, decreased expansion of cells in culture, halted

differentiation to less stem-like progenitors, and enrichment in the G_0/G_1 phase of the cell

cycle.
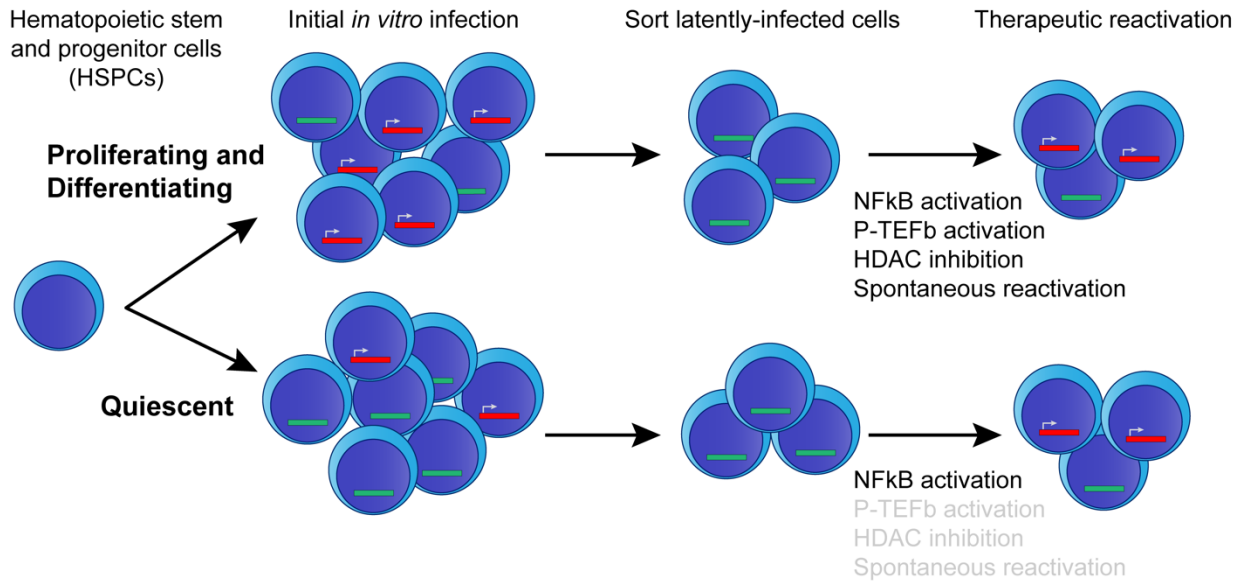
Fig. 4.1: Summary diagram of results presented in Chapter 2. Blue cells represent a heterogenous population of cord blood-derived hematopoietic stem and progenitor cells (HSPCs). HSPCs can be cultured in two states, proliferating and differentiating or quiescent. Quiescent cells preferentially establish latent infections, and these latent infections are resistant to spontaneous reactivation and reactivation by HDAC inhibitors and P-TEFb activators. *Red* represents a transcriptionally active provirus; *green* represents a transcriptionally silent latent provirus. Grey text represents mechanisms that are inefficient for reactivation.

Importantly, we observed that quiescent HSPCs remained susceptible to HIV

infection, and that infection of quiescent cells with HIV was significantly skewed to favor

latent rather than active infection, whereas HSPCs that were actively proliferating and

differentiating were significantly more likely to harbor transcriptionally-active HIV

proviruses. Furthermore, latent proviruses under quiescent conditions were significantly

less likely to reactivate spontaneously during extended culture periods, indicating that

latency was maintained and not simply the result of delayed kinetics of active infection at

the reduced temperature. Latent HIV proviruses in quiescent HSPCs were, however,

inducible following TNFα stimulation, which acts by potently activating NFκB to induce transcription at the promoter in the HIV 5' LTR. Taken together, the findings described in Chapter 2 represent a significant advance to the study of HIV latency, providing an *in vitro* system where inducible post-integration latency is established in quiescent primary cells (Fig. 4.1).

One key aspect of this experiment setup is the addition of raltegravir after removing actively infected cells, which ensures that all subsequent investigations of latent provirus represent true post-integration latency rather than delayed integration or transcription from labile, unintegrated forms of the HIV genomic DNA. The experimental approach also uses a single-round infection with a defective reporter virus for which fluorescence of GFP is used as the readout for active infection, ensuring that cells that are deemed to be actively infected have sufficient RNA expression to produce viral proteins. This increases the likelihood that sufficient virus-derived epitopes to trigger CTL-mediated clearance are present in the cells that are deemed to be actively infected based on GFP expression.

All models have limitations and it is impossible to know in advance whether the findings in the model system will translate to the clinical setting. Nevertheless, this model offers reasonable hope of being valuable due to the preferential establishment and maintenance of latency in quiescent primary cells, with particular focus on an under-studied reservoir that exists in a quiescent state *in vivo*. The development of this model system to study the dynamics of HIV latency in quiescent HSPCs enabled us to begin making fundamental observations about the nature of latency and latency reversal in these cells. One initial observation was that, in quiescent HSPCs, loss of stemness was associated with a higher frequency of spontaneous reactivation from latency. Thus, we

concluded that differentiation into increasingly more lineage-committed cell types could correlate with reactivation from latency.

This points to the hypothesis that a long-lived, quiescent, stem-like progenitor cell could be infected with HIV, establish a latent infection, and maintain it in a transcriptionally-silent state for decades. As a cell undergoes asymmetric cell division, daughter cells that maintain stemness will remain in a quiescent state, associated with stable and enduring latency. The presence of daughter cells that differentiate into increasingly lineage-committed progenitors, however, could lead to reactivation of a clonal provirus. As opposed to terminally-differentiated resting memory T cells, this provides a mechanism by which the HSPC reservoir can spontaneously and continuously contribute to residual and rebound viremia. While this is unlikely to be the sole source of viremia during ART or ART interruption due to the low proportion of infected HSPCs[8], Zaikos et al. demonstrated that plasma virus during ART is disproportionally identical to HSPC-derived provirus[9]. Taken together, recent *in vivo* studies and the results obtained from the *in vitro* model described in Chapter 2 support a model where HSPCs are a long-lived reservoir of HIV capable of contributing to the clonal expansion of replication-competent HIV as well as residual viremia during ART.

Another interesting aspect of the studies described in Chapter 2 was the observation that the relationship between HIV proviral latency and quiescence is an ongoing process, requiring the active maintenance of the quiescent state. HIV latency could be regulated at two levels: establishment and maintenance. Upon integration, the provirus may immediately enter a transcriptionally-silent latent state, as is observed in HSPCs in Chapter 2, or could actively transcribe HIV genes initially before becoming

latent, as is observed in some T cell models of latency[4,6,7]. This initial fate decision can be described as the establishment of latency. The maintenance of latency, however, could be a dynamic and active process, or a semi-permanent result of the events that occur at establishment. For instance, if quiescent cells show an integration site bias for HIV, where the chromosomal location of integration is permanently unlikely to result in activation of the viral promoter, this would be regulated primarily at the time of latency establishment.

We infected HSPCs in a quiescent or proliferating state with HIV, removed actively infected cells, and prevented new integrations with raltegravir. Thus, we were studying only post-integration latent proviruses in each cellular state. We subsequently maintained some of the cells in their original state while switching others to the alternative. We observed that the frequency with which HIV proviruses reactivate spontaneously was determined by the current state of the cell rather than the state of the cell at the time of integration. These findings were confirmed whether quiescence was induced via hypothermia or inhibition of HSP90. Thus, the increased frequency of latent HIV infection in quiescent cells is not the result of differences in integration site or other factors established at the time of integration, but rather is an active and dynamic interplay between the provirus and the cellular state. We did not investigate the possibility that inducing cellular quiescence could cause an actively infected cell to revert to latency, but did demonstrate that inducing quiescence can cause latent proviruses to enter a more stable form of latency with a low likelihood of spontaneous reactivation, and that exiting the quiescent state causes formerly-stable latent proviruses to spontaneously reactivate at a high frequency. This has direct ramifications for targeting HIV proviruses in quiescent

cells *in vivo*, which are unlikely to exit the quiescent state and therefore represent long-lived, stable latent reservoirs.

With the goal of determining whether leading LRAs could stimulate reactivation of latent proviruses in quiescent cells, we tested a panel of common drugs capable of inducing HIV gene expression in T cell models of latency. TNFα was used as a positive control, as robust reactivation was observed in both quiescent and proliferating cells following TNFα stimulation. The PKC agonist bryostatin-1 was able to reactivate an equivalent proportion of the inducible latent reservoir in both proliferating and quiescent HSPCs, suggesting that the susceptibility of a latent provirus to NFκB stimulation is not altered by the cellular state. Alternatively, while the histone deacetylase (HDAC) inhibitors vorinostat and romidepsin and the P-TEFb activator HMBA were able to reactivate a portion of the inducible latent HIV in proliferating HSPCs, these were significantly less effective in quiescent HSPCs. This was not a result of the drugs being inactive at lower temperatures, as they were able to synergize with bryostatin at 30°C, and vorinostat led to histone acetylation with the same magnitude and kinetics in HSPCs at 37°C and 30°C.

Similar to what was observed for spontaneous reactivation from latency, sensitivity to LRAs was determined by the current state of the cell rather than the state at the time of integration. Proviruses that were established in a latent state at 37°C were susceptible to reactivation by HDAC inhibitors or HMBA at 37°C but not at 30°C or in the presence of 17-AAG, and proviruses that were established at 30°C were susceptible to HDAC inhibitors or HMBA if they were reactivated at 37°C. These findings confirm that the susceptibility to reactivation following treatment with a given LRA is reversible, related to the current cellular state, and is not permanently established at the time of integration. A

provirus may be rendered more or less susceptible to a given stimulus as the cell harboring that provirus exits or enters a quiescent state, further validating the need for LRAs or combinations of LRAs that can broadly induce HIV gene expression, particularly in quiescent primary cells. The model system described in Chapter 2 enables more informative testing of latency reversing agents *in vitro* by establishing a higher threshold for reactivation that is associated with quiescence in primary cells, representing the state of many cells that make up the latent HIV reservoir *in vivo*. In fact, the susceptibility to various LRAs observed in quiescent HSPCs closely resembles that for the Greene and Planelles models of HIV latency, which use T cells maintained in a relatively quiescent state, while other models respond to LRAs in a manner that is more similar to proliferating HSPCs[7].

In addition to its utility for testing the efficacy of proposed LRAs or LRA combinations in quiescent primary cells, the model described in Chapter 2 will also be useful to understand the precise mechanisms regulating HIV latency in quiescent cells. We were able to determine that quiescent HSPCs are more likely to establish latent infections, less likely to spontaneously reactivate from latency, and were less susceptible to reactivation in response to certain stimuli. Understanding the cellular mechanisms regulating these effects could inform the development of targeted latency reversing approaches in the future. We began by taking a hypothesis-driven approach to interrogate possible mechanisms influencing HIV gene expression in quiescent HSPCs.

First, since both TNFα and bryostatin could reactivate quiescent HSPCs, we hypothesized that these cells may have a deficiency in NFκB expression or activation relative to their proliferating counterparts. Yet we failed to detect any differences in the

abundance of NFκB p65 in either the cytoplasm or the nucleus of quiescent HSPCs when compared to proliferating HSPCs. Furthermore, the steady-state level of activated NFκB capable of binding to DNA, which represents the pool of NFκB capable of driving transcription, was identical in quiescent and proliferating HSPCs, as was the induction of activated NFκB following TNFα stimulation. We also assessed the translocation of NFκB to the nucleus following TNFα stimulation as determined by ImageStream analysis and found no defect in quiescent HSPCs. Thus, while robust NFκB activation is able to overcome the restrictions on HIV gene expression in a portion of quiescent cells, a deficiency in NFκB is not responsible for the association between quiescence and latency. This could be explained by robust NFκB activation compensating for a deficiency in a different activating factor, overcoming the activity of a repressive factor, or overcoming a chromatin environment that is generally unfavorable to transcription.

The fact that HMBA was unable to induce reactivation led to the hypothesis that steady-state levels of P-TEFb may be low in quiescent HSPCs, as HMBA cannot stimulate P-TEFb activity if it is not present in the cell. Levels of cyclin T1 and an activating phosphorylated form of CDK9 in both the cytoplasm and the nucleus, however, were unchanged when comparing quiescent and proliferating HSPCs. With deficiencies in NFκB and P-TEFb failing to explain the association between quiescence and latency, we considered the possibility that quiescence induced by hypothermia was causing broader defects in the expression of cellular or viral genes. This system allowed us to take advantage of the fact that GFP is expressed in the *env* open reading frame, and thus GFP fluorescence intensity is a proxy for HIV protein production. Within the GFP+ subset of cells, there was no decrease in GFP MFI in quiescent cells, either in the context of initial

217

active infection or upon latency reversal. This observation suggests that the effect on viral gene expression in quiescent cells is strictly limited to the likelihood that a given provirus is transcribed, but does not alter the level of expression from proviruses that do become activated.

We also quantified GAPDH protein expression per cell equivalent and observed no deficiency of GAPDH expression at 30°C. Furthermore, in qPCR experiments on cell-associated RNA from HSPCs, we observed no deficiency of Pol2a mRNA expression at 30°C. Throughout the study, TNFα was capable of inducing GFP expression and NFκB activation at 30°C in the same time frame as at 37°C, suggesting *de novo* transcription and translation of GFP and NFκB activation pathways are not delayed at 30°C. Even more, vorinostat induced histone acetylation with the same kinetics and to the same extent at 30°C as 37°C, demonstrating that protein modification is not delayed at 30°C. Taken together, these results demonstrate that mRNA transcription and protein translation and turnover are not reduced at 30°C in HSPCs, and broad effects on viral and host gene expression do not appear to explain the relationship between quiescence and latency.

Some studies have suggested that HIV latency is almost exclusively a product of stochastic activation of a Tat-driven positive feedback loop. Expression of HIV gene products is inefficient in the absence of Tat, yet Tat itself is an HIV gene product with Tat-dependent transcription. Thus, initial activation of the HIV promoter requires a low-level expression of Tat that can subsequently facilitate high levels of expression for all of the viral genes[10,11]. If this framework is taken as a hypothesis to explain the relationship between quiescence and latency, the expectation would be that quiescent cells have

broadly lower levels of transcription, and thus are less likely to stochastically express sufficient levels of Tat to establish an active infection. This hypothesis aligns in an intriguing way with the observation that latent proviruses in proliferating HSPCs are significantly more likely to reactivate spontaneously in the absence of additional stimuli when compared to those in quiescent HSPCs. The evidence thus far does not support the hypothesis that quiescent cells have lower transcriptional activity, however, as quiescent and proliferating HSPCs produce virus-derived GFP with the same magnitude and kinetics and show the same steady-state levels of host RNA and proteins. A model based exclusively on the likelihood of stochastic Tat activation also fails to account for the differential sensitivity of proviruses in quiescent and proliferating HSPCs to HDAC inhibitors and HMBA. In summary, though the importance of the stochastic Tat mechanism has not been disproven in the model described in Chapter 2, it is unlikely to be the sole contributor to the observed relationship between quiescence and latency.

Future directions: mechanisms regulating latency in quiescent cells

Although clear mechanistic answers have thus far remained elusive, this model of HIV latency in both proliferating and quiescent HSPCs will enable us to interrogate four critical questions about the mechanisms regulating HIV latency: 1) Why do some cells in a given state, either proliferating or quiescent, establish active infections while other cells establish latent infections? 2) Why are some cells in a given state, either proliferating or quiescent, responsive to a given LRA while others are unresponsive? 3) Why are quiescent cells particularly likely to establish latent infections? 4) Why are HIV proviruses in quiescent cells responsive to a narrow range of stimuli? Within each of these questions,

the effects of differentiation and loss of stemness on HIV latency in a heterogenous pool of progenitor cells is also of interest.

Four potential mechanistic categories could be contributing to or solely responsible for explaining the divergent outcomes for proviruses at the levels articulated in each of those four questions (Fig. 4.2). First, it is possible that cells harboring proviruses that become activated possess an activating factor that is lacking in cells that harbor proviruses that remain transcriptionally silent. This difference could manifest at the level of the transcription or translation of the activating factor, or through post-translational modifications rendering the factor more active in cells with active HIV or less active in cells with latent HIV. Second, the same could be said about the existence of a negative factor that suppresses gene expression from the HIV promoter. Third, genome-wide epigenetic differences affecting chromatin accessibility could influence the efficiency of HIV gene expression, either through changes in activating or suppressive epigenetic modifications of histones or DNA. Lastly, epigenetic differences specific to the HIV 5' LTR or the region of HIV integration could specifically enhance or repress the transcription of HIV genes.
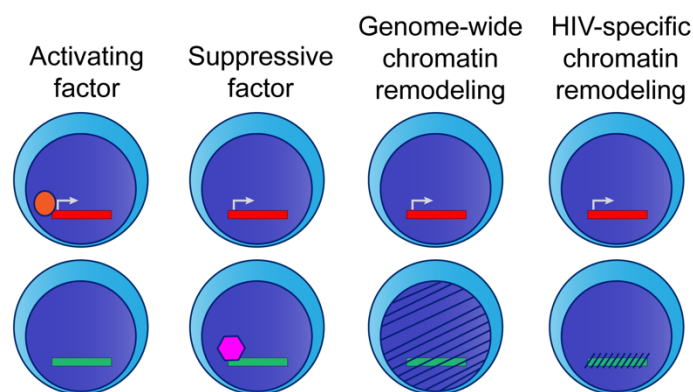
Fig. 4.2: Diagram of possible mechanisms contributing to HIV latency in quiescent cells. *Red* represents a transcriptionally active provirus; *green* represents a transcriptionally silent latent provirus.

With the failure to elucidate the mechanisms behind any of these questions using bulk analyses testing specific hypotheses, the need for unbiased approaches with single-cell resolution has become abundantly clear. HSPCs isolated from cord blood and cultured as described in Chapter 2 yield a heterogenous population of progenitor cells. While this heterogeneity can obscure population-level analyses, approaches with single-cell resolution can leverage the existing heterogeneity to identify parameters associated with divergent outcomes, in this case transcriptional activation or silencing of the HIV promoter.

Future directions: single-cell transcriptomic and epigenomic approaches

Single-cell RNA sequencing (scRNA-seq) and single-cell assay for transposase-accessible chromatin sequencing (scATAC-seq) can together provide transcriptomic and epigenomic data with single-cell resolution. In collaboration with Maria Virgilio and members of Joshua Welch's lab, in particular Chen Li, we have begun to perform scRNA-seq and scATAC-seq experiments on proliferating and quiescent HSPCs infected with HIV. A critical technical advancement enabling these studies was the development of a dual-reporter HIV construct by Valeri Terry. Named VT1, this construct expresses GFP driven by the constitutive promoter from spleen focus-forming virus and mCherry driven from the promoter in the HIV 5' LTR. With this construct, we are able to isolate pure populations of both latently infected and actively infected cells, which was not possible in the experiments described in Chapter 2. The use of VT1 significantly improves the ability to accurately interrogate the mechanisms driving HIV latency by enabling single-cell analysis of definitive populations of actively- and latently infected cells.

Our aim is to use single-cell transcriptomic and epigenomic data from purified actively- and latently infected primary HSPCs in both quiescent and proliferating cells for unbiased approaches to identify parameters associated with HIV latency. The general experimental setup is presented in Fig. 4.3. Quiescent and proliferating HSPCs will be infected with VT1, pure populations of actively- and latently infected cells will be isolated, and scRNA-seq and scATAC-seq will be performed. Since the transcriptomic data can be used to identify cells expressing HIV RNA, we elected to pool actively- and latently infected cells 1:1 as a cost-saving measure, while performing scATAC-seq on pure samples of either actively- or latently infected cells. From this experiment we will obtain epigenomic data from proliferating cells with active infections, proliferating cells with latent infections, quiescent cells with active infections, and quiescent cells with latent infections. We will also have transcriptomic data for a sample of 50% actively- and 50% latently infected cells for both quiescent and proliferating HSPCs, which can be segregated *in silico* into the same four populations based on HIV RNA expression.

These data will be analyzed with a priority on identifying differences that correlate with the likelihood that a cell harbors an active or latent provirus. In addition to looking at the expression of single host genes, we will also identify gene expression patterns characteristic of the activity of known transcription factors or signaling pathways. Mechanisms identified by the unbiased approaches described here will have to be tested directly for their influence on latency in HSPCs through knockout and overexpression experiments, and pharmacologic stimulation or inhibition where possible.
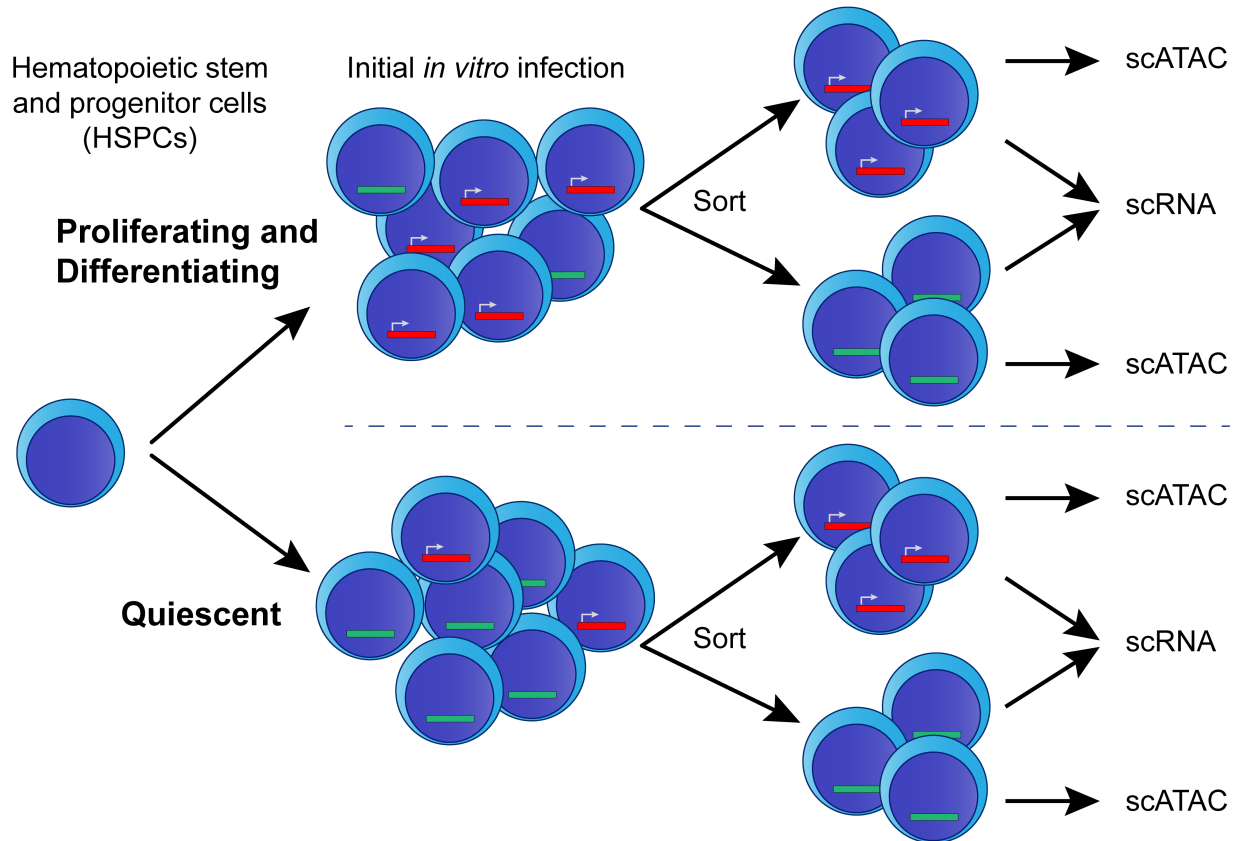
Fig. 4.3: Summary diagram of future directions for sc-RNAseq and sc-ATACseq. Blue cells represent a heterogenous population of cord blood-derived hematopoietic stem and progenitor cells (HSPCs). HSPCs can be cultured in two states, proliferating and differentiating or quiescent. Quiescent cells preferentially establish latent infections, but pure populations of both actively- and latently infected cells can be isolated using the novel dual-reporter virus VT1. These populations can be pooled at a 1:1 ratio for scRNA-seq, as transcriptomic data will enable them to be distinguished, while ATAC-seq samples are kept pure. *Red* represents a transcriptionally active provirus; *green* represents a transcriptionally silent latent provirus.

Given the heterogeneity of the HSPC population and the observation that differentiation correlates with reactivation from latency, as described in Chapter 2, cells will likely cluster by transcriptomic and epigenomic profiles according to their differentiation state, and some of these clusters will be more or less associated with HIV latency. Indeed, preliminary observations support this hypothesis. This allows for multi-layered analysis of the data to identify key differences regulating HIV gene expression. First, if cells of a certain profile are strongly enriched for latency or active infection, the

parameters that most clearly define that cluster of cells from the rest of the heterogeneous population are likely to contain clues about mechanisms regulating latency in HSPCs. Furthermore, even if a certain profile is enriched for latent infections, there will likely be some similar cells that harbor a transcriptionally-active provirus. The differences between otherwise similar cells that differentiate between active and latent cells will be another key point of comparison to identify possibly latency-regulating aspects of the host cell biology. Thus, both inter- and intra-cluster differences are likely to provide critical information toward the identification of the mechanism or mechanisms regulating latency in quiescent HSPCs.

Actively infected cells express high levels of viral RNA and thus, in time, produce high levels of the viral proteins. Expression of viral proteins is necessary for reactivation of sufficient magnitude to drive killing and is thus essential to the success of a shock and kill strategy. For this reason, it is generally a strength of our studies that we use fluorescent protein expression as a readout for active infection or reactivation, as these fluorescent proteins are expressed from the viral promoter and likely represent high-level production of the other viral proteins as well. The experiments described in Chapter 3 support this understanding, as expression of GFP or PLAP reporter genes is universally associated with downregulation of MHC-I and CD4 from the cell surface, hallmarks of Nef activity. Latently infected cells, on the other hand, do not express viral proteins. Thus, in addition to whatever differences caused a cell to actively transcribe HIV genes, many differences associated with the activities of the HIV proteins themselves will be different in actively- and latently infected cells. This represents a major obstacle to the successful identification of mechanisms responsible for the activation or silencing of the HIV

promoter, as many of the differences identified from the analyses described above will be consequences of HIV protein expression rather than causes that preceded the expression of HIV genes. Without a way to distinguish causes from consequences of HIV expression, time and resources will be spent exploring mechanisms with no veritable relationship to latency.

A key preliminary result sheds light on previously enigmatic results described in Chapter 2 and may offer a path forward to resolve this problem. In Chapter 2, when proliferating cells infected at 37°C harboring latent proviruses were transferred to 30°C or treated with 17-AAG, inducing quiescence, the frequency of spontaneous reactivation from latency was suppressed. However, the frequency was not suppressed to the levels of latent proviruses from cells that had always been kept in a quiescent state at 30°C, instead producing an intermediate phenotype. This was perplexing, especially given the result that responsiveness to LRAs was not intermediate, but instead completely mirrored cells that had been at 30°C from the time of infection. Surprisingly, when we analyzed the scRNA-seq results from HSPCs at 37°C, which had been sorted by FACS and re-pooled to have 50% actively- and 50% latently infected cells based on HIV protein expression as reported by mCherry, we observed that over 50% of the cells were expressing HIV transcripts. A similar result was not observed at 30°C, where cells have a low frequency of spontaneous reactivation.

Although this observation needs to be repeated in an experiment where the submitted samples are analyzed to confirm 50% expression of mCherry protein, these preliminary results lead me to hypothesize that, since the frequency of spontaneous reactivation is high at 37°C, a proportion of the population of cells is always in the state

of having been recently reactivated and thus having produced HIV RNA but not yet having translated large quantities of HIV proteins. This could explain the intermediate suppression of spontaneous reactivation when switching cells to a quiescent state, as a portion of those GFP-negative cells were already transcribing the HIV genes at the time of the switch and could not be suppressed. These cells appeared latent, as they were not yet expressing sufficient levels of GFP protein to be detected by flow cytometry, but were in fact actively infected at the time of the sort. Thus, the switch to the quiescent state likely halted all *de novo* reactivation but did not halt the expression of viral proteins from already-reactivated cells.

This hypothesis could be tested by repeating the experiments in Chapter 2 that yielded intermediate effects on spontaneous reactivation, but sorting again for GFP⁻ cells after an additional 24 hours. After the sort, cells that had spent the previous 24 hours in a quiescent state could be returned to the same culture conditions as before, either 30°C or in the presence of 17-AAG. If this hypothesis is correct, the frequency of spontaneous reactivation will now match the low frequency observed in cells that have always been at 30°C, as any cells that had been transcriptionally activated at 37°C would by now be sorted away.

Should this hypothesis prove true, the implications for attempts at distinguishing between consequences and causes of HIV reactivation are substantial. In our preliminary experiments, we observed a greater-than-expected ratio of active:latent proviruses at the level of HIV RNA expression when compared to what was observed by measuring HIV protein expression. This would imply that some cells that are negative for HIV proteins, and thus not experiencing the multitude of consequences that result from the activity of

these proteins, are indeed actively transcribing HIV RNA. The existence of these cells would resolve the major obstacle described above. Comparing HIV RNA-positive, protein-negative cells to HIV RNA-negative cells eliminates the confounding differences that are consequences of HIV protein expression and focuses solely on the differences in the host cell that may be regulating HIV gene expression. If we avoid re-pooling cells after sorting, we will yield three populations of interest: RNA$^+$protein$^+$ (actively infected), RNA$^+$protein$^-$ (recently reactivated), and RNA$^-$protein$^-$ (latently infected). Since our goal is to identify the differences responsible for the initial activation of HIV expression, the comparison most likely to reveal the key parameters is between recently reactivated and latently infected cells. That said, it could also be informative to identify features that are shared between actively infected and recently reactivated cells, but different from latently infected cells, so long as the expression of HIV proteins does not interfere with the mechanisms that initially led to reactivation.

While these studies are of great interest and will likely be useful to identify the mechanisms regulating latency in the quiescent primary cell model described in Chapter 2, several further questions will remain. Should we succeed in identifying the mechanisms regulating latency in the *in vitro* system, it will be of great interest to determine whether these mechanisms may be contributing to latency in HSPCs *in vivo*. For instance, if the absence of an activating factor seems critical for maintaining the latent state, it would be important to determine the level of expression and activation of that factor in HSPCs in the bone marrow. Furthermore, though the latent reservoir of HIV in HSPCs is likely to be important to persistence and will need to be eliminated for the success of a shock and kill cure strategy, the primary reservoir of latent HIV resides in quiescent, resting CD4$^+$ T

cells. Thus, it will also be of great interest to determine whether the mechanisms regulating latency in our *in vitro* model of quiescent primary cells are also involved in regulating latency in quiescent CD4$^+$ T cells *in vivo*.

Lastly, should the mechanisms regulating latency in quiescent cells be identified, there will be great interest in designing therapeutics aimed at reactivating latent proviruses by targeting these mechanisms. The model system describe in Chapter 2 will be a vital resource in testing possible targeted LRAs in quiescent primary cells. The results in Chapter 2 demonstrate that HIV expression can be induced in quiescent cells in this model by a narrower panel of stimuli compared to proliferating cells. Notably, combination therapies of bryostatin, which is effective in quiescent cells, with agents that did not induce reactivation independently, such as HDAC inhibitors and HMBA, resulted in robust reactivation greater than bryostatin alone. Thus, in addition to single targeted therapies aimed at counteracting the mechanisms maintaining latency in quiescent cells, combination therapies should be considered to achieve maximal reactivation in the broadest possible range of cells that make up the heterogeneous reservoir of HIV *in vivo*.

The Role of CTLs in Reservoir Clearance: Open Questions

In the event that the approaches described above successfully identify therapeutic approaches capable of achieving robust and broad reactivation of the latent reservoir of HIV, this will only guarantee one branch of the shock and kill approach to an HIV cure. Upon reactivation from latency, cells harboring reactivated provirus need to be killed before they can proliferate, leading to clonal expansion of the provirus and/or return to

latency, potentially as a result of the host cell returning to a more quiescent state. This is particularly pertinent, given that the estimated half-life of HIV-infected cells *in vivo* is approximately 2 days[12-14], but activated T cells can proliferate in as little as 6-8 hours[15-17]. Thus, proliferation and clonal expansion of the virus may theoretically outpace decay in some circumstances in the absence of efficient killing mechanisms that reduce the half-life of HIV-infected cells.

HIV-specific CTLs are the effectors of the adaptive immune system most responsible for the clearance of virus-infected cells. Robust CTL responses are induced early in HIV infection[18-20] and exert notable selective pressures on the virus[21-23], though they are not sufficient to control the infection in the vast majority of individuals[19,20]. With antiretroviral therapy suppressing viral replication, however, effective anti-HIV CTLs may play a key role in clearing reactivated viral reservoirs as part of a shock and kill strategy to cure HIV.   The efficacy of anti-HIV CTLs on clearance of the reactivated HIV reservoir is an area of ongoing investigation. A recent study from Huang et al. demonstrated that cells harboring replication-competent latent HIV proviruses are intrinsically less susceptible to CTL killing[24]. This study aimed to explore the capacity of a patient's CTLs to eliminate their autologous latent reservoir of HIV in an *ex vivo* co-culture system known as the HIV eradication (HIVE) assay, in which the replication-competent reservoir is measured by a quantitative viral outgrown assay. Using the HIVE assay in donors whose latent virus did not possess mutations to escape their immunodominant CTL responses, they observed that co-culture of CD8+ T cells with *ex vivo* CD4+ T cells stimulated with potent LRAs resulted in a reduction in HIV proviral DNA, but no reduction in the inducible replication-competent reservoir. This was observed despite the fact that the CTLs were

capable of killing autologous CD4^{+} T cells infected *in vitro* with the exact virus that emerged in the HIVE assays. Thus, the cells harboring latent provirus *in vivo* appear to be intrinsically resistant to CTL killing.

The authors discuss two possible mechanisms that could contribute to these observations. First, it is known that CTLs exert selective pressures that shape the HIV proviral reservoir, suggesting that the cells harboring provirus have already undergone selection for those cells that are most resistant to CTL-mediated clearance[21,24]. This hypothesis is supported by other recent findings focused on the expression of the anti-apoptotic factor BCL-2. In two independent studies, Cummins et al. demonstrated that BCL-2 expression protects HIV-infected CD4^{+} T cells from the cytopathic effects of infection, and that antagonism of BCL-2 reduces HIV persistence *in vitro*[25,26]. By performing transcriptomic profiling of the peptide-pulsed *ex vivo* CD4^{+} T cells that evaded CTL killing in a co-culture assay, Ren et al. identified BCL-2 overexpression as being associated with survival[27]. They proceeded to show that HIV-specific CTLs preferentially eliminate BCL-2^{low} cells, and that replication-competent HIV proviruses are enriched in BLC-2^{high} cells *ex vivo*. The BCL-2 antagonist ABT-199 was unable to drive reductions in the intact reservoir *ex vivo*, even in combination with the potent LRA bryostatin, although this combination did lead to reservoir reduction in an *in vitro* latency model, as observed by Cummins et al. However, when co-cultured with CTLs, ABT-199 and bryostatin led to a modest reduction in the inducible reservoir of HIV, which was more striking when bryostatin was replaced by potent T cell activating stimulation using anti-CD3/CD28 antibodies. This study demonstrates that BCL-2 is one barrier to the CTL-mediated clearance of cells harboring the latent reservoir of HIV after reactivation, although even

potent reactivation and BCL-2 antagonism did not overcome every obstacle to clearance. This indicates that other mechanisms likely contribute as well, possibly including Nef-mediated downregulation of MHC-I.

Importantly, Ren et al. demonstrated that the efficiency with which CTLs eliminate the reactivated reservoir of HIV is dependent on the LRA used to induce reactivation. Robust reactivation resulting in antigen presentation sufficient to induce detectable CTL-mediated clearance generally requires the use of agents that cause T cell activation, such as bryostatin, PMA and ionomycin, or anti-CD3/CD28[24,27]. HDAC inhibitors, while failing to induce high levels of HIV gene expression, also have suppressive effects on CTL function. HDAC inhibitors were shown to reduce IFNγ production and impair the cytolytic functions of CTLs, reducing their ability to successfully eliminate cells harboring reactivated HIV provirus[28]. Furthermore, HDAC inhibitors were shown to induce HIV gene expression, but did not generate spliced HIV transcripts or promote expression of HIV proteins, and thus did not lead to an increase in virus production[29]. As expected, the lack of splicing and virion production was associated with a lack of antigen presentation, as cells reactivated with HDAC inhibitors failed to induce degranulation from HIV-specific CTLs. This finding is in line with our observations in quiescent HSPCs, in which HDAC inhibitors fail to induce GFP expression, which would be produced from the singly-spliced *env* transcript. In combination with the negative effects of HDAC inhibitors on CTL function, the use of these agents to achieve reactivation may directly prevent successfully killing of cells harboring reactivated provirus.

Jones et al. investigated a wide panel of single agents to determine their ability to promote degranulation of HIV-specific CTLs, a readout of successful antigen

231

presentation. This study determined that HDAC inhibitors and HMBA failed to induce HIV-specific CTL activation, consistent once again with our findings that these agents do not induce potent reactivation and HIV protein expression in quiescent HSPCs[30]. Alternatively, they observed that reactivation using PKC agonists can induce CTL responses. However, a very recent report shows that reactivation using PKC agonists, such as bryostatin, increases the activity of BCL-2 and protects reactivated cells from elimination[31], and thus these agents may need to be used in combination with BCL-2 inhibitors. In addition to PKC inhibitors, Jones et al., determined that IL-15, IL-15 superagonists such as ALT-803, IL-2, a TLR2-ligand could also reactivate latent proviruses and promote CTL recognition of cells harboring reactivated provirus. They focused particularly on ALT-803, which did not induce T cell activation, did induce HIV RNA expression, and was able to promote modest clearance of HIV-infected cells in CTL co-cultures[30]. The modest nature of CTL clearance of reactivated reservoirs may reflect the presence of Nef, as higher expression of viral proteins and subsequent presentation of abundant viral peptide antigens will be accompanied by higher expression of HIV Nef and greater reductions in cell-surface MHC-I. In the absence of therapies to counteract Nef, other approaches are being investigated to enhance CTL responsiveness to HIV-infected cells. Priming CTLs prior to reactivation has also been shown to enhance clearance of reactivated reservoirs *in vitro*, indicating that vaccination strategies to prime HIV-specific CTLs in patients prior to shock may aid in reservoir clearance[32], although inhibition of Nef would also likely be beneficial in restoring antigen presentation to these primed CTLs.

In contrast to the doubts about the efficiency of CTL-mediated clearance of reactivated HIV reservoirs, CD8^{+} T cells are known to be important in the control of SIV infection and the maintenance of undetectable viral loads during antiretroviral therapy in SIV models[33-36]. Antibody-mediated depletion of CD8^{+} T cells leads to rebound viremia even if ART is maintained, suggesting that the ongoing activity of CD8^{+} T cells is essential even for the efficacy of ART[37,38]. However, two independent studies used mathematical modeling of plasma viral decay upon re-initiation of ART to assess the lifespan of HIV-infected cells, and saw no increase in lifespan when CD8^{+} T cells were depleted[39,40]. The authors and many in the field have taken this to indicate that the cytolytic activities of CD8^{+} T cells are not responsible for exerting control over HIV and SIV, but rather other, non-cytolytic functions. This is supported by the well-characterized observation that CD8^{+} T cells exert a suppressive effect on HIV replication *in vivo* and *in vitro* independent of cytolytic functions, though the specific mechanism by which this occurs has remained elusive[41-49].

However, an alternative interpretation of the observation that the lifespan of virus-producing cells is not reduced by the presence of CD8^{+} T cells is that by the time a cell is producing virus, it is protected from CTL killing, likely through the activity of some viral gene product. In this hypothesis, cytolytic functions of CD8^{+} T cells are important for the clearance of a portion of HIV-infected cells before infection has proceeded to the stage of virion production. Once sufficient viral gene expression to produce virus has been achieved, however, the virus is able to evade cytolytic responses by CTLs. The activity of the viral accessory protein Nef, which downregulates MHC-I in productively-infected cells, could explain this phenomenon. Indeed, Nef also downregulates CD4 from the cell

surface, and the majority of HIV virions are produced by CD4^{-} CD8^{-} T cells, indicating that Nef is already active and offering protection to virus-producing cells[50]. Of note, while they did not observe an increase in the lifespan of virus-producing cells after CD8^{+} T cell depletion, both studies observed a higher initial level of plasma virus, suggesting that more virus-producing cells were present at the time of ART-initiation in the absence of CD8^{+} T cells, and thus that CD8^{+} T cells may kill some HIV-infected cells prior to virion production[39,40]. In summary, it remains likely that the cytolytic activities of CD8^{+} T cells are important for eliminating some infected cells before they are able to produce virus, but subsequent protection by Nef allows virus-producing, CD4^{-} cells to evade CTL killing.

The Need for a Nef Inhibitor

Given that Nef has a multitude of functions that aid viral replication and persistence and many of the key resides of Nef are essential for several of these processes, the study of genetic mutants of Nef provides only limited understanding of the contributions of MHC-I downregulation to HIV fitness or reservoir dynamics. The existence of a potent inhibitor of HIV Nef would allow this alternative hypothesis to be tested directly. If true, Nef inhibition would lead to faster kinetics of viral load suppression upon ART initiation, reflecting a reduction in the lifespan of virus-producing cells that are no longer protected by Nef, and this effect would be dependent on the presence of CD8^{+} T cells.

B9 was identified as an inhibitor of Nef-mediated activation of Src-family kinases, although it also inhibited Src-family kinases in the absence of Nef, calling into question the conclusion that this activity is truly Nef-specific[51]. B9 was later shown to interfere with

dimerization of Nef and to bind directly to the dimerization interface, as the mutants at N126 abrogated B9 binding to Nef by surface plasmon resonance, and they demonstrated that these mutants at N126 were able to activate Src family kinases equivalently to wild-type Nef. Intriguingly, the authors neglected to perform the critical experiment demonstrating that these mutants, which do not bind B9, are not susceptible to B9-mediated inhibition of Src family kinase activation, an experiment that would have been exceedingly simple in the context of the other experiments that were performed. They went on to clearly demonstrate that B9 reduces Nef dimerization in cells, but do not correlate this with any functional activity of B9[51]. A recent paper showed small but statistically significant effects of B9 on CTL clearance and the authors claimed these effects were mediated through reversal of Nef-dependent MHC-I downregulation[52]. However, the authors failed to demonstrate restoration of MHC-I to the surface of Nef-expressing cells, a simple experiment that was dubious to exclude, and the CTL killing assays lacked a control without CTLs added, rendering any attribution of the effects of B9 to CTL-mediated killing impossible.

It has been proposed that Nef acts as a dimer to perform its various functions within host cells, but the requirement for dimerization in MHC-I and CD4 downregulation and enhanced viral replication was based on the impacts of mutations in the dimerization interface of Nef[53,54]. Crystal structures of Nef in complex with MHC-I, however, indicate Nef present as a monomer. Interestingly, the residues believed to be important for dimerization were making important contacts with residues on other proteins within the structure, supporting the hypothesis that previous experiments may have been overinterpreted in attributing the defects associated with mutations in these residues to

deficiencies in dimerization[55,56]. Moreover, the myristoylated form of Nef exists primarily as a monomer[57], and myristoylation is essential for all functions of Nef[58-61]. This brings clarity to the observation in Chapter 3 that B9 fails to restore MHC-I to the cell surface, as it is proposed to function as an inhibitor of Nef dimerization, which may not be involved in this process.

Alternatively, we were able to confirm the recent report that Lovastatin, which was not proposed to affect Nef dimerization, does restore MHC-I to the surface of Nef-expressing cells[62]. However, Lovastatin is over 1,000-fold less potent than CMA and requires supratherapeutic concentrations, acts with slower kinetics, and does not achieve comparable levels of MHC-I restoration. Thus, the discovery of concanamycin A (CMA) as a potent inhibitor of HIV Nef is a major development in the study of the effects of Nef on CTL-mediated clearance of HIV. Our evidence indicates that CMA is a selective inhibitor of MHC-I downregulation by Nef, as the lysosome remains functional and CD4 is internalized and degraded in a Nef-dependent manner.

Studies with CMA will be able to interrogate the importance of MHC-I downregulation to the survival of HIV-infected cells upon ART initiation, as described in the SIV models above[39,40]. Indeed, as detailed in Chapter 3, we confirmed previous studies and observed that Nef protects a significant portion of HIV-infected cells from CTL killing. Even though Nef was already highly-expressed in these cells, treatment with CMA restored killing and led to the elimination of virtually every HIV-infected cell. Thus, it is reasonable to predict that CMA could enhance the clearance of even hard-to-kill virus-producing cells that already express high levels of Nef, presuming functional CTLs recognizing autologous viral epitopes are present.

The notion that, due to the activity of Nef, HIV-infected cells are only susceptible to clearance by CTLs during a narrow window after the initiation of viral gene expression but before virion production has interesting implications for the dynamics of HIV persistence in lymph nodes, where the majority of HIV DNA and HIV RNA is found[63]. In particular, HIV RNA is detected in B cell follicles in both SIV and HIV infection, even during ART[64-66]. This points to the importance of T follicular helper cells (T_{FH}), which are the dominant T cell population in B cell follicles and are more susceptible than other CD4^{+} T cell subsets to HIV infection *in vitro*[67], as critical sources of the latent reservoir of HIV[68]. Ongoing RNA expression during ART causes T_{FH} to contribute disproportionately to residual viremia, similar to HSPCs[69,70]. The B cell follicle may represent a sanctuary for HIV, as only cells expressing CXCR5 enter the follicle, and thus few CTLs are present despite the relatively large number of cells expressing HIV RNA[71]. Elite controller monkeys with potent CTLs still show ongoing replication in T_{FH}[72], further confirming the inability of CTLs to control HIV in the follicle. Some CTLs do enter the follicle during SIV and HIV infection, although there is disagreement over whether these cells have a regulatory phenotype that suppresses anti-HIV responses[73] or have especially potent cytolytic function, which thus requires further investigation[74,75].

Nonetheless, the reservoir of HIV in T_{FH} represents an additional barrier to a cure, as CTL-based kill strategies will likely require cytolytic CXCR5^{+} CTLs to enter the follicle. The relative lack of CTLs in the B cell follicle may allow T_{FH} cells beginning to express HIV RNA sufficient time to express high levels of Nef and downregulate MHC-I before encountering an HIV-specific CTL. Interestingly, ALT-803, the IL-15 superagonist that reactivates latent HIV, was shown to enhance the proliferation and activation of CTLs and

increased their expression of CXCR5, leading them to accumulate in the B-cell follicle. This led to reductions in the number of SIV RNA$^+$ and DNA$^+$ cells in the lymph nodes of elite controller macaques treated with ALT-803. While SIV RNA was reduced, it was not eliminated, suggesting that other mechanisms, including possibly the expression of Nef, enable T$_{FH}$ cells to evade even potent CTL responses in elite controller monkeys. The discovery of CMA as the first potent inhibitor of HIV Nef will enable the exploration of the contributions of MHC-I downregulation to HIV persistence in lymph nodes.

The identification of CMA as a potent Nef inhibitor also makes it possible to determine the contributions of MHC-I downregulation by Nef to the observed inefficiency of CTL-mediated clearance of cells harboring induced HIV proviruses following latency reversing treatments[24,27]. While other mechanisms described above may contribute to these effects, such as off-target effects of the selected LRA[28-30] or the expression of the inhibitory molecule BCL-2[25,27], Nef could also play an important role. The use of CMA in HIVE assays is thus an area of intense interest moving forward, with the aim of determining the optimal combination therapy to simultaneously achieve potent reactivation with single or combinations of LRAs, such as ALT-803, and maximize CTL-mediated clearance, with CMA restoring antigen presentation and BCL-2 inhibitors, such as ABT-199, supporting apoptosis.

Concanamycin A (CMA): A Promising Lead Compound for Enhancing CTL-Mediated Clearance of HIV Reservoirs

As described in Chapter 3, we performed high-throughput screening of large libraries of small molecules and natural products with the goal of identifying potent inhibitors of HIV Nef that could restore MHC-I to the surface of Nef-expressing cells. The screen was designed to provide the greatest likelihood of identifying a *bona fide* Nef inhibitor, as hits emerging from the secondary screen would have demonstrated restoration of MHC-I in cells expressing Nef both from and adenoviral delivery vector and in the context of integrated HIV infection, eliminating compounds that would reduce Nef expression at the transcriptional level. The screen also guaranteed a minimal tolerability of any identified compounds in cells, as the cells would have to tolerate 16-hour exposure to the drug without losing the capacity to restore MHC-I to the cell surface.

After a library of known small-molecules yielded no hits, we established a collaboration with Dr. David Sherman's lab at the Life Sciences Institute. This allowed us access to their library of natural product extracts, among which we found 11 strains producing Nef inhibitors. The Nef inhibitory activity in several of these strains was attributed to a single family of molecules known as the plecomacrolide antibiotics. In response to this discovery, we tested a small panel of plecomacrolide family members, including several of the bafilomycins, which have a 16-member ring, and concanamycin A (CMA), which has an 18-member ring. Though the screen was performed in the CEM T cell line, which is a useful model of the activated CD4$^+$ T cells that are the primary targets of HIV infection, we proceeded to assess the efficacy of the plecomacrolides in primary CD4$^+$ T cells infected with HIV. While all of these compounds were able to inhibit Nef, CMA had the greatest potency, with an extremely low 50% effective concentration of 70pM.

While CMA was by far the most potent inhibitor of Nef ever described and the most potent in our panel, the goal of identifying a therapeutic Nef inhibitor requires not only potent anti-Nef activity, but also tolerability. Thus, we assessed the toxicity of plecomacrolide family members in primary human $CD4^+$ T cells. In contrast to Nef inhibition, which occurs rapidly in the first 24 hours of plecomacrolide treatment, toxicity to primary cells required sustained exposure. However, after 3 days of culture, we observed marked toxicities with sufficient concentrations of each plecomacrolide tested. Importantly, however, the 50% toxic concentration for CMA was 11-fold higher than the 50% effective concentration for Nef inhibition, providing a small but essential therapeutic window in which Nef is inhibited without notable toxicity in primary cells. Thus, CMA was identified as a promising lead compound for further development as a therapeutic inhibitor of Nef, based on its exceedingly high potency and ability to counteract Nef at non-toxic concentrations.

CMA mechanism of action: summary of results and hypotheses to explore

Though the plecomacrolides had never been described as inhibitors of HIV Nef capable of restoring antigen presentation in HIV-infected cells, the molecules are well-known inhibitors of the vacuolar-type H^+ ATPase (V-ATPase), the enzyme responsible for acidifying intracellular organelles, particularly the lysosome[76]. Bafilomycins were the first plecomacrolides identified as potent and selective inhibitors of V-ATPase[77], and the concanamycins were subsequently determined to be even more potent than the bafilomycins[78], although this original study may have overstated the degree to which concanamycins are more potent as inhibitors of V-ATPase[79]. Plecomacrolides likely

inhibit V-ATPase through direct, high-affinity binding to the V_0 subunit[80], ultimately resulting in the neutralization of the lysosome in cells, disrupting its degradative functions[81]. A structurally-related molecule, elaiophylin, has no effect on V-ATPase at all[78]. Thus, comparisons between elaiophylin and CMA could yield informative mechanistic insights regarding the requirement for V-ATPase inhibitory activity.

Nef downregulates MHC-I by redirecting it from the trans-Golgi network (TGN) into the endolysosomal system, from which it transits to the lysosome and is degraded[82,83]. Thus, we hypothesized that restoration of MHC-I to the surface of Nef-expressing cells following CMA treatment must somehow be a consequence of inhibiting V-ATPase, neutralizing the lysosome and preventing MHC-I degradation. We were surprised, then, to discover that the concentrations of CMA needed to neutralize the lysosomes of primary monocyte-derived-macrophages or intracellular compartments in primary T cells were much higher than those that were required to restore MHC-I. This led us to assess lysosomal function directly, as the maintenance of an acidic lysosome is necessary for degradation of lysosome-targeted proteins.

For this we took advantage of the fact that Nef directs both CD4 and MHC-I to the lysosome for degradation, though by different mechanisms. Nef recruits AP-1 to the MHC-I cytoplasmic tail in the TGN, forming the AP-1:Nef:MHC-I complex that promotes transit of MHC-I in an ARF1- and β-COP-dependent manner through late endosomes and ultimately to the lysosome[82-85]. Alternatively, Nef binds both CD4 and AP-2 at the plasma membrane, leading to CD4 internalization from the cell surface in clathrin-coated vesicles, from which CD4 also transits through late endosomes and ultimately to the lysosome[86-88]. Based on assays using Lysotracker Red staining intensity to assess the neutralization

of intracellular organelles in T cells, we predicted that 2.5nM CMA would neutralize the lysosome, while 0.5nM would not. Importantly, while both concentrations of CMA restored MHC-I to the cell surface, CD4 was not restored with either treatment, indicating that not all lysosome-targeted proteins have mechanisms for re-establishing surface expression after CMA treatment. We subsequently observed that degradation of both CD4 and MHC-I was blocked by 2.5nM CMA, while 0.5nM CMA prevented MHC-I degradation without blocking CD4 degradation. These experiments definitively demonstrated that MHC-I is restored to the cell surface and avoids degradation in cells that have functional lysosomes. We conclude that CMA specifically alters Nef-mediated trafficking of MHC-I but not CD4, such that CD4 transit to the lysosome via AP-2 is unaffected, and CD4 is degraded upon arrival in a functional, acidified lysosome, while MHC-I never reaches the lysosome and instead goes to the cell surface, avoiding degradation.

Since the effect of CMA is unique to MHC-I and not CD4, we focused on the differences in the trafficking pathways hijacked by Nef for targeting these two proteins. Coimmunoprecipitation experiments of HLA-A2 confirmed that both Nef and components of the AP-1 complex show significantly and reproducibly reduced association with the MHC-I cytoplasmic tail in cells treated with CMA. Given that the formation of this complex is necessary for MHC-I trafficking to the lysosome, this observation is sufficient to explain the restoration of MHC-I to the cell surface. However, questions remain about precisely how CMA interferes with the AP-1:Nef:MHC-I complex. Despite the specific effect on this the AP-1:Nef:MHC-I complex, CMA does not show signs of binding directly to AP-1, MHC-I, Nef, or ARF-1 *in vitro*, either as individual proteins or in complexes. These *in vitro* assays with purified recombinant proteins do not definitively prove that CMA does not

interact with these proteins or complexes in living cells, and further investigation of CMA binding partners in cells is warranted. Nevertheless, the absence of evidence of direct binding points to alternative hypotheses to explain the mechanism by which low-dose CMA that maintains lysosomal degradative functions reduces the prevalence of the AP-1:Nef:MHC-I complex in cells and results in successful trafficking of properly-loaded MHC-I to the cell surface.

Since plecomacrolides, especially CMA, are known to be extremely potent and selective inhibitors of V-ATPase, it remains possible that the target of CMA is the V-ATPase complex, even if the lysosome is not ultimately neutralized. Preliminary data indicate that Nef inhibitory potency correlates with neutralization potency among different plecomacrolide family members, although this association is not perfect. Furthermore, diphyllin, a V-ATPase inhibitor that is structurally unrelated to plecomacrolides, also counteracts Nef to restore MHC-I to the cell surface (data not shown), supporting the hypothesis that plecomacrolides inhibit Nef through interactions with their known high-affinity binding partner, V-ATPase. Additionally, exposing cells to high concentrations of NH_4Cl, though toxic, partially restores MHC-I to the cell surface (data not shown). NH_4Cl functions as a weak base, neutralizing organelles within the cell without interacting with V-ATPase. While these results are preliminary and certainly not definitive, they collectively support the hypothesis that plecomacrolides inhibit Nef through a mechanism that involves V-ATPase and organellar acidification. This, however, is puzzling, as the experiments presented in Chapter 3 clearly and definitively demonstrate that primary $CD4^+$ T cells treated with low-dose CMA restore MHC-I in Nef-expressing cells where the lysosome remains acidified and capable of degrading lysosome-targeted proteins.

This opens a series of questions regarding the possible roles of V-ATPase in MHC-I trafficking. If V-ATPase is being inhibited in a way that impacts Nef function, why is the lysosome not being neutralized? And why would V-ATPase or acidification affect Nef-mediated trafficking of MHC-I? A deep exploration of the protein trafficking and V-ATPase literature, which has been extensively reviewed elsewhere[89-93] begins to shed insights on these questions that point to a testable hypothesis moving forward.

First, β-COP binding to the Golgi membranes was shown to require myristoylated ARF and occurs temporally after ARF binding, and ARF binding requires an additional membrane protein that was not identified[94]. Furthermore, recruitment of ARF to membranes from the cytoplasm is pH-dependent and requires the activity of V-ATPase[95]. β-COP also associates with endosomal membranes in a pH-dependent manner and is required for transport from early to late endosomes[96]. An additional study confirmed that association of COP proteins with endosomes requires acidic endosomal pH and is dependent on ARF1, which is the factor responds to endosomal pH and renders COP association pH-dependent. The association of ARF1 and COP proteins with endosomal membranes is critical for the formation of transport intermediates destined for late endosomes[97].

Fitting with this observation, several studies have shown that plecomacrolide treatment interferes with transport from early to late endosomes. Baf A1 did not interfere with internalization from the plasma membrane or recycling back to the plasma membrane, but caused morphological changes in early endosomes and blocked trafficking from early endosomes to late endosomes[98]. Bafilomycin was also found to block transport from early to late endosomes after receptor-mediated endocytosis[99].

Another study showed that Baf A1 causes a lysosomal protease to be secreted into the media. Thus, a protein that would normally be targeted to the lysosome was redirected through the secretory pathway and released at the cell surface, similar to what we observe for MHC-I in primary T cells treated with low-dose CMA[100].

Other studies give results that are more difficult to interpret and associate with the observation that plecomacrolide treatment restores trafficking of MHC-I from the ER, through the Golgi, and to the cell surface. Concanamycin B blocks intra-Golgi and Golgi to plasma membrane transport without affecting ER to Golgi transport. Trafficking to the plasma membrane was delayed, and glycosylation was modified to a lesser extent than in cells without V-ATPase inhibition, showing that concanamycin B interfered with processing in the Golgi and reduces transport to the plasma membrane[101]. Baf A1 can also block the endocytic pathway after internalization and blocks recycling between the plasma membrane and the TGN, which would seem to reduce the likelihood of MHC-I trafficking from the TGN to the cell surface[102].

In addition to being essential for β-COP recruitment to Golgi membranes, ARF1 was also found to be essential for AP-1 recruitment[103]. Taken together, the literature supports a model in which V-ATPase acidifies Golgi and early endosomal compartments, and this low pH is required for ARF1 and subsequently β-COP association with endosomal, and perhaps Golgi membranes[95,96,104]. If the lumen of these compartments is neutralized, an unknown membrane-spanning factor responsible for relaying information about the luminal pH discourages ARF1 binding, which would subsequently reduce the recruitment of both AP-1 and β-COP to these membranes, preventing trafficking to late endosomes and ultimately to the lysosome. This pathways could be altered by neutralizing the luminal

pH of a critical compartment in the trafficking pathway, or by directly binding to and interfering with any of the key players, including the yet-to-be-identified pH sensor that transmits information to ARF1. CMA was not observed to bind directly to ARF1, AP-1, Nef, or MHC-I, but the pH sensor could theoretically be a target of CMA.

V-ATPase itself has been implicated as a pH sensor with both transmembrane (V_0) and cytoplasmic (V_1) domains. During endocytosis at the plasma membrane, association of ARF6 and ARNO with endosomes is pH-sensitive and dependent on a transmembrane protein to relay luminal pH information, akin to ARF1 and β-COP[105-107]. Hurtado-Lorenzo et al. identified V-ATPase as the protein complex required to relay luminal pH information to ARNO and ARF6. The a-subunit of V_0, specifically the a2 isoform, which is specifically targeted to early endosomes, associated with ARNO. The c-subunit of V_0 associated with ARF6. The interaction between a2 and ARNO was pH-dependent and essential for downstream events after endocytosis from the plasma membrane, with bafilomycin treatment specifically impairing the pathway leading to protein degradation rather than recycling to the plasma membrane[108]. This opens the possibility that the unidentified pH sensor relaying pH information via ARF1 could be a component of the V_0 subunit of V-ATPase, and a generalizable mechanism by which V-ATPase could serve as the pH sensing protein has been proposed[109]. Thus, CMA could target V-ATPase to disrupt the luminal pH itself, or possibly to disrupt the recruitment of ARF1 to membranes even when acidic pH is maintained. That diphyllin achieves equivalent MHC-I restoration to CMA in Nef-expressing cells while NH_4Cl has only a partial effect could support either mechanism.

Since MHC-I is normally transported to the plasma membrane in the absence of AP-1 recruitment, disruptions in the ARF1:AP-1:β-COP axis that prevent AP-1 recruitment in Nef-expressing cells could explain the restoration of cell surface MHC-I. The results described in Chapter 3, however, clearly demonstrate that low-dose CMA does not reduce the abundance of acidic compartments within the cell by Lysotracker staining intensity and does not impair the degradative capacity of the lysosome, suggesting the acidic pH is maintained. How, then, could a pH-sensitive pathway be responsible for the Nef inhibitory activity of CMA?

The secretory and endolysosomal pathways are made up of a series of organelles possessing increasingly acidic luminal pH as proteins are transported toward the lysosome, either from the ER or the plasma membrane[110,111]. V-ATPase is the primary host complex responsible for establishing the acidic environment in each of these organelles, and thus the lysosome is not the exclusive organelle into which V-ATPase actively pumps H^+ ions to maintain an acidic pH. Yet, in spite of this fact, not all organelles are as acidic as the lysosome. The Na^+/H^+ exchangers (NHEs) are integral membrane proteins that exchange H^+ for Na^+ to regulate pH at the plasma membrane (NHE1-5) or in organelles (NHE6-9)[112]. The organellar NHEs have a particularly important role in fine-tuning the pH of organelles by counteracting V-ATPase. Each organellar NHE is localized to the membrane of a distinct organelle: NHE6 is found in early recycling endosomes[113], NHE7 in the TGN[114], NHE8 in the mid- and trans-Golgi, and NHE9 in late endosomes[115]. Overexpression of the NHE proteins causes the neuralization of their respective compartments to the cytosolic pH, and knockdown leads to acidification equivalent to what is seen in the lysosome, supporting the hypothesis that a delicate balance between

V-ATPase and NHE activities regulates pH in the secretory and endolysosomal pathways[115-117].

Considering the activity and distribution of the NHE proteins, it is possible that a slight but incomplete impairment of V-ATPase activity at low doses of CMA could disrupt the delicate balance of H^+ flow that maintains the pH through the Golgi apparatus, the TGN, and the early and late endosomes without affecting the pH of the lysosome, since the lysosome does not have any NHEs counteracting V-ATPase. If the majority or entirety of LysoTracker staining is attributed to lysosomes rather than organelles with slightly acidic pH, organellar acidification could appear intact by that assay under conditions that neutralize a key trafficking compartment, such as the TGN or early endosomes. Neutralizing of these compartments could thus impair the recruitment of AP-1 to MHC-I, as we observed by coimmunoprecipitation, as a consequence of reduced pH-dependent ARF1 association with membranes (hypothesis in Fig. 4.4).
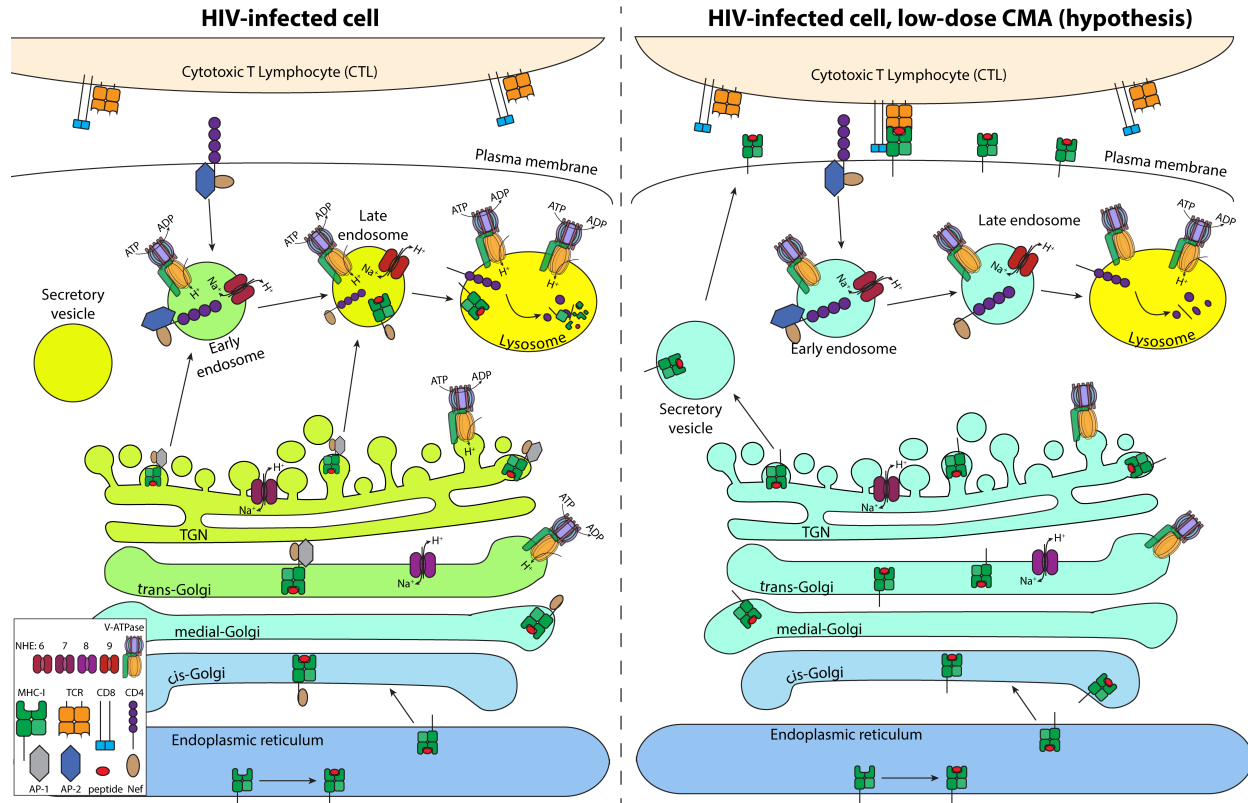
Fig. 4.4: Untested hypothesis that Nef inhibition by low-dose CMA is mediated by partial inhibition of V-ATPase. Left panel: a cell infected with HIV expresses Nef, and Nef recruits AP-1 to redirect MHC-I to the lysosome. AP-1 recruitment requires the acidification of organelles in the secretory and endolysosomal pathways, which is mediated by the activity of V-ATPase and balanced by the counteractivity of NHEs. Right: low-dose CMA partially but incompletely impairs V-ATPase, leaving the lysosome acidified but neutralizing organelles that express NHEs. Neutralization leads to reduced Nef and AP-1 binding to MHC-I, which reaches the cell surface to successfully present HIV-derived peptides to CTLs. Nef also downregulates CD4 by a different mechanism, as indicated, which is unaffected by low-dose CMA. Color gradient: yellow = low pH, blue = high pH.

This model warrants further exploration by a number of different approaches. First, the pH of organelles throughout the secretory and endolysosomal pathways should be determined in primary T cells treated with low-dose CMA. If no alterations in organellar pH are observed, then the mechanism by which CMA alters Nef-mediated trafficking of MHC-I is likely to be pH-independent. These assays may be challenging in primary T cells, as past approaches have required either an active endocytic pathway[118] or the expression of transgenic fusion proteins targeted to certain organelles[110,111,119].

Knockdown or overexpression of NHEs may be a more informative and feasible approach to test this hypothesis. If low-dose CMA functions by increasing the pH of a key trafficking compartment, then knockdown of NHEs should prevent restoration of MHC-I by low-dose CMA, requiring complete rather than partial inhibition of V-ATPase to achieve neutralization, and thus shifting the curve of Nef inhibitory activity to the right. Alternatively, overexpression of NHEs will neutralize the compartment in the absence of CMA treatment, leading to a lesser degree of Nef-mediated downregulation in these cells and no effect of CMA on MHC-I expression. The organelle-specific localization of each NHE protein would also enable the identification of the organelle or organelles in which acidic pH is critical for Nef-mediated downregulation of MHC-I. As a means to test these hypotheses, we are developing an HIV construct that will enable the overexpression of individual NHE genes, or any gene, from an IRES element in the context of Nef-expressing HIV infection (Fig. 4.5).
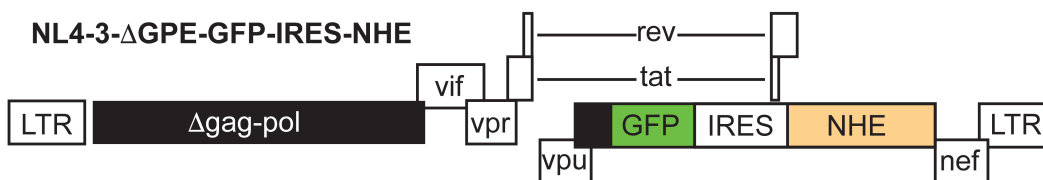
Fig. 4.5: Schematic of HIV construct to be used for overexpressing NHE genes.

If the mechanism by which low-dose CMA counteracts Nef requires the neutralization of key organelles and a subsequent defect in clathrin-mediated trafficking through association of ARF1, AP-1, and COP with membranes, then MHC-I is unlikely to be the only host protein that experiences aberrant trafficking in cells treated with low-dose CMA. The observation that CD4 is still internalized from the plasma membrane and degraded in the lysosome supports the conclusion that clathrin coat formation,

endocytosis, transport from early endosomes to late endosomes, and transport from late endosomes to the lysosome are not impaired. Mannose-6-phosphate receptors (M6PRs) are the canonical host factors sorted by AP-1 along the pathway hijacked by Nef to target MHC-I to the lysosome[120]. Experiments to determine the effects of low-dose CMA on the trafficking of M6PRs in primary T cells are of critical importance. First, immunofluorescence experiments can determine the localization of M6PRs in primary T cells treated with low-dose CMA compared to control cells. Alterations in localization would indicate that the effects of CMA are not specific for Nef and MHC-I but affect AP-1-mediated trafficking more broadly. It is of interest to determine whether M6PRs also appear on the cell surface, as this is where MHC-I is delivered in Nef-expressing cells treated with low-dose CMA. Assays measuring the successful sorting of cathepsin D by M6PRs, as previously published, could be used to further determine whether CMA impairs M6PR function[121-124].

There is also the possibility that different V-ATPase isoforms may be expressed in different cell types or in different organelles within a cell. In this case, different isoforms could have different roles in trafficking and organellar acidification, as V-ATPase has many isoforms with little known about their functional differences[125]. Though this is speculative, the identification of isoforms unique to primary T cells or unique to the secretory pathway could explain the observations that primary T cells are uniquely sensitive to low-dose CMA and that Nef-mediated trafficking can be disrupted without affecting the lysosome, respectively. Proteomic and transcriptomic analyses of primary T cells will be necessary to determine which isoforms of V-ATPase are present under the conditions of our experiments. Should multiple or unique isoforms be detected in primary

T cells, this line of investigation will warrant further study. If the activity of low-dose CMA does not appear to be mediated by alterations in pH or any of the aforementioned mechanisms, unbiased proteomic analyses will be necessary to determine whether V-ATPase subunits function in Nef-specific trafficking independent of effects on pH or to identify other non-V-ATPase host factors that interact with CMA in primary T cells.

CMA restores cellular adaptive immunity to HIV-infected cells and shows broad therapeutic promise

Although the precise mechanism by which CMA restores MHC-I to the cell surface requires further investigation, results in Chapter 3 provide many clues regarding the biology and processing of MHC-I in cells treated with low-dose CMA. While restoration of MHC-I to the cell surface was likely to correlate with increased CTL responsiveness to Nef-expressing target cells[126-130], it remained possible that this MHC-I may not be properly loaded with HIV-derived peptides. To address this question functionally, we performed co-culture assays of HIV-infected primary T cells with HIV-specific CTLs. CTLs efficiently eliminated cells infected with a virus in which Nef was genetically deleted but failed to eliminate a portion of cells infected with Nef-competent HIV. Thus, we confirmed that downregulation of MHC-I by Nef offers protection to at least a subset of HIV-infected cells, posing a major obstacle to the success of shock and kill approaches to eliminate the latent HIV reservoir. Impressively, low-dose CMA enhanced the killing of HIV-infected cells equivalent to genetic deletion of Nef, while providing no enhancement to the killing of cells infected with a Nef-deleted virus. The increase in CTL-mediated clearance of infected cells was complete despite the fact that restoration of MHC-I to the surface was

incomplete when compared to Nef-negative cells. This suggests that CTLs required a certain threshold of MHC-I expression to achieve efficient killing in these assays, and that CMA successfully increased MHC-I expression above the threshold for these CTLs. Furthermore, CTLs did not kill HIV-infected cells from an HLA-mismatched donor in the presence or in the absence of CMA, confirming that the observed killing was due to specific recognition of peptide:MHC-I by CTLs. Taken together, these results provide proof-of-concept that Nef can protect HIV-infected cells from even potent CTLs, and that CMA can reverse this to aid in the elimination of these hard-to-kill cells.

These findings clearly demonstrate that the cell-surface MHC-I that is restored in Nef-expressing cells is properly loaded with HIV-derived peptides. This indicates that the trafficking pathway is not altered too radically from what occurs in the absence of Nef, such that MHC-I would not be exposed to HIV-derived peptides or would not retain peptides as it migrates toward the cell surface. This also confirms that CMA does not interfere with the generation of peptide antigens from HIV proteins that are suitable for MHC-I presentation. Thus, the cytoplasmic proteasome and peptide importing machinery in the ER are unlikely to be affected. Furthermore, low-dose CMA did not impair the responsiveness of primary T cells to the lytic signals from CTLs, which would work directly against the goal of enhancing killing of these cells and has been observed for some LRAs[29].

Chapter 3 concludes with a series of experiments demonstrating that CMA works to counteract Nef in diverse contexts, pointing to the broad therapeutic potential of CMA. Studies of MHC-I are rendered difficult by the tremendous diversity of HLA alleles present in the human population[131], and antibodies targeting specific alleles without cross-

reactivity to other alleles are rare[132]. Nonetheless, capturing the impacts of this diversity is essential for the therapeutic development of any drug aimed at MHC-I, as it must be broadly active on a wide array of HLA alleles to be useful in more than a small subset of patients. While we focused predominantly on HLA-A2, as it is the most common allele of MHC-I in many populations[133-137] and is recognized by the highly specific BB7.2 monoclonal antibody[138,139], we aimed to determine whether CMA could enhance antigen presentation in the context of other alleles of MHC-I, particularly alleles of HLA-B. Nef downregulates both HLA-A and HLA-B[83], but HLA-B alleles are the most strongly associated with control or accelerated progression of HIV infection[140-142].

Using a donor with minimal HLA cross-reactivity with the antibodies recognizing the Bw4 and Bw6 epitopes, we were able to interrogate the effects of Nef and CMA on two alleles of HLA-B, B*51:01 and B*07:02, in primary CD4$^+$ T cells infected with HIV. Both alleles of HLA-B were downregulated by Nef and restored by CMA with similar magnitude and over a similar range of concentrations. This result confirmed that the results obtained using HLA-A2 were likely to be broadly conserved across HLA-A and -B alleles in primary CD4$^+$ T cells. These experiments employed the lab-adapted HIV strain NL4-3. We expanded these findings by infecting primary cells from the same donor with a primary isolate of HIV. This isolate is of particular interest in the context of the work presented in Chapters 2 and 3, as it was isolated from the residual plasma virus of an optimally-treated patient and is associated with a provirus found in bone marrow HSPCs[9]. Thus, this isolate represents precisely the source of HIV that, following reactivation of the HSPC reservoir, may require enhanced CTL responsiveness to facilitate clearance. This virus downregulated HLA- B*51:01, -B*07:02, and -A*02:01 with impressive magnitude,

and CMA strongly counteracted Nef from this virus to restore all three alleles of MHC-I. This confirms that Nef from proviruses residing in long-lived cells in the bone marrow can downregulate both HLA-A and HLA-B and is likely to offer protection from CTLs, based on the data from the CTL killing assay described above. In summary, CMA was able to enhance antigen presentation by diverse alleles of HLA-A and HLA-B in primary cells targeted by both lab-adapted and a primary isolate of HIV from a patient's latent reservoir.

To extend these findings, we used a vector derived from the murine stem cell virus that allows expression of individual Nef alleles in CEM cells. Using this system, we tested a panel of Nef alleles derived from diverse clades of HIV and one Nef allele from simian immunodeficiency virus (SIV) targeting 4 alleles of MHC-I: HLA-A*02, HLA-B*08, HLA-B*27, and HLA-B*57. All 4 alleles of MHC-I were downregulated by each allele of Nef, to varying degrees. CMA counteracted every allele of Nef targeting each allele of MHC-I, with more complete restoration of MHC-I in cells expressing weaker Nef alleles, but a greater magnitude of MHC-I restoration in cells expressing stronger Nef alleles. This suggests that CMA is likely to enhance CTL responses in every clinical setting, regardless of whether Nef is offering a small or large degree of protection to HIV-infected cells. CMA was also active with the same potency against each allele of Nef, indicating that variations in Nef even across clades of HIV do not alter sensitivity to CMA. These results indicate that CMA is likely to have broad therapeutic utility despite the tremendous diversity of both HIV and MHC-I sequences in the population. These findings are important because CTL responses in an individual are polyclonal and restricted to multiple HLA alleles presenting a diverse array of peptides. Furthermore, the diversity of HIV is high even within a single individual, and escape mutations often develop to evade immunodominant

CTL responses. Thus, enhancing CTL responses broadly is likely to improve the overall cellular adaptive immune response to HIV as a means of enhancing clearance of reactivated latent reservoirs.

Despite the many promising findings, some limitations exist that will require further investigation. First, CMA is known to target V-ATPase with high affinity, which is associated with many off-target effects unrelated to restoration of MHC-I. We clearly demonstrated that the 50% effective concentration was 11-fold lower than the 50% toxic concentration (therapeutic index). This is acceptable for a lead compound for further development, but may not be feasible for clinical use without making modifications to the compound to widen the separation between active and toxic effects. A recent inhibitor of HIV CA protein, for instance, shows a 1,000,000-fold separation between activity and toxicity[143]. CMA used in the clinic would likely require extremely careful dosing and clinical monitoring. We also demonstrated a significant separation between inhibition of the lysosome and restoration of MHC-I in Nef-expressing primary T cells. While this is also encouraging for CMA as a lead compound, increasing the specificity of the compound for Nef inhibition relative to V-ATPase inhibition is another priority of derivatization approaches.

CMA is also a known inhibitor of CTL functions, a critically important off-target effect that would counteract any efforts to use CMA as part of a combination therapy to achieve shock and kill. The possibility that CMA could affect CD8^{+} T cell function was addressed in Chapter 3. While at higher concentrations CMA has been reported to inhibit the perforin-mediated cytolytic activity of CTLs[144], inhibition of CTL-mediated lysis was not observed with CMA concentrations less than 1nM[144,145]. We confirmed these findings,

demonstrating that we observed no reduction in the specific killing of peptide-pulsed cells by CTL clones in the presence of 0.5 nM CMA. While this once again suggests that Nef-mediated downregulation of MHC-I is more sensitive to CMA than other known off-target effects, the separation between these two activities is small, and the development of modified compounds that promote antigen presentation without risking impaired CTL functionality may be essential.

It will be of great interest to perform structure-activity studies for the plecomacrolide family of compounds comparing their effects on toxicity, lysosomal neutralization, and Nef inhibition in primary CD4$^+$ T cells. These studies will provide information on two fronts. First, they will help define the key components of the structure of concanamycin that enhance activity relative to other plecomacrolides, as well as various modifications that can improve or decrease these activities. This work will help to define the pharmacophore for plecomacrolides targeting Nef and will reveal whether this is different from the pharmacophore for inhibition of V-ATPase. Second, to that end, these studies will reveal whether there are significant separations between the potency of these activities for different plecomacrolide compounds. If V-ATPase is the target responsible for Nef inhibition, lysosomal degradation, and toxicity, then the relationship between these three activities will likely be comparable for all plecomacrolides, and structural modifications will be unlikely to substantially improve the therapeutic index. Based on the results of structure-activity studies, it will be paramount to attempt guided derivatization of CMA with the aims of improving potency of Nef inhibition, reducing toxicity, increasing the therapeutic index, decreasing negative effects on CTL function, and making CMA readily bioavailable for easier use in the clinic.

Taken together, the results in Chapter 3 strongly support the conclusion that CMA is a potent and broad inhibitor of HIV Nef that restores CTL-mediated clearance of HIV-infected cells in primary cell cultures. The success of CMA in primary cells *in vitro* necessitates the completion of *in vivo* studies to determine the tolerability and efficacy of CMA in the context of a living organism. Toxicity studies *in vitro* provide valuable information, but it is possible that CMA is more or less toxic to other cell types than it is to primary T cells. For instance, data presented in Chapter 3 indicate that much higher concentrations of CMA are required to neutralize the lysosomes of primary monocyte-derive-macrophages than primary T cells. Encouragingly, initial dosing studies indicated that mice could tolerate sequential injections of CMA at two-day intervals for 18 days. Mice were sacrificed 2 hours after the final injection, and CMA levels in plasma and lymph nodes were determine by mass spectrometry. Despite the fact that no toxicity was observed in the mice based on weight or the appearance of fur, CMA concentrations in both plasma and lymph nodes were above those that were required to achieve Nef inhibition *in vitro*. Furthermore, plasma from mice injected with CMA inhibited Nef in our primary cell cultures with potency equivalent to what would have been predicted based on the concentration as determined by mass spectrometry (data not shown). Taken together, early *in vivo* studies somewhat surprisingly indicate that CMA can be tolerated *in vivo* at concentrations that can inhibit Nef. Further studies using immunodeficient mice injected with HIV-infected human PBMCs or HSPCs will be necessary to determine whether CMA administered by injection can indeed increase the expression of MHC-I on the surface of HIV-infected cells circulating in a living animal.

Even a potent inhibitor of Nef will not be able to cure HIV in isolation. CMA alone will not reactivate latent reservoirs, necessitating the development of effective LRAs capable of inducing the entire replication-competent reservoir of HIV despite its cellular and proviral heterogeneity, as described above. These LRAs will also need to induce HIV gene expression to levels sufficient to produce enough HIV peptide epitopes for CTL recognition[28,29]. Furthermore, while a Nef inhibitor can enhance antigen presentation to CTLs and thus improve the efficiency of CTL-mediated clearance of cells harboring reactivated proviruses, this depends on the presence of functional CTLs within the individual. CTLs in HIV-infected individuals can often become exhausted[146,147], reducing their functionality and providing an obstacle to enhanced killing following Nef inhibition. The latent reservoir of HIV can sometimes contain escape mutants that evade immunodominant CTLs[148]. These barriers will likely necessitate approaches to prime CTLs prior to shock and kill[32], even in the presence of a Nef inhibitor like CMA. Checkpoint inhibitor therapies may at least temporarily restore function to exhausted CTLs, and vaccine strategies should be developed to simultaneously prime existing CTL responses and enhance the breadth of the anti-HIV CTL repertoire to counter reservoir viruses with escape mutants evading already-present CTLs, preferably by targeting highly-networked epitopes associated with elite control[149]. Additionally, as described above, the cells that make up the latent reservoir of HIV may be particularly hard to kill, due to the expression of BCL-2 and potentially other mechanisms[24,27]. Together, the parallel development of each of these approaches could collectively comprise a combination shock and kill therapy to achieve an HIV cure. Even if all of these approaches were to be successful, it is unlikely that a single round of latency reversal will truly eliminate every replication-

competent provirus from the body. Thus, successive bursts of CTL priming followed by latency reversal in the presence of a Nef inhibitor, all while maintaining ART, will likely be necessary to have any hope of truly achieving a cure.

Concluding Statements

Collectively, the work presented here describes recent advancements in the study of HIV persistence and therapeutic approaches to achieve a cure for HIV. Particular focus was given to 1) the mechanisms contributing to HIV latency in quiescent cells, which represent a major reservoir of HIV in optimally-treated people and may be resistant to the approaches to reactivate latent viruses that are currently in development, and 2) enhancing the clearance of the cells harboring reactivated virus by HIV-specific cytotoxic T lymphocytes through the inhibition of the accessory factor Nef. This work represents a significant contribution to the field of HIV persistence and the search for a shock and kill approach to an HIV cure. The findings herein were presented in the broader context of retroviral biology and HIV persistence, with discussion of the limitations to the work as currently constituted and future directions that lie ahead.

Although ART has radically altered the trajectory of the HIV pandemic, 700,000 people died in 2019 as a result of being infected with this virus, joining the millions whose lives have been taken too soon, and the millions more currently living with the stigma associated with HIV infection. While this work does little for the needs of these people today, I humbly offer this small contribution in the hopes that one day, through the dedicated of countless scientists, we will reach the goals outlined in these pages.

References

1. Arai F, Hirao A, Ohmura M, et al. Tie2/angiopoietin-1 signaling regulates hematopoietic stem cell quiescence in the bone marrow niche. *Cell.* 2004;118(2):149-161.
2. Cheng T, Rodrigues N, Shen H, et al. Hematopoietic stem cell quiescence maintained by p21cip1/waf1. *Science.* 2000;287(5459):1804-1808.
3. Dobrowolski C, Valadkhan S, Graham AC, et al. Entry of polarized effector cells into quiescence forces HIV latency. *MBio.* 2019;10(2).
4. Kim M, Hosmane NN, Bullen CK, et al. A primary CD4+ T cell model of HIV-1 latency established after activation through the T cell receptor and subsequent return to quiescence. *nature protocols.* 2014;9(12):2755.
5. Brooks DG, Kitchen SG, Kitchen CM, Scripture-Adams DD, Zack JA. Generation of HIV latency during thymopoiesis. *Nat Med.* 2001;7(4):459-464.
6. Bosque A, Planelles V. Induction of HIV-1 latency and reactivation in primary memory CD4+ T cells. *Blood, The Journal of the American Society of Hematology.* 2009;113(1):58-65.
7. Spina CA, Anderson J, Archin NM, et al. An in-depth comparison of latent HIV-1 reactivation in multiple cell model systems and resting CD4+ T cells from aviremic patients. *PLoS Pathog.* 2013;9(12):e1003834.
8. Sebastian NT, Zaikos TD, Terry V, et al. CD4 is expressed on a heterogeneous subset of hematopoietic progenitors, which persistently harbor CXCR4 and CCR5-tropic HIV proviral genomes in vivo. *PLoS Pathogens.* 2017;13(7):e1006509.
9. Zaikos TD, Terry VH, Kettinger NTS, et al. Hematopoietic stem and progenitor cells are a distinct HIV reservoir that contributes to persistent viremia in suppressed patients. *Cell Reports.* 2018;25(13):3759-3773. e3759.
10. Weinberger LS, Burnett JC, Toettcher JE, Arkin AP, Schaffer DV. Stochastic gene expression in a lentiviral positive-feedback loop: HIV-1 Tat fluctuations drive phenotypic diversity. *Cell.* 2005;122(2):169-182.
11. Singh A, Weinberger LS. Stochastic gene expression as a molecular switch for viral latency. *Current opinion in microbiology.* 2009;12(4):460-466.
12. Wei X, Ghosh SK, Taylor ME, et al. Viral dynamics in human immunodeficiency virus type 1 infection. *Nature.* 1995;373(6510):117-122.
13. Perelson AS, Neumann AU, Markowitz M, Leonard JM, Ho DD. HIV-1 dynamics in vivo: virion clearance rate, infected cell life-span, and viral generation time. *Science.* 1996;271(5255):1582-1586.
14. Ho DD, Neumann AU, Perelson AS, Chen W, Leonard JM, Markowitz M. Rapid turnover of plasma virions and CD4 lymphocytes in HIV-1 infection. *Nature.* 1995;373(6510):123-126.

15. Dummer W, Ernst B, LeRoy E, Lee D-S, Surh CD. Autologous regulation of naive T cell homeostasis within the T cell compartment. *The Journal of Immunology.* 2001;166(4):2460-2468.

16. Kieper WC, Troy A, Burghardt JT, et al. Cutting edge: recent immune status determines the source of antigens that drive homeostatic T cell expansion. *The Journal of Immunology.* 2005;174(6):3158-3163.

17. Min B, Yamane H, Hu-Li J, Paul WE. Spontaneous and homeostatic proliferation of CD4 T cells are regulated by different mechanisms. *The Journal of Immunology.* 2005;174(10):6039-6044.

18. Koup R, Safrit JT, Cao Y, et al. Temporal association of cellular immune responses with the initial control of viremia in primary human immunodeficiency virus type 1 syndrome. *Journal of virology.* 1994;68(7):4650-4655.

19. Borrow P, Lewicki H, Wei X, et al. Antiviral pressure exerted by HIV-I-specific cytotoxic T lymphocytes (CTLs) during primary infection demonstrated by rapid selection of CTL escape virus. *Nature medicine.* 1997;3(2):205.

20. Ndhlovu ZM, Kamya P, Mewalal N, et al. Magnitude and kinetics of CD8+ T cell activation during hyperacute HIV infection impact viral set point. *Immunity.* 2015;43(3):591-604.

21. Pollack RA, Jones RB, Pertea M, et al. Defective HIV-1 proviruses are expressed and can be recognized by cytotoxic T lymphocytes, which shape the proviral landscape. *Cell host & microbe.* 2017;21(4):494-506. e494.

22. Leslie A, Pfafferott K, Chetty P, et al. HIV evolution: CTL escape mutation and reversion after transmission. *Nature medicine.* 2004;10(3):282-289.

23. Goulder PJ, Brander C, Tang Y, et al. Evolution and transmission of stable CTL escape mutations in HIV infection. *Nature.* 2001;412(6844):334-338.

24. Huang S-H, Ren Y, Thomas AS, et al. Latent HIV reservoirs exhibit inherent resistance to elimination by CD8+ T cells. *The Journal of clinical investigation.* 2018;128(2):876-889.

25. Cummins NW, Sainski-Nguyen AM, Natesampillai S, Aboulnasr F, Kaufmann S, Badley AD. Maintenance of the HIV reservoir is antagonized by selective BCL2 inhibition. *Journal of virology.* 2017;91(11).

26. Cummins NW, Sainski AM, Dai H, et al. Prime, shock, and kill: priming CD4 T cells from HIV patients with a BCL-2 antagonist before HIV reactivation reduces HIV reservoir size. *Journal of virology.* 2016;90(8):4032-4048.

27. Ren Y, Huang SH, Patel S, et al. BCL-2 antagonism sensitizes cytotoxic T cell–resistant HIV reservoirs to elimination ex vivo. *The Journal of Clinical Investigation.* 2020;130(5):2542-2559.

28. Jones RB, O'Connor R, Mueller S, et al. Histone deacetylase inhibitors impair the elimination of HIV-infected cells by cytotoxic T-lymphocytes. *PLoS Pathog.* 2014;10(8):e1004287.

29. Mota TM, McCann CD, Danesh A, et al. Integrated Assessment of Viral Transcription, Antigen Presentation, and CD8+ T Cell Function Reveals Multiple Limitations of Class I-Selective Histone Deacetylase Inhibitors during HIV-1 Latency Reversal. *Journal of Virology.* 2020;94(9).

30.   Jones RB, Mueller S, O'Connor R, et al. A subset of latency-reversing agents expose HIV-infected resting CD4+ T-cells to recognition by cytotoxic T-lymphocytes. *PLoS pathogens.* 2016;12(4):e1005545.

31.   French AJ, Natesampillai S, Krogman A, et al. Reactivating latent HIV with PKC agonists induces resistance to apoptosis and is associated with phosphorylation and activation of BCL2. *PLoS Pathog.* 2020;16(10):e1008906.

32.   Shan L, Deng K, Shroff NS, et al. Stimulation of HIV-1-specific cytolytic T lymphocytes facilitates elimination of latent viral reservoir after virus reactivation. *Immunity.* 2012;36(3):491-501.

33.   Jin X, Bauer DE, Tuttleton SE, et al. Dramatic rise in plasma viremia after CD8+ T cell depletion in simian immunodeficiency virus–infected macaques. *The Journal of experimental medicine.* 1999;189(6):991-998.

34.   Lifson JD, Rossio JL, Piatak M, et al. Role of CD8+ lymphocytes in control of simian immunodeficiency virus infection and resistance to rechallenge after transient early antiretroviral treatment. *Journal of virology.* 2001;75(21):10187-10199.

35.   Matano T, Shibata R, Siemon C, Connors M, Lane HC, Martin MA. Administration of an anti-CD8 monoclonal antibody interferes with the clearance of chimeric simian/human immunodeficiency virus during primary infections of rhesus macaques. *Journal of virology.* 1998;72(1):164-169.

36.   Schmitz JE, Kuroda MJ, Santra S, et al. Control of viremia in simian immunodeficiency virus infection by CD8+ lymphocytes. *Science.* 1999;283(5403):857-860.

37.   Cao Y, Cartwright EK, Silvestri G, Perelson AS. CD8+ lymphocyte control of SIV infection during antiretroviral therapy. *PLoS pathogens.* 2018;14(10):e1007350.

38.   Cartwright EK, Spicer L, Smith SA, et al. CD8+ lymphocytes are required for maintaining viral suppression in SIV-infected macaques treated with short-term antiretroviral therapy. *Immunity.* 2016;45(3):656-668.

39.   Klatt NR, Shudo E, Ortiz AM, et al. CD8+ lymphocytes control viral replication in SIVmac239-infected rhesus macaques without decreasing the lifespan of productively infected cells. *PLoS Pathog.* 2010;6(1):e1000747.

40.   Wong JK, Strain MC, Porrata R, et al. In vivo CD8+ T-cell suppression of siv viremia is not mediated by CTL clearance of productively infected cells. *PLoS Pathog.* 2010;6(1):e1000748.

41.   McBrien JB, Mavigner M, Franchitti L, et al. Robust and persistent reactivation of SIV and HIV by N-803 and depletion of CD8+ cells. *Nature.* 2020;578(7793):154-159.

42.   Cocchi F, DeVico AL, Garzino-Demo A, Arya SK, Gallo RC, Lusso P. Identification of RANTES, MIP-1α, and MIP-1β as the major HIV-suppressive factors produced by CD8+ T cells. *Science.* 1995;270(5243):1811-1815.

43.   Levy JA. The search for the CD8+ cell anti-HIV factor (CAF). *Trends in immunology.* 2003;24(12):628-632.

44.   Mackewicz CE, Blackbourn DJ, Levy JA. CD8+ T cells suppress human immunodeficiency virus replication by inhibiting viral transcription. *Proceedings of the National Academy of Sciences.* 1995;92(6):2308-2312.

45. Mackewicz CE, Wang B, Metkar S, Richey M, Froelich CJ, Levy JA. Lack of the CD8+ cell anti-HIV factor in CD8+ cell granules. *Blood.* 2003;102(1):180-183.

46. Mackewicz CE, Yuan J, Tran P, et al. α-Defensins can have anti-HIV activity but are not CD8 cell anti-HIV factors. *Aids.* 2003;17(14):F23-F32.

47. Walker C, Levy J. A diffusible lymphokine produced by CD8+ T lymphocytes suppresses HIV replication. *Immunology.* 1989;66(4):628.

48. Walker CM, Moody DJ, Stites DP, Levy JA. CD8+ lymphocytes can control HIV infection in vitro by suppressing virus replication. *Science.* 1986;234(4783):1563-1566.

49. Yang OO, Kalams SA, Trocha A, et al. Suppression of human immunodeficiency virus type 1 replication by CD8+ cells: evidence for HLA class I-restricted triggering of cytolytic and noncytolytic mechanisms. *Journal of virology.* 1997;71(4):3120-3128.

50. Kaiser P, Joos B, Niederöst B, Weber R, Günthard HF, Fischer M. Productive human immunodeficiency virus type 1 infection in peripheral blood predominantly takes place in CD4/CD8 double-negative T lymphocytes. *Journal of virology.* 2007;81(18):9693-9706.

51. Emert-Sedlak LA, Narute P, Shu ST, et al. Effector kinase coupling enables high-throughput screens for direct HIV-1 Nef antagonists with antiretroviral activity. *Chemistry & biology.* 2013;20(1):82-91.

52. Mujib S, Saiyed A, Fadel S, et al. Pharmacologic HIV-1 Nef blockade promotes CD8 T cell–mediated elimination of latently HIV-1–infected cells in vitro. *JCI insight.* 2017;2(17).

53. Poe JA, Smithgall TE. HIV-1 Nef dimerization is required for Nef-mediated receptor downregulation and viral replication. *Journal of molecular biology.* 2009;394(2):329-342.

54. Liu LX, Heveker N, Fackler OT, et al. Mutation of a conserved residue (D123) required for oligomerization of human immunodeficiency virus type 1 Nef protein abolishes interaction with human thioesterase and results in impairment of Nef biological functions. *Journal of Virology.* 2000;74(11):5310-5319.

55. Jia X, Singh R, Homann S, Yang H, Guatelli J, Xiong Y. Structural basis of evasion of cellular adaptive immunity by HIV-1 Nef. *Nature structural & molecular biology.* 2012;19(7):701-706.

56. Shen QT, Ren X, Zhang R, Lee IH, Hurley JH. HIV-1 Nef hijacks clathrin coats by stabilizing AP-1:Arf1 polygons. *Science.* 2015;350(6259):aac5137.

57. Breuer S, Gerlach H, Kolaric B, Urbanke C, Opitz N, Geyer M. Biochemical indication for myristoylation-dependent conformational changes in HIV-1 Nef. *Biochemistry.* 2006;45(7):2339-2349.

58. Peng B, Robert-Guroff M. Deletion of N-terminal myristoylation site of HIV Nef abrogates both MHC-1 and CD4 down-regulation. *Immunology letters.* 2001;78(3):195-200.

59. Niederman TM, Hastings WR, Ratner L. Myristoylation-Enhanced Binding of the HIV-1 Net Protein to T Cell Skeletal Matrix. *Virology.* 1993;197(1):420-425.

60. Kaminchik J, Margalit R, Yaish S, et al. Cellular distribution of HIV type 1 Nef protein: identification of domains in Nef required for association with membrane

and detergent-insoluble cellular matrix. *AIDS research and human retroviruses.* 1994;10(8):1003-1010.

61. Macrae D, Bruss V, Ganem D, et al. The role of myristoylation in the interactions between human immunodeficiency virus type I Nef and cellular proteins. *Virology.* 1983;181:359-363.

62. Liu B, Zhang X, Zhang W, et al. Lovastatin inhibits HIV-1-induced MHC-I downregulation by targeting Nef–AP-1 complex formation: A new strategy to boost immune eradication of HIV-1 infected cells. *Frontiers in Immunology.* 2019;10:2151.

63. Estes JD, Kityo C, Ssali F, et al. Defining total-body AIDS-virus burden with implications for curative strategies. *Nature medicine.* 2017;23(11):1271.

64. Tenner-Racz K, Stellbrink H-J, Van Lunzen J, et al. The unenlarged lymph nodes of HIV-1–infected, asymptomatic patients with high CD4 T cell counts are sites for virus replication and CD4 T cell proliferation. The impact of highly active antiretroviral therapy. *The Journal of experimental medicine.* 1998;187(6):949-959.

65. Deleage C, Wietgrefe SW, Del Prete G, et al. Defining HIV and SIV reservoirs in lymphoid tissues. *Pathogens & immunity.* 2016;1(1):68.

66. Deleage C, Turkbey B, Estes JD. Imaging lymphoid tissues in nonhuman primates to understand SIV pathogenesis and persistence. *Current opinion in virology.* 2016;19:77-84.

67. Kohler SL, Pham MN, Folkvord JM, et al. Germinal center T follicular helper cells are highly permissive to HIV-1 and alter their phenotype during virus replication. *The Journal of Immunology.* 2016;196(6):2711-2722.

68. Perreau M, Savoye A-L, De Crignis E, et al. Follicular helper T cells serve as the major CD4 T cell compartment for HIV-1 infection, replication, and production. *Journal of Experimental Medicine.* 2013;210(1):143-156.

69. Pallikkuth S, Sharkey M, Babic DZ, et al. Peripheral T follicular helper cells are the major HIV reservoir within central memory CD4 T cells in peripheral blood from chronically HIV-infected individuals on combination antiretroviral therapy. *Journal of virology.* 2016;90(6):2718-2728.

70. Banga R, Procopio FA, Noto A, et al. PD-1+ and follicular helper T cells are responsible for persistent HIV-1 transcription in treated aviremic individuals. *Nature medicine.* 2016;22(7):754-761.

71. Connick E, Mattila T, Folkvord JM, et al. CTL fail to accumulate at sites of HIV-1 replication in lymphoid tissue. *The Journal of Immunology.* 2007;178(11):6975-6983.

72. Fukazawa Y, Lum R, Okoye AA, et al. B cell follicle sanctuary permits persistent productive simian immunodeficiency virus infection in elite controllers. *Nature medicine.* 2015;21(2):132-139.

73. Miles B, Miller SM, Folkvord JM, et al. Follicular regulatory CD8 T cells impair the germinal center response in SIV and ex vivo HIV infection. *PLoS pathogens.* 2016;12(10):e1005924.

74. Petrovas C, Ferrando-Martinez S, Gerner MY, et al. Follicular CD8 T cells accumulate in HIV infection and can kill infected cells in vitro via bispecific antibodies. *Science translational medicine.* 2017;9(373).

75. He R, Hou S, Liu C, et al. Follicular CXCR5-expressing CD8+ T cells curtail chronic viral infection. *Nature.* 2016;537(7620):412-416.

76. Dröse S, Altendorf K. Bafilomycins and concanamycins as inhibitors of V-ATPases and P-ATPases. *J Exp Biol.* 1997;200(1):1-8.

77. Bowman EJ, Siebers A, Altendorf K. Bafilomycins: a class of inhibitors of membrane ATPases from microorganisms, animal cells, and plant cells. *Proceedings of the National Academy of Sciences.* 1988;85(21):7972-7976.

78. Droese S, Bindseil KU, Bowman EJ, Siebers A, Zeeck A, Altendorf K. Inhibitory effect of modified bafilomycins and concanamycins on P-and V-type adenosinetriphosphatases. *Biochemistry.* 1993;32(15):3902-3906.

79. Dröse S, Boddien C, Gassel M, Ingenhorst G, Zeeck A, Altendorf K. Semisynthetic derivatives of concanamycin A and C, as inhibitors of V-and P-type ATPases: structure− activity investigations and developments of photoaffinity probes. *Biochemistry.* 2001;40(9):2816-2825.

80. Huss M, Ingenhorst G, König S, et al. Concanamycin A, the specific inhibitor of V-ATPases, binds to the Vo subunit c. *Journal of Biological Chemistry.* 2002;277(43):40544-40548.

81. Yoshimori T, Yamamoto A, Moriyama Y, Futai M, Tashiro Y. Bafilomycin A1, a specific inhibitor of vacuolar-type H (+)-ATPase, inhibits acidification and protein degradation in lysosomes of cultured cells. *Journal of Biological Chemistry.* 1991;266(26):17707-17712.

82. Roeth JF, Williams M, Kasper MR, Filzen TM, Collins KL. HIV-1 Nef disrupts MHC-I trafficking by recruiting AP-1 to the MHC-I cytoplasmic tail. *J Cell Biol.* 2004;167(5):903-913.

83. Wonderlich ER, Williams M, Collins KL. The tyrosine binding pocket in the adaptor protein 1 (AP-1) mu1 subunit is necessary for Nef to recruit AP-1 to the major histocompatibility complex class I cytoplasmic tail. *The Journal of biological chemistry.* 2008;283(6):3011-3022.

84. Wonderlich ER, Leonard JA, Kulpa DA, Leopold KE, Norman JM, Collins KL. ADP ribosylation factor 1 activity is required to recruit AP-1 to the major histocompatibility complex class I (MHC-I) cytoplasmic tail and disrupt MHC-I trafficking in HIV-1-infected primary T cells. *Journal of virology.* 2011;85(23):12216-12226.

85. Schaefer MR, Wonderlich ER, Roeth JF, Leonard JA, Collins KL. HIV-1 Nef targets MHC-I and CD4 for degradation via a final common beta-COP-dependent pathway in T cells. *PLoS Pathog.* 2008;4(8):e1000131.

86. Jin YJ, Cai CY, Zhang X, Zhang HT, Hirst JA, Burakoff SJ. HIV Nef-mediated CD4 down-regulation is adaptor protein complex 2 dependent. *J Immunol.* 2005;175(5):3157-3164.

87. Greenberg ME, Bronson S, Lock M, Neumann M, Pavlakis GN, Skowronski J. Co-localization of HIV-1 Nef with the AP-2 adaptor protein complex correlates with Nef-induced CD4 down-regulation. *Embo J.* 1997;16(23):6964-6976.

88. Coleman SH, Van Damme N, Day JR, et al. Leucine-specific, functional interactions between human immunodeficiency virus type 1 Nef and adaptor protein complexes. *J Virol.* 2005;79(4):2066-2078.

89. Weisz OA. Acidification and protein traffic. *International review of cytology.* 2003:259-320.
90. Toei M, Saum R, Forgac M. Regulation and isoform function of the V-ATPases. *Biochemistry.* 2010;49(23):4715-4723.
91. Schumacher K, Krebs M. The V-ATPase: small cargo, large effects. *Current opinion in plant biology.* 2010;13(6):724-730.
92. Paroutis P, Touret N, Grinstein S. The pH of the secretory pathway: measurement, determinants, and regulation. *Physiology.* 2004;19(4):207-215.
93. Marshansky V, Futai M. The V-type H+-ATPase in vesicular trafficking: targeting, regulation and function. *Current opinion in cell biology.* 2008;20(4):415-426.
94. Palmer DJ, Helms J, Beckers C, Orci L, Rothman J. Binding of coatomer to Golgi membranes requires ADP-ribosylation factor. *Journal of Biological Chemistry.* 1993;268(16):12083-12089.
95. Zeuzem S, Feick P, Zimmermann P, Haase W, Kahn RA, Schulz I. Intravesicular acidification correlates with binding of ADP-ribosylation factor to microsomal membranes. *Proceedings of the National Academy of Sciences.* 1992;89(14):6619-6623.
96. Aniento F, Gu F, Parton RG, Gruenberg J. An endosomal beta COP is involved in the pH-dependent formation of transport vesicles destined for late endosomes. *The Journal of cell biology.* 1996;133(1):29-41.
97. Gu F, Gruenberg J. ARF1 regulates pH-dependent COP functions in the early endocytic pathway. *Journal of Biological Chemistry.* 2000;275(11):8154-8160.
98. Clague MJ, Urbe S, Aniento F, Gruenberg J. Vacuolar ATPase activity is required for endosomal carrier vesicle formation. *Journal of Biological Chemistry.* 1994;269(1):21-24.
99. Bayer N, Schober D, Prchla E, Murphy RF, Blaas D, Fuchs R. Effect of bafilomycin A1 and nocodazole on endocytic transport in HeLa cells: implications for viral uncoating and infection. *Journal of virology.* 1998;72(12):9645-9655.
100. Oda K, Nishimura Y, Ikehara Y, Kato K. Bafilomycin A1 inhibits the targeting of lysosomal acid hydrolases in cultured hepatocytes. *Biochemical and biophysical research communications.* 1991;178(1):369-377.
101. Yilla M, Tan A, Ito K, Miwa K, Ploegh H. Involvement of the vacuolar H (+)-ATPases in the secretory pathway of HepG2 cells. *Journal of Biological Chemistry.* 1993;268(25):19092-19100.
102. Reaves B, Banting G. Vacuolar ATPase inactivation blocks recycling to the trans-Golgi network from the plasma membrane. *FEBS letters.* 1994;345(1):61-66.
103. Stamnes MA, Rothman JE. The binding of AP-1 clathrin adaptor particles to Golgi membranes requires ADP-ribosylation factor, a small GTP-binding protein. *Cell.* 1993;73(5):999-1005.
104. Zeuzem S, Zimmermann P, Schulz I. Association of a 19-and a 21-kDa GTP-binding protein to pancreatic microsomal vesicles is regulated by the intravesicular pH established by a vacuolar-type H+-ATPase. *The Journal of membrane biology.* 1992;125(3):231-241.
105. Marshansky V, Ausiello DA, Brown D. Physiological importance of endosomal acidification: potential role in proximal tubulopathies. *Current opinion in nephrology and hypertension.* 2002;11(5):527-537.

106. Maranda B, Brown D, Bourgoin S, et al. Intra-endosomal pH-sensitive recruitment of the Arf-nucleotide exchange factor ARNO and Arf6 from cytoplasm to proximal tubule endosomes. *Journal of Biological Chemistry.* 2001;276(21):18540-18550.

107. El Annan J, Brown D, Breton S, Bourgoin S, Ausiello DA, Marshansky V. Differential expression and targeting of endogenous Arf1 and Arf6 small GTPases in kidney epithelial cells in situ. *American Journal of Physiology-Cell Physiology.* 2004;286(4):C768-C778.

108. Hurtado-Lorenzo A, Skinner M, El Annan J, et al. V-ATPase interacts with ARNO and Arf6 in early endosomes and regulates the protein degradative pathway. *Nature cell biology.* 2006;8(2):124-136.

109. Marshansky V. The V-ATPase a2-subunit as a putative endosomal pH-sensor. In: Portland Press Ltd.; 2007.

110. Anderson R, Orci L. A view of acidic intracellular compartments. *The Journal of Cell Biology.* 1988;106(3):539-543.

111. Miesenböck G, De Angelis DA, Rothman JE. Visualizing secretion and synaptic transmission with pH-sensitive green fluorescent proteins. *Nature.* 1998;394(6689):192-195.

112. Ohgaki R, van IJzendoorn SC, Matsushita M, Hoekstra D, Kanazawa H. Organellar Na+/H+ exchangers: novel players in organelle pH regulation and their emerging functions. *Biochemistry.* 2011;50(4):443-450.

113. Brett CL, Wei Y, Donowitz M, Rao R. Human Na+/H+ exchanger isoform 6 is found in recycling endosomes of cells, not in mitochondria. *American Journal of Physiology-Cell Physiology.* 2002;282(5):C1031-C1041.

114. Numata M, Orlowski J. Molecular cloning and characterization of a novel (Na+, K+)/H+ exchanger localized to the trans-Golgi network. *Journal of Biological Chemistry.* 2001;276(20):17387-17394.

115. Nakamura N, Tanaka S, Teko Y, Mitsui K, Kanazawa H. Four Na+/H+ exchanger isoforms are distributed to Golgi and post-Golgi compartments and are involved in organelle pH regulation. *Journal of Biological Chemistry.* 2005;280(2):1561-1572.

116. Roxrud I, Raiborg C, Gilfillan GD, Strømme P, Stenmark H. Dual degradation mechanisms ensure disposal of NHE6 mutant protein associated with neurological disease. *Experimental cell research.* 2009;315(17):3014-3027.

117. Ohgaki R, Matsushita M, Kanazawa H, Ogihara S, Hoekstra D, van IJzendoorn SC. The Na+/H+ exchanger NHE6 in the endosomal recycling system is involved in the development of apical bile canalicular surface domains in HepG2 cells. *Molecular biology of the cell.* 2010;21(7):1293-1304.

118. Demaurex N, Furuya W, D'Souza S, Bonifacino JS, Grinstein S. Mechanism of acidification of the trans-Golgi network (TGN) In situ measurements of pH using retrieval of TGN38 and furin from the cell surface. *Journal of Biological Chemistry.* 1998;273(4):2044-2051.

119. Llopis J, McCaffery JM, Miyawaki A, Farquhar MG, Tsien RY. Measurement of cytosolic, mitochondrial, and Golgi pH in single living cells with green fluorescent proteins. *Proceedings of the National Academy of Sciences.* 1998;95(12):6803-6808.

120. Kornfeld S. Structure and function of the mannose 6-phosphate/insulinlike growth factor II receptors. *Annual review of biochemistry.* 1992;61(1):307-330.

121. Johnson KF, Kornfeld S. The cytoplasmic tail of the mannose 6-phosphate/insulin-like growth factor-II receptor has two signals for lysosomal enzyme sorting in the Golgi. *The Journal of cell biology.* 1992;119(2):249-257.

122. Gieselmann V, Pohlmann R, Hasilik A, Von Figura K. Biosynthesis and transport of cathepsin D in cultured human fibroblasts. *The Journal of cell biology.* 1983;97(1):1-5.

123. Johnson KF, Kornfeld S. A His-Leu-Leu sequence near the carboxyl terminus of the cytoplasmic domain of the cation-dependent mannose 6-phosphate receptor is necessary for the lysosomal enzyme sorting function. *Journal of Biological Chemistry.* 1992;267(24):17110-17115.

124. Faust PL, Wall DA, Perara E, Lingappa VR, Kornfeld S. Expression of human cathepsin D in Xenopus oocytes: phosphorylation and intracellular targeting. *The Journal of cell biology.* 1987;105(5):1937-1945.

125. Gogarten JP, Starke T, Kibak H, Fishman J, Taiz L. Evolution and isoforms of V-ATPase subunits. *J Exp Biol.* 1992;172(1):137-147.

126. Anmole G, Kuang XT, Toyoda M, et al. A robust and scalable TCR-based reporter cell assay to measure HIV-1 Nef-mediated T cell immune evasion. *Journal of immunological methods.* 2015;426:104-113.

127. Stevanovic S, Schild H. Quantitative aspects of T cell activation—peptide generation and editing by MHC class I molecules. Paper presented at: Seminars in immunology1999.

128. Christinck ER, Luscher MA, Barber BH, Williams DB. Peptide binding to class I MHC on living cells and quantitation of complexes required for CTL lysis. *Nature.* 1991;352(6330):67.

129. Brower R, England R, Takeshita T, et al. Minimal requirements for peptide mediated activation of CD8+ CTL. *Molecular immunology.* 1994;31(16):1285-1293.

130. Valitutti S, Müller S, Cella M, Padovan E, Lanzavecchia A. Serial triggering of many T-cell receptors by a few peptide–MHC complexes. *Nature.* 1995;375(6527):148.

131. Robinson J, Halliwell JA, Hayhurst JD, Flicek P, Parham P, Marsh SG. The IPD and IMGT/HLA database: allele variant databases. *Nucleic acids research.* 2014;43(D1):D423-D431.

132. Yarzabek B, Zaitouna AJ, Olson E, et al. Variations in HLA-B cell surface expression, half-life and extracellular antigen receptivity. *Elife.* 2018;7:e34961.

133. Cao K, Hollenbach J, Shi X, Shi W, Chopek M, Fernández-Viña MA. Analysis of the frequencies of HLA-A, B, and C alleles and haplotypes in the five major ethnic groups of the United States reveals high levels of diversity in these loci and contrasting distribution patterns in these populations. *Human immunology.* 2001;62(9):1009-1030.

134. Hollenbach JA, Thomson G, Cao K, et al. HLA diversity, differentiation, and haplotype evolution in Mesoamerican Natives. *Human immunology.* 2001;62(4):378-390.

135. Bugawan T, Klitz W, Blair A, Erlich H. High-resolution HLA class I typing in the CEPH families: analysis of linkage disequilibrium among HLA loci. *Tissue antigens.* 2000;56(5):392-404.

136. Lázaro AM, Moraes ME, Marcos CY, Moraes JR, Fernández-Viña MA, Stastny P. Evolution of HLA-class I compared to HLA-class II polymorphism in Terena, a South-American Indian tribe. *Human immunology.* 1999;60(11):1138-1149.

137. Li S, Jiao H, Yu X, et al. Human leukocyte antigen class I and class II allele frequencies and HIV-1 infection associations in a Chinese cohort. *JAIDS Journal of Acquired Immune Deficiency Syndromes.* 2007;44(2):121-131.

138. Hilton HG, Parham P. Direct binding to antigen-coated beads refines the specificity and cross-reactivity of four monoclonal antibodies that recognize polymorphic epitopes of HLA class I molecules. *Tissue antigens.* 2013;81(4):212-220.

139. Brodsky FM, Parham P, Barnstable CJ, Crumpton M, BOdmer WF. Monoclonal antibodies for analysis of the HLA system. *Immunological reviews.* 1979;47(1):3-61.

140. Carrington M, O'Brien SJ. The influence of HLA genotype on AIDS. *Annual review of medicine.* 2003;54(1):535-551.

141. Kaslow RA, Carrington M, Apple R, et al. Influence of combinations of human major histocompatibility complex genes on the course of HIV–1 infection. *Nature medicine.* 1996;2(4):405.

142. Study IHC. The major genetic determinants of HIV-1 control affect HLA class I peptide presentation. *Science.* 2010;330(6010):1551-1557.

143. Link JO, Rhee MS, Winston CT, et al. Clinical targeting of HIV capsid protein with a long-acting small molecule. *Nature.* 2020;584(7822):614-618.

144. Kataoka T, Shinohara N, Takayama H, et al. Concanamycin A, a powerful tool for characterization and estimation of contribution of perforin-and Fas-based lytic pathways in cell-mediated cytotoxicity. *The Journal of Immunology.* 1996;156(10):3678-3686.

145. Togashi K-i, Kataoka T, Nagai K. Characterization of a series of vacuolar type H+-ATPase inhibitors on CTL-mediated cytotoxicity. *Immunology letters.* 1997;55(3):139-144.

146. Zhang J-Y, Zhang Z, Wang X, et al. PD-1 up-regulation is correlated with HIV-specific memory CD8+ T-cell exhaustion in typical progressors but not in long-term nonprogressors. *Blood.* 2007;109(11):4671-4678.

147. Day CL, Kaufmann DE, Kiepiela P, et al. PD-1 expression on HIV-specific T cells is associated with T-cell exhaustion and disease progression. *Nature.* 2006;443(7109):350-354.

148. Deng K, Pertea M, Rongvaux A, et al. Broad CTL response is required to clear latent HIV-1 due to dominance of escape mutations. *Nature.* 2015;517(7534):381-385.

149. Gaiha GD, Rossin EJ, Urbach J, et al. Structural topology defines protective CD8+ T cell epitopes in the HIV proteome. *Science.* 2019;364(6439):480-484.